



UiT The Arctic University of Norway

The Faculty of Biosciences, Fisheries and Economics

The Norwegian College of Fishery Science

Engineering novel bacterial biosensors for the characterization of membrane active natural products

Céline Sarah Marine Richard

A dissertation for the degree of Philosophiae Doctor, April 2024



Engineering novel bacterial biosensors for the characterization of membrane active natural products

A dissertation for the degree of Philosophiae Doctor



Céline Sarah Marine Richard

Tromsø, April 2024

Marine Bioprospecting Group

The work for this thesis was carried out from September 2018 to May 2023 at the Norwegian College of Fishery Science (NFH), UiT – The Arctic University of Norway. The work was funded by UiT – The Arctic University of Norway as an independent PhD position.

Table of Contents

Summary	iv
Acknowledgment	vi
List of papers.....	ii
Abbreviations	iii
List of Tables.....	iv
List of Figures	iv
1 Introduction	1
1.1 Antibiotics: a blessing or a curse?	1
1.2 Bioprospecting and natural products discovery.....	6
1.3 Bacterial biosensors as tools in biodiscovery	11
2 Research Aim	19
3 Summary of papers	20
4 General discussion.....	23
4.1 Luciferases as universal tools for assessment of bacterial viability and membrane integrity 23	
4.2 Adapting next generation reporter genes to natural product discovery.....	25
4.3 Combining reporter elements for more efficient activity testing.....	29
4.4 The outer-membrane as a potential target and an obstacle in natural product discovery.....	30
5 Conclusion	33
6 Future perspectives	34
Works cited	35
Paper I, II and III	

Summary

Treatment of bacterial infections has become more challenging due to the expansion of antibiotic resistance. Especially, resistant Gram-negative pathogens are burdening healthcare systems worldwide. This increases the need for new antibiotics able to penetrate the outer-membrane (OM) of Gram-negatives. Natural products (NPs) from the marine environment e.g. antimicrobial peptides (AMPs) are interesting drug lead candidates as they often show potent activity against bacterial membranes and are still under-studied compared to NPs from the terrestrial environment. Mode of action (MoA) specific drug lead discovery requires new tools, which can be based on engineered bacterial cells as biosensors. To identify MoA of peptides in general, and the impact of AMPs on bacterial membranes specifically, bacterial whole-cell biosensors (BWCBs) based on different reporter gene constructs are one possible solution to facilitate effective discovery pipelines.

The work conducted in this thesis aims to engineer novel BWCBs with relatively new reporter genes to facilitate a better understanding of the impact of marine AMPs on the bacterial membranes already during screening steps of drug discovery.

In **paper I**, as part of the ongoing research for antimicrobial NPs, the BWCBs *Escherichia coli* (for Gram-negative) and *Bacillus subtilis* (for Gram-positive) carrying the bacterial luciferase *lux* operon or the eukaryotic click beetle luciferase *lucGR* were used to study the impact of compounds extracted from the arctic bryozoan *Securiflustra securifrons*, on the cell viability or membrane integrity, respectively. One of them, the Securamine H, was found to inhibit the viability of Gram-positive bacteria and reduce metabolic activity of *B. subtilis* but the MoA on this intracellular target still needs to be identified.

In **paper II**, a recently discovered reporter gene, *unaG*, from the Japanese eel *Anguilla japonicas*, was used to engineer a novel MoA specific BWCB to investigate OM integrity of Gram-negative bacteria. We used the *E. coli* wild-type strain MC4100 and its isogenic OM-impaired mutant strain NR698 as well as different OM-active compounds and cyclic marine AMP derivatives to show that the uptake of Bilirubin (BR), the ligand of UnaG, and thus fluorescence depends on a leaky OM. Those properties of the UnaG-BR couple might be applied as a BWCB and as an alternative to the OM integrity assays currently in use.

In **paper III**, the reporter gene *unaG* has been combined with luciferase-based reporter systems in the same BWCB to distinguish OM from OM- and plasma-membrane (PM) disruption or to run simultaneous cell viability measurements. These novel BWCBs allow for one step evaluation of OM and PM or OM and viability. Marine AMPs from the Spider Crab *Hyas araneus* and from the Green Sea Urchin *Strongylocentrotus droebachiensis* were used to study their impact on bacterial membranes. Centrocin HC has a strong effect on the PM and OM of *E. coli* while the fragment Centrocin HC (1-20)

exhibited less activity towards PM and more against OM, and shorter fragments remained completely inactive. This indicates that most of the first 20 amino acids are required to exhibit OM activity but not sufficient to efficiently penetrate the PM. The latter could be explained by the loss of a positively charge arginine compared to the full-length peptide.

Acknowledgment

“The one who falls and gets up is stronger than the one who never tried. Do not fear failure but rather fear not trying.”

— Roy T. Bennett

What a journey, a PhD.

I think it was one of the most difficult but also rewarding experience in my life so far. Done with blood, sweat and tears, we say. It has been exciting, frustrating, fun, difficult, interesting, terrifying, my best friend and my worst enemy: a whole roller-coaster of emotions. I thought many times about giving up, but at the same time I just couldn't let it go, because I loved my project. I am thankful about this opportunity. But mostly, I am feeling blessed to be surrounded by kind-hearted people who really helped me to go through this journey.

The PhD was carried out at the Norwegian College of Fishery Science, UiT – The Arctic University of Norway, Tromsø, from 2018 to 2024. UiT provided the financial support.

First of all, I want to give my biggest thanks to my principal supervisor, Associated Professor Hans-Matti Blencke, who helped, supported, and guided me through the PhD but also in my new life in Tromsø. Thank you for all your advice, knowledge, patience, calmness and support. Thank you for helping me when I had problems with my health, and my body was giving me some struggling times. I will always cheer for you when I will drink kombucha. Also, I am thankful to my co-supervisor, Dr Chun Li, for all the feedback and valuable suggestions.

I extend my deepest gratitude to the PhD evaluation committee, Prof. Sven Halbedel, Prof. Trygve Brautaset and Associated Prof. Eva-Stina Edholm for your willingness to be part of my PhD journey. Thank you for accepting to evaluate my thesis and taking this time out of your busy schedules. Also, thank you for coming all the way to Tromsø for the defense.

Thank you for all of my colleagues inside and outside the Marine Bioprospecting research group, for the amazing working environment, the coffee breaks, the laughter, and good discussions. Thank you to the engineers, Hege, Ida and mostly Frode, for all the help in the lab. I would like to express my special gratitude to Andrea, we started together, had our adventures in different parts of Norway but also Svalbard, sharing many difficult and beautiful moments of our PhDs. I will never forget this amazing hot chocolate from Gdańsk we shared one of the Christmas times.

Big thank you to all my friends, Daniela, Nathanaël, Emilie, Reinhardt, Jasmine, Matthias, Claire, Herman, Kate, Julien, Louis, Silvia, Vidar, Jarad, Alexis, Maxime, Laurine, and the others, close or far away, for your support, your kindness, and being my sunshine during this journey. It would have been a lot harder without you. Thank you, my dear friend Kate, for proof-reading my dissertation.

Thank you to my dear family. Mom, dad, I would not be here without you. I am feeling blessed to have such supportive parents.

My last words for my special person, my partner in crime, Bert. Thank you for believing in me, supporting me, for your patience during the hardest time, I would have completely lost myself without you. I cherish all the moments with you. Ik hou van jou.

Céline Richard

“We must find time to stop and thank the people who make a difference in our lives.”

List of papers

The following three publications form the basis of this thesis:

Paper I

Kine Ø. Hansen, Ida K. Ø. Hansen, Céline S. M. Richard, Marte Jenssen, Jeanette H. Andersen, and Espen H. Hansen

Antimicrobial Activity of Securamines from the Bryozoan *Securiflustra securifrons*

Natural Product Communication (2021). doi: 10.1177/1934578X21996180

Paper II

Céline S. M. Richard, Hymonti Dey, Frode Øyen, Munazza Maqsood and Hans-Matti Blencke

Outer Membrane Integrity-Dependent Fluorescence of the Japanese Eel UnaG Protein in Live *Escherichia coli* Cells

Biosensors (2023). doi: 10.3390/bios13020232

Paper III

Céline S. M. Richard, Hymonti Dey, Emma Murvold, Frode Øyen, Chun Li, and Hans-Matti Blencke

Cloning of a dual biosensor relying on UnaG and luciferase for detection of outer and plasma membrane disruption and its application to characterizing the membranolytic effects of green sea urchin *Strongylocentrotus droebachiensis* Centroci-1-based antimicrobial peptides.

Manuscript

Contributions

	Paper I	Paper II	Paper III
Concept and idea	KØH, IKØH, JHA, EHH	CSMR, MM, HMB	CSMR, HMB
Study design and methods	KØH, IKØH, JHA, EHH	CSMR, HD, HMB	CSMR, HD, HMB
Data gathering and interpretation	KØH, IKØH, CSMR, MJ	CSMR, HD, MM, FØ, HMB	CSMR, HD, EM, FØ, HMB
Manuscript preparation	KØH, IKØH, CSMR, EHH	CSMR, HD, HMB	CSMR, HD, CL, HMB

CSMR = Céline Sarah Marine Richard, CL = Chun Li, EHH = Espen Holst Hansen, EM = Emma Murvold, FØ = Frode Øyen, HD = Hymonti Dey, HMB = Hans-Matti Blencke, IKØH = Ida Kristine Østnes Hansen, JHA = Jeanette Hammer Andersen, KØH = Kine Østnes Hansen, MJ = Marte Jenssen, MM = Munazza Maqsood.

Abbreviations

AB = Antibiotic

AMP = Antimicrobial peptide

BR = Bilirubin

BV = Biliverdin

BWCB = Bacterial whole-cell biosensor

CAT = Chloramphenicol Acetyltransferase

CHX = Chlorhexidine

EtBr = ethidium bromide

FABP = Fatty-acid-binding protein

FP = Fluorescent protein

FR = Far red

GFP = Green Fluorescent protein

HBC = (4-((2-hydroxyethyl)(methyl)amino)benzyl-idene)-cyanophenylacetonitrile

HC = Heavy chain

ICU = Intensive care units

LC = Light chain

mAb = Monoclonal antibodies

MBC = Minimum bactericidal concentration

MDR = Multi-drug resistant

MIC = Minimum inhibitory concentration

MoA = Mode of action

NIR = Near-infrared

NP = Natural product

NPN = N-phenyl-1-naphthylamine

OM = Outer membrane

PDR = Pan-drug resistant

PM = Plasma membrane

RBS = Ribosome-binding site

smURFP= Small ultra-red fluorescent protein

WHO = The World Health Organization

WT = Wild type

XDR = Extensively drug-resistant

List of Tables

Table 1. Common reporter genes.....	12
-------------------------------------	----

List of Figures

All the illustrations are made with BioRender.com, and graphs with GraphPad Prism.

Figure 1. Common uses of antibiotics in different sectors like health care, agriculture and aquaculture.	2
Figure 2. Antibiotic action and resistance mechanisms.....	4
Figure 3. Possible integration of whole cell biosensors into current bioassays-guided screening and purification platforms for natural products discovery.	8
Figure 4. Elements of biosensors.	10
Figure 5. Examples of applications of biosensors. (references: a ⁹⁹ , b ¹⁰⁰ , c ¹⁰¹ , d ¹⁰² , e ¹⁰³ , f ¹⁰⁴ , g ¹⁰⁵ , h ¹⁰⁶ , i ¹⁰⁷ , j ¹⁰⁸ , k ¹⁰⁹ , l ¹¹⁰ , m ¹¹¹ , n ¹¹²).....	11
Figure 6. Basics of genetic engineering to construct a bacterial biosensor.	16
Figure 7. Example of bacterial biosensors with combined fluorescent and bioluminescent reporter genes.	17
Figure 8. Kinetics of the relative luminescence emission by A) <i>B. subtilis</i> (pCSS962) and B) <i>E. coli</i> (pCSS962) treated with ranging concentrations of securamine H (1) or chlorhexidine (CHX). Each point is the mean of three independent measurements.	20
Figure 9. Kinetics of the relative luminescence emission by A) <i>B. subtilis</i> (pCGLS-11) and B) <i>E. coli</i> (pCGLS-11) treated with ranging concentrations of securamine H (1) or chlorhexidine (CHX). Each point is the mean of three independent measurements.....	20
Figure 10. Schematic of the use of the reporter protein UnaG as an OM permeabilization whole-cell biosensor.	21
Figure 11. Schematic of the use of the dual biosensor for OM and PM permeabilization.....	22
Figure 12. Representation of the 8pepper-GFP BWCB project.	28

1 Introduction

1.1 Antibiotics: a blessing or a curse?

Antibiotics (ABs) are a group of drugs most people in modern society have heard of. Surveys conducted around the world have shown that the general population to a large extent, knows that ABs are used to treat or prevent bacterial infections. However, even in western countries, large groups of the population still harbor critical misconceptions concerning ABs. For instance, around 37 % of the respondents in a cross-sectional study recently conducted in Italy agreed with false claims such as ABs being effective against viruses or being useful in pain relief. In the same study only roughly around a quarter of the respondents agreed with the correct claim that there are bacteria that are resistant to antibiotics ¹. In Turkey, 13% responded that ibuprofen was an antibiotic and 27% that antibiotics were effective against a cold or flu. On the positive side, 87% agreed that antibiotics are effective against bacteria ². Even farther to the east, in Bangkok 55% of the respondents believed that ABs could treat colds and flu including 38% not knowing that ABs could not treat measles, and 70% misunderstanding that ABs resistance occurs as a consequence of the human body becoming resistant ³. Public misconceptions like these might well be seen as the original drivers of today's frantic search for novel antimicrobials.

How did ABs gain the important role they have in today's society and where did they originate from? It all seemed to start with the first renowned discovery of an AB by Alexander Fleming in 1928: Penicillin from the fungus *Penicillium notatum*. His observation that fungal contaminants inhibited bacterial growth of *Staphylococcus aureus* can be seen as the steppingstone into the golden age of ABs a few decades later. Fleming, along with Florey and Chain, was awarded the Nobel Prize in Physiology and Medicine for this discovery in 1945. But mankind started to harvest the power of antibiotics long before the advent of modern medicine. Already 3 000 years ago in the ancient China, they were using moldy soybeans as remedies to cure infected wounds ⁴. Mold in general has also been used to cure infections in folk medicine stretching back to antiquity with moldy bread, milk, cheese, etc ⁵. The first antimicrobial drug that has been used in the hospital setting of modern history was called pyocyanase, discovered by Rudolph Emmerich and Oscar Löw in the late 1890 from the cultivation of *Pseudomonas aeruginosa* ⁶. This was followed by the introduction of Salvarsan in 1909 by Paul Ehrlich ⁷, and finally the milestone discovery of penicillin. Since then, many more ABs have been discovered, mostly during the "Golden Era" of antibiotics from the 1940s - 1960s. Nowadays, ABs are widely used in our society, and they have drastically changed how we live and when we die. ABs revolutionized the practice of medicine and healthcare directly by rendering formerly lethal infections, such as pneumonia, bacterial meningitis or sepsis, treatable ⁸, and by ensuring treatment of recurring bacterial infections and chronic conditions. Indirectly, the availability of these effective antibacterial drugs made organ transplants and other invasive surgical interventions possible by preventing postoperative infection ⁹. However, the impact of ABs was not limited to human healthcare but also strongly affected the development of

agriculture, aquaculture, and biotechnology, as illustrated in figure 1 below. Even in biotechnology, ABs are routinely used in combination with resistance cassettes as selection markers ¹⁰ and as ingredients of cell culture media to prevent bacterial contamination ^{11,12}. Consequently, ABs are fundamental pillars of society today and we heavily rely on the availability of effective ABs.

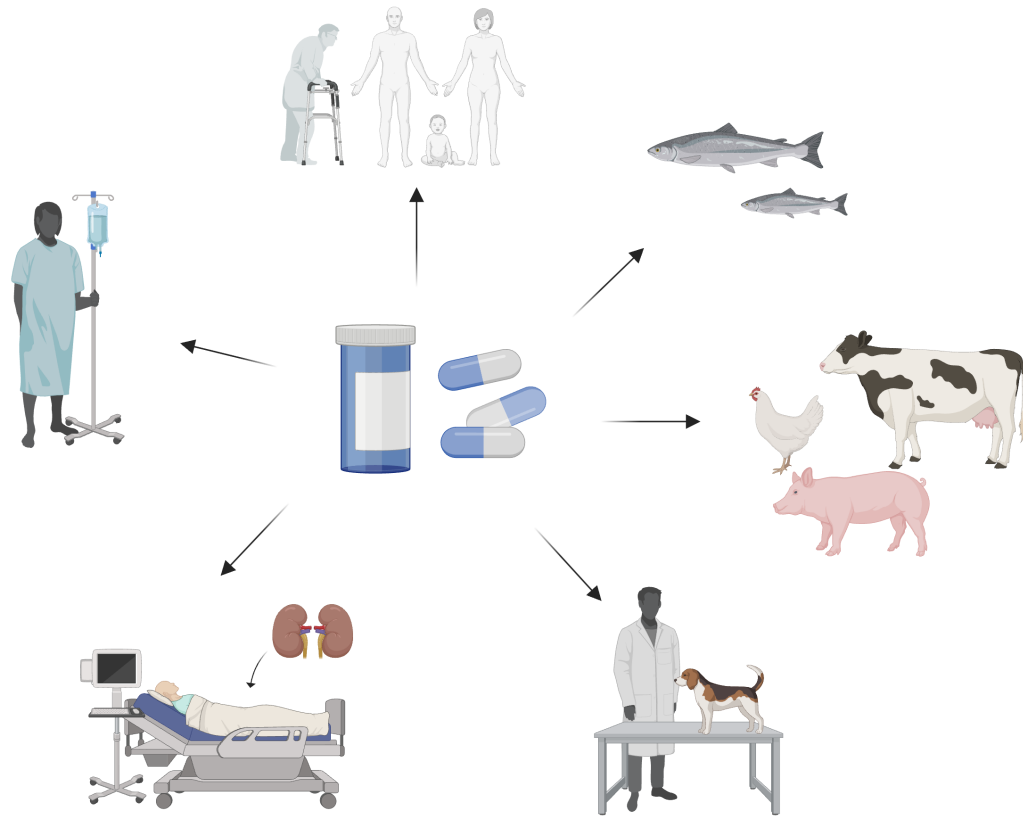


Figure 1. Common uses of antibiotics in different sectors like health care, agriculture and aquaculture.

ABs in use today are produced as natural, semi-synthetic and synthetic substances. Generally, they affect bacteria through five major modes of action, which are based on the interference with enzymes required for the peptidoglycan biosynthesis, nucleic acid synthesis, protein synthesis and metabolism, but also with membrane integrity ¹³, as summarized in figure 2. A single antibiotic can have one or several modes of action.

The introduction of ABs strongly affected both the human species and their microbiome. It has lifted the co-evolution between humans as the host and their bacterial pathogens into a new accelerated phase where the host's response is based on biotechnological progress rather than genetic change. Unfortunately, this race between human society and bacterial pathogens specifically, but also microbiota in general, is in danger of approaching the post-antibiotic era ^{14,15} with bacterial pathogenic yeast, molds, and protists rendering themselves and each other resistant to previously effective cures ^{16,17}. Bacterial

infections, which until recently could be treated with antibiotics risk becoming an issue. This has worldwide consequence through the increase of resistance against antibiotics rendering traditional treatment of bacterial infections ineffective. Common diseases like bloodstream, urinary tract and respiratory tract infections are becoming untreatable and countries like the Russian Federation, North Macedonia, Italy, Turkey or Greece already are alarmed due to high levels of resistance against carbapenems, third-generation cephalosporins, fluoroquinolones, and other antibiotics¹⁸. Already in 2019, 1.2 million deaths worldwide were linked to antibiotic resistance¹⁹. The World Health Organization (WHO) estimates that if no action is taken, untreatable diseases caused by drug-resistant bacteria could result in up to 10 million annual deaths globally by 2050²⁰. Most of the resistance spread is provoked by the overuse or misuse of antibiotics in health care, agriculture, and aquaculture^{21,22}. Recent studies also demonstrated that antibiotic resistance genes can be disseminated by air pollution particles²³, microplastics²⁴ and even nonnutritive sweeteners²⁵. This issue is perceived strongly in Intensive Care Units (ICU), where complications often arise from resistant Gram-negative bacteria. For example, in 2019, *Escherichia coli* was responsible for the most common cause of community-acquired bloodstream infections and urinary tract infection. This bacterium shows resistance to fluoroquinolones between 10% and 50% of the cases in the EU-EEA and could exceed 50% in some countries like the Russian Federation or in North Macedonia²⁶. Moreover, several multidrug resistant Gram-negative bacteria are present in the WHO high-priority list of pathogens like *Acinetobacter baumannii*, *Pseudomonas aeruginosa* and *Escherichia coli*²⁷. The resistance to antibiotics can have two origins: either an error in the DNA replication that gave a selection for drug-insensitive mutants with vertical propagation through bacterial populations or by the acquisition of mobilized resistance genes by horizontal transfer facilitated by conjugation, transduction or transformation. Different mechanisms can be responsible for microbial resistance (figure 2), like the activation of the efflux pumps to extrude toxic compounds, lessening AB penetration by decreasing the permeability of the membranes, enzymatic inactivation of the ABs, or target bypass²⁸. Bacteria accumulating more than one AB resistance are classified in three different categories. The multi-drug resistant (MDR) bacteria, which has acquired resistance to at least one agent from three or more antimicrobial categories; the extensively drug-resistant (XDR) bacteria, which has acquired resistance to at least one agent from all but two or fewer antimicrobial categories; and the pan-drug-resistant (PDR) bacteria, which acquired resistance to all antimicrobial categories^{29,30}. Already in 2011, Dr. Margaret Chan of the WHO paraphrased the situation with the slogan “no action today, no cure tomorrow”, arguing for a more responsible use of the currently available antibiotics. At the same time, she pointed out that the antimicrobial drug development pipelines are practically running dry. Obviously, a combination of many approaches is needed to combat the impact of antimicrobial resistance on society. To compensate this slow antibiotic discovery, WHO made a classification database of antibiotics called Be AWaRe list, to preserve the available ABs as well as possible. Three different classifications are presented: “Access” to indicate the AB recommended as

first- or second-line therapies; “Watch” for the ones sensitive to development of resistance that should be focus on stewardship programs; and “Reserve” for the ones recommended as last-line therapies ³¹. Also, the recognition of antimicrobial drug discovery resulted in the creation of different funding initiatives such as CARB-X (combating antibiotic-resistant bacteria), GARDP (global antibiotic research + development partnership), and the REPAIR (Replenishing and Enabling the Pipeline for Anti-Infective Resistance) impact fund that finance late-stage antibiotic discovery and clinical trials to bring medicines to the market ³². Increasing drug discovery efforts today will start to have an impact on treatment of infections with pathogens resistant to today’s antibiotics after a lag of several decades. Nevertheless, it is an important part of the strategies to combat resistance.

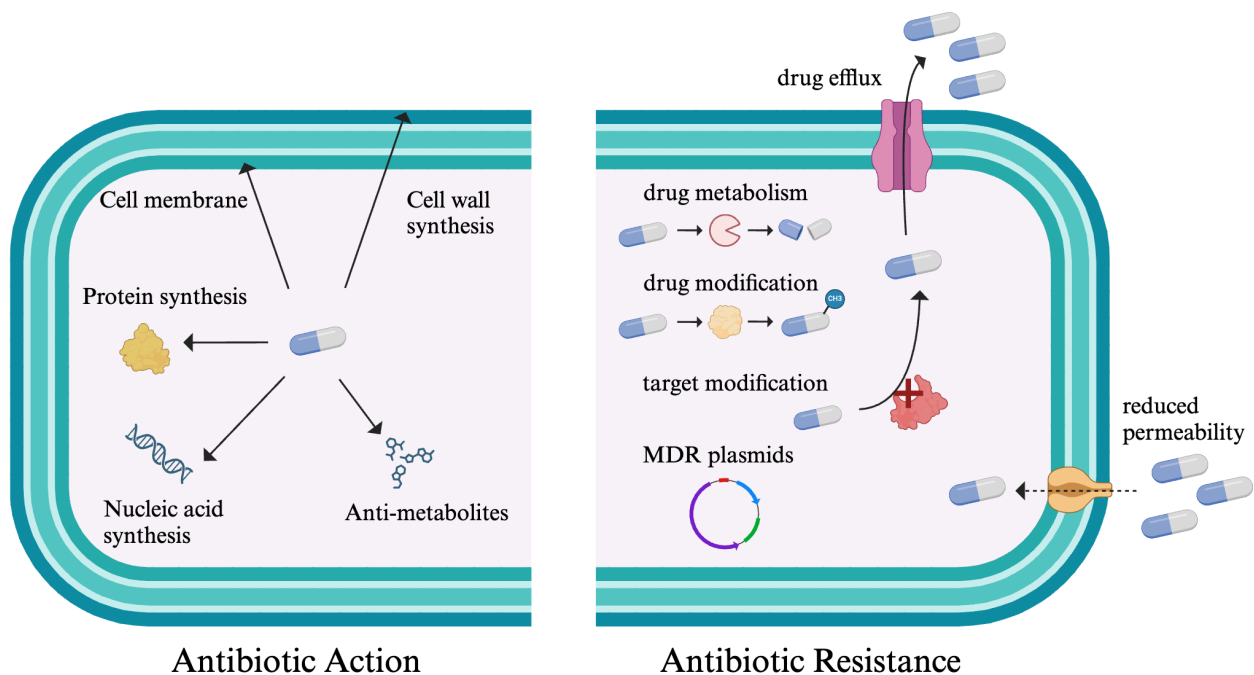


Figure 2. Antibiotic action and resistance mechanisms.

Several alternative approaches are promising to reduce the pressure exerted by ABs resistance spread, as novel but also old and almost forgotten treatment regimens are on the way to (re-)enter the market of anti-infection drugs. One promising approach is the development of anti-virulence medication, which suppresses the virulence of the targeted pathogens. This method is intrinsically narrow-spectrum but often needs to be paired with an antibiotic to remove the pathogen for high-risk patients ^{33,34}. For instance, inhibitors of *Escherichia coli* adhesin FimH, GSK3882347 and EB8018/Sibofimloc are interesting candidates. Sibofimloc has successfully completed the phase 1 trials ³⁵ and has been shown to block the attachment of pathogenic *E. coli* to the host epithelia. An example for the revival of pre-antibiotic treatment strategies is the use of bacteriophages. These bacterial viruses were discovered already early in the 20th century and were rapidly deployed for infection control. In 2006 the first commercial phage product approved by FDA was introduced, LMP-102 from Intralytix Incorporated

(USA). Since then species-specific phages have been used extensively in food industry and agriculture for quality control by removing pathogens like *Listeria monocytogenes*, *Salmonella* spp., and *Shigella* spp., with more than a dozen products on the market ³⁶. Now the use of phage therapy to treat highly drug-resistant infections becomes increasingly attractive as an alternative to antibiotics in medicine. Already more than a dozen active clinical trials in phases 1 and 2 are prompted. One disadvantage of bacteriophages is that bacteria employ a host of different mechanisms to become resistant to phage attacks, with the CRISPR system possibly being the most prominently known. In its function, it resembles adaptive immunity but it greatly differs among bacterial species ³⁷. Finally, the pharmaceutical industry focuses on harnessing adaptive immunity. Monoclonal antibodies (mAb) are showing promising results also in the treatment of bacterial infection. Indeed, mAbs are one of the fastest-growing pharmaceutical sectors with more than 100 FDA-approved mAbs already on the market and hundreds more in clinical development ³⁸. But also classical vaccination strategies are applied to prevention of bacterial infections. By reducing the rates of infection and disease spread, it is possible to suppress the dissemination of the resistance to antibiotics by preventing infection and thus, antibiotic use. Maybe the main advantage of vaccines is the fact that they do not select for resistance. Already dozens of vaccine candidates targeting pathogenic bacteria are present in all stages of clinical trials ³⁹. Most advanced are vaccines for the prevention of *Clostridium difficile* infection and pneumococcal vaccines that target 20 serotypes, with others directed to *Shigella*, *E. coli*, *Salmonella*, and *S. aureus* in the pipeline ⁴⁰. Another way is the use of drugs relieving bacteria of their inherent resistance mechanisms and allowing for the reactivation and repurposing of ABs. For example, bioactive compounds specifically attacking the outer membrane (OM) of Gram-negative bacteria, to use ABs that would not work on Gram-negative bacteria otherwise due to the OM barrier.

Unfortunately, current ABs have other downsides than just resistance. They also have a negative effect on the human microbiome, which is a key contributor to health. AB treatment reduces richness and diversity of the microbiome, including commensal bacteria ^{41,42}. Furthermore, ABs have also been likened to cancerogenesis ⁴³, microbial dysbiosis ⁴², obesity and diabetes ⁴⁴, allergies ⁴⁵, bowel diseases ⁴⁶, etc. emphasizing the fact that for ABs not to become a curse, diligence is due.

The discovery of ABs was a blessing, which revolutionized our society and helped us to extend our lifetime. Unfortunately, AB over- and misuse only boosted by public misconceptions eventually led to the resistance crisis we are experiencing today. It resembles a vicious circle, as humanity seems to be cursed to invent novel cures to diseases, which seemed to be under control. The only way to break out seems to be a combination of end-user education and intensified drug discovery. This thesis focuses on the roots of the original AB drug discovery by contributing to the groundwork of providing tools for natural product discovery of antimicrobial substances with potential new modes of action.

1.2 Bioprospecting and natural products discovery

The term bioprospecting was defined for the first time in 1993 by Walter V. Reid *et al.* as “the exploration of biodiversity for commercially valuable genetic resources and biochemicals”⁴⁷. From it, bioprospecting nowadays is defined as an organized and systematic research for beneficial products derived from bioresources, called natural products (NPs). The discovery of NPs represents indeed a fascinating and essential field of scientific exploration of chemical compounds produced by living organisms, encompassing plants, microorganisms and animals^{48–52}. Those natural products can be produced by organisms from terrestrial and marine environments, and can be developed further for commercialization, to the benefit of society. This field has played a significant role in shaping the world of medicine, agriculture, and biotechnology^{53–55}. The biosynthetic pathways for secondary metabolite synthesis evolved over billions of years to generate chemical structures that interact with biological targets, either in the producing organism itself or in those present in the surrounding environment. Consequently, it can be assumed that an important part of secondary metabolites possesses biological activities, although we may not yet have assays to detect these^{56,57}.

For the first time, a pure bioactive compound was isolated from an organism by Friedrich Wilhelm Sertürner in 1804. It was isolated from the poppy *Papaver somniferum* and is called morphine⁵⁸. Since then, the traditional way of approaching NP discovery was based on the isolation of bioactive compounds from potential producers and then screening the extracts or separated fractions in a variety of bioassays, as shown in figure 3. This ongoing quest continues to yield remarkable discoveries. Scientists have identified natural products with potent anticancer properties^{59–61}, antimicrobial agents vital for combating drug-resistant pathogens^{62–65}, and bioactive molecules with potential applications in neurodegenerative diseases^{66–68}. Even today natural ecosystems represent a reservoir of NPs as potential solutions to contemporary global challenges. In fact, over 50% of all pharmaceutical drugs currently on the market are directly derived from or inspired by NPs⁶⁹. Rapid development of technologies has led to new methods that dramatically increase the potential for natural product discovery like the growth-independent mining of bacterial genomes for new bioactive NPs. The power of genome sequencing technologies was complemented with advanced computational analyses of DNA sequences. Indeed, the biosynthetic pathways of NPs are organized in gene clusters with highly conserved modules. These gene clusters have been observed in genomes of filamentous fungi and bacteria. Most of these NPs are based on polyketides or have peptide cores, involving specific enzymes for synthesis: polyketide synthases (PKSs) like anthraquinone biosynthesis⁷⁰ and non-ribosomal peptide synthetases (NRPSs) like cyclopeptides biosynthesis⁷¹, respectively⁷². Some can even be hybrids involving both pathways (NRPS-PKS) like the aspcandine biosynthesis⁷³.

One interesting source of NPs is the marine environment. It represents more than 70% of the Earth’s surface encompassing between 50% and 80% of all lifeforms and is yet insufficiently explored for

potential bioactive molecules by natural product discovery⁷⁴. Aqueous by nature, sea water is an ideal medium for spreading pathogenic bacteria between the immersed hosts. Sea water contains around 10⁶ bacteria/mL sea water on average. One potential and attractive source of secondary metabolites, with potential commercial value, are microalgae^{75,76}. They are the source of many economically interesting compounds such as biofuels (bioethanol⁷⁷, biodiesel⁷⁸, etc.), high value products like carotenoids⁷⁹, proteins, lutein and lipids⁸⁰. However, the foremost resource of new NPs from the marine environment so far are mostly marine fungi and bacteria, but also from invertebrates like sponges or cnidarians^{57,81}. As most of them are sedentary creatures, they are constantly in presence of bacteria. Lacking adaptive immunity, they need to produce a multitude of secondary metabolites as adaptive strategies to environmental fluctuations and as defense mechanisms. Thus, those marine animals rely solely on innate immunity, including antimicrobial peptides (AMPs), to combat infectious agents, rendering the marine environment unique in terms of AMP evolution⁸². Marine AMPs differ from their terrestrial counterparts by the prevalence of the amino acids arginine and leucine. This is interpreted as an adaptation to a unique feature of bacterial membranes in the cold marine environment where polyunsaturated fatty acids are more frequent⁸³⁻⁸⁹. In addition, brominated amino acids have been observed in AMPs from the marine environment for example in strongylocins and centrocins⁹⁰. The function of bromination might be to improve proteolytic stability as was shown for hagfish cathelicidins⁹¹. These features make them interesting for drug discovery. The first marine AMP was discovered by Nakamura *et al.*⁹², named tachyplesin, from the hemocytes of horseshoe crab *Tachypleus tridentatus*. The most prevalent mode of action of AMPs is membrane disruption^{90,93,94}.

One of the main tools to find novel natural products is bioassay-guided discovery, linking chemical extraction and purification methods to biological activity based analysis in modern bioprospecting. Typically, bioassay guided bioprospection is initiated by extensive screening of the crude natural extracts with a fraction of the sample, followed by the isolation and characterization of the bioactive compounds, as shown in figure 3.

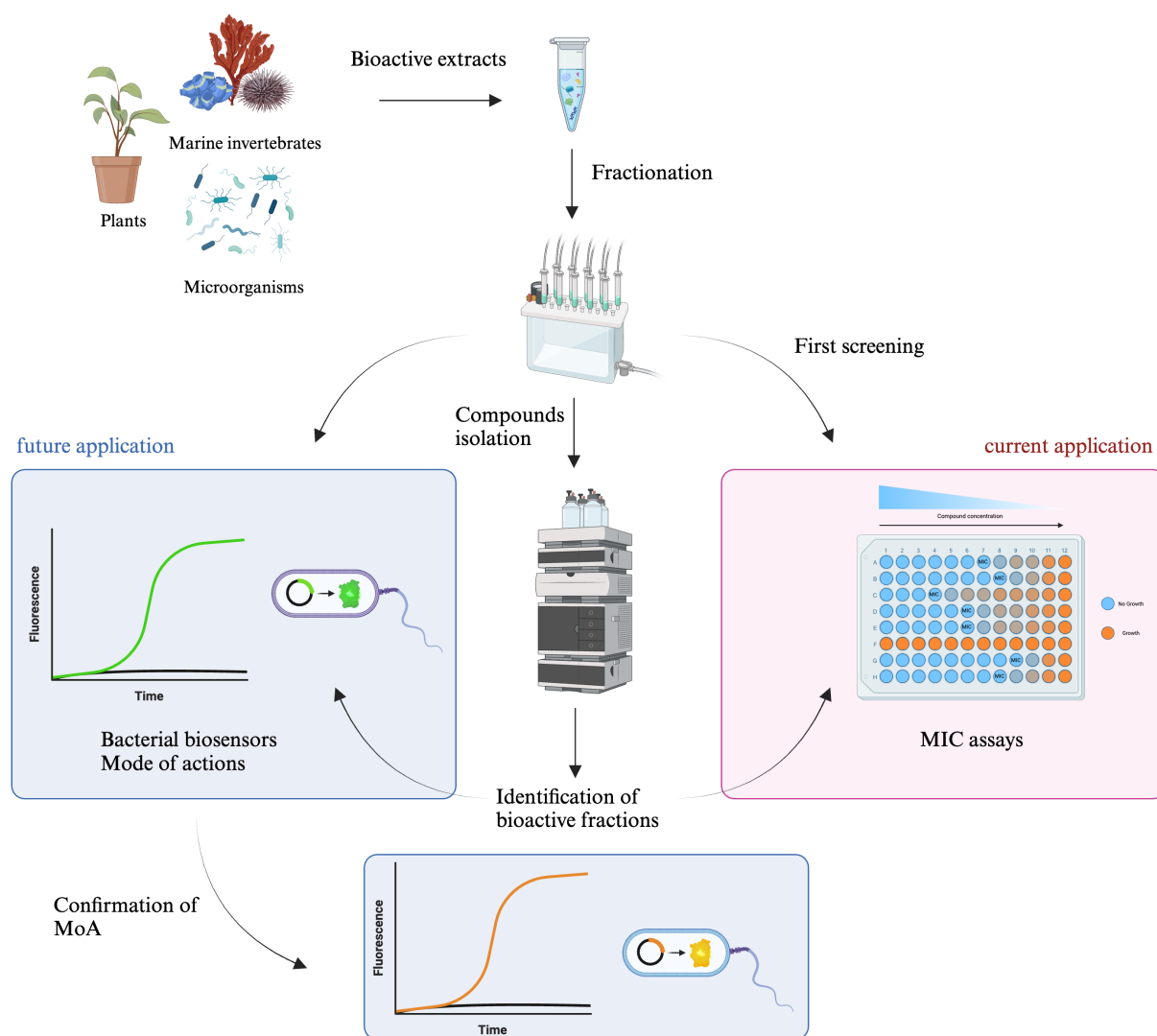


Figure 3. Possible integration of whole cell biosensors into current bioassays-guided screening and purification platforms for natural products discovery.

To identify extracts and fractions with antimicrobial activity potentially containing one or several novel NPs *in vitro*, the most common bioassay is based on growth inhibition and testing of serial dilutions to establish a dose dependence. It will determine the highest dilution of an antimicrobial compound that still prevents visible or measurable growth of a microorganism, which is defined as the minimal inhibitory concentration (MIC) if the concentration of a pure compounds is known. Growth based assays can be conducted in different media and formats, for example as broth micro- or macrodilution, agar dilution and Kirby-Bauer disc diffusion susceptibility assays⁹⁵. MIC assays are cost-effective, accurate, reproducible, versatile, sensitive, standardized, and quantitative⁹⁶. However, to establish the minimum bactericidal concentration (MBC), further assays are needed. There are also several limitations to MIC assays. First, growth dependent assays usually require 24 hours incubation making them slow in terms of result availability. Second, solubility of organic extracts and compounds can be challenging in broth

media and affect the testable concentration. Third, growth media and *in vitro* conditions will not necessarily represent compound activity *in vivo*. Finally, the choice of solvent for the dilution series might affect growth of the microorganism⁹⁷. Most importantly, by merely assaying for growth inhibition, a MIC assay can't provide information on the mechanism of action of the studied compounds and is by definition limited to detection of compounds affecting bacterial growth.

As we need new bioactive compounds with innovative modes of action, it is important to expand NP discovery but, at the same time, not limiting the bioassays to mere growth inhibition during the screening process. For example, biochemical assays investigating enzyme inhibition, cell based studies combined with imaging techniques visualizing morphological changes of target cells and mode of action specific biosensors can be relatively cost effective and rapid enough to integrate into screening platforms. Other approaches such as methods based on genomics, transcriptomics, proteomics, x-ray crystallography and metabolomics allow for the elucidation of resistance determinants, expression profiles, protein-modifications, molecular target interactions and metabolic fluxes, respectively, currently require large quantities of the compound, are rather time-consuming and costly, thus suited for downstream confirmation and further characterization of compounds rather than screening. While many of the methods mentioned above can be applied to elucidate mechanisms of action and find the properties of the bioactive compounds, within the different bioactivities like for example antimicrobials, anti-cancer compounds and antioxidants, especially biosensors seem to harbor potential to revolutionize natural product discovery.

Biosensors can serve as cost-efficient and rapid alternatives to traditional approaches. They are devices capable of detecting changes through biological systems and translating them into a measurable signal. They consist of three main components: a biological sensing element, a transducer and the signal processing system⁹⁸, as shown in the figure 4. The biological sensing element can be tissues, organelles, enzymes, antibodies, microorganisms, cell receptors, or nucleic acids, and is responsible for detecting the presence and/or the concentration of an analyte. Ideally this sensory element would be highly specific to the analyte. The transducer converts the biochemical signal received from the biological sensing element into a measurable and quantifiable signal, which can be optical or electrochemical. Ideally, a biosensor should be sensitive, selective and stable, thus generating reproducible results.

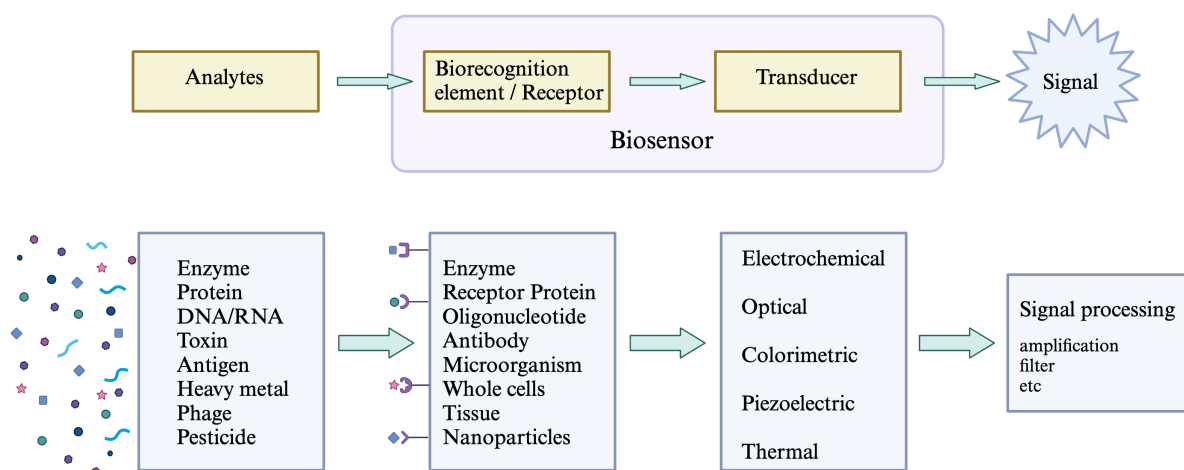


Figure 4. Elements of biosensors.

Figure 5 summarizes how biosensors are frequently applied to different fields such as biomedicine^{99,100}, food safety and processing^{101,102}, disease diagnosis^{100,103,104}, environmental monitoring^{105–107}, and also natural product / drug discovery¹⁰⁸.

Effective bioprospecting requires a wide range of methods to discover and characterize novel NPs providing value for society. Ultimately, it is the screening steps, where compounds are flagged as valuable or to be discarded, which determine if innovative discoveries are made in the first place. Thus, the biodiscovery success of bioassay guided purification pipelines could be substantially improved by merely replacing or adding novel bioassays to the established platform. In antimicrobial compounds discovery, biosensors seem to be well suited to build on and improve bioassay-guided purification platforms, which are built on detection of growth inhibition.

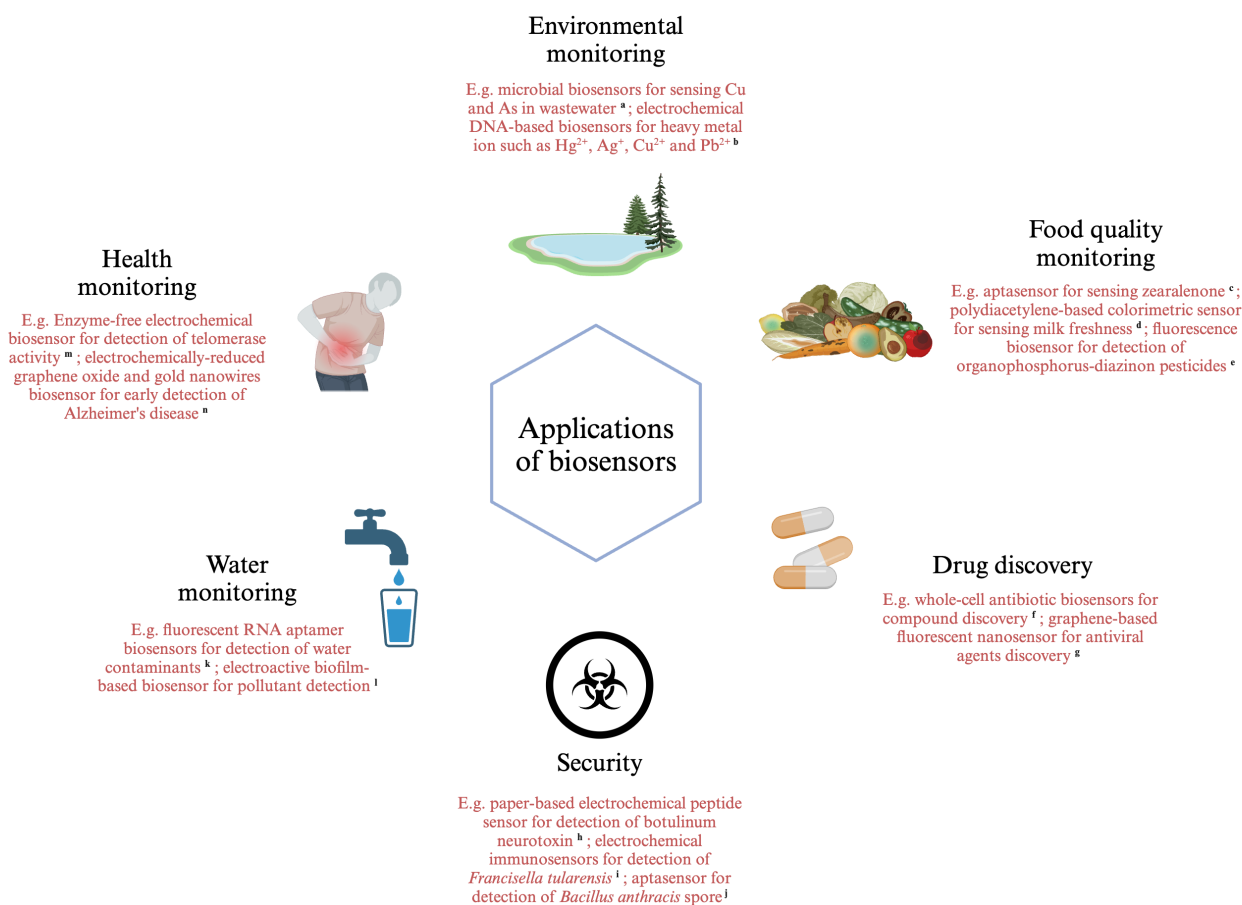


Figure 5. Examples of applications of biosensors. (references: a ⁹⁹, b ¹⁰⁰, c ¹⁰¹, d ¹⁰², e ¹⁰³, f ¹⁰⁴, g ¹⁰⁵, h ¹⁰⁶, i ¹⁰⁷, j ¹⁰⁸, k ¹⁰⁹, l ¹¹⁰, m ¹¹¹, n ¹¹²)

Generally, biosensors can either be cell-free or cellular systems. This thesis focuses on the use of cellular biosensors, so called whole-cell biosensors. They are based on genetically modified organisms where the biological sensing element is coupled to reporter genes functioning as transducers, which can be interrogated by mostly optical devices from populations or single cells. As self-replicating units such biosensors are easy to maintain and replicate providing a cost-effective platform for screening and compound characterization purposes.

1.3 Bacterial biosensors as tools in biodiscovery

Biosensors are particularly suited for discovery of novel compounds with potential application in treatment of bacterial infectious diseases. Especially bacterial whole-cell biosensors (BWCB) can be easily integrated into established workflows based on MIC assays as they are based on conventional bacterial cells. Instead of merely monitoring bacterial growth the bacterial cell provides the chassis for expression and coupling of the sensory element and the transducer, thus the BWCB is functioning as a

miniature genetic machine. Construction of BWCBs is assisted by the bacteria carrying out their biological functions, which include sensing a wide range of environmental stimuli like presence of nutrients, environmental stressors, and autoinducers, thus already efficiently processing information and producing a range of chemical and physical responses, which can be interrogated through reporter genes as genetic transducer modules. BWCBs are already widely used for detection of for example heavy metals in environmental monitoring ^{109–113}, and monitoring several diseases in clinical applications ^{114,115}. The advancements of synthetic biology has accelerated the development of a variety of BWCBs in recent years. BWCBs benefit from inherent robustness, as the bacterial chassis must function reliably in harsh real-world environments; they are highly sensitive and specific as they are based on sensory proteins, which evolved to distinguish analytes from a large number of molecules in their environment, and they are by nature continuously active throughout the lifetime of the BWCB cell or population. BWCBs can be used in two different settings: real-time sensing or endpoint measurements. In the latter case the measurement is stopped in order to acquire, which is often the case when using β -galactosidase as the reporter ^{116,117}. Real-time sensing on the other hand allows for continuous tracking of changes.

Designing and engineering BWCBs relies heavily on genetic engineering and molecular biology. In this context reporter genes represent invaluable tools, enabling the quantification and visualization of gene expression and thereby also regulatory processes. They are typically placed under the control of a promoter which responds to the conditions of interest by inducing their expression. These genes are usually heterologous and fused with the respective promoter elements by genetic engineering. The encoded reporter proteins can be detected, measured, and/or localized within the cell or the organism to track the activity of specific promoters, monitor gene expression levels, or visualize cellular processes. The aim of reporter genes is to translate promoter activity into easily detectable signals and providing a measurable or visible output from the organism. They have been used for different applications like the gene expression analysis ^{118–120}, promoter characterization ^{121–123}, high-throughput screening ^{124–126}, and for cellular imaging and localization ^{127–129}. Some of the most common reporter genes are listed in the table 1 below, indicating their distinct output, advantages and disadvantages in term of detection methods, time, sensitivity and efficiency.

Table 1. Common reporter genes.

Reporter gene	Origin	Description	Advantages	Disadvantages
Green Fluorescent Protein (<i>gfp</i>) ¹³⁰	Victoria jellyfish	Fluorescent protein that emits green light upon excitation	Stable, online and in-situ monitoring, no need of exogenous substances and ATP	Delayed expression, low sensitivity, need of O ₂ , background fluorescence

Flavin-binding fluorescent protein (<i>fbfp</i>) ¹³¹	<i>Pseudomonas putida</i>	Flavin-binding fluorescent protein	O ₂ -independent fluorescence, rapid maturation, broad operational pH range	Metabolic burden if overexpressed, weak fluorescence emission
Red Fluorescent Protein (<i>dsred</i>) ¹³²	Coral <i>Discosoma</i>	Red fluorescent protein	No substrate, high stability, low background fluorescence, wide selection of mutants such as mCherry	Slow maturation, moderate sensitivity
Luciferases		Enzymes that catalyze oxidation of luciferin, or fatty aldehyde, resulting in emission of luminescence		
<i>luxAB</i> ¹³³	<i>Vibrio fischeri</i>		Easy detection, quick response, high signal to noise ratio	Need FMNH ₂ and O ₂ , thermal instability
<i>luxABCDE</i> ¹³⁴	<i>Vibrio harveyi</i>		High sensitivity, quick response	Need exogenous substrate and O ₂
<i>Luc</i> ¹³⁵	Firefly		Can have different colors	
<i>LucGR</i> ¹³³	Click beetle <i>Pyrophorus plagiophthalmus</i>			
β-Galactosidase (<i>lacZ</i>) ¹¹⁶	<i>Escherichia coli</i>	Enzyme that cleaves artificial substrates, turning them blue or yellow. Colorimetric detection	Observation with naked eye, high stability, applicable in anaerobic environment	Requires prolonged incubation times, may have endogenous activity in mammalian cells
β-lactamase (<i>bla</i>) ¹³⁶	<i>Escherichia coli</i>	Colorimetric detection	Easy to detect	Need of substrate
Chloramphenicol Acetyltransferase (<i>cat</i>) ¹³⁷		Enzyme that inactivates chloramphenicol. Resistance detection.	No endogenous activity	Need of substrate and co-factor, narrow linear range
β-Glucuronidase (<i>uidA</i>) ¹³⁸	<i>Escherichia coli</i>	Enzyme that hydrolyzes glucuronides, generating blue precipitate.	Very straightforward, quantification by fluorometric and spectrophotometric analysis	Expensive chemicals

Bioluminescence is widely used as the output of reporter constructs. The eukaryotic luciferase *luc* has been expressed in *E. coli* as reporter gene for the first time in 1985 by De Wet *et al.*¹³⁹ while the bacterial luciferase *lux* in 1982 by Belas *et al.*¹⁴⁰. The reporter proteins responsible for bioluminescence are called luciferases and their light emission relies on an enzymatic reaction, which requires a substrate as well as energy from the cells metabolism. The chemical energy is used to excite the substrate, which subsequently gets oxidized with the concomitant emission of a photon in the visible light spectrum¹⁴¹. The substrates and donors of chemical energy needed for catalyzing the reaction vary between luciferases of bacterial and eukaryotic origin. Bacterial luciferases are typically encoded in the *luxCDABE* operon and require long chain fatty aldehydes as substrate, while they rely on FMNH₂ as electron donors. In addition to the luciferase subunits (*luxAB*) the *lux* operon also encodes an ATP and NADPH dependent multi-enzyme fatty acid reductase (*luxCDE*), which recycles the oxidation product of the luciferase reaction, thus making the reaction independent of external substrate addition but highly responsive to changes in the metabolic state of the cell¹⁴². Eukaryotic luciferases, for example the firefly luciferase, require the exogenous addition of their substrate D-luciferin for the light reaction to occur and ATP for the adenylation of its carboxylate group¹⁴³. It is important to note that also the eukaryotic luciferases require energy in form of ATP from the cell metabolism, thus the current metabolic state of the cells will always affect real-time bioluminescence measurements. This is an important detail to consider for the choice of the reporter gene, as the eukaryotic luciferases, apart from being expressed, will only exert additional metabolic stress on the bacterial chassis when D-luciferin is available for the luciferase and thus when light is emitted. In contrast, the bacterial *lux* operon will exhibit constant metabolic stress on the bacterial chassis as light is produced continuously once the operon is expressed and long chain fatty acids are recycled. Finally, eukaryotic and bacterial luciferases are both dependent on oxygen for light production and signal intensity is usually too low to measure from single cells, until the enhanced *ilux* operon which permits the single-cell imaging¹⁴⁴. The major advantages of luciferases as reporter genes is the lack of background luminescence and the relatively fast response times compared to fluorescent proteins.

Fluorescent proteins (FPs) are also very efficient reporter proteins. They are intrinsically fluorescent once produced and correctly folded, which means that unlike bioluminescence from luciferases, they are not burdening cell metabolism and can therefore fluoresce also in nonviable cells. They are highly stable and do not depend on any substrate to emit light. However, they are not suitable for rapid detection of compounds due to delayed expression and slow maturation. The first fluorescent protein that was discovered and purified is avGFP from the hydrozoan jellyfish species *Aequorea victoria* in 1962 by Simomura *et al.*^{130,145}. This protein emits a green light with a peak at 510 nm when excited with blue light. Since then, several mutations have been introduced to improve fluorescence like for the enhanced green FP (eGFP)¹⁴⁶, alter the fluorescence emission spectra to ass fluorescent proteins with new colors like blue (BFP)^{147,148}, cyan (CFP)^{149,150}, or yellow (YFP)^{151,152}, but also to improve protein folding at

37 °C like the superfolder avGFP. The result of these efforts is a large panel of tools for imaging or reporter fusions. Another family of FPs are the red fluorescent proteins. The first to be purified from the coral *Discosoma* is called DsRed¹³². The original DsRed exhibits a particularly long maturation time and requires days at room temperature in order to reach its maximum red fluorescence¹³² while GFP fluorescence peaks after several hours. Unfortunately, the GFP signal overlaps with cellular autofluorescence which usually results in noisy background fluorescence, that can affect the results. In the red spectrum of DsRed based FPs on the other hand, bacterial autofluorescence background is minimal. Both groups of reporter require oxygen for maturation and are therefore limited to use in aerobic conditions.

More recently, the bili-FPs, another family of FPs, was discovered and received interest because of its characteristics. The chromophore, a linear tetrapyrrole molecule, originates in vertebrates from the degradation of heme: bilirubin (BR), from its metabolic precursor, biliverdin (BV). This emerging class of fluorophores dependent FPs contains bilin-FPs like Sandercyanin¹⁵³, miRFPs¹⁵⁴, smURFP¹⁵⁵ and UnaG¹⁵⁶. Their potential for high brightness, photoswitching and the far-red emission, allowing for a high signal-to-noise ratio are making them very good candidates as reporter proteins. UnaG is a oxygen-independent green FP belonging to the fatty-acid-binding protein (FABP) family, extracted from the Japanese eel *Anguilla japonica*¹⁵⁶. Its ability of becoming fluorescent via noncovalent, high-affinity, high-specificity binding to unconjugated BR, and the fact that UnaG is not limited to aerobic conditions make it a very good reporter gene in conditions where GFP is not maturing. Moreover, it has been shown that UnaG emits brighter green fluorescence than eGFP^{156,157}. Sandercyanin is a small size blue colored protein-ligand complex isolated from the skin mucus of walleye *Sander vitreus*. It has a non covalent ligand-inducible far-red fluorescence in presence of BV with a large spectral shift¹⁵³. In the category of near-infrared (NIR) FPs, miRFPs are monomeric and 2-5-fold brighter in mammalian cells than other monomeric NIR FPs. They emit red-shifted fluorescence when binding to BV and are very photostable¹⁵⁴. Finally, the small ultra-red FP (smURFP) is the brightest far-red (FR) and NIR FPs created, with a better photostability than eGFP but comparable in terms of brightness, with BV as its ligand.

Aptamers, also known as chemical antibodies, are single-stranded oligonucleotides that can bind specific ligands or target molecules with a good selectivity, high specificity and sensitivity¹⁵⁸. They can be used in biosensors and thus are called aptasensors. When the aptasensors are binding with the target or ligand, the conformation changes and they emit a detectable signal, which can be for example electrochemical¹⁵⁹ or fluorescence¹⁶⁰⁻¹⁶³. Fluorescent aptamers are called light-up aptamers. They are RNA sequences that can bind their cognate non-fluorescent fluorogens and strongly activate their fluorescence at different wavelengths. Several light-up aptamers, like malachite green which was one of the first probes developed, followed by Spinach¹⁶⁴, Spinach2¹⁶⁵, Baby Spinach¹⁶⁶, Mango¹⁶⁷, Broccoli¹⁶⁸, Corn¹⁶⁹, Pepper and others, are now widely used in bioimaging^{163,170-173} and biosensing

¹⁷⁴⁻¹⁷⁸ for *in vitro* sensing ^{179,180}, turn-on sensors, or ratiometric sensors ¹⁸¹. For example, Pepper is a short 46-nt sequence RNA light-up aptamer reported by Chen *et al.* in 2019 ¹⁸². It emits fluorescence through its high affinity toward to the fluorogen (4-((2-hydroxyethyl)(methyl)amino)-benzyl-idene)-cyanophenylacetonitrile (HBC) with excitation and emission wavelengths of 485 nm and 530 nm, respectively. The color of its fluorescence can also be modulated through different HBC derivatives with emission spectra covering visible light between cyan (485 nm) and red (620 nm). The use of light-up aptamers in live bacteria seems to be limited to expression by strong phage polymerases.

The science of engineering biology is called synthetic biology. This is a new discipline, which emerged quite recently and is interdisciplinary ¹⁸³ with a combination of biology, engineering and computational sciences to design and build novel biological systems or redesign existing organisms for specific purposes ¹⁸⁴. It offers exceptional potential to revolutionize industries and address pressing societal challenges. Synthetic biology involves the application of standardized and modular genetic components, such as genes, pathways, and regulatory elements, to engineer biological entities with enhanced functionalities or entirely new traits. To build organisms that can perform useful activities in response to specified conditions, molecular biology techniques to manipulate genetic material including DNA synthesis, editing and assembly, are central.

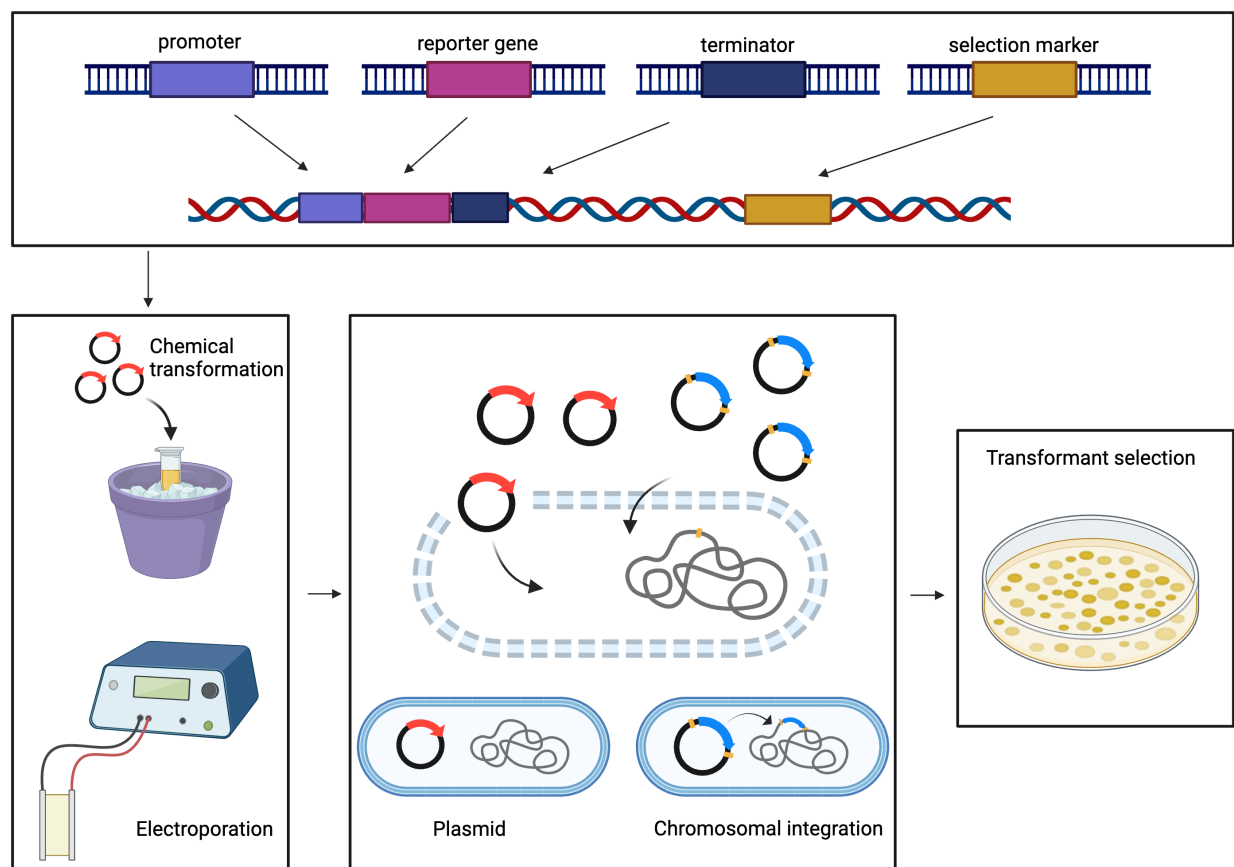


Figure 6. Basics of genetic engineering to construct a bacterial biosensor.

To construct bacterial biosensors with reporter genes as represented in the figure 7, genetic engineering relies on a wide range of techniques and methodologies to modify the genetic material of the organisms. This manipulation primarily involves the alteration, addition, or deletion of specific genes or parts of genes in the genome of an organism. The essentials of genetic engineering (figure 6) of new organisms requires developing of several basic tools such as functional promoters, terminators, other genetic elements like reporter genes, and selection markers. Once the set of DNA elements has been established, they can be combined into an expression vector through a cloning system. The traditional way of cloning by restriction digests and ligation for assembly of DNA has been largely replaced by techniques with standard systems for cloning allowing for simultaneous and seamless assembly of multiple gene parts, for example Gibson assembly¹⁸⁵ or Golden Gate cloning^{186,187}. When the plasmid is assembled, it can be transferred into the bacterial cell through different methods like chemical transformation, electrotransformation, biolistic transformation, or sonic transformation¹⁸⁸. The construct can be then plasmid-based or being integrated in the chromosome in specific recombination sites. The bacterial biosensors containing the constructs will then be selected for by conditions alleviated by the selection marker used in the construct.

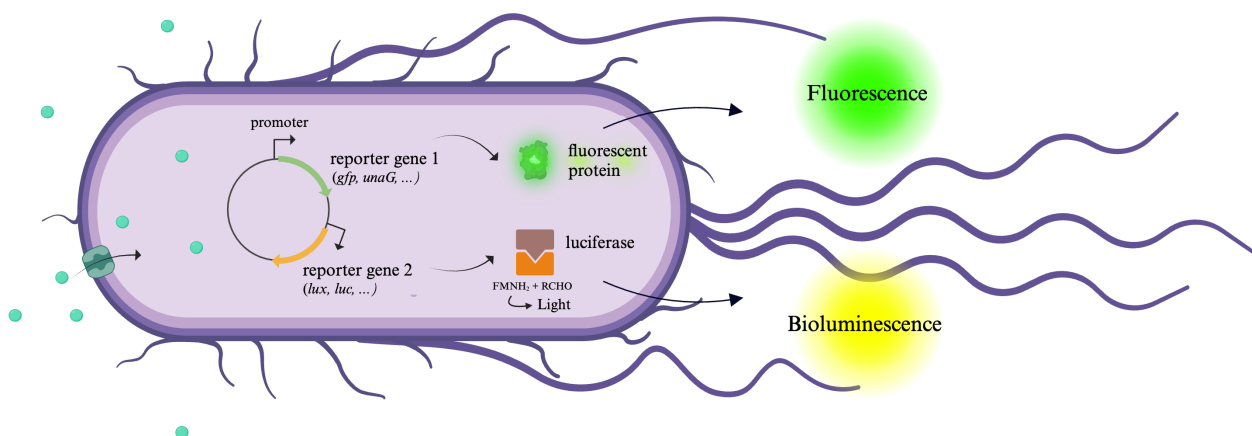


Figure 7. Example of bacterial biosensors with combined fluorescent and bioluminescent reporter genes.

Synthetic biology has the potential to transform how we interact with our environment and how we approach human health. The programmability of DNA sequences through replicating digital decision in living organisms aims to develop genetic circuits, cellular networks, and organisms with application spanning various domains from healthcare and pharmaceuticals to environmental sustainability and sensing, and industrial processes. The process of engineering biological systems typically involves repetitive cycles of design, modeling, construction, and testing. Computer-aided design tools assist in the predictive modeling of genetic circuits and metabolic pathways, aiding in creating functional biological constructs before their physical implementation. Through these methods, synthetic biologists seek to address societal challenges by designing organisms capable of producing pharmaceuticals,

biofuels, bioremediation agents, and other valuable products in a sustainable and efficient manner. The two main purposes of synthetic biology are to develop novel tools and the pursuit of new discoveries through these tools. This will be the present and the future of engineering toolbox of biosensors with all different genetics elements ready to be assemble for the NPs discovery.

2 Research Aim

The research group of marine bioprospecting conducts research to better understand marine molecules, particularly the bioactive secondary metabolites. The work focuses on the areas of isolation and characterization of antimicrobial compounds from marine animals, plants, microorganisms, and algae. Thus, another important point of this research group is the study of mechanisms of action for these antimicrobial compounds.

In this project, the main aim was to construct and establish novel biosensors as tools to characterize the modes of action of novel antimicrobial peptides (AMPs), with the introduction of new reporter genes.

The first part of the project was to improve existing luciferase based bacterial biosensors by transferring plasmid-based reporter constructs to the chromosomes of sensor strains in order to have stable and more reproducible assays, reducing the need of antibiotics for selection.

The second part of the project was to construct the new biosensors with new reporter genes, UnaG and the light-up aptamer pepper.

Light-up aptamer-based biosensors should allow for differentiating translation from transcription inhibition in simple whole cell bacterial assays.

The UnaG based biosensor should allow to identify the effect of AMPs on the membrane integrity by dissociating the action on the outer membrane (OM) of the Gram-negative bacteria only.

The last goal was to combine at least two reporter constructs in one bacterial strain in order to sense more than one mode of action in a single assay.

Finally, the functionality of the novel biosensors for the study of novel modes of action of marine AMPs should be shown.

3 Summary of papers

Paper I. Antimicrobial Activity of Securamines from the Bryozoan *Securiflustra securifrons*

Kine Ø. Hansen, Ida K. Ø. Hansen, Céline S. M. Richard, Marte Jenssen, Jeanette H. Andersen, and Espen H. Hansen

Natural Product Communication (2021). doi: 10.1177/1934578X21996180

In this study,

- Securamine H was extracted from the Bryozoan *Securiflustra securifrons*.
- bacterial biosensors based on *Escherichia coli* and *Bacillus subtilis* carrying the reporter gene *lucGR* were used to assess the membrane integrity after exposure to Securamine H. No effect on *E. coli* and a slight effect *B. subtilis* plasma membrane integrity, which is more bacteriostatic than bactericidal, was observed.
- *E. coli* and *B. subtilis* biosensors carrying the reporter operon *luxABCDE* were used to assess the effect of Securamine H on viability. The compound was found to reduce viability of Gram-positive bacteria and reduce metabolic activity of *Bacillus subtilis*.
- no evidence was found that interference with DNA replication, transcription, translation, fatty acid, cell wall or folic acid synthesis was responsible for the bacteriostatic effect.

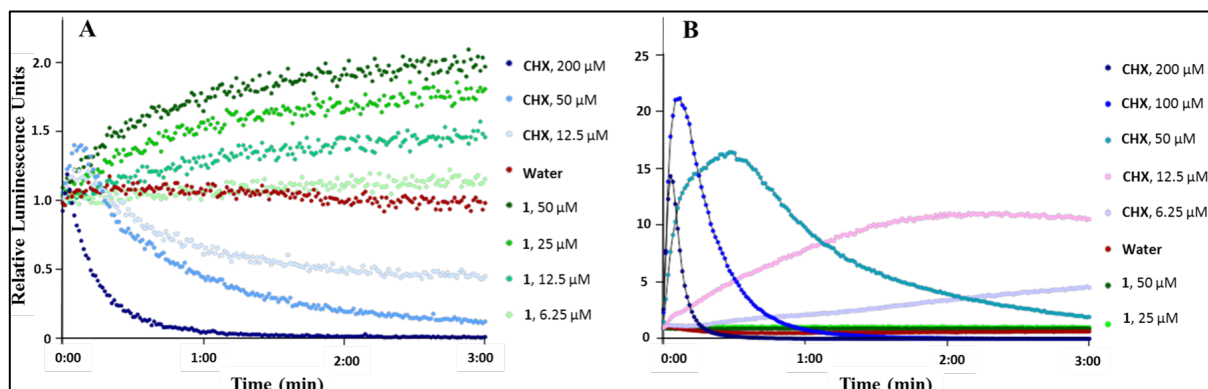


Figure 8. Kinetics of the relative luminescence emission by A) *B. subtilis* (pCSS962) and B) *E. coli* (pCSS962) treated with ranging concentrations of securamine H (1) or chlorhexidine (CHX). Each point is the mean of three independent measurements.

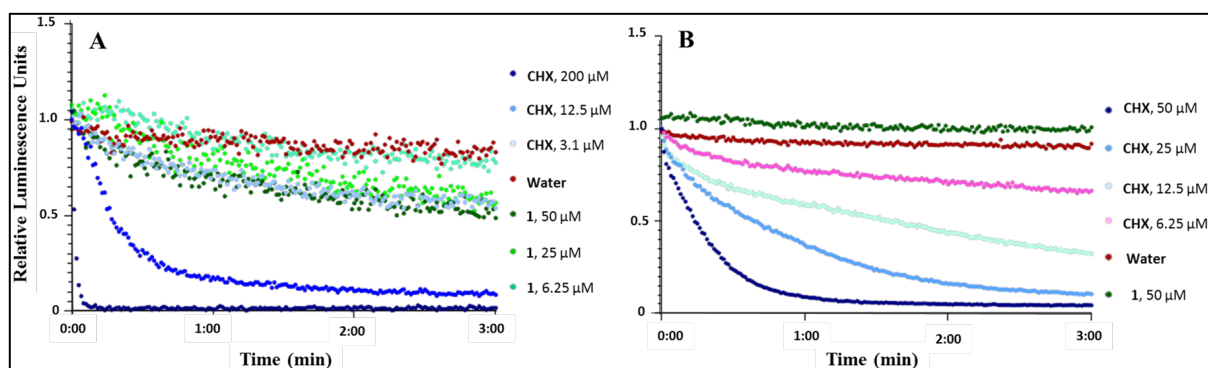


Figure 9. Kinetics of the relative luminescence emission by A) *B. subtilis* (pCGLS-11) and B) *E. coli* (pCGLS-11) treated with ranging concentrations of securamine H (1) or chlorhexidine (CHX). Each point is the mean of three independent measurements.

Paper II. Outer Membrane Integrity-Dependent Fluorescence of the Japanese Eel UnaG Protein in Live *Escherichia coli* Cells

Céline S. M. Richard, Hymonti Dey, Frode Øyen, Munazza Maqsood and Hans-Matti Blencke

Biosensors (2023). doi: 10.3390/bios13020232

In this study,

- a new *E. coli* bacterial biosensor was engineered to detect of outer membrane (OM) integrity compromising compounds.
- UnaG, a fatty-acid-binding protein (FABP) and relatively young reporter gene originating from the Japanese eel *Anguilla japonica*, which emits green fluorescence when bound to its ligand bilirubin (BR) was used.
- we showed that at low BR concentrations (5 $\mu\text{g}/\text{mL}$), diffusion and subsequent fluorescence is dependent on OM disruption.
- we confirmed that BR does not affect plasma membrane (PM) integrity or the survival of *E. coli* cells negatively.

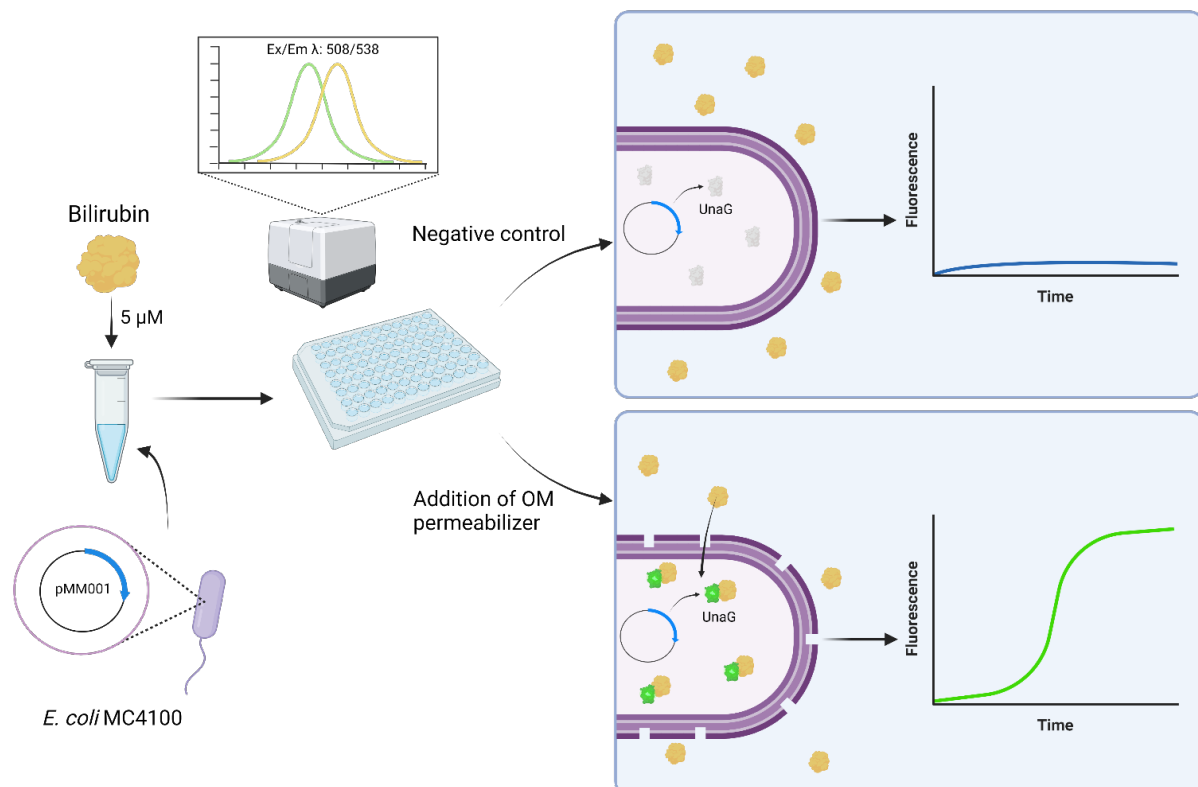


Figure 10. Schematic of the use of the reporter protein UnaG as an OM permeabilization whole-cell biosensor.

Paper III. Cloning of a dual biosensor relying on UnaG and luciferase LucGR for detection of outer and plasma membrane disruption and its application to characterizing the membranolytic effects of green sea urchin *Strongylocentrotus droebachiensis* Centrocin-1-based antimicrobial peptides

Céline S. M. Richard, Hymonti Dey, Emma Murvold, Frode Øyen, Chun Li, and Hans-Matti Blencke

In this study,

- a combination of two reporter genes, UnaG and luciferase LucGR in an *E. coli* dual sensor strain of OM and PM integrity.
- three antimicrobial peptides from marine invertebrates, originally isolated from the spider crab *Hyas aranaeus* (Arasin, Hyasin) and the green sea urchin *Strongylocentrotus* (Centrocin) were characterized by the dual biosensor *E. coli* carrying the plasmid pCSMR01 with *unaG* and *lucGR*.
- the original heavy chain (HC) Centrocin showed strong and fast PM activity.
- the fragment Centrocin HC (1-20) is mostly affects OM integrity.
- Centrocin HC caused PM damages on Gram-positive *B. subtilis* while Centrocin HC (1-20) did not, confirming the results on Gram-negative *E. coli*.
- neither Arasin or Hyasin seem to affect PM and OM integrity

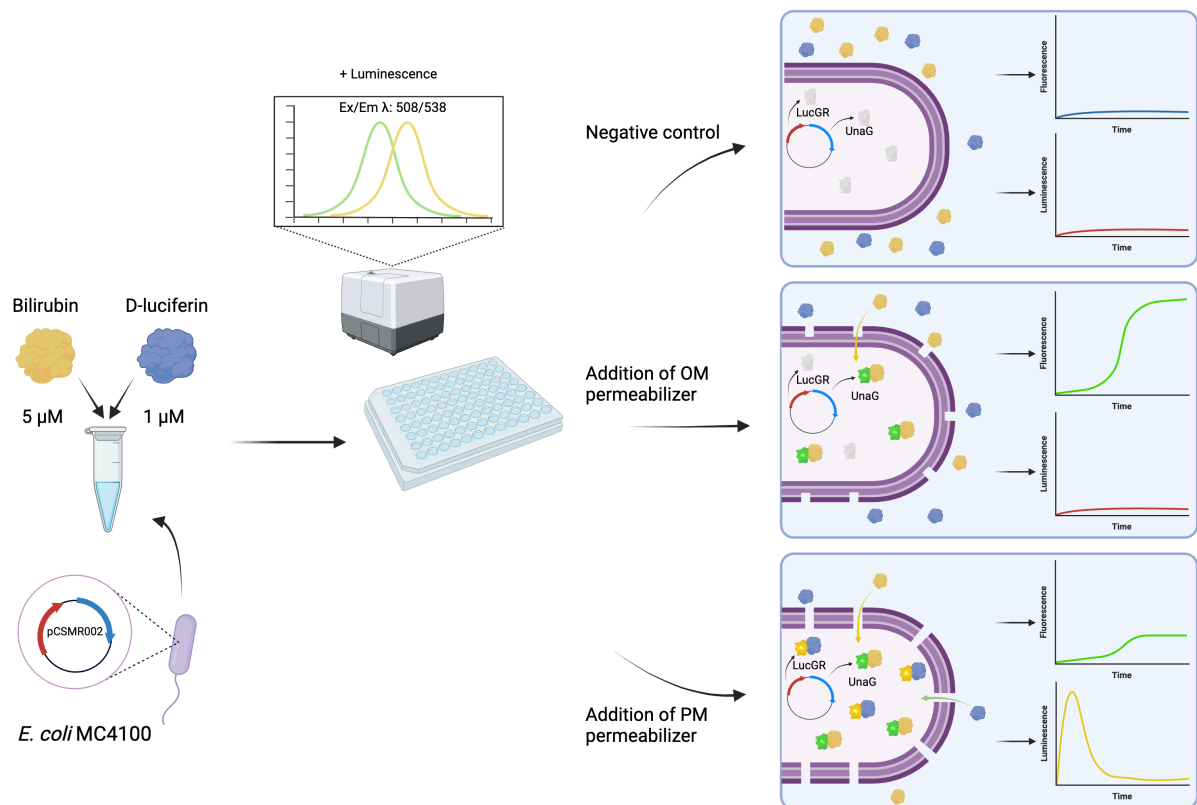


Figure 11. Schematic of the use of the dual biosensor for OM and PM permeabilization.

4 General discussion

The Marine Bioprospecting research group aims on finding new bioactive natural products (NPs) from the marine environment. In the pipeline of NPs discovery, it is important to detect bioactivity and identify the modes of action of newly discovered compounds as early as possible. The general aim of this thesis project was to expand the repertoire of reporter genes in bacterial whole cell biosensors (BWCB) available at the research group and to provide sensors to study the membrane-specific modes of action typical for AMPs, in particular. In the future BWCBs will likely replace MIC based screening in the natural products discovery pipeline of the bioprospecting group.

4.1 Luciferases as universal tools for assessment of bacterial viability and membrane integrity

Luciferases emit light in a strictly energy dependent manner and can exert a substantial metabolic strain on bacterial cells^{189,190}. In spite of this energy dependence, luciferases have been used in reporter constructs since the discovery of the respective genes in the beginning of the 1980s (*cf introduction*). For instance, the bacterial luciferase *luxAB* has been used in BWCB for the first time in 1990 for the detection of naphthalene¹⁹¹, and henceforth applied to different fields e.g. for the detection of blood in urine¹⁹², environmental monitoring^{193–196}, gene expression studies¹⁹⁷, autoinducers sensing¹⁹⁸, and compounds investigations like DNA damages¹⁹⁹. However, it is the energy dependence of luciferases, which allows for their use in assessing cell viability with light emission as a proxy for active metabolism and cell survival. Luciferases are therefore applied in both prokaryotic and eukaryotic whole cell biosensors to monitor cell survival^{200–202}. In addition, eukaryotic firefly and click beetle luciferases depend on the presence of the substrate D-luciferin, which must be externally added. Free diffusion of D-luciferin into the cell is prevented by an intact plasma membrane (PM). Hence eukaryotic luciferases have been exploited to assess PM integrity¹³³.

At the beginning of this project, the bioprospecting research group at the UiT - The Arctic University of Norway used biosensors based on luciferases to evaluate both bacterial viability and membrane integrity of different NPs. The use of luciferase-based biosensors is relatively inexpensive, fast and can easily be integrated into existing bioassay-guided discovery pipelines. For example, by using biosensors constitutively expressing the bacterial *lux*-operon the bactericidal concentrations of antimicrobial molecules can be elucidated in a matter of hours and a time resolution of minutes with the same effort as conventional MIC assays. This saves time and labor necessary for running MIC assays based on dilution plating and allows for a substantially higher throughput. Also, when comparing to other reporter proteins, for example GFP, the background noise is rather low. However, there are also drawbacks. First, each measurement done from wells in a plate reader merely represents the average output of a

given population at the measurement timepoint. A mean value can indicate that most cells in the population emit light around the mean, but also that two or more subpopulations in the well with substantially different emission profiles result in the measured mean luminescence intensity. This is also true for other reporter genes measured in similar setups, however fluorescent reporter genes can also be measured from single cells by for example flow cytometry. Current luminescent systems are not emitting sufficient light for single cell analysis in conventional flow cytometry although the efficiency of luciferases has been adjusted in recent years^{203,204}. In **paper I**, the membrane potential of cells treated with different antimicrobial substances was analyzed by flow cytometry after staining with the membrane potential reactive indicator dye DiOC₂(3). In presence of different concentrations of chlorhexidine (CHX) or Securamine H (compound 1), different subpopulations were discernible, indicating different levels of loss of membrane integrity. This difference in subpopulations was not evident from the bioluminescence signals of the BWCBs and the membrane integrity assay. Moreover, it has been shown to have also heterogeneities in bacterial responses to AMPs, with two distinct subpopulations in an isogenic bacterial culture; one group that retain the AMP after their growth is inhibited and a group of surviving cells²⁰⁵. Unfortunately, this kind of information is not possible with our BWCBs. However, the use of the biosensors allowed for a real-time approach, and thus understand the kinetics behind the loss of membrane integrity, which was not resolvable by the flow cytometry-based system.

The luciferases reporter constructs applied in **paper I** to assess bacterial membrane integrity and viability, like most other constructs described in this work, are plasmid-based. The membrane integrity assay in both *Bacillus subtilis* 168 and *Escherichia coli* K12 relies on the plasmid pCSS962¹³³ expressing the eukaryotic luciferase *lucGR* constitutively. Hence, these biosensors must be grown in presence of chloramphenicol to apply selection pressure for plasmid stability. In spite of the applied selection pressure, one problem with these plasmid-based assays is day to day variation in luminescence intensities, which can only be avoided by testing the overnight cultures in time consuming control experiments to confirm the cultures suitability for further experiments. We hypothesized that transferring the sensor elements from the plasmid to the chromosome might alleviate these variations as the chromosomal copy number remains stable and the loss of the sensor element in absence of selection pressure is less likely.

To investigate this hypothesis, the membrane integrity and cell viability reporter constructs were integrated into the chromosomes of sensor bacteria. Genetic engineering tools like the pBS1C vector from the Biobrick²⁰⁶ for the chromosomal integration in *B. subtilis* and pOSIP vector for the cloneteintegration²⁰⁷ in *E. coli* (**results not published**) were used for integrating the constructs into the genomes of a single sensor strain each. The chromosomal integration seems to indeed decrease the batch variation observed in the plasmid-based system. However, bioluminescence signals were reduced

substantially most likely because the reporter constructs were transferred from high copy plasmids into a single copy in the chromosome. Furthermore, chromosomal integration reduces the flexibility of the plasmid-based BWCBs as transferring chromosomal integration from one strain to another or even between different species is rather cumbersome, compared to the simple transformation of plasmids. In conclusion, chromosomal integration in *B. subtilis* is easy to achieve, but reduces signal intensities. It worked well for the viability strain and with further optimizations it might be a good alternative for stabilizing membrane integrity biosensors for stable screening environment. For example, we could try to optimize the luminescence production by integrating the reporter gene in other locations in the chromosome as there are different transcriptional levels and/or also by integrating several copies of the gene in different high transcriptional locations in the genome, as Yin *et al.* showed the importance of the gene location and the gene copy numbers in their study²⁰⁸. Moreover, a study²⁰⁹ comparing the production of melanin in *E. coli* through plasmid-based or chromosomal integration showed that overall the chromosomal integration was genetically more stable and resulted in higher growth capacity due to the reduced metabolic burden compared to the high copy plasmid number. Also, they showed that antibiotics selective pressure may not be sufficient to maintain homogeneous cell population over long time spans as 40% of the population lost their plasmid after 12h and in presence of the antibiotic the same loss occurred after 72h. Thus, for basic screening assays like the viability and the membrane integrity assays, it would be more efficient after some optimization to use the chromosomal integration-based bacterial strains. But in our hands, the flexibility of the plasmid-based approach outweighed the advantage of increased stability and absence of selective antibiotics for other assays. Therefore, we continued the use of plasmid-encoded sensing elements for the outer-membrane (OM) assay in **paper II**.

4.2 Adapting next generation reporter genes to natural product discovery

As we continue the race of antibiotic discovery to counteract resistance spread, we need more efficient tools to discover and characterize hit compounds. Reporter genes have been used in many research fields and are still the object of interest, even though discovery of novel reporter genes has become relatively rare.

One way to improve biosensors as tools for NPs discovery is to apply reporter genes in a novel context. One of the more recently discovered reporter genes is UnaG. It belongs to the fatty-acid-binding protein (FABP) family and has not been used in BWCB for natural product discovery yet. It was discovered by Kumagai *et al.* in 2013¹⁵⁶ from the Japanese eel *Anguilla japonica* and requires presence of Bilirubin (BR) as a fluorogen. It has been mostly used in bacteria for imaging in anaerobic environment²¹⁰, in rotavirus for imaging in infected cells²¹¹, mammalian cells imaging²¹², sensors in eukaryotic cell-based

assays¹⁵⁷, or engineering conditional protein stability system²¹³. In **paper II**, we describe a novel application of UnaG in a new *E. coli* BWCB carrying a plasmid coding for this new fluorescent protein. We observed very low fluorescence emission when expressing UnaG in *E. coli* in presence of BR. We therefore speculated that BR was excluded from entering bacterial cells by the cell wall of Gram-negative bacteria²¹⁰. We hypothesized that the UnaG-BR couple might be a good candidate for an outer-membrane (OM) integrity BWCB. In order to confirm this hypothesis, two different *E. coli* strains were transformed with a plasmid designed for constitutive expression of UnaG, one wild-type (WT; *E. coli* MC4100) and its isogenic OM impaired mutant (*E. coli* NR698). At low BR concentration, no UnaG specific fluorescence was observed for the MC4100 based construct, while the OM impaired NR698 mutant became strongly fluorescent. In addition also the OM specific Polymyxin B nonapeptide induced fluorescence in the WT strain when added in presence of BR. These results indicated that the OM indeed excludes BR from entering the cell.

This new WT biosensor might be a good candidate for screening natural product libraries for OM specific disruption. Fluorescence levels are dependent on cell survival and therefore only pick-up OM disruption from populations with intact plasma-membranes (PM). Its plasmid-based design proved fairly stable with little batch variation and still is flexible with regards to screening strains. This also turned-out as an advantage in the current work where different genetic backgrounds were needed to prove the constructs OM specificity.

Novel compounds that specifically impair OM integrity would permit to use antibiotics, which are excluded from entering Gram-negative bacteria by the OM barrier. Antibiotics with relatively high molecular weights currently only used for treatment of infections caused by Gram-positive bacteria, could be expanded for the use against diseases caused by Gram-negative bacteria. In **paper III** we showed synergistic activity of OM active antimicrobial peptides (AMPs) with Erythromycin and Vancomycin, which are Gram-positive specific antibiotics. Using an UnaG-based sensors would allow for specific discovery of such compounds, which are likely not detected in a conventional MIC assay, as OM impairment is not picked-up by growth dependent assays. One of the drawbacks of this approach would be that compounds that impact the OM, but also affect translation, as might be the case for intracellularly active AMPs, might not be picked-up in this assay as it is strongly dependent on active translation of UnaG. However, these compounds would be picked-up by the general growth arrest of the cell.

Technically, the UnaG-based OM assay resembles the LucGR based PM integrity assay mentioned earlier as both are based on exclusion of a ligand/substrate. Interestingly, the response of the OM sensor is substantially slower than in the LucGR system where light emission is instant. It is not likely to be related to the binding kinetics of the protein and its ligand as purified recombinant UnaG fluorescence is instantaneous when combined with BR *in vitro*¹⁵⁶. By timed induction studies in **paper III**, we

showed that BR only induces fluorescence in freshly translated UnaG, indicating the active degradation of apoUnaG as likely reason. This is in agreement with the observations published on a mouse fibroblast cell line where WT UnaG expressed in the absence of BR was shown to render fusion protein constructs with mCherry less fluorescent and less stable than BR treated controls, indicating active degradation of the apoUnaG²¹³. Moreover, another study with another FABP, SmFABP, showed similar results with the apoprotein, which was significantly degraded at 1h and almost completely degraded at 18h, while the holoprotein with palmitic acid was stable over time²¹⁴. A last example found in the study of Sripa *et al*²¹⁵, where the apo-forms of the FABP, *Ov*-FABP were also readily degraded while the holo-forms with oleic acid, palmitic acid and linoleic acid were stable. This feature of rapid degradation of apo-forms of proteins, which preserve from misfolding, aggregation and regulate the cellular processes and homeostasis would be an advantage in the BWCBs to avoid aggregation and metabolic burden in the bacterial cells, and would show a real state of translation activity as only freshly translated proteins would be detected. It would be then interesting to use the UnaG mutant from the study of Navarro *et al.*²¹³ with an increased sensitivity in *E. coli* in further work. The rather sensitive and quick response of UnaG fluorescence to translation inhibitors in the OM impaired background of the NR698 strain might be a valuable second line BWCBs for rapid confirmation of translation inhibition.

Another reporter gene we tried to integrate into our toolbox is the light-up aptamer pepper (**results not published**). Light-up aptamers, like UnaG, are relatively recent reporter genes. They are based on artificial RNA sequences that can bind to their cognate non-fluorescent fluorogens, which activate their fluorescence. One such aptamer is pepper, a short 46-nt sequence RNA light-up aptamer reported by Chen *et al.* in 2019¹⁸². It emits fluorescence in presence of its fluorogen (4-((2-hydroxyethyl)(methyl)amino)benzyl-idene)-cyanophenylacetonitrile (HBC). The interesting part of this fluorogen, the color of the fluorescence can be modulated from the cyan (485 nm) to red (620 nm) through different HBC derivatives allowing concomitant interrogation with other fluorescent reporter constructs. We wanted to couple pepper with GFP and therefore used HBC620 generating red fluorescence from pepper. We tried the original monomer and a tandem of 8 peppers described by Chen *et al*¹⁸² which was shown to emit stronger fluorescence. The aim was to construct a BWCB with the ability to discriminate between transcription inhibition and translation inhibition by expressing both reporter genes in an operon-like structure. One of the constructs is shown in figure 12. The final BWCB was supposed to be used as a confirmation assay for transcription/translation inhibition activities detected by promoter activity based *B. subtilis* BWCB also used in **paper I**. This part of the thesis did not progress past *E. coli* BWCB proof of concept studies as fluorescence expression of the construct with native polymerases in live *E. coli* cells is still elusive.

We engineered several constructs with different inducible promoters (Tac, pBAD) and switched positions of GFP and pepper. Each construct also carried an upstream T7 promoter for control expression in T7 polymerase inducible BL21 strains.

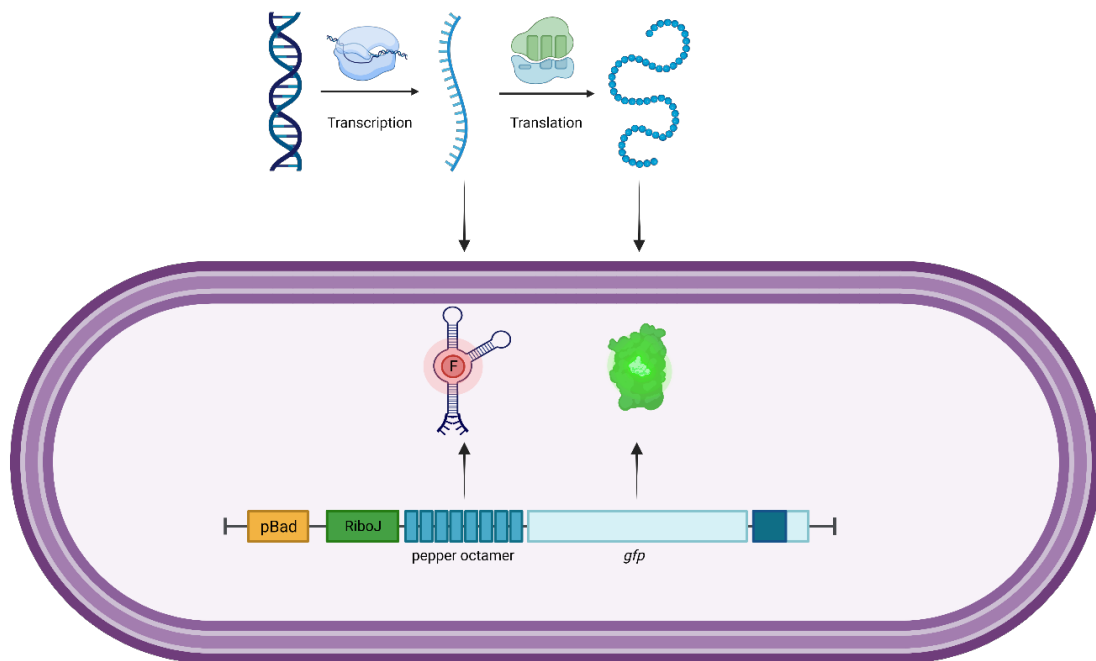


Figure 12. Representation of the 8pepper-GFP BWCB project.

Unfortunately, pepper fluorescence in live *E. coli* appears limited in terms of the conditions where it is transcribed by the powerful phage polymerases from the upstream T7 promoter while the coupled GFP protein could be expressed and was fluorescent also with the bacterial promoters. This indicates that the promoters are indeed active and that the upstream sequence of the pepper construct is also transcribed by bacterial promoters as downstream GFP is translated. We concluded that either transcription speed will affect the folding pattern of the fluorescent aptamer or the RNA turnover in *E. coli* is too high to accumulate sufficient concentrations for detectable fluorescence when transcribed from bacterial promoters. A recent study showed for the first time that other light-up aptamers are transcribed and emit fluorescence in *E. coli* with strong bacterial promoters when expressed from a high copy plasmid background. In this study, Climent-Catala *et al.* showed that light-up aptamers have shorter response times than fluorescent proteins²¹⁶. Their results indicate that it should indeed be possible to construct BWCBs which can discriminate between transcription and translation inhibitors in real-time. Most other studies performed in live bacteria with aptamers relied on T7 promoter^{182,217,218}.

4.3 Combining reporter elements for more efficient activity testing

The biggest advantage of using assays based on BWCB in screening for novel natural products is the relative simplicity and efficiency with respect to time and cost. However, each novel biosensors integrated into a screening platform requires biomass. Fraction biomass being a limited resource, running many different biosensors and/or MIC assays is usually not an option during screening. To still deeply screen the limited biomass for novel interesting activities, one option is to combine two or more BWCBs to screen for activities in a single well. This could be achieved by combining two or more BWCBs with compatible reporter genes, for example fluorescent proteins, which emit different colors, like the combination of GFP (green fluorescence) and mCherry (red fluorescence) in one assay. This should allow for distinguishable signals in response to different signals at the same time. Similar approaches have been applied to visualization and tracking of different bacterial strains in a biofilm ²¹⁹ and in co-culture ²²⁰, but also in biosensors like *E. coli*-based toxicity and genotoxicity biosensor with the combination of eGFP and DsRed fluorescent proteins ²²¹ or for monitoring simultaneously mercury and cadmium with eGFP and mCherry ²²².

In **paper III**, we used this approach to prove the concept of combining PM and OM assays. We checked if the luminescence and fluorescence signals are detectable in the presence of luciferase substrate D-luciferin and the UnaG ligand BR at the same time and confirmed suitable assay conditions. However, combining two BWCBs for each assay complicates screening and most likely reduces reproducibility. Therefore we combined the OM reporter system based on UnaG-BR system with different luciferase-based reporter genes genetically by designing synthetic operons to be used as two-in-one step BWCBs. The first one, UnaG coupled with the eukaryotic luciferase lucGR permits to distinguish OM from OM- and plasma-membrane (PM) active compounds in real-time. The second one, UnaG coupled with the bacterial luciferase *lux* operon sensing OM disruption and cell viability measurements into one biosensor strain allowing for one step evaluation. These combinations of different reporter genes allow for either studying MoAs of natural products for two different MoAs in one assay, or measuring cell survival in combination with OM integrity, gaining time, effort and fraction biomass. This permits us to confirm if a compound is only OM active or if it also impacts the PM of the sensor bacteria, which seems to be often only a concentration based difference. However, the signal strength in these double sensors was reduced, possibly because of the metabolic load of *lux* operon/*lucGR* combined with UnaG. This phenomenon of biosensing signal attenuation due to multiple-signal output often occurs as a result of an increased metabolic burden and excessive energy consumption in a single cell. Similar effects were observed by Hui *et al.* ²²² when combining two fluorescent proteins eGFP and mCherry for the simultaneous sensing of mercury and cadmium. They found that fluorescent signals significantly decreased in the double sensor when sensing mercury (green fluorescence). However, the intensity of red fluorescence while sensing cadmium was similar to the single sensor. In general, the signals are still

strong enough to detect the effects on the bacterial cells although there is room for optimization in future work. For example, by adjusting the respective Shine-Dalgarno sequences to fine tune the relative expression of each reporter gene in the operon. In addition, it would be interesting to test UnaG expression in *B. subtilis* to see if BR is freely passing to the cytoplasm of Gram-positives, confirming the relevance of OM dependent BR exclusion.

4.4 The outer-membrane as a potential target and an obstacle in natural product discovery

Several Gram-negative antibiotic resistant pathogens are strongly impacting the healthcare systems. Among them are pathogenic carbapenem-resistant *Enterobacteriaceae* (CRE) ²²³⁻²²⁵, extended-spectrum β -lactamase (ESBLs) ²²⁶⁻²²⁸ and more recently Colistin-resistant *E. coli* ²²⁹⁻²³¹. The OM as a distinctive feature of Gram-negative bacteria functions as an effective permeability barrier and thus, contributes to their resistance against a large number of antimicrobial compounds ^{232,233}. In addition, modification of the OM lipid and protein composition of drug-resistance bacterial species have been observed frequently ²³⁴. Consequently, the OM is an interesting target for the new drug discovery ²³⁵⁻²³⁷. Discovery of NPs specifically targeting the OM might help against pathogenic Gram-negative bacteria. We engineered several BWCBs to study the effect of marine AMPs and other bioactive compounds on the PM (**paper I**), the OM of *E. coli* (**paper II**) and designed an assay to detect both activities at the same time (**paper III**).

Thus, the biosensor based on UnaG and BR from **paper II** could serve in primary screening for OM active compounds while the OM/PM double sensor described in **paper III** could be used to confirm the OM as the main target. The plasmid-based nature of these sensor strains allows for transformation of different AB resistant isolates with modified OM structures into biosensors to determine the activity spectrum of positive hits in the primary assays.

Other assays for assessing the OM integrity are routinely used like the fluorescence assay with the lipophilic dye N-phenyl-1-naphthylamine (NPN) for example. Already used in the 80's, this molecule will emit a weak fluorescence in aqueous environment while it will emit a high fluorescence in hydrophobic environment like in the lipidic membranes. This dye cannot pass through the bacterial membranes, but if AMPs are disturbing the OM, then it will have access to the lipid layers in the OM and/or in the cytoplasmic membrane, increasing greatly the fluorescence ²³⁸⁻²⁴¹. This assay has many advantages as it is sensitive, relatively quick and straightforward, which is a good point for high-throughput screening purposes. But compared to our BWCBs, this presents a lack of specificity as it is only sensitive to changes in membrane integrity, it is easier to get false-positive or false-negative results, the assay is limited to bacterial cells with intact membranes, and it is harder to standardize the assay. In

the **paper II**, we compared our single OM BWCB with NPN assay, and it seemed that NPN assay quantified the combined membrane damage of both OM and PM, making our assay more specific towards OM integrity only. To distinguish OM from OM and PM with the NPN assay, it would need to be combined with, for example, the fluorescent probe ethidium bromide (EtBr) assay, like used in the study of Zou *et al.* ²⁴², which is based on the same mechanism except that EtBr needs to permeate both PM and OM membrane to fluoresce. But then two different assays need to be done to assess compounds with OM specific activities, and EtBr is carcinogenic and so require careful handling thus, also is susceptible to get interference from extracellular DNA or RNA. Another method to study OM integrity would be through electron microscopy ^{243,244}. This method has several advantages as it provides direct visualization of OM structure and can be combined with immunogold labeling for specific protein localization. Unfortunately, the method is only suitable for detailed studies on compound interaction with the OM as the electron microscopy requires specialized equipment, is a time consuming and static, therefore is not suitable for real-time monitoring like our BWCBs.

On the other hand, the OM might prevent discovery of novel non-membrane active compounds by excluding NPs from their intracellular targets. In **paper III** we observed that the intracellularly active AMP PR-39 (1-26) induced a stress response in the *B. subtilis* based biosensor, which indicates inhibition of translational processes. The response was stronger than against Erythromycin, serving as the positive control antibiotic. As many intracellular active AMPs also show membrane activities at high concentrations as it is the case for Arasin 1 ^{245,246}, we tried to exclude that the translation inhibition indicated by the assay in *B. subtilis* interferes with the OM assay, which is based on the fresh expression of UnaG. However, when repeating the PM/OM double sensor assay in presence of different concentrations of PR39 (1-26) in the background of the OM impaired *E. coli* strain NR698, UnaG specific fluorescence was absent in the active concentrations of PR-39 (1-26) in spite of the fact that the bacterial cells were still alive as confirmed by light emission from the luciferase in the sensor strain. Thus, the bioactivity of peptides and other compounds above the porin determined exclusion size around 600 Da ²⁴⁷ might only be detected when screened in the genetic background of OM impaired strains. Other studies used OM deficient strain *E. coli* NR698 but mostly to confirm a MoA in *E. coli* for a compound not able to cross the OM like the study of Krüger *et al* ²⁴⁸ to confirm that chlorophyll is effective on Gram-positive bacteria and Gram-negative bacteria but is blocked by the OM in wild-type *E. coli*, or the one of Sherman *et al.* ²⁴⁹ where they used it to validate the inhibition of an ABC transporter could kill *E. coli* if this compound could penetrate the cell wall. Screening strategies with new biosensors for discovery of NPs inhibiting metabolic processes in the cytoplasm or periplasm of Gram-negative bacteria should assess the interest in compounds of higher molecular weight compounds before deciding on the genetic background of the screening assay.

Combining screening hits from OM integrity assays with hits from OM impaired mutants could be used to find NP combinations, which sensitize Gram-negative bacteria to the intracellularly active compounds by concomitant treatment with OM active products. As discovering new antibiotics is difficult, combinations for a synergistic effect is a good alternative in order to use for example Gram-positive antibiotics on Gram-negative bacteria. For example, the AMPs β -naphthylalanine end-tagged S1-Nal and S-Nal-Nal, were found to be used in synergy with vancomycin to fight against Gram-negative bacterial infection²⁵⁰. In our **paper III**, we also found this synergetic effect by combining an OM active AMP, Centrocin (1-20) with Erythromycin and Vancomycin on *E. coli*. However, not only non-natural combinations are interesting. Natural synergism between several AMPs is typical for the innate immunity, as eukaryotes need an effective killing of microorganisms through simultaneous targeting of multiple critical cellular functions of bacteria. This synergism elicits a much higher antimicrobial effect than each AMP alone, and it can be beneficial for reducing the risk of resistance evolution. The effects between AMPs can also be potentiated, so one AMP can enable or enhance the activity of others. The most common would be to have some AMPs that are permeabilizing the membrane of the bacterial cell to enable the entry of other AMPs with intracellular targets. For example, a first study showed the AMP abaecin from bumblebees was active against *E. coli* D22, which has a deficient cell envelope²⁵¹. So in another study, they found that this AMP abaecin had no effect on a wild-type *E. coli*, as well as the AMP hymenoptaecin from the same bumblebee²⁵². However, when *E. coli* is in presence of both AMPs, its growth is completely suppressed through the synergism of hymenoptaecin, which opens the pores of the OM to allow abaecin to enter and bind to DnaK, abolishing the bacterial chaperone network and thus, protein folding and ribosomal biogenesis. Another example would be the perforins from vertebrates, which open pores and allow lethal cationic cargo to reach the cytoplasm of bacterial cells²⁵³. These synergetic effects of AMPs could be assessed with our BWCBs, as we could screen for OM active compounds with the OM integrity assay, for intracellular target with the deficient OM strain, and confirm both with the double sensor OM integrity assay combined with cell viability for example, in future work.

5 Conclusion

The marine environment is an interesting of novel antimicrobial compounds and might therefore be part of the solution to resolve the resistance crisis currently shadowing healthcare systems. However, efficient bioprospecting efforts will require approaches beyond simple MIC assays. Bacterial whole cell biosensors allow for mode of action specific search for compounds potentially valuable as leads for future development of antimicrobial drugs. Integrating novel biosensors into existing platforms for bioassay-guided purification of antimicrobial compounds might therefore substantially improve the output of marine bioprospecting efforts.

The first part of this thesis was dedicated to gain knowledge about the first generation of biosensors in use at the research group. Biosensor based assays were used to try to characterize the mode of action of Securamine H from an arctic Bryozoan species. The results were not conclusive and require further investigation to identify the mode of action as described in **paper I**.

Subsequently the plasmid-based sensor-elements were transferred to the chromosomes of the *E. coli* and *B. subtilis*, which increased assay reproducibility but reduced assay sensitivity. The results from chromosomal integration are not published yet.

In the second part the use of UnaG as a reporter gene in bacterial biosensors was analyzed. It was confirmed that Bilirubin is efficiently excluded from the cytoplasm in cells with intact OMs. Compromised OMs allowed for uptake of Bilirubin and activation of UnaG based fluorescence in a manner that requires survival of the cell. The system was suggested to be used as an assay for OM integrity as described in **paper II**.

Also, novel reporter genes called light-up aptamers like pepper were tested for inducible fluorescence in live *E. coli* cells with limited success. Only the very strong viral T7-promoter-polmerase combination resulted in red fluorescence. While the inducible reporter systems for identification of transcription inhibition, did not result in detectable fluorescence levels. This work is still ongoing and not part of a manuscript in this thesis.

Finally, the first-generation luciferase-based sensor systems for PM damage and viability were combined with the novel OM sensor that allows for concomitant testing for both OM and PM integrity (**Paper III**) In addition, using the dual biosensors in the OM deficient background to run timed translation arrest and Bilirubin addition showed that UnaG stability depends on the presence of Bilirubin. Furthermore, sensor activity for population-based measurements is not improved by UnaG export to the periplasm.

6 Future perspectives

To improve OM damage responsive feedback from UnaG in the double sensor background, expression of the reporter genes should be optimized with respect to expression of the luciferase genes possible by reducing translation efficiency of the luciferases by tuning the Shine-Dalgarno sequences.

Securamine H should be tested with the new double sensor to exclude potential effects on the OM of *E. coli*. Possible long term viability studies should be run to see how cell viability changes over time.

Recent publications have shown that light-up aptamers can be successfully expressed from strong bacterial promoters when located on high copy plasmids. This approach should be tested for the pepper construct used in this study.

A dual biosensor with UnaG and a light-up aptamer should be constructed for a rapid biosensor detecting and discriminating translation and transcription inhibition.

Attempts to stabilize apoUnaG in absence of BR by mutagenesis studies should be made in order to make the OM assay independent of the current translation rate.

Finally, the improved versions of the biosensors should be used to screen NP libraries to identify novel hit compounds for future drug leads

Works cited

- (1) Francesca Pennino; Maria Luisa Maccauro; Michele Sorrentino; Mariagiovanna Gioia; Simonetta Riello; Giuseppe Messineo; Carmela Di Rosa; Paolo Montuori; Maria Triassi; Antonio Nardone. Insights from a Cross-Sectional Study on Knowledge, Attitudes and Behaviors Concerning Antibiotic Use in a Large Metropolitan Area: Implications for Public Health and Policy Interventions. *Antibiotics* **2023**, *12* (10), 1476.
- (2) Timo J. Lajunen; Mark J. M. Sullman; Buket Baddal; Burcu Tekeş; Menelaos Apostolou. Antibiotics Knowledge, Attitudes and Behaviours among the Population Living in Greece and Turkey. *Antibiotics* **2023**, *12* (8), 1279. <https://doi.org/10.3390/antibiotics12081279>.
- (3) Atsadaporn Niyomyart; Susan Ka Yee Chow; Wunwisa Bualoy; Nipaporn Butsing; Xingjuan Tao; Xuejiao Zhu. Antibiotic Knowledge, Antibiotic Resistance Knowledge, and Antibiotic Use: A Cross-Sectional Study among Community Members of Bangkok in Thailand. *Antibiotics* **2023**, *12* (8), 1312. <https://doi.org/10.3390/antibiotics12081312>.
- (4) L. Bickel. Rise up to Life: A Biography of Howard Walter Florey Who Gave Penicillin to the World. *Angus and Robertson* **1972**, 60–61.
- (5) Milton Wainwright. Moulds in Folk Medicine. *Folklore* **1989**, *100* (2), 162–166.
- (6) Carl Ruttloff. Pyocyanase. *The Dental Register* **1910**, *64* (9), 455–459.
- (7) F. Bosch; L. Rosich. The Contributions of Paul Ehrlich to Pharmacology: A Tribute on the Occasion of the Centenary of His Nobel Prize. *Pharmacology* **2008**, *82*, 171–179.
- (8) Brad Spellberg; John G. Bartlett; David N. Gilbert. The Future of Antibiotics and Resistance. *The New England Journal of Medicine* **2013**, *368*, 299–302.
- (9) Dale W. Bratzler; E. Patchen Dellinger; Keith M. Olsen; Trish M. Perl; Paul G. Auwaerter; Maureen K. Bolon; Douglas N. Fish; Lena M. Napolitano; Robert G. Sawyer; Douglas Slain; James P. Steinberg; Robert A. Weinstein. Clinical Practice Guidelines for Antimicrobial Prophylaxis in Surgery. *American Journal of Health-System Pharmacy* **2013**, *70* (3), 195–283.
- (10) John M. Hardham; Everett L. Rosey. Antibiotic Selective Markers and Spirochete Genetics. *Journal of Molecular Microbiology and Biotechnology* **2000**, *2* (4), 425–432.
- (11) D. Perlman. Use of Antibiotics in Cell Culture Media. *Methods in Enzymology* **1979**, *58*, 110–116. [https://doi.org/10.1016/S0076-6879\(79\)58128-2](https://doi.org/10.1016/S0076-6879(79)58128-2).
- (12) Victor Lorian. *Antibiotics in Laboratory Medicine*; Lippincott Williams & Wilkins, 2005.
- (13) Michael A. Kohanski; Daniel J. Dwyer; James J. Collins. How Antibiotics Kill Bacteria: From Target to Networks. *Nature Reviews Microbiology* **2010**, *8*, 423–435.
- (14) Emad M. Abdallah; Bader Y. Alhatlani; Ralciane de Paula Menezes; Carlos Henrique Gomes Martins. Back to Nature: Medicinal Plants as Promising Sources for Antibacterial Drugs in the Post-Antibiotic Era. *Plants* **2023**, *12* (17), 3077. <https://doi.org/10.3390/plants12173077>.
- (15) Youshun Jin; Wei Li; Huaiyu Zhang; Xuli Ba; Zhaocai Li; Jizhang Zhou. The Post-Antibiotic Era: A New Dawn for Bacteriophages. *Biology* **2023**, *12* (5), 681. <https://doi.org/10.3390/biology12050681>.
- (16) Shawn R. Lockhart; Anuradha Chowdhary; Jeremy A. W. Gold. The Rapid Emergence of Antifungal-Resistant Human-Pathogenic Fungi. *Nature Reviews Microbiology* **2023**, *21*, 818–832.
- (17) Hafiz Muhammad Rizwan; Haider Abbas; Muhammad Sohail Sajid; Mahvish Maqbool; Malcolm K. Jones; Muhammad Irfan Ullah; Nabeel Ijaz. Drug Resistance in Protozoal Infections. In *Biochemistry of Drug Resistance*; Springer, 2021; pp 95–142.
- (18) World Health Organization. *Antimicrobial Resistance Surveillance in Europe - 2020 Data*; 2022.
- (19) Reza Ranjbar; Mostafa Alam. Antimicrobial Resistance Collaborators. Global Burden of Bacterial Antimicrobial Resistance in 2019: A Systematic Analysis. *Lancet* **2022**, *399*, 629–655.
- (20) Interagency Coordination Group on Antimicrobial Resistance. *No Time to Wait: Securing the Future from Drug-Resistant Infections. Report to the Secretary-General of the United Nations*; 2019.
- (21) Alison H Holmes; Luke S P Moore; Arnfinn Sundsfjord; Martin Steinbakk; Sadie Regmi; Abhilasha Karkey; Philippe J Guerin; Laura J V Piddock. Understanding the Mechanisms and Drivers of Antimicrobial Resistance. *The Lancet* **2016**, *387*, 176–187.
- (22) Hyejun Jo; Shahbaz Raza; Adeel Farooq; Jungman Kim; Tatsuya Unno. Fish Farm Effluents as a Source of Antibiotic Resistance Gene Dissemination on Jeju Island, South Korea. *Environmental Pollution* **2021**, 276.
- (23) Guibing Zhu; Xiaomin Wang; Ting Yang; Jianqiang Su; Yu Qin; Shanyun Wang; Michael Gillings; Cheng Wang; Feng Ju; Bangrui Lan; Chunlei Liu; Hu Li; Xi-En Long; Xuming Wang; Mike S. M. Jetten; Zifa Wang; Yong-Guan Zhu. Air Pollution Could Drive Global Dissemination of Antibiotic Resistance Genes. *The ISME Journal* **2021**, *15*, 270–281.
- (24) Ruilong Li; Longji Zhu; Kai Yang; Hongzhe Li; Yong-Guan Zhu; Li Cui. Impact of Urbanization on Antibiotic Resistome in Different Microplastics: Evidence from a Large-Scale Whole River Analysis. *Environmental Science & Technology* **2021**, *55*, 8760–8770.

- (25) Zhigang Yu; Yue Wang; Ji Lu; Philip L. Bond; Jianhua Guo. Nonnutritive Sweeteners Can Promote the Dissemination of Antibiotic Resistance through Conjugative Gene Transfer. *The ISME Journal* **2021**, *15*, 2117–2130.
- (26) World Health Organization. *Central Asian and European Surveillance of Antimicrobial Resistance - Annual Report 2020*; 2020.
- (27) Evelina Tacconelli; Elena Carrara; Alessia Savoldi; Stephan Harbarth; Marc Mendelson; Dominique L. Monnet; Céline Pulcini; Gunnar Kahlmeter; Jan Kluytmans; Yehuda Carmeli; Marc Ouellette; Kevin Outterson; Jean Patel; Marco Cavaleri; Edward M Cox; Chris R Houchens; M Lindsay Grayson; Paul Hansen; Nalini Singh; Ursula Theuretzbacher; Nicola Magrini; the WHO Pathogens Priority List Working Group. Discovery, Research, and Development of New Antibiotics: The WHO Priority List of Antibiotic-Resistant Bacteria and Tuberculosis. *The Lancet Infectious Diseases* **2018**, *18* (3), 318–327.
- (28) Thiruchelvi Pulingam; Thaigarajan Parumasivam; Amirah Mohd Gazzali; Azlinah Mohd Sulaiman; Jiun Yee Chee; Manoj Lakshmanan; Chai Fung Chin; Kumar Sudesh. Antimicrobial Resistance: Prevalence, Economic Burden, Mechanisms of Resistance and Strategies to Overcome. *European Journal of Pharmaceutical Sciences* **2022**, *170*, 106103. <https://doi.org/10.1016/j.ejps.2021.106103>.
- (29) A.-P. Magiorakos; A. Srinivasan; R. B. Carey; Y. Carmeli; M. E. Falagas; C. G. Giske; S. Harbarth; J. F. Hindler; G. Kahlmeter; B. Olsson-Liljequist; D. L. Paterson; L. B. Rice; J. Stelling; M. J. Struelens; A. Vatopoulos; J. T. Weber; D. L. Monnet. Multidrug-Resistant, Extensively Drug-Resistant and Pandrug-Resistant Bacteria: An International Expert Proposal for Interim Standard Definitions for Acquired Resistance. *Clinical Microbiology and Infection* **2012**, *18* (3), 268–281.
- (30) Silpi Basak; Priyanka Singh; Monali Rajurkar. Multidrug Resistant and Extensively Drug Resistant Bacteria: A Study. *Journal of Pathogens* **2016**.
- (31) 23rd WHO Expert Committee on Selection and Use of Essential Medicines, Classifying Antibiotics in the WHO Essential Medicines List for Optimal Use-Be AWaRe. *WHO Technical Report Series* **2021**, No. No. 1035.
- (32) Kevin Outterson; John H. Rex. Evaluating For-Profit Public Benefit Corporations as an Additional Structure for Antibiotic Development and Commercialization. *Translational Research* **2020**, *220*, 182–190. <https://doi.org/10.1016/j.trsl.2020.02.006>.
- (33) Camilla Pecoraro; Daniela Carbone; Barbara Parrino; Stella Cascioferro; Patrizia Diana. Recent Developments in the Inhibition of Bacterial Adhesion as Promising Anti-Virulence Strategy. *International Journal of Molecular Sciences* **2023**, *24* (5), 4872. <https://doi.org/10.3390/ijms24054872>.
- (34) Wing Yin Venus Lau; Patrick K. Taylor; Fiona S. L. Brinkman; Amy H. Y. Lee. Pathogen-Associated Gene Discovery Workflows for Novel Antivirulence Therapeutic Development. *eBioMedicine* **2023**, *88*, 104429. <https://doi.org/10.1016/j.ebiom.2022.104429>.
- (35) Walter Reinisch; Xavier Hébuterne; Anthony Buisson; Stefan Schreiber; Pierre Desreumaux; Christian Primas; Jean-Michel Paillarse; Grégoire Chevalier; Christophe Bonny. Safety, Pharmacokinetic, and Pharmacodynamic Study of Sibofimloc, a Novel FimH Blocker in Patients with Active Crohn's Disease. *Journal of Gastroenterology and Hepatology* **2022**, *37*, 832–840.
- (36) Marzena Polaska; Barbara Sokolowska. Bacteriophages-a New Hope or a Huge Problem in the Food Industry. *AIMS Microbiology* **2019**, *5* (4), 324–346.
- (37) Graham F. Hatfull; Rebekah M. Dedrick; Robert T. Schooley. Phage Therapy for Antibiotic-Resistant Bacterial Infections. *Annual Review of Medicine* **2022**, *73*, 197–211.
- (38) Rwei-Min Lu; Yu-Chyi Hwang; I-Ju Liu; Chi-Chiu Lee; Han-Zen Tsai; Hsin-Jung Li; Han-Chung Wu. Development of Therapeutic Antibodies for the Treatment of Diseases. *Journal of Biomedical Science* **2020**, *27* (1).
- (39) Kathrin U. Jansen; William C. Gruber; Raphael Simon; James Wassil; Annaliesa S. Anderson. The Impact of Human Vaccines on Bacterial Antimicrobial Resistance. A Review. *Environmental Chemistry Letters* **2021**, *19*, 4031–4062.
- (40) Isabel Frost; Hatim Sati; Pilar Garcia-Vello; Mateusz Hasso-Agopsowicz; Christian Lienhardt; Valeria Gigante; Peter Beyer. The Role of Bacterial Vaccines in the Fight against Antimicrobial Resistance: An Analysis of the Preclinical and Clinical Development Pipeline. *Lancet Microbe* **2023**, *4* (2), E113–E125. [https://doi.org/10.1016/S2666-5247\(22\)00303-2](https://doi.org/10.1016/S2666-5247(22)00303-2).
- (41) Benjamin P. Willing; Shannon L. Russell; B. Brett Finlay. Shifting the Balance: Effects on Host-Microbiota Mutualism. *Nature Reviews Microbiology* **2011**, *9*, 233–243.
- (42) Lucy McDonnell; Alexander Gilkes; Mark Ashworth; Victoria Rowland; Timothy Hugh Harries; David Armstrong; Patrick White. Association between Antibiotics and Gut Microbiome Dysbiosis in Children: Systematic Review and Meta-Analysis. *GUT MICROBES* **2021**, *13* (1), e1870402. <https://doi.org/10.1080/19490976.2020.1870402>.
- (43) Tsvetelina Velikova; Boris Krastev; Stefan Lozenov; Radostina Gencheva; Monika Peshevska-Sekulovska; Georgi Nikolaev; Milena Peruhova. Antibiotic-Related Changes in Microbiomes: The Hidden Villain behind

- Colorectal Carcinoma Immunotherapy Failure. *International Journal of Molecular Sciences* **2021**, *22* (4), 1754. <https://doi.org/10.3390/ijms22041754>.
- (44) Patrice D. Cani; Rodrigo Bibiloni; Claude Knauf; Aurélie Waget; Audrey M. Neyrinck; Nathalie M. Delzenne; Rémy Burcelin. Changes in Gut Microbiota Control Metabolic Endotoxemia-Induced Inflammation in High-Fat Diet-Induced Obesity and Diabetes in Mice. *Diabetes* **2008**, *57* (6), 1470–1481. <https://doi.org/10.2337/db07-1403>.
- (45) Mairi C. Noverr; Nicole R. Falkowski; Rod A. McDonald; Andrew N. McKenzie; Gary B. Huffnagle. Development of Allergic Airway Disease in Mice Following Antibiotic Therapy and Fungal Microbiota Increase: Role of Host Genetics, Antigen, and Interleukin-13. *Infection and Immunity* **2005**, *73* (1). <https://doi.org/10.1128/iai.73.1.30-38.2005>.
- (46) Long H. Nguyen; Anne K. Örtqvist; Yin Cao; Tracey G. Simon; Bjorn Roelstraete; Mingyang Song; Amit D. Joshi; Kyle Staller; Andrew T. Chan; Hamed Khalili; Ola Olén; Jonas F. Ludvigsson. Antibiotic Use and the Development of Bowel Disease: A National Case-Control Study in Sweden. *Gastroenterology & Hepatology* **2020**, *5* (11), 986–995. [https://doi.org/10.1016/S2468-1253\(20\)30267-3](https://doi.org/10.1016/S2468-1253(20)30267-3).
- (47) Walter V. Reid; Sarah A. Laird; Rodrigo Gámez; Ana Sittenfeld; Daniel H. Janzen; Michael A. Gollin; Calestous Juma. Biodiversity Prospecting: Using Genetic Resources for Sustainable Development. *A World Resources Institute Book* **1993**, 1–52.
- (48) Arnold L. Demain. From Natural Products Discovery to Commercialization: A Success Story. *Journal of Industrial Microbiology and Biotechnology* **2006**, *33* (7), 486–495. <https://doi.org/10.1007/s10295-005-0076-x>.
- (49) Arnold L. Demain. Importance of Microbial Natural Products and the Need to Revitalize Their Discovery. *Journal of Industrial Microbiology and Biotechnology* **2014**, *41* (2), 185–201. <https://doi.org/10.1007/s10295-013-1325-z>.
- (50) Tobias AM Gulder; Bradley S. Moore. Chasing the Treasure of the Sea - Bacterial Marine Natural Products. *Current Opinion in Microbiology* **2009**, *12* (3), 252–260. <https://doi.org/10.1016/j.mib.2009.05.002>.
- (51) M. D. Ivorra; M. Payá; A. Villar. A Review of Natural Products and Plants as Potential Antidiabetic Drugs. *Journal of Ethnopharmacology* **1989**, *27*, 243–275.
- (52) Adam M. Burja; Bernard Banaigs; Eliane Abou-Mansour; J. Grant Burgess; Phillip C. Wright. Marine Cyanobacteria - a Prolific Source of Natural Products. *Tetrahedron* **2001**, *57*, 9347–9377.
- (53) Martin J. Rice; Mike Legg; Keith A. Powell. Natural Products in Agriculture - A View from the Industry. *Pesticide Science* **1998**, *52* (2), 184–188. [https://doi.org/Pestic.Sci.0031-613X/98/\\$17.5](https://doi.org/Pestic.Sci.0031-613X/98/$17.5).
- (54) A. Bhanot; R. Sharma; Malleshappa N. Noolvi. Natural Sources as Potential Anti-Cancer Agents: A Review. *International Journal of Phytomedicine* **2011**, *3* (1), 09–26.
- (55) Franck E. Dayan; Charles L. Cantrell; Stephen O. Duke. Natural Products in Crop Protection. *Bioorganic & Medicinal Chemistry* **2009**, *17*, 4022–4034. <https://doi.org/doi:10.1016/j.bmc.2009.01.046>.
- (56) Berhanu M. Abegaz; Henok H. Kinfe. Secondary Metabolites, Their Structural Diversity, Bioactivity, and Ecological Functions: An Overview. *Physical Sciences Reviews* **2019**, 20180100. <https://doi.org/DOI:10.1515/psr-2018-0100>.
- (57) Ya-Nan Wang; Ling-Hong Meng; Bin-Gui Wang. Progress in Research on Bioactive Secondary Metabolites from Deep-Sea Derived Microorganisms. *Marine Drugs* **2020**, *18* (12), 614. <https://doi.org/10.3390/md18120614>.
- (58) Rudolf Schmitz. Friedrich Wilhelm Sertürner and the Discovery of Morphine. *Pharmacy in History* **1985**, *27* (2), 61–74.
- (59) D. C. Zhou; R. Zittoun; J. P. Marie. Homoharringtonine: An Effective New Natural Product in Cancer Chemotherapy. *Bull Cancer* **1995**, *82* (12), 987–995.
- (60) Dennis R. A. Mans; Adriana B. Rocha; Gilberto Schwartzmann. Anti-Cancer Drug Discovery and Development in Brazil: Targeted Plant Collection as a Rational Strategy to Acquire Candidate Anti-Cancer Compounds. *The Oncologist* **2000**, *5* (3), 185–198. <https://doi.org/10.1634/theoncologist.5-3-185>.
- (61) M. Gordaliza. Natural Products as Leads to Anticancer Drugs. *Clinical and Translational Oncology* **2007**, *9*, 767–776.
- (62) L. Silver; K. Bostian. Screening of Natural Products for Antimicrobial Agents. *European Journal of Clinical Microbiology & Infections Diseases* **1990**, *9*, 455–461.
- (63) Peter J. Petersen; T. Z. Wang; Russel G. Dushin; Patricia A. Bradford. Comparative *In Vitro* Activities of AC98-6446, a Novel Semisynthetic Glycopeptide Derivative of the Natural Product Mannopeptimycin α , and Other Antimicrobial Agents against Gram-Positive Clinical Isolates. *Antimicrobial Agents and Chemotherapy* **2004**, *48* (3), 739–746. <https://doi.org/10.1128/2FAAC.48.3.739-746.2004>.
- (64) Haiyin He. Mannopeptimycins, a Novel Class of Glycopeptide Antibiotics Active against Gram-Positive Bacteria. *Applied Microbiology and Biotechnology* **2005**, *67* (4), 444–452. <https://doi.org/doi:10.1007/s00253-004-1884-z>.

- (65) Christian Hobson; Andrew N. Chan; Gerard D. Wright. The Antibiotic Resistome: A Guide for the Discovery of Natural Products as Antimicrobial Agents. *Chemical Reviews* **2021**, *121*, 3464–3494. <https://dx.doi.org/10.1021/acs.chemrev.0c01214?ref=pdf>.
- (66) Pranay Srivastava; Rajesh Singh Yadav. Efficacy of Natural Compounds in Neurodegenerative Disorders. In *Advances in Neurobiology*; 2016; Vol. 12, pp 107–123.
- (67) Dmitri Leonoudakis; Anand Rane; Suzanne Angeli; Gordon J. Lithgow; Julie K. Andersen; Shankar J. Chinta. Anti-Inflammatory and Neuroprotective Role of Natural Product Securinine in Activated Glial Cells: Implications for Parkinson's Disease. *Mediators of Inflammation* **2017**, *2017*. <https://doi.org/10.1155/2017/8302636>.
- (68) Siva S. Panda; Nancy Jhanji. Natural Products as Potential Anti-Alzheimer Agents. *Current Medicinal Chemistry* **2020**, *27*, 5887–5917. <https://doi.org/10.1080/13652077.2020.1875533>.
- (69) David J. Newman; Gordon M. Cragg. Natural Products as Sources of New Drugs from 1981 to 2014. *Journal of Natural Products* **2016**, *79*, 629–661.
- (70) Nitesh Kumar Mund; Eva Cellárová. Recent Advances in the Identification of Biosynthetic Genes and Gene Clusters of the Polyketide-Derived Pathways for Anthraquinone Biosynthesis and Biotechnological Applications. *Biotechnology Advances* **2023**, *63*, 108104. <https://doi.org/10.1016/j.biotechadv.2023.108104>.
- (71) Jacob M. Wurlitzer; Aleksa Stanišić; Ina Wasmuth; Sandra Jungmann; Dagmar Fischer; Hajo Kries; Markus Gressler. Bacterial-Like Nonribosomal Peptide Synthetases Produce Cyclopeptides in the Zygomycetous Fungus *Mortierella Alpina*. *Applied and Environmental Microbiology* **2021**, *87* (3). <https://doi.org/10.1128/AEM.02051-20>.
- (72) Nadine Ziemert; Mohammad Alanjary; Tilmann Weber. The Evolution of Genome Mining in Microbes - a Review. *Natural Product Report* **2016**, *33*, 988–1005. <https://doi.org/10.1039/c6np00025h>.
- (73) Lin Chen; Jian-Wei Tang; Yan Yee Liu; Yudai Matsuda. Aspcandine: A Pyrrolobenzazepine Alkaloid Synthesized by a Fungal Nonribosomal Peptide Synthetase-Polyketide Synthase Hybrid. *Organic Letters* **2022**, *24* (26), 4816–4819. <https://doi.org/10.1021/acs.orglett.2c01918>.
- (74) Laila Ziko; Omnia AbdelRaheem; Marina Nabil; Ramy K. Aziz; Rania Siam. Bioprospecting the Microbiome of Red Sea Atlantis II Brine Pool for Peptidases and Biosynthetic Genes with Promising Antibacterial Activity. *Microbial Cell Factories* **2022**, *21*.
- (75) Michele Greque de Moraes; Bruna da Silva Vaz; Etiele Greque de Moraes; Jorge Alberto Vieira Costa. Biologically Active Metabolites Synthesized by Microalgae. *Biomedical Research International* **2015**, *2015*. <https://doi.org/10.1155/2015/835761>.
- (76) Wendy A. Stirk; Johannes van Staden. Bioprospecting for Active Compounds in Microalgae: Antimicrobial Compounds. *Biotechnology Advances* **2022**, *59*. <https://doi.org/10.1016/j.biotechadv.2022.107977>.
- (77) Carlos Eduardo de Garias Silva; Alberto Bertucco. Bioethanol from and Cyanobacteria: A Review and Technological Outlook. *Process Biochemistry* **2016**, *51*, 1833–1842. <https://doi.org/10.1016/j.procbio.2016.02.016>.
- (78) Teresa M. Mata; António A. Martins; Nidia. S. Caetano. Microalgae for Biodiesel Production and Other Applications: A Review. *Renewable and Sustainable Energy Reviews* **2010**, *14* (1), 217–232. <https://doi.org/10.1016/j.rser.2009.07.020>.
- (79) Kunal Seth; Ashwani Kumar; Rajesh P. Rastogi; Mukesh Meena; Vandana Vinayak; Harish. Bioprospecting of Fucoxanthin from Diatoms - Challenges and Perspectives. *Algal Research* **2021**, *60*. <https://doi.org/10.1016/j.algal.2021.102475>.
- (80) Anil Kumar Patel; Akash Pralhad Vadrale; Yi-Sheng Tseng; Chiu-Wen Chen; Cheng-Di Dong; Reeta Rani Singhanian. Bioprospecting of Marine Microalgae from Kaohsiung Seacoast for Lutein and Lipid Production. *Bioresource Technology* **2022**, *351*.
- (81) Anthony R. Carroll; Brent R. Copp; Rohan A. Davis; Robert A. Keyzers; Michèle R. Prinsep. Marine Natural Products. *Natural Product Reports* **2023**, *40*, 275–325.
- (82) Brandt Bertrand; Carlos Munoz-Garay. Marine Antimicrobial Peptides: A Promising Source of New Generation Antibiotics and Other Bio-Active Molecules. *International Journal of Peptide Research and Therapeutics* **2019**, *25*, 1441–1450.
- (83) Annarita Falanga; Lucia Lombardi; Gianluigi Franci; Mariateresa Vitiello; Maria Rosaria Iovene; Giancarlo Morelli; Massimiliano Galdiero; Stefania Galdiero. Marine Antimicrobial Peptides: Nature Provides Templates for the Design of Novel Compounds against Pathogenic Bacteria. *International Journal of Molecular Sciences* **2016**, *17* (785). <https://doi.org/10.3390/ijms17050785>.
- (84) Raymond C. Valentine; David L. Valentine. Omega-3 Fatty Acids in Cellular Membranes: A Unified Concept. *Progress in Lipid Research* **2004**, *42* (5), 383–402.
- (85) Nicholas J. Russel; David S. Nichols. Polyunsaturated Fatty Acids in Marine Bacteria - a Dogma Rewritten. *Microbiology* **145**, 767–779.
- (86) Randy Chi Fai Cheung; Tzi Bun Ng; Jack Ho Wong. Marine Peptides: Bioactivities and Applications. *Marine Drugs* **2015**, *13* (7), 4006–4043. <https://doi.org/10.3390/md13074006>.

- (87) Sigmund V. Sperstad; Tor Haug; Hans-Matti Blencke; Olaf B. Styrvoid; Chun Li; Klara Stensvåg. Antimicrobial Peptides from Marine Invertebrates: Challenges and Perspectives in Marine Peptide Discovery. *Biotechnology Advances* **2011**, *29*, 519–530. <https://doi.org/10.1016/j.biotechadv.2011.05.021>.
- (88) Mohammad H. Semreen; Mohammed I. El-Gamal; Shifaa Abdin; Hajar Alkhazraji; Leena Kamal; Saba Hammad; Faten El-Awady; Dima Waleed; Layal Kourbaj. Recent Updates of Marine Antimicrobial Peptides. *Saudi Pharmaceutical Journal* **2018**, *26*, 396–409.
- (89) Shuocun Wang; Liming Fan; Hanyu Pan; Yingying Li; Yan Qiu; Yiming Lu. Antimicrobial Peptides from Marine Animals: Sources, Structures, Mechanisms and the Potential for Drug Development. *Frontiers in Marine Science* **2023**. <https://doi.org/10.3389/fmars.2022.1112595>.
- (90) Chun Li; Tor Haug; Morten K. Moe; Olaf B. Styrvoid; Klara Stensvåg. Centrocins: Isolation and Characterization of Novel Dimeric Antimicrobial Peptides from the Green Sea Urchin, *Strongylocentrotus Droebachiensis*. *Developmental and Comparative Immunology* **2010**, *34*, 959–568. <https://doi.org/10.1016/j.dci.2010.04.004>.
- (91) Ann Eisenberg Shinnar; Kathryn L. Butler; Hyon Ju Park. Cathelicidin Family of Antimicrobial Peptides: Proteolytic Processing and Protease Resistance. *Bioorganic Chemistry* **2003**, *31* (6), 425–436. [https://doi.org/10.1016/S0045-2068\(03\)00080-4](https://doi.org/10.1016/S0045-2068(03)00080-4).
- (92) Takanori Nakamura; Hiromi Furunaka; Toshiyuki Miyata; Fuminori Tokunaga; Tatsushi Muta; Sadaaki Iwanaga. Tachyplesin, a Class of Antimicrobial Peptide from the Hemocytes of the Horseshoe Crab (*Tachypleus Tridentatus*). Isolation and Chemical Structure. *The Journal of Biological Chemistry* **1988**, *263* (32), 16709–16713.
- (93) Chun Li; Hans-Matti Blencke; L. Courtney Smith; Matti T. Karp; Klara Stensvåg. Two Recombinant Peptides, SpStrongylocins 1 and 2, from *Strongylocentrotus Purpuratus*, Show Antimicrobial Activity against Gram-Positive and Gram-Negative Bacteria. *Developmental and Comparative Immunology* **2009**, *34*, 286–292. <http://dx.doi.org/10.1016/j.dci.2009.10.006>.
- (94) Rathi Saravanan; Harini Mohanram; Mangesh Joshi; Prerna N. Domadia; Jaume Torres; Christiane Ruedl; Surajit Bhattachariya. Structure, Activity and Interactions of the Cysteine Deleted Analog of Tachyplesin-I with Lipopolysaccharide Micelle: Mechanistic Insights into Outer-Membrane Permeabilization and Endotoxin Neutralization. *Biochimica et Biophysica Acta* **2012**, *1818* (7), 1613–1624.
- (95) Jan Hudzicki. Kirby-Bauer Disk Diffusion Susceptibility Test Protocol. *American Society for Microbiology* **2009**.
- (96) Irith Wiegand; Kai Hilpert; Robert E. W. Hancock. Agar and Broth Dilution Methods to Determine the Minimal Inhibitory Concentration (MIC) of Antimicrobial Substances. *Nature Protocols* **2008**, *3* (2), 163–175.
- (97) Teena Wadhvani; Komal Desai; Dhara Patel; Deepmala Lawani; Priyadarshani Bahaley; Priyanka Joshi; Vijay Kothari. Effect of Various Solvents on Bacterial Growth in Context of Determining MIC of Various Antimicrobials. *Internet Journal of Microbiology* **2009**, *7* (1).
- (98) Phumlani Tetyana; Poslet Morgan Shumbula; Zikhona Njengele-Tetyana. Biosensors: Design, Development and Applications. *Nanopores*. <https://doi.org/10.5772/intechopen.97576>.
- (99) Adam Bieniek; Artur P. Terzyk; Marek Wiśniewski; Katarzyna Roszek; Piotr Kowalczyk; Lev Sarkisov; Seda Keskin; Katsumi Kaneko. MOF Materials as Therapeutic Agents, Drug Carriers, Imaging Agents and Biosensors in Cancer Biomedicine: Recent Advances and Perspectives. *Progress in Materials Science* **2021**, *117*, 100743. <https://doi.org/10.1016/j.pmatsci.2020.100743>.
- (100) P. Mohankumar; J. Ajayan; T. Mohanraj; R. Yasodharan. Recent Developments in Biosensors for Healthcare and Biomedical Applications: A Review. *Measurement* **2021**, *167*, 108293. <https://doi.org/10.1016/j.measurement.2020.108293>.
- (101) Christian Griesche; Antje J. Baeumner. Biosensors to Support Sustainable Agriculture and Food Safety. *TrAC Trends in Analytical Chemistry* **2020**, *128*, 115906. <https://doi.org/10.1016/j.trac.2020.115906>.
- (102) Zheng Hua; Ting Yu; Donghong Liu; Yunlei Xianyu. Recent Advances in Gold Nanoparticles-Based Biosensors for Food Safety Detection. *Biosensors and Bioelectronics* **2021**, *179*, 113076. <https://doi.org/10.1016/j.bios.2021.113076>.
- (103) Laís Canniatti Brazaca; Isabella Sampaio; Valtencir Zucolotto; Bruno Campos Janegitz. Applications of Biosensors in Alzheimer's Disease Diagnosis. *Talanta* **2020**, *210*, 120644. <https://doi.org/10.1016/j.talanta.2019.120644>.
- (104) Richa Pandey; Yang Lu; Erin M. McConnell; Enas Osman; Alexander Scott; Jimmy Gu; Todd Hoare; Leyla Soleymani; Yingfu Li. Electrochemical DNAzyme-Based Biosensors for Disease Diagnosis. *Biosensors and Bioelectronics* **2023**, *224*, 114983. <https://doi.org/10.1016/j.bios.2022.114983>.
- (105) Erin M. McConnell; Julie Nguyen; Yingfu Li. Aptamer-Based Biosensors for Environmental Monitoring. *Frontiers in Chemistry* **2020**, *8*, 434. <https://doi.org/10.3389/fchem.2020.00434>.

- (106) Simona Gavrilas; Claudiu Stefan Ursachi; Simona Perta-Crisan; Florentina-Daniela Munteanu. Recent Trends in Biosensors for Environmental Quality Monitoring. *Sensors* **2022**, *22* (4), 1513. <https://doi.org/10.3390/s22041513>.
- (107) Chi-Wei Huang; Chitsan Lin; Minh Ky Nguyen; Adnan Hussain; Xuan-Thanh Bui; Huu Hao Ngo. A Review of Biosensor for Environmental Monitoring: Principle, Application, and Corresponding Achievement of Sustainable Development Goals. *Bioengineered* **2023**, *14* (1), 58–80. <https://doi.org/10.1080/21655979.2022.2095089>.
- (108) Firoozeh Piroozmand; Fatemeh Mohammadipanah; Farnoush Faridbod. Emerging Biosensors in Detection of Natural Products. *Synthetic and Systems Biotechnology* **2020**, *5* (4), 293–303. <https://doi.org/10.1016/j.synbio.2020.08.002>.
- (109) Francisco F. Roberto; Joni M. Barnes; Debby F. Bruhn. Evaluation of a GFP Reporter Gene Construct for Environmental Arsenic Detection. *Talanta* **2002**, *58*, 181–188.
- (110) N. Carol Casavant; Dan Thompson; Gwyn A. Beattie; Gregory J. Phillips; Larry J. Halverson. Use of a Site-Specific Recombination-Based Biosensor for Detecting Bioavailable Toluene and Related Compounds on Roots. *Environmental Microbiology* **2003**, *5* (4), 238–249. <https://doi.org/10.1046/j.1462-2920.2003.00420.x>.
- (111) Shrute Kannappan; Bhaskar Chandra Mohan Ramisetty. Engineering Whole-Cell-Based Biosensors: Sensing Environmental HeavyMetal Pollutants in Water-a Review. *Applied Microbiology and Biotechnology* **2022**, *194*, 1814–1840.
- (112) Yueqian Chen; Yingying Guo; Yanwei Liu; Yuping Xiang; Guangliang Liu; Qinghua Zhang; Yongguang Yin; Yong Cai; Guibin Jiang. Advances in Bacterial Whole-Cell Biosensors for the Detection of Bioavailable Mercury: A Review. *Science of the Total Environment* **2023**, *686*, 161709. <http://dx.doi.org/10.1016/j.scitotenv.2023.161709>.
- (113) Robin Tecon; Siham Beggah; Kamila Czechowska; Vladimir Sentchilo; Panagiota-Myrsini Chronopoulou; Terry J. McGenity; Jan Roelof van der Meer. Development of a Multistrain Bacterial Bioreporter Platform for the Monitoring of Hydrocarbon Contaminants in Marine Environments. *Environmental Science & Technology* **2010**, *44* (3), 1049–1055. <https://doi.org/10.1073/pnas.97.22.11984>.
- (114) Sherwin Reyes; Nga Le; Mary Denneth Fuentes; Jonathan Upegui; Emre Dikici; David Broyles; Edward Quinto; Sylvia Daunert; Sapna K. Deo. An Intact Cell Bioluminescence-Based Assay for the Simple and Rapid Diagnosis of Urinary Tract Infection. *International Journal of Molecular Sciences* **2020**, *21* (14). <https://doi.org/doi:10.3390/ijms21145015>.
- (115) Seung-Gyun Woo; Sung-Je Moon; Seong Keun Kim; Tae Hyun Kim; Hyun Seung Lim; Gun-Hwi Yeon; Bong Hyun Sung; Chul-Ho Lee; Seung-Goo Lee; Jung Hwan Hwang; Dae-Hee Lee. A Designed Whole-Cell Biosensor for Live Diagnosis of Gut Inflammation through Nitrate Sensing. *Biosensors and Bioelectronics* **2020**, *168*, 112523. <https://doi.org/10.1016/j.bios.2020.112523>.
- (116) Grant R. MacGregor; Garry P. Nolan; Steven Fiering; Mario Roederer; Leonard A. Herzenberg. Use of *E. Coli lacZ* (β -Galactosidase) as a Reporter Gene. *Methods in Molecular Biology* **1991**, *7*, 217–234.
- (117) Jorrit Schaefer; Goran Jovanovic; Loly Kotta-Loizou; Martin Buck. Single-Step Method for β -Galactosidase Assays in *Escherichia Coli* Using a 96-Well Microplate Reader. *Analytical Biochemistry* **2016**, *503*, 56–57. <https://doi.org/10.1016/j.ab.2016.03.017>.
- (118) Chhandak Basu; Albert P. Kausch; Joel M. Chandlee. Use of β -Glucuronidase Reporter Gene for Gene Expression Analysis in Turfgrasses. *Biochemical and Biophysical Research Communications* **2004**, *320* (1), 7–10. <https://doi.org/10.1016/j.bbrc.2004.05.128>.
- (119) Niels C. Adams; Nicholas W. Gale. High Resolution Gene Expression Analysis in Mice Using Genetically Inserted Reporter Genes. *Mammalian and Avian Transgenesis - New Approaches* **2006**, 131–172.
- (120) Xiang Liu; Jine Li; Yue Li; Junyue Li; Huiying Sun; Jiazhen Zheng; Jihui Zhang; Huarong Tan. A Visualization Reporter System for Characterizing Antibiotic Biosynthetic Gene Clusters Expression with High-Sensitivity. *Communications Biology* **2022**, *5*, 901.
- (121) Shu-Ye Jiang; Jeevanandam Vanitha; Yanan Bai; Srinivasan Ramachandran. A Novel Binary T-Vector with the GFP Reporter Gene for Promoter Characterization. *PLOS ONE* **2014**, *9* (9), e107328. <https://doi.org/doi:10.1371/journal.pone.0107328>.
- (122) Villao L.; Sánchez E.; Romero C.; Galarza L.; Flores J.; Santos-Ordóñez E. Activity Characterization of the Plantain Promoter from the Heavy Metal-Associated Isoprenylated Plant Gene (MabHIPP) Using the Luciferase Reporter Gene. *Plant Gene* **2019**, *19*, 100187. <https://doi.org/10.1016/j.plgene.2019.100187>.
- (123) M. Mardalisa; S. Suhandono; M. Ramdhani. Isolation and Characterization of Str Promoter from Bacteria *Escherichia Coli* DH5 α Using Reporter Gene AmilCP (*Acropora Millepora*). *IOP Conference Series: Earth and Environmental Science* **2020**, *430*, 012014. <https://doi.org/doi:10.1088/1755-1315/430/1/012014>.
- (124) Priya Kunapuli; Richard Ransom; Kathy L. Murphy; Doug Pettibone; Julie Kerby; Sarah Grimwood; Paul Zuck; Peter Hodder; Raul Lacson; Ira Hoffman; James Inglese; Berta Strulovici. Development of an

- Intact Cell Reporter Gene β -Lactamase Assay for G Protein-Coupled Receptors for High-Throughput Screening. *Analytical Biochemistry* **2003**, *314* (1), 16–29. [https://doi.org/10.1016/S0003-2697\(02\)00587-0](https://doi.org/10.1016/S0003-2697(02)00587-0).
- (125) Ellen Siebring-van Olst; Christie Vermeulen; Renee X. de Menezes; Michael Howell; Egbert F. Smit; Victor W. van Beusechem. Affordable Luciferase Reporter Assay for Cell-Based High-Throughput Screening. *Journal of Biomolecular Screening* **2013**, *18* (4), 453–461. <https://doi.org/10.1177/1087057112465184>.
- (126) Heather M. Froggatt; Brook E. Heaton; Nicholas S. Heaton. Development of a Fluorescence-Based, High-Throughput SARS-CoV-2 3CLpro Reporter Assay. *American Society for Microbiology* **2020**, *94* (22). <https://doi.org/10.1128/jvi.01265-20>.
- (127) Yajing Yu; Alexander J. Annala; Jorge R. Barrio; Tatsushi Toyokuni; Nagichettiar Satyamurthy; Mohammad Namavari; Simon R. Cherry; Michael E. Phelps; Harvey R. Herschman; Sanjiv S. Gambhir. Quantification of Target Gene Expression by Imaging Reporter Gene Expression in Living Animals. *Nature Medicine* **2000**, *6*, 933–937.
- (128) Hyewon Youn; June-Key Chung. Reporter Gene Imaging. *AJR* **2013**, *201* (2). <https://doi.org/10.2214/AJR.13.10555>.
- (129) Candice Ashmore-Harris; Madeleine Lafrate; Adeel Saleem; Gilbert O. Fruhwirth. Non-Invasive Reporter Gene Imaging of Cell Therapies, Including T Cells and Stem Cells. *Molecular Therapy* **2020**, *28* (6), 1392–1416. <https://doi.org/10.1016/j.ymthe.2020.03.016>.
- (130) Marc Zimmer. Green Fluorescent Protein (GFP): Applications, Structure, and Related Photophysical Behavior. *Chemical Reviews* **2002**, *102* (3), 759–782. <https://doi.org/10.1021/cr010142r>.
- (131) Arnab Mukherjee; Kevin B. Weyant; Joshua Walker; Charles M. Schroeder. Directed Evolution of Bright Mutants of an Oxygen-Independent Flavin-Binding Fluorescent Protein from *Pseudomonas Putida*. *Journal of Biological Engineering* **2012**, *6* (20).
- (132) Geoffrey S. Baird; David A. Zacharias; Roger Y. Tsien. Biochemistry, Mutagenesis, and Oligomerization of DsRed, a Red Fluorescent Protein from Coral. *PNAS* **2000**, *97* (22), 11984–11989. <https://doi.org/10.1073/pnas.97.22.11984>.
- (133) Marko Virta; Karl E. O. Åkerman; Petri Saviranta; Christian Oker-Blom; Matti T. Karp. Real-Time Measurement of Cell Permeabilization with Low-Molecular-Weight Membranolytic Agents. *Journal of Antimicrobial Chemotherapy* **1995**, *36*, 303–315.
- (134) Joanne Engebrecht; Kenneth Nealson; Michael Silverman. Bacterial Bioluminescence: Isolation and Genetic Analysis of Functions from *Vibrio Fischeri*. *Cell* **1983**, *32* (3), 773–781. [https://doi.org/10.1016/0092-8674\(83\)90063-6](https://doi.org/10.1016/0092-8674(83)90063-6).
- (135) Stephen J. Gould; Suresh Subramani. Firefly Luciferase as a Tool in Molecular and Cell Biology. *Analytical Biochemistry* **1988**, *175*, 5–13.
- (136) Sohail A. Qureshi. β -Lactamase: An Ideal Reporter System for Monitoring Gene Expression in Live Eukaryotic Cells. *BioTechniques* **2018**, *42* (1). <https://doi.org/10.2144/000112292>.
- (137) W. V. Shaw; A. G. W. Leslie. Chloramphenicol Acetyltransferase. *Annual Review of Biophysics and Biophysical Chemistry* **1991**, *20*, 363–386. <https://doi.org/10.1146/annurev.bb.20.060191.002051>.
- (138) Richard A. Jefferson. Assaying Chimeric Genes in Plants: The GUS Gene Fusion System. *Plant molecular biology reporter* **1987**, *5* (1), 387–405.
- (139) Jeffrey E. De Wet; Keith V. Wood; Donald R. Helinski; Marlene DeLuca. Cloning of Firefly Luciferase cDNA and the Expression of Active Luciferase in *Escherichia Coli*. *PNAS* **1985**, *82* (23), 7870–7873. <https://www.jstor.org/stable/26480>.
- (140) Robert Belas; Alan Mileham; Daniel Cohn; Marcia Hilman; Melvin Simon; Michael Silverman. Bacterial Bioluminescence: Isolation and Expression of the Luciferase Genes from *Vibrio Harveyi*. *Science* **1982**, *218* (4574), 791–793. <https://doi.org/DOI:10.1126/science.10636771>.
- (141) Thérèse Wilson; J. Woodland Hastings. Bioluminescence. *Annual Review of Cell and Developmental Biology* **1998**, *14*, 197–230. <https://doi.org/10.1146/annurev.cellbio.14.1.197>.
- (142) Kaisa Hakkila; Mikael Maksimow; Matti Karp; Marko Virta. Reporter Genes lucFF, luxCDABE, Gfp, and Dsred Have Different Characteristics in Whole-Cell Bacterial Sensors. *Analytical Biochemistry* **2002**, *301*, 235–242. <https://doi.org/doi:10.1006/abio.2001.5517>.
- (143) Dan M. Close; Steven Ripp; Gary S. Saylor. Reporter Proteins in Whole-Cell Optical Bioreporter Detection Systems, Biosensor Integrations, and Biosensing Applications. *Sensors* **2009**, *9* (11), 9147–9174. <https://doi.org/10.3390/s91109147>.
- (144) Carola Gregor; Klaus C. Gwosch; Steffen J. Sahl; Stefan W. Hell. Strongly Enhanced Bacterial Bioluminescence with the *lux* Operon for Single-Cell Imaging. *PNAS* **2018**, *115* (5), 962–967. <https://doi.org/10.1073/pnas.1715946115>.
- (145) Shimomura, O.; Johnson, F. H.; Saiga, Y. Extraction, Purification and Properties of Aequorin, a Bioluminescent Protein from the Luminous Hydromedusan, *Aequorea*. *J Cell Comp Physiol* **1962**, *59*, 223–239. <https://doi.org/10.1002/jcp.1030590302>.

- (146) Te-Tuan Yang; Linzhao Cheng; Steven R. Kain. Optimized Codon Usage and Chromophore Mutations Provide Enhanced Sensitivity with the Green Fluorescent Protein. *Nucleic Acids Research* **1996**, *24* (22), 4592–4593.
- (147) Yoshihito Kitamura; Satoshi Mori; Wen Chen; Jun Sumaoka; Makoto Komiyama. Recombination of GFP Gene to the BFP Gene Using a Man-Made Site-Selective DNA Cutter. *Journal of Biological Inorganic Chemistry* **2006**, *11*, 13–16.
- (148) Etienne Joly. Optimising Blue Fluorescent Protein (BFP) for Use as Mammalian Reporter Gene in Parallel with Green Fluorescent Protein (GFP). *Nature Precedings* **2007**.
- (149) Dmitry M. Chudakov; Vladislav V. Verkhusha; Dmitry B. Staroverov; Ekaterina A. Souslova; Sergey Lukyanov; Konstantin A. Lukyanov. Photoswitchable Cyan Fluorescent Protein for Protein Tracking. *Nature Biotechnology* **2004**, *22*, 1435–1439. <https://doi.org/10.1038/nbt1025>.
- (150) Iona D. Raymond; Alejandro Vila; Uyen-Chi N. Huynh; Nicholas C. Brecha. Cyan Fluorescent Protein Expression in Ganglion and Amacrine Cells in a Thyl-CFP Transgenic Mouse Retina. *Molecular Vision* **2008**, *14*, 1559–1574.
- (151) Marc-Jan Gubbels; Catherine Li; Boris Striepen. High-Throughput Growth Assay for *Toxoplasma Gondii* Using Yellow Fluorescent Protein. *Antimicrobial Agents and Chemotherapy* **2003**, *47* (1). <https://doi.org/10.1128/aac.47.1.309-316.2003>.
- (152) Agata Rekas; Jean-René Alattia; Takeharu Nagai; Atsushi Miyawaki; Mitsuhiro Ikura. Crystal Structure of Venus, a Yellow Fluorescent Protein with Improved Maturation and Reduced Environmental Sensitivity. *Protein Structure and Folding* **2002**, *277* (52), 50573–50578. <https://doi.org/10.1074/jbc.M209524200>.
- (153) Swagatha Ghosh; Chi-Li Yu; Daniel J. Ferraro; Sai Sudha; Samir Kumar Pal; Wayne F. Schaefer; David T. Gibson; S. Ramaswamy. Blue Protein with Red Fluorescence. *PNAS* **2016**, *113* (41), 11513–11518.
- (154) Daria M. Shcherbakova; Mikhail Baloban; Alexander V. Emelyanov; Michael Brenowitz; Peng Guo; Vladislav V. Verkhusha. Bright Monomeric Near-Infrared Fluorescent Proteins as Tags and Biosensors for Multiscale Imaging. *Nature communications* **2016**, *7*, 12405. <https://doi.org/10.1038/ncomms12405>.
- (155) Erik A. Rodriguez; Geraldine N. Tran; Larry A. Gross; Jessica L. Crisp; Xiaokun Shu; John Y. Lin; Roger Y. Tsien. A Far-Red Fluorescent Protein Evolved from a Cyanobacterial Phycobiliprotein. *Nature Methods* **2016**, *13* (9), 763–769. <https://doi.org/doi:10.1038/nmeth.3935>.
- (156) Akiko Kumagai; Ryoko Ando; Hideyuki Miyatake; Peter Greimel; Toshihide Kobayashi; Yoshio Hirabayashi; Tomomi Shimogori; Atsushi Miyawaki. A Bilirubin-Inducible Fluorescent Protein from Eel Muscle. *Cell* **2013**, *153*, 1602–1611.
- (157) Johannes T.-H. Yeh; Kwangho Nam; Joshua T.-H. Yeh; Norbert Perrimon. eUnaG: A New Ligand-Inducible Fluorescent Reporter to Detect Drug Transporter Activity in Live Cells. *Scientific reports* **2017**, *7* (41619), 1–9.
- (158) Andrew D. Ellington; Jack W. Szostak. In Vitro Selection of RNA Molecules That Bind Specific Ligands. *NATURE* **1990**, *346*, 818–822.
- (159) Brian R. Baker; Rebecca Y. Lai; McCall S. Wood; Elaine H. Doctor; Alan J. Heeger; Kevin W. Plaxco. An Electronic, Aptamer-Based Small-Molecule Sensor for the Rapid, Label-Free Detection of Cocaine in Adulterated Samples and Biocidal Fluids. *Journal of the American Chemical Society* **2006**, *128*, 3138–3139. <https://doi.org/10.1021/ja056957p>.
- (160) Milan N. Stojanovic; Paloma de Prada; Donald W. Landry. Aptamer-Based Folding Fluorescent Sensor for Cocaine. *Journal of the American Chemical Society* **2001**, *123*, 4928–4931. <https://doi.org/10.1021/ja0038171>.
- (161) Nobuko Hamaguchi; Andrew D. Ellington; Martin Stanton. Aptamer Beacons for the Direct Detection of Proteins. *Analytical Biochemistry* **2001**, *294*, 126–131. <https://doi.org/10.1006/abio.2001.5169>.
- (162) Milan N. Stojanovic; Dmitry M. Kolpashchikov. Modular Aptameric Sensors. *Journal of the American Chemical Society* **2004**, *126* (30), 9266–9270.
- (163) Jeremy S. Paige; Thinh Nguyen-Duc; Wenjiao Song; Samie R. Jaffrey. Fluorescence Imaging of Cellular Metabolites with RNA. *Science* **2012**, *335* (6073), 1194.
- (164) Jeremy S. Paige; Karen Y. Wu; Samie R. Jaffrey. RNA Mimics of Green Fluorescent Protein. *Science* **2011**, *333*, 642–646. <https://doi.org/10.1126/science.1207339>.
- (165) Rita L. Strack; Matthew D. Disney; Samie R. Jaffrey. A Superfolding Spinach2 Reveals the Dynamic Nature of Trinucleotide Repeat-Containing RNA. *Nature Methods* **2013**, *10* (12), 1219–1224. <https://doi.org/doi:10.1038/nmeth.2701>.
- (166) Katherine Deigan Warner; Michael C. Chen; Wenjiao Song; Rita L. Strack; Andrea Thorn; Samie R. Jaffrey; Adrian R. Ferré-D'Amaré. Structural Basis for Activity of Highly Efficient RNA Mimics of Green Fluorescent Protein. *Nature structural & molecular biology* **2014**, *21* (8), 658–663. <https://doi.org/doi:10.1038/nsmb.2865>.
- (167) Elena V. Dolgosheina; Sunny C. Y. Jeng; Shanker Shyam S. Panchapakesan; Razvan Cojocaru; Patrick S. K. Chen; Peter D. Wilson; Nancy Hawkins; Paul A. Wiggins; Peter J. Unrau. RNA Mango Aptamer-

- Fluorophore: A Bright, High-Affinity Complex for RNA Labeling and Tracking. *ACS chemical biology* **2014**, *9*, 2412–2420. <https://doi.org/dx.doi.org/10.1021/cb500499x>.
- (168) Grigory S. Filonov; Jared D. Moon; Nina Svensen; Samie R. Jaffrey. Broccoli: Rapid Selection of an RNA Mimic of Green Fluorescent Protein by Fluorescence-Based Selection and Directed Evolution. *Journal of the American Chemical Society* **2014**, *136*, 16299–16308. <https://doi.org/dx.doi.org/10.1021/ja508478x>.
- (169) Wenjiao Song; Grigory S. Filonov; Hyaeyeong Kim; Markus Hirsch; Xing Li; Jared D. Moon; Samie R. Jaffrey. Imaging RNA Polymerase III Transcription Using a Photostable RNA-Fluorophore Complex. *Nature Chemical Biology* **2017**, *13*, 1187–1194. <https://doi.org/doi:10.1038/nchembio.2477>.
- (170) Rita L. Strack; Wenjiao Song; Samie R. Jaffrey. Using Spinach-Based Sensors for Fluorescence Imaging of Intracellular Metabolites and Proteins in Living Bacteria. *Nature Protocols* **2014**, *9* (1), 146–155. <https://doi.org/10.1038/nprot.2014.001>.
- (171) Maho Okuda; Dominique Fourmy; Satoko Yoshizawa. Use of Baby Spinach and Broccoli for Imaging of Structured Cellular RNAs. *Nucleic Acids Research* **2017**, *45* (3), 1404–1415. <https://doi.org/10.1093/nar/gkw794>.
- (172) Rita L. Strack; Samie R. Jaffrey. Live-Cell Imaging of Mammalian RNAs with Spinach2. *Methods in Enzymology* **2015**, *550*. <http://dx.doi.org/10.1016/bs.mie.2014.10.044>.
- (173) Aruni P. K. K. Karunanayake Mudiyansele; Qikun Yu; Mark A. Leon-Duque; Bin Zhao; Rigumula Wu; Mingxu You. Genetically Encoded Catalytic Hairpin Assembly for Sensitive RNA Imaging in Live Cells. *Journal of the American Chemical Society* **2018**, *140*, 8739–8745. <https://doi.org/doi:10.1021/jacs.8b03956>.
- (174) Puchakayala Swetha; Ze Fan; Fenglin Wang; Jian-Hui Jiang. Genetically Encoded Light-up RNA Aptamers and Their Applications for Imaging and Biosensing. *Journal of Materials Chemistry B* **2020**, *8*, 3382–3392. <https://doi.org/10.1039/c9tb02668a>.
- (175) Khalid K. Alam; Kwaku D. Tawiah; Matthew F. Lichte; David Porciani; Donald H. Burke. A Fluorescent Split Aptamer for Visualizing RNA-RNA Assembly *In Vivo*. *ACS Synthetic Biology* **2017**, *6*, 1710–1721. <https://doi.org/10.1021/acssynbio.7b00059>.
- (176) Na Li; Xin Huang; Jiawei Zou; Gangyi Chen; Getong Liu; Mei Li; Juan Dong; Feng Du; Xin Cui; Zhuo Tang. Evolution of Microbial Biosensor Based on Functional RNA through Fluorescence-Activated Cell Sorting. *Sensors and Actuators B* **2018**, *258*, 550–557. <https://doi.org/10.1016/j.snb.2017.11.015>.
- (177) Arghya Sett; Lorena Zara; Eric Dausse; Jean-Jacques Toulmé. Engineering Light-up Aptamers for the Detection of RNA Hairpins through Kissing Interaction. *Analytical Chemistry* **2020**, *92*, 9113–9117. <https://dx.doi.org/10.1021/acs.analchem.0c01378>.
- (178) Wenjiao Song; Rita L. Strack; Samie R. Jaffrey. Imaging Bacterial Protein Expression Using Genetically Encoded RNA Sensors. *Nature Methods* **2013**, *10* (9), 873–875. <https://doi.org/doi:10.1038/nmeth.2568>.
- (179) Simon Ausländer; David Fuchs; Samuel Hürlemann; David Ausländer; Martin Fussenegger. Engineering a Ribozyme Cleavage-Induced Split Fluorescent Aptamer Complementation Assay. *Nucleic Acids Research* **2016**, *44* (10). <https://doi.org/10.1093/nar/gkw117>.
- (180) Mingxu You; Jacob L. Litke; Rigumula Wu; Samie R. Jaffrey. Detection of Low-Abundance Metabolites in Live Cells Using an RNA Integrator. *Cell Chemical Biology* **2019**, *26*, 471–481. <https://doi.org/10.1016/j.chembiol.2019.01.005>.
- (181) Rigumula Wu; Aruni P. K. K. Karunanayake Mudiyansele; Fatemeh Shafiei; Bin Zhao; Yousef Bagheri; Qikun Yu; Kathleen McAuliffe; Kewei Ren; Mingxu You. Genetically Encoded Ratiometric RNA-Based Sensors for Quantitative Imaging of Small Molecules in Living Cells. *Angewandte Chemie International Edition* **2019**, *58* (50), 18271–18275.
- (182) Xianjun Chen; Dasheng Zhang; Ni Su; Bingkun Bao; Xin Xie; Fangting Zuo; Lipeng Yang; Hui Wang; Li Jiang; Qiuning Lin; Mengyue Fang; Ningfeng Li; Xin Hua; Zhengda Chen; Chunyan Bao; Jinjin Xu; Wenli Du; Lixin Zhang; Yuzheng Zhao; Linyong Zhu; Joseph Loscalzo; Yi Yang. Visualizing RNA Dynamics in Live Cells with Bright and Stable Fluorescent RNAs. *Nature Biotechnology* **2019**, *37*, 1287–1293. <https://doi.org/10.1038/s41587-019-0249-1>.
- (183) Jay D. Keasling. Synthetic Biology and the Development of Tools for Metabolic Engineering. *Metabolic Engineering* **2012**, *14*, 189–195. <https://doi.org/doi:10.1016/j.ymben.2012.01.004>.
- (184) Priscilla E. M. Purnick; Ron Weiss. The Second Wave of Synthetic Biology: From Modules to Systems. *Nature Reviews Molecular Cell Biology* **2009**, *10*, 410–422.
- (185) Daniel G. Gibson; Lei Young; Ray-Yuan Chuang; J. Craig Venter; Clyde A. Hutchison III; Hamilton O. Smith. Enzymatic Assembly of DNA Molecules up to Several Hundred Kilobases. *Nature Methods* **2009**, *6* No. 5, 343–345.
- (186) Carola Engler; Sylvestre Marillonnet. Golden Gate Cloning. *DNA Cloning and Assembly Methods* **2013**, 119–131.
- (187) Carola Engler; Romy Kandzia; Sylvestre Marillonnet. A One Pot, One Step, Precision Cloning Methods with High Throughput Capability. *PLOS ONE* **2008**, *3* (11).

- (188) Naoto Yoshida; Misa Sato. Plasmid Uptake by Bacteria: A Comparison of Methods and Efficiencies. *Applied Microbiology and Biotechnology* **2009**, *83*, 791–798. <https://doi.org/10.1007/s00253-009-2042->
- (189) K. Koga; T. Harada; H. Shimizu; K. Tanaka. Bacterial Luciferase Activity and the Intracellular Redox Pool in *Escherichia Coli*. *Molecular Genetics and Genomics* **2005**, *274*, 180–188. <https://doi.org/DOI.10.1007/s00438-005-0008-5>.
- (190) Lorenzo Galluzzi; Matti Karp. Intracellular Redox Equilibrium and Growth Phase Affect the Performance of Luciferase-Based Biosensors. *Journal of Biotechnology* **2007**, *127* (2). <https://doi.org/10.1016/j.jbiotec.2006.06.019>.
- (191) J. M. H. King; P. M. Digrazia; B. Applegate; R. Burlage; J. Sanseverino; P. Dunbar; F. Larimer; G. S. Saylor. Rapid, Sensitive Bioluminescent Reporter Technology for Naphthalene Exposure and Biodegradation. *Science* **1990**, *249* (4970), 778–781. <https://doi.org/DOI:10.1126/science.249.4970.778>.
- (192) Natalia Barger; Ilan Oren; Ximing Li; Mouna Habib; Ramez Daniel. A Whole-Cell Bacterial Biosensor for Blood Markers Detection in Urine. *ACS Synthetic Biology* **2021**, *10* (5), 1132–1142. <https://doi.org/10.1021/acssynbio.0c00640>.
- (193) Armin Heitzer; Ken Malachowsky; Janeen E. Thonnard; Paul R. Bienkowski; David C. White; Gary S. Saylor. Optical Biosensor for Environmental On-Line Monitoring of Naphthalene and Salicylate Bioavailability with an Immobilized Bioluminescent Catabolic Reporter Bacterium. *Applied and Environmental Microbiology* **1994**, *60* (5), 1487–1494. <https://doi.org/10.1128/aem.60.5.1487-1494.1994>.
- (194) Suzanne Leth; Susanna Maltoni; Remigijus Simkus; Bo Mattiasson; Philippe Corbisier; Ingo Klimant; Otto S. Wolfbeis; Elisabeth Csöregi. Engineered Bacteria Based Biosensors for Monitoring Bioavailable Heavy Metals. *Electroanalysis* **2002**, *14* (1), 35–42. [https://doi.org/10.1002/1521-4109\(200201\)14:1<35::AID-ELAN35>3.0.CO;2-W](https://doi.org/10.1002/1521-4109(200201)14:1<35::AID-ELAN35>3.0.CO;2-W).
- (195) Suk Tai Chang; Hyun Joo Lee; Man Bock Gu. Enhancement in the Sensitivity of an Immobilized Cell-Based Soil Biosensor for Monitoring PAH Toxicity. *Sensors and Actuators B: Chemical* **2004**, *97* (2–3), 272–276. <https://doi.org/10.1016/j.snb.2003.08.027>.
- (196) Andrew G. Kessenikh; Uliana S. Novoyatlova; Sergey V. Bazhenov; Eugeniya A. Stepanova; Svetlana A. Khrulnova; Eugeny Yu. Gnuchikh; Vera Yu. Kotova; Anna A. Kudryavtseva; Maxim V. Bermeshev; Ilya V. Manukhov. Constructing of *Bacillus Subtilis*-Based Lux-Biosensors with the Use of Stress-Inducible Promoters. *International Journal of Molecular Sciences* **2021**, *22* (17), 9571. <https://doi.org/10.3390/ijms22179571>.
- (197) Michael S. Allen; John R. Wilgus; Christopher S. Chewning; Gary S. Saylor; Michael L. Simpson. A Destabilized Bacterial Luciferase for Dynamic Gene Expression Studies. *Systems and Synthetic Biology* **2007**, *1*, 3–9. <https://doi.org/10.1007/s11693-006-9001-5>.
- (198) Rafael Jose Vivero-Gomez; Gustavo Bedoya Mesa; Jorge Higueta-Castro; Sara M. Robledo; Claudia X. Moreno-Herrera; Gloria Cadavid-Restrepo. Detection of Quorum Sensing Signal Molecules, Particularly N-Acyl Homoserine Lactones, 2-Alkyl-4-Quinolones, and Diketopiperazines, in Gram-Negative Bacteria Isolated From Insect Vector of Leishmaniasis. *Frontiers in Tropical Diseases* **2021**, *2*. <https://doi.org/10.3389/ftd.2021.760228>.
- (199) Amy C. Vollmer; Shimshon Belkin; Dana R. Smulski; Tina K. Van Dyk; Robert A. Larossa. Detection of DNA Damage by Use of *Escherichia Coli* Carrying *recA*'::Lux, *uvrA*'::Lux, or *alkA*'::Lux Reporter Plasmids. *Applied and Environmental Microbiology* **1997**, *63* (7), 2566–2571. <https://doi.org/10.1128/aem.63.7.2566-2571.1997>.
- (200) Deirdre R. Coombe; Anne-Marie Nakhoul; Sandra M. Stevenson; Susanne E. Peroni; Colin J. Sanderson. Expressed Luciferase Viability Assay (ELVA) for the Measurement of Cell Growth and Viability. *Journal of Immunological Methods* **1998**, *215* (1–2), 145–150. [https://doi.org/10.1016/S0022-1759\(98\)00081-7](https://doi.org/10.1016/S0022-1759(98)00081-7).
- (201) Siouxsie Wiles; Kathryn Ferguson; Martha Stefanidou; Douglas B. Young; Brian D. Robertson. Alternative Luciferase for Monitoring Bacterial Cells under Adverse Conditions. *Applied and Environmental Microbiology* **2005**, *71* (7), 3427–3432. <https://doi.org/10.1128/AEM.71.7.3427-3432.2005>.
- (202) Melissa L. Sykes; Vicky M. Avery. A Luciferase Based Viability Assay for ATP Detection in 384-Well Format for High Throughput Whole Cell Screening of *Trypanosoma Brucei Brucei* Bloodstream Form Strain 427. *Parasites & Vectors* **2009**, *2*, 54. <https://doi.org/10.1186/1756-3305-2-54>.
- (203) Hideto Hoshino; Yoshihiro Nakajima; Yoshihiro Ohmiya. Luciferase-YFP Fusion Tag with Enhanced Emission for Single-Cell Luminescence Imaging. *Nature Methods* **2007**, *4*, 637–639. <https://doi.org/10.1038/nmeth1069>.
- (204) Sunil Nooti; Madison Naylor; Trevor Long; Brayden Groll; Manu. LucFlow: A Method to Measure Luciferase Reporter Expression in Single Cells. *PLOS ONE* **2023**, *18* (10), e0292317. <https://doi.org/10.1371/journal.pone.0292317>.
- (205) Medhi Snoussi; John Paul Talledo; Nathan-Alexander Del Rosario; Salimeh Mohammadi; Bae-Yeun Ha; Andrej Kosmrlj; Sattar Taheri-Araghi. Heterogeneous Absorption of Antimicrobial Peptide LL37 in

- Escherichia Coli* Cells Enhances Population Survivability. *eLIFE* **2018**, *7*, e38174. <https://doi.org/10.7554/eLife.38174>.
- (206) Jara Radek; Korinna Kraft; Julia Bartels; Tamara Cikovic; Franziska Dürr; Jennifer Emenegger; Simon Kelterborn; Christopher Sauer; Georg Fritz; Susanne Gebhard; Thorsten Mascher. The Bacillus BioBrick Box: Generation and Evaluation of Essential Genetic Building Blocks for Standardized Work with *Bacillus Subtilis*. *Journal of Biological Engineering* **2013**, *7*:29. <https://doi.org/10.1186/1754-1611-7-29>.
- (207) Francois St-Pierre; Lun Cui; David G. Priest; Drew Endy; Ian B. Dodd; Keith E. Shearwin. One-Step Cloning and Chromosomal Integration of DNA. *ACS Synthetic Biology* **2013**, *2*, 537–541. <https://doi.org/10.1021/sb400021j>.
- (208) Jin Yin; Huan Wang; Xiao-Zhi Fu; Xue Cao; Qiong Wu; Guo-Qiang Chen. Effects of Chromosomal Gene Copy Number and Locations on Polyhydroxyalkanoate Synthesis by *Escherichia Coli* and *Halomonas Sp.* *Applied Microbiology and Biotechnology* **2015**, *99*, 5523–5534. <https://doi.org/doi:10.1007/s00253-015-6510-8>.
- (209) Andrea Sabido; Luz María Martínez; Ramón de Anda; Alfredo Martínez; Francisco Bolívar; Guillermo Gosset. A Novel Plasmid Vector Designed for Chromosomal Gene Integration and Expression: Use for Developing a Genetically Stable *Escherichia Coli* Melanin Production Strain. *Plasmid* **2013**, *69*, 16–23. <http://dx.doi.org/10.1016/j.plasmid.2012.04.005>.
- (210) Hannah E. Chia; E. Neil G. Marsh; Julie S. Biteen. Extending Fluorescence Microscopy into Anaerobic Environments. *Current Opinion in Chemical Biology* **2019**, *51*, 98–104. <https://doi.org/10.1016/j.cbpa.2019.05.008>.
- (211) Asha A. Philip; Jacob L. Perry; Heather E. Eaton; Maya Shmulevitz; Joseph M. Hyser; John T. Patton. Generation of Recombinant Rotavirus Expressing NSP3-UnaG Fusion Protein by a Simplified Reverse Genetics Systems. *Journal of Virology* **2019**, *93* (24), e01616-19. <https://doi.org/10.1128/JVI.01616-19>.
- (212) Jiwoong Kwon; Jong-Seok Park; Minsu Kang; Soobin Choi; Jumi Park; Gyeong Tae Kim; Changwook Lee; Sangwon Cha; Hyun-Woo Rhee; Sang-Hee Shim. Bright Ligand-Activable Fluorescent Protein for High-Quality Multicolor Live-Cell Super-Resolution Microscopy. *Nature communications* **2020**, *11* (273).
- (213) Raul Navarro; Ling-chun Chen; Rishi Rakhit; Thomas J. Wandless. A Novel Destabilizing Domain Based on a Small-Molecule Dependent Fluorophore. *ACS chemical biology* **2016**, *11* (8), 2101–2104.
- (214) Shinan Liu; Fei Gao; Ruijie Wang; Wen Li; Siyao Wang; Xi Zhang. Molecular Characteristics of the Fatty-Acid-Binding Protein (FABP) Family in *Spirometra Mansoni* - A Neglected Medical Tapeworm. *Animals* **2023**, *13* (18). <https://doi.org/10.3390/ani13182855>.
- (215) Jittiyawadee Sriipa; Thewarach Laha; Banchob Sriipa. Characterization and Functional Analysis of Fatty Acid Binding Protein from the Carcinogenic Liver Fluke, *Opisthorchis Viverrini*. *Parasitology International* **2017**, *66* (4), 419–425. <https://doi.org/10.1016/j.parint.2016.04.009>.
- (216) Alicia Climent-Catala; Ivan Casas-Rodrigo; Suhasini Iyer; Rodrigo Ledesma-Amaro; Thomas E. Ouldridge. Evaluating DFHBI-Responsive RNA Light-Up Aptamers as Fluorescent Reporters for Gene Expression. *ACS Synthetic Biology* **2023**, *12* (12), 3754–3765. <https://doi.org/10.1021/acssynbio.3c00599>.
- (217) Alicia Climent-Catala; Thomas E. Ouldridge; Guy-Bart V. Stan; Wooli Bae. Building an RNA-Based Toggle Switch Using Inhibitory RNA Aptamers. *ACS Synthetic Biology* **2022**, *11* (2), 562–569. <https://doi.org/10.1021/acssynbio.1c00580>.
- (218) Ru Zheng; Rigumula Wu; Yuanchang Liu; Zhining Sun; Yousef Bagheri; Zhaolin Xue; Lan Mi; Qian Tian; Raymond Pho; Sidrat Siddiqui; Kewei Ren; Mingxu You. Multiplexed Sequential Imaging in Living Cells with Orthogonal Fluorogenic RNA Aptamer/Dye Pairs. *bioRxiv [Preprint]* **2023**. <https://doi.org/doi:10.1101/2023.04.20.537750>.
- (219) Ellen L. Legendijk; Shamil Validov; Gerda E. M. Lamers; Sandra De Weert; Guido V. Bloemberg. Genetic Tools for Tagging Gram-Negative Bacteria with mCherry for Visualization *in Vitro* and in Natural Habitats, Biofilm and Pathogenicity Studies. *FEMS Microbiology Letters* **2010**, *305* (1), 81–90. <https://doi.org/10.1111/j.1574-6968.2010.01916.x>.
- (220) Fuminori Kato; Motoki Nakamura; Motoyuki Sugai. The Development of Fluorescent Protein Tracing Vectors for Multicolor Imaging of Clinically Isolated *Staphylococcus Aureus*. *Scientific reports* **2017**, *7*, 2865. <https://doi.org/10.1038/s41598-017-02930-7>.
- (221) N. Hever; S. Belkin. A Dual-Color Bacterial Reporter Strain for the Detection of Toxic and Genotoxic Effects. *Engineering in Life Sciences* **2006**, *6* (3), 319–323. <https://doi.org/10.1002/elsc.200620132>.
- (222) Chang-Ye Hui; Yan Guo; Han Li; Yu-ting Chen; Juan Yi. Differential Detection of Bioavailable Mercury and Cadmium Based on a Robust Dual-Sensing Bacterial Biosensor. *Frontiers in Microbiology* **2022**, *13*. <https://doi.org/10.3389/fmicb.2022.846524>.
- (223) P. L. Ho; Y. Y. Cheung; Y. Wang; W. U. Lo; E. L. Y. Lai; K. H. Chow; V. C. C. Cheng. Characterization of Carbapenem-Resistant *Escherichia Coli* and *Klebsiella Pneumoniae* from a Healthcare Region in Hong Kong. *European Journal of Clinical Microbiology & Infectious Diseases* **2016**, *35*, 379–385.

- (224) Rabab R. Makharita; Iman El-kholy; Helal F. Hetta; Moahmed H. Abdelaziz; Fatma I. Hagagy; Amara A. Ahmed; Abdelazeem M. Algammal. Antibigram and Genetic Characterization of Carbapenem-Resistant Gram-Negative Pathogens Incriminated in Healthcare-Associated Infections. *Infection and Drug Resistance* **2020**, *13*, 3991–4002.
- (225) A. Balkhair; K. Al. Saadi; B. Al Adawi. Epidemiology and Mortality Outcome of Carbapenem- and Colistin-Resistant *Klebsiella Pneumoniae*, *Escherichia Coli*, *Acinetobacter Baumannii*, and *Pseudomonas Aeruginosa* Bloodstream Infections. *IJID Regions* **2023**, *7*, 1–5. <https://doi.org/10.1016/j.ijregi.2023.01.002>.
- (226) Sarah S. Tang; Anucha Apisarnthanarak; Li Yang Hsu. Mechanisms of β -Lactam Antimicrobial Resistance and Epidemiology of Major Community- and Healthcare-Associated Multidrug-Resistant Bacteria. *Advanced Drug Delivery Reviews* **2014**, *78*, 3–13.
- (227) Borna Mehrdad; Nina M. Clark; George G. Zhanel; Lynch Joseph. Antimicrobial Resistance in Hospital-Acquired Gram-Negative Bacterial Infections. *Contemporary Reviews in Critical Care Medicine* **2015**, *147* (5), 1413–1421. <https://doi.org/10.1378/chest.14-2171>.
- (228) Yihiene M. Bezabih; Alemayehu Bezabih; Michel Dion; Eric Batard; Samson Tekla; Abiy Obole; Noah Dessalegn; Alelegn Enyew; Anna Roujeinikova; Endalkachew Alamneh; Corinne Mirkazemi; Gregory M. Peterson; Wolde Sellassie M. Bezabhe. Comparison of the Global Prevalence and Trend of Human Intestinal Carriage of ESBL-Producing *Escherichia Coli* between Healthcare and Community Settings: A Systematic Review and Meta-Analysis. *JAC-Antimicrobial Resistance* **2022**, *4* (3). <https://doi.org/10.1093/jacamr/dlac048>.
- (229) Hadir A. El-Mahallawy; Marwa El Swify; Asmaa Abdul Hak; Mai M. Zafer. Increasing Trends of Colistin Resistance in Patients at High-Risk of Carbapenem-Resistant *Enterobacteriaceae*. *Annals of Medicine* **2022**, *54* (1), 2748–2756. <https://doi.org/10.1080/07853890.2022.2129775>.
- (230) Yasuhide Kawamoto; Norihito Kaku; Norihiko Akamatsu; Kei Sakamoto; Kosuke Kosai; Yoshitomo Morinaga; Norio Ohmagari; Koichi Izumikawa; Yoshihiro Yamamoto; Hiroshige Mikamo; Mitsuo Kaku; Kazunori Oishi; Katsunori Yanagihara. The Surveillance of Colistin Resistance and Mobilized Colistin Resistance Genes in Multidrug-Resistant *Enterobacteriaceae* Isolated in Japan. *International Journal of Antimicrobial Agents* **2022**, *59* (1). <https://doi.org/10.1016/j.ijantimicag.2021.106480>.
- (231) Masoud Dadashi; Fatemeh Sameni; Nazila Bostanshirin; Somayeh Yaslianifard; Nafiseh Khosravi-Dehaghi; Mohammad Javad Nasiri; Mehdi Goudarzi; Ali Hashemi; Bahareh Hajikhani. Global Prevalence and Molecular Epidemiology of Mcr-Mediated Colistin Resistance in *Escherichia Coli* Clinical Isolates: A Systematic Review. *Journal of Global Antimicrobial Resistance* **2022**, *29*, 444–461. <https://doi.org/10.1016/j.jgar.2021.10.022>.
- (232) Umji Choi; Chang-Ro Lee. Distinct Roles of Outer Membrane Porins in Antibiotic Resistance and Membrane Integrity in *Escherichia Coli*. *Frontiers in Microbiology* **2019**, *10*. <https://doi.org/10.3389/fmicb.2019.00953>.
- (233) Hiroshi Nikaiko. Outer Membrane Barrier as a Mechanism of Antimicrobial Resistance. *Antimicrobial Agents and Chemotherapy* **1989**, *33* (11), 1831–1836.
- (234) Anne H. Delcour. Outer Membrane Permeability and Antibiotic Resistance. *Biochimica et Biophysica Acta* **2009**, *1794* (5), 808–816.
- (235) Kristina Klobucar; Eric D. Brown. New Potentiators of Ineffective Antibiotics: Targeting the Gram-Negative Outer Membrane to Overcome Intrinsic Resistance. *Current Opinion in Chemical Biology* **66**. <https://doi.org/10.1016/j.cbpa.2021.102099>.
- (236) Scott S. Walker; Todd A. Black. Are Outer-Membrane Targets the Solution for MDR Gram-Negative Bacteria? *Drug Discovery Today* **2021**, *26* (9), 2152–2158. <https://doi.org/10.1016/j.drudis.2021.03.027>.
- (237) Craig R. MacNair; Caressa N. Tsai; Eric D. Brown. Creative Targeting of the Gram-Negative Outer Membrane in Antibiotic Discovery. *Annals of the New York Academy of Sciences* **2020**, *1459*, 69–85. <https://doi.org/10.1111/nyas.14280>.
- (238) Robert E. W. Hancock; Patrick G. W. Wong. Compounds Which Increase the Permeability of the *Pseudomonas Aeruginosa* Outer Membrane. *Antimicrobial Agents and Chemotherapy* **1984**, *26* (1), 48–52. <https://doi.org/10.1128/aac.26.1.48>.
- (239) Robert E. W. Hancock; Susan W. Farmer. Mechanism of Uptake of Deglucoteicoplanin Amide Derivatives across Outer Membranes of *Escherichia Coli* and *Pseudomonas Aeruginosa*. *Antimicrobial Agents and Chemotherapy* **1993**, *37* (3), 453–456. <https://doi.org/10.1128/aac.37.3.453>.
- (240) Juan Carlos Espeche; Melina Martínez; Patricia Maturana; Andrea Cutró; Liliana Semorile; Paulo C. Maffia; Axel Hollmann. Unravelling the Mechanism of Action of “de Novo” Designed Peptide P1 with Model Membranes and Gram-Positive and Gram-Negative Bacteria. *Archives of Biochemistry and Biophysics* **2020**, *693*, 108549. <https://doi.org/10.1016/j.abb.2020.108549>.
- (241) Swaleeha Jaan Abdullah; Bernice Tan Siu Yan; Nithya Palanivelu; Vidhya Bharathi Dhanabal; Juan Pablo Bifani; Surajit Bhattachariya. Outer-Membrane Permeabilization, LPS Transport Inhibition: Activity,




- Interactions, and Structures of Thanatin Derived Antimicrobial Peptides. *International Journal of Molecular Sciences* **2024**, *25* (4), 2122. <https://doi.org/10.3390/ijms25042122>.
- (242) S. Betty Zou; Steven J. Hersch; Hervé Roy; J. Brad Wiggers; Andrea S. Leung; Stephen Buranyi; Jinglin Lucy Xie; Kiley Dare; Michael Ibba; William Wiley Navarre. Loss of Elongation Factor P Disrupts Bacterial Outer Membrane Integrity. *Journal of Bacteriology* **2012**, *194* (2). <https://doi.org/10.1128/jb.05864-11>.
- (243) Mareike Hartmann; Marina Berditsch; Jacques Hawecker; Mohammad Fotouhi Ardakani; Dagmar Gerthsen; Anne S. Ulrich. Damage of the Bacterial Cell Envelope by Antimicrobial Peptides Gramicidin S and PGLa as Revealed by Transmission and Scanning Electron Microscopy. *Antimicrobial Agents and Chemotherapy* **2010**, *54* (8). <https://doi.org/10.1128/aac.00124-10>.
- (244) Attila Farkas; Gergely Maróti; Attila Kereszt; Éva Kondorosi. Comparative Analysis of the Bacterial Membrane Disruption Effect of Two Natural Plant Antimicrobial Peptides. *Frontiers in Microbiology* **2017**, *8*. <https://doi.org/10.3389/fmicb.2017.00051>.
- (245) Klara Stensvåg; Tor Haug; Sigmund V. Sperstad; Oystein Rekdal; Bård Indrevoll; Olaf B. Styrvold. Arasin 1, a Proline-Arginine-Rich Antimicrobial Peptide Isolated from the Spider Crab, *Hyas Araneus*. *Developmental and Comparative Immunology* **2007**, *32* (3), 275–285. <https://doi.org/10.1016/j.dci.2007.06.002>.
- (246) Victoria S. Paulsen; Hans-Matti Blencke; Monica Benincasa; Tor Haug; Jacobus J. Eksteen; Olaf B. Styrvold; Marco Scocchi; Klara Stensvåg. Structure-Activity Relationships of the Antimicrobial Peptide Arasin 1 - And Mode of Action Studies of the N-Terminal, Proline-Rich Region. *PLOS ONE* **2013**, *8* (1).
- (247) Gary M. Decad; Hiroshi Nikaiko. Outer Membrane of Gram-Negative Bacteria XII. Molecular-Sieving Function of Cell Wall. *Journal of Bacteriology* **1976**, *128*, No. 1, 325–336.
- (248) Marcus Krüger; Peter Richter; Sebastian M. Strauch; Adeel Nasir; Andreas Burkovski; Camila A. Antunes; Tina Meißgeier; Eberhard Schlücker; Stefan Schwab; Michael Lebert. What an *Escherichia Coli* Mutant Can Teach Us About the Antibacterial Effect of Chlorophyllin. *Microorganisms* **2019**, *7* (2), 59. <https://doi.org/10.3390/microorganisms7020059>.
- (249) David J. Sherman; Suguru Okuda; William A. Denny; Daniel Kahne. Validation of Inhibitors of an ABC Transporter Required to Transport Lipopolysaccharide to the Cell Surface in *Escherichia Coli*. *Bioorganic & Medicinal Chemistry* **2013**, *21* (16), 4846–4851. <https://doi.org/10.1016/j.bmc.2013.04.020>.
- (250) Chih-Lung Wu; Kuang-Li Peng; Bak-Sau Yip; Ya-Han Chih; Jya-Wei Cheng. Boosting Synergistic Effects of Short Antimicrobial Peptides With Conventional Antibiotics Against Resistant Bacteria. *Frontiers in Microbiology* **2021**, *12*, 747760. <https://doi.org/10.3389/fmicb.2021.747760>.
- (251) Jane A. Rees; Marc Moniatte; Philippe Bulet. Novel Antibacterial Peptides Isolated from a European Bumblebee, *Bomus Pascuorum* (Hymenoptera, Apoidea). *Insect Biochemistry and Molecular Biology* **1997**, *27* (5), 413–422. [https://doi.org/10.1016/S0965-1748\(97\)00013-1](https://doi.org/10.1016/S0965-1748(97)00013-1).
- (252) Mohammad Rahnamaeian; Małgorzata Cytryńska; Agnieszka Zdybicka-Barabas; Kristin Dobszlaff; Jochen Wiesner; Richard M. Twyman; Thole Zuchner; Ben M. Sadd; Roland R. Regoes; Paul Schmid-Hempel; Andreas Vilcinskas. Insect Antimicrobial Peptides Show Potentiating Functional Interactions against Gram-Negative Bacteria. *Proceedings Royal Society B* **2015**, *282*, 20150293. <http://dx.doi.org/10.1098/rspb.2015.0293>.
- (253) Sarah E. Stewart; Stephanie C. Kondos; Antony Y. Matthews; Michael E. D’Angelo; Michelle A. Dunstone; James C. Whisstock; Joseph A. Trapani; Phillip I. Bird. The Perforin Pore Facilitates the Delivery of Cationic Cargos. *The Journal of Biological Chemistry* **2014**, *289* (13), 9172–9181. <https://doi.org/DOI.10.1074/jbc.M113.544890>.

Paper I

Antimicrobial Activity of Securamines From the Bryozoan *Securiflustra securifrons*

Natural Product Communications
Volume 16(2): 1–8
© The Author(s) 2021
DOI: 10.1177/1934578X21996180
journals.sagepub.com/home/npx



Kine Ø. Hansen¹ , Ida K. Ø. Hansen², Céline S. Richard² , Marte Jenssen¹, Jeanette H. Andersen¹, and Espen H. Hansen¹ 

Abstract

Natural products and their derivatives have served as powerful therapeutics against pathogenic microorganisms and are the mainstay of our currently available treatment options to combat infections. As part of our ongoing search for antimicrobial natural products from marine organisms, one fraction prepared from the Arctic marine bryozoan *Securiflustra securifrons* was found to be active against the human pathogenic bacterium *Streptococcus agalactiae* (gr. B). Chemical investigation of the fraction revealed that it contained several variants of the highly modified secondary metabolites known as securamines. The securamines are alkaloids sharing a common isoprene-histamine-tryptamine backbone. In this study, we describe the antimicrobial activities of securamine C, E, and H – J (4, 5, and 1-3) and the attempt to deconvolute the mode of action of 1.

Keywords

marine bryozoan, *Securiflustra securifrons*, alkaloids, bioactivity, marine bioprospecting

Received: December 4th, 2020; Accepted: January 13th, 2021.

The increasing prevalence of antibiotic resistant pathogens is recognized as one of the most serious global threats to human health in the 21st century. Extensive use of antimicrobials together with declining investments into discovery and development of new treatment options to combat pathogens have aggravated the problem.¹ Novel classes of antibiotics are therefore urgently needed for the future. In the search for new antimicrobial agents, nature remains the richest and most versatile source.^{2,3} In fact, close to 80% of all marketed anti-infective agents originate from a natural source.⁴

Bryozoans are a phylum of suspension-feeding mainly colonial invertebrates found in aquatic benthic ecosystems throughout the world.⁵ They generally form sessile colonies of genetically identical, polymorphic units termed zooids.^{6,7} These colonies are extremely vulnerable to biofouling, predation by grazers and pathogenic attacks.^{8,9} In order to thrive in this hostile environment, bryozoans have developed a chemical defense strategy, in which potent secondary metabolites are produced to combat these external threats. As a result, bryozoan biomass has yielded several structurally diverse bioactive secondary metabolites. The best known examples are the bryostatins, isolated from *Bugula neritina* (Linnaeus, 1758), some of which are under clinical development as an anticancer drug candidate for combination therapy¹⁰ and neurological disorders.¹¹⁻¹³

As part of our ongoing search for bioactive secondary metabolites from marine organisms, the organic extract of *Securiflustra securifrons* (Pallas, 1766) was prepared into eight

fractions and tested for antibacterial activity. Fraction three was found to be active against the pathogenic bacterium *Streptococcus agalactiae* (Gr. B). Previously, fraction five of the same extract was found to be active against a human melanoma cancer cell line.^{14,15} The components found to be responsible for the cytotoxicity in this fraction were the hexacyclic alkaloids securamine C (4), E (5), and H – J (1-3) (Figure 1). The structures and cytotoxic properties of 1-5 have been reported by our group.¹⁴ HRMS analysis of the fraction showing antibacterial activity revealed the presence of securamines. The antimicrobial properties of the securamines have not been previously examined. This, coupled with the knowledge that nature has provided a wealth of promising lead structures for antimicrobial development,¹⁶⁻¹⁸ motivated an investigation into the antimicrobial potential of the securamines.

¹Marbio, UiT–The Arctic University of Norway, Breivika, Tromsø, Norway

²Norwegian College of Fishery Science, UiT - The Arctic University of Norway, Breivika, Norway

Corresponding Author:

Kine Ø. Hansen, Marbio, UiT–The Arctic University of Norway, Breivika, Tromsø N-9037, Norway.
Email: kine.o.hanssen@uit.no



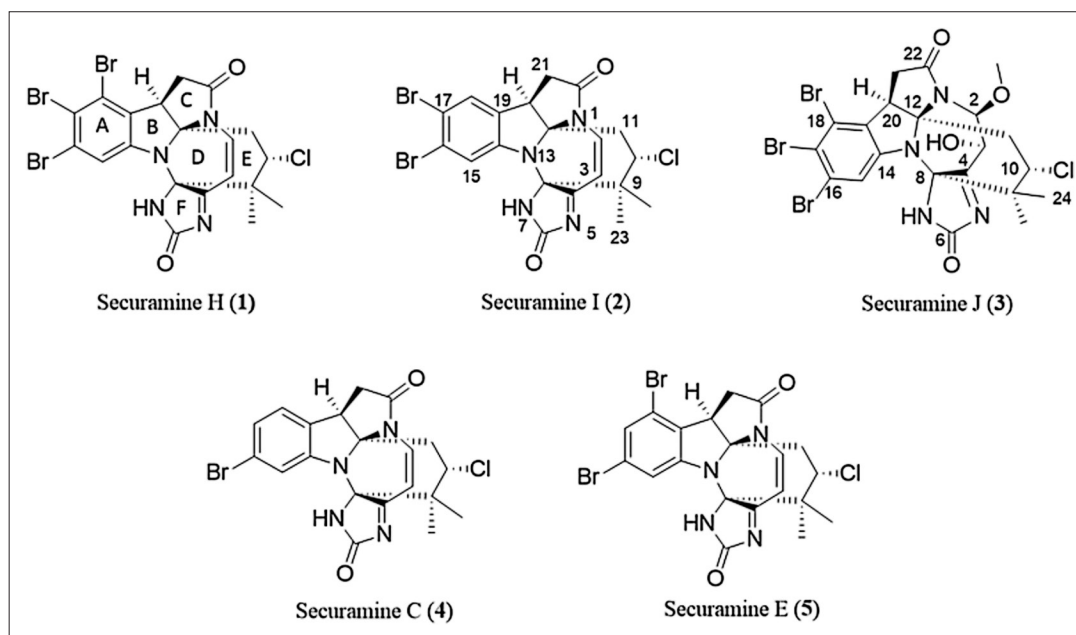


Figure 1. Structures of securamine C, E, and H – J (4, 5, and 1-3) isolated from the organic extract of the Arctic marine bryozoan *Securiflustra securifrons*.

Results and Discussion

Biomass, Extraction, Fractionation, Compound Isolation, and Structure Elucidation

The biomass of *S. securifrons* was collected off the coast of Hjelmsøya, freeze dried and subjected to liquid-liquid extraction, providing an aqueous and an organic extract. The organic extract was fractionated into eight fractions using flash

Table 1. MIC (μM) of Securamine H-J, C, and E (1-5) Against four G+ and two G- Bacterial Strains, Against *Staphylococcus epidermidis* Biofilm Formation, and Against three Yeast Strains.

Microorganisms	Minimum inhibitory concentration (μM)				
	1	2	3	4	5
G+ bacteria:					
<i>Bacillus subtilis</i>	6.25	>50	>50	>50	>50
<i>Staphylococcus aureus</i>	3.13	12.5	>50	>50	25
<i>Enterococcus faecalis</i>	6.25	25	>50	>50	50
<i>Streptococcus agalactiae</i> (Gr. B)	6.25	25	>50	>50	25
G- bacteria:					
<i>Escherichia coli</i>	>50	>50	>50	>50	>50
<i>Pseudomonas aeruginosa</i>	>50	>50	>50	>50	>50
Biofilm formation:					
<i>Staphylococcus epidermidis</i>	>50	>50	>50	>50	>50
Yeast:					
<i>Candida albicans</i>	>50	>50	>50	>50	>50
<i>Rhodotorula sp.</i>	>50	>50	>50	>50	>50
<i>Aureobasidium pullulans</i>	>50	>50	>50	>50	>50

chromatography. Compounds 1-5 were isolated using mass guided semi-preparative HPLC and their structures elucidated using spectroscopic methods (HRMS, 1D- and 2D-MNR), as previously described.¹⁴

Antibacterial Screening and Chemical Investigation of the Flash Fractions of *S. securifrons*

The flash fractions of the organic *S. securifrons* extract were assayed for activity against the pathogenic bacterial strains *S. aureus*, *E. faecalis*, *E. coli*, *P. aeruginosa*, and *S. agalactiae* (Gr. B) at 250 $\mu\text{g}/\text{mL}$. Flash fraction three (eluting at 50% MeOH) was found to be active against the G+ bacterium *S. agalactiae* (Gr. B). Fraction three was inactive against the remaining bacteria and the remaining fractions were inactive against all bacteria. Chemical analysis of the fraction using UHPLC-HRMS revealed that it contained compounds belonging to the securamine family, including compounds 1, 2, 4, and 5.

Antimicrobial Activity of 1-5

The MIC values of compounds 1-5 were determined against four G+ and two G- bacterial strains, three yeast strains and toward the biofilm formation capability of *S. epidermidis* (Table 1, online supplementary file). Compounds 1, 2, and 5 showed activity against all or most of the G+ strains. No activity was found toward the G- bacteria, the yeast strains or against biofilm formation at the highest assay concentration (50 μM).

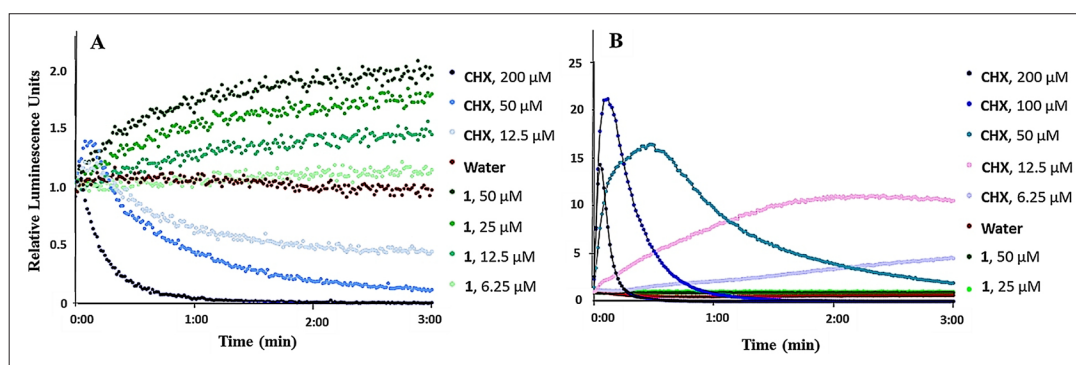


Figure 2. Kinetics of the relative luminescence emission by **A)** *B. subtilis* (pCSS962) and **B)** *E. coli* (pCSS962) treated with ranging concentrations of either securamine H (**1**) or chlorhexidine (CHX). Each point is the mean of three independent measurements. CHX and water were used as positive and negative controls, respectively.

Based on these results it appears that a double bond in the D-ring between C-2 and C-3 and more than one bromine on the A-ring at C-16, C-17, and/or C-18 are important for the antibacterial activity of the securamines. This observed structure activity relationship (SAR) correlates well with the previously reported SAR of the securamines against melanoma, lung and breast cancer cell lines,¹⁴ where **1**, **2**, **4**, and **5** inhibited cell viability. The lowest MIC value, 3.13 μM , was measured for **1** against *S. aureus*. Compound **1** is brominated at C-16, C-17, and C-18, and has a double bond between C-2 and C-3. This could indicate that the activities of the securamines against both bacteria and cancer cell lines are caused by an unspecific interaction with and disruption of biological membrane integrity. This is, however, unlikely, as the herein assayed eukaryotic yeast strains were unaffected by the securamines at the highest assayed concentration (50 μM), indicating an unrelated intracellular target in the cancer- and bacteria cells. Compound **1** showed the broadest and most potent inhibition, with MIC values ranging from 3.13 to 6.25 μM against the G+ bacteria, and was, therefore, chosen for further investigation.

Real-Time Measurement of Membrane Integrity of Bacteria When Exposed to **1**

B. subtilis and *E. coli*, carrying the pCSS962 plasmid with the LucGR gene, were used to assess the membrane disruptive properties of **1**. The strains express eukaryotic luciferase and will emit luminescence if their membrane is disrupted and D-luciferin from the growth medium is allowed to diffuse into the cell.¹⁹ If the bacterial cells die following membrane disruption, an initial rise in relative luminescence units (RLU) caused by D-luciferin influx, will be followed by declining RLU values as bacterial ATP reserves are exhausted and the enzymatic reaction consequently stopped. The luminescence measurements of *B. subtilis* and *E. coli* after exposure to ranging concentrations of **1** or chlorhexidine (CHX, positive control), an antibiotic known for its cell wall and membrane-disruptive activities,²⁰ can be seen in Figure 2. CHX treated *B. subtilis* gave

an initial increase followed by a decrease in RLU values. In contrast to this, **1** caused a persistent increase in light emission from the cells within the 3 minutes assay time at the 3 hours highest concentrations tested (12.5, 25, and 50 μM ; 2, 4, and 8 \times the MIC value of 6.25 μM , respectively). This increase was most likely caused by an increased D-luciferin influx into the cells caused by effects on the membrane. This effect does however not appear to affect the viability of *B. subtilis*, as the ATP reserves in the bacteria are not exhausted and resultantly no delayed drop in RLU was observed, indicating that the effect of **1** was different from that of CHX. The lack of a drop in ATP reserves following *B. subtilis* exposure to **1** furthermore indicates that **1** is bacteriostatic rather than bactericidal at the highest assayed concentrations. At 6.25 μM (and at lower concentrations, data not shown) **1** did not cause an influx of D-luciferin, as relative light emission remained equal to the water control. In contrast to CHX, no substantial increase in D-luciferin uptake and thus no effect on plasma membrane integrity of *E. coli* could be detected for **1**, even at the highest assayed concentrations (Figure 2(B)).

Assessment of the Membrane Potential of Bacteria When Exposed to **1**

To elucidate further if **1** affected the membrane integrity of *B. subtilis* directly, the membrane potential of *B. subtilis* was measured after 3 minutes exposure to ranging concentrations of **1**. Bacterial cells were stained with a membrane potential sensitive dye and subsequently analyzed by flow cytometry. The assay is based on the use of 3,3'-diethylcarbocyanine iodide (DiOC₂(3)), the fluorescence of which shifts from green to red in response to higher cytosolic concentrations in cells with active membrane potential where the dye aggregates. Ratiometric analysis of green to red fluorescence allows for estimating changes in membrane potential of bacteria.²¹ CHX and carbonyl cyanide m-chlorophenylhydrazone (CCCP) were used as positive and negative controls, respectively. CCCP blocks the generation of the electrochemical proton gradient, and thus lowers the

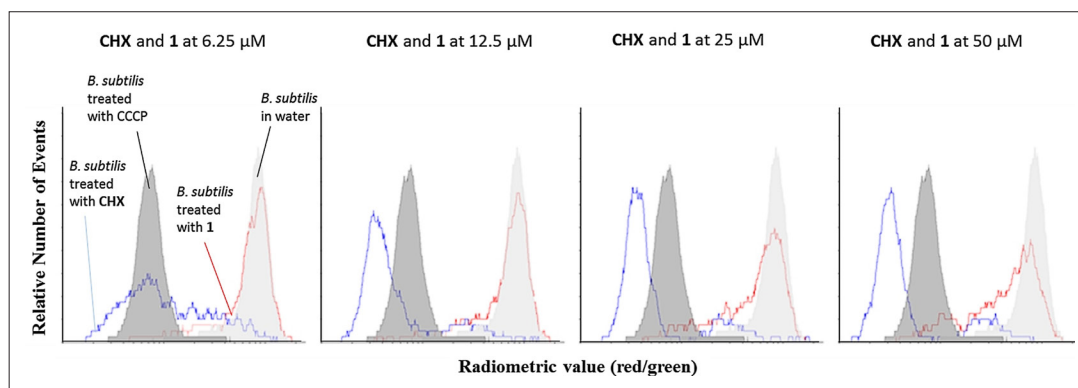


Figure 3. The effect of securamine H (**1**) in comparison to chlorhexidine (CHX) on the membrane potential of *B. subtilis*. The bacteria were treated for 3 minutes with ranging concentrations of either **1** or CHX and subsequently incubated for at least 30 minutes with 30 μM $\text{DiSO}_2(3)$. The overlaid histograms show the positive and the negative controls treated with 5 μM carbonyl cyanide m-chlorophenylhydrazone (CCCP) (shaded dark grey) and water (shaded light grey), respectively. Measurements depicting analysis of **1** are highlighted. The radiometric values (red/green) are depicted on the x axis, and the relative number of events on the y axis.

membrane potential in bacteria.²² Increasing concentrations of CHX decreased the ratio of red/green, showing that higher CHX concentrations result in a higher fraction of bacteria with disrupted membranes. For **1**, increased concentrations resulted in a decreased red/green ratio, but this decrease was significantly less marked compared to the CCCP and CHX controls. At the observed MIC (6.25 μM), only a slight shift was visible, further indicating that the activity of **1** was not due to direct membrane integrity disruption (Figure 3).

Effect of **1** on Bacterial Metabolism

We proceeded to evaluate whether **1** affected bacterial metabolism. *B. subtilis* carrying a chromosomal integration of a *lux-ABCDE*²³ operon and *E. coli* carrying the pCGLS-11²⁴ plasmid with a *Photobabidus luminescens* *lux* operon (*luxCDABE*) were used to assess the effect of **1** on bacterial cell viability measured in real-time. From these operons, the strains express a bacterial luciferase and fatty acid reductases for regeneration of long-chain fatty aldehydes, which serve as substrates for light production. Light production is therefore linked to

several metabolic processes, which in turn depend on the regeneration of reduction equivalents and ATP.^{25,26} While light production indicates active metabolism, loss of light production indicates a decrease in metabolic activity, and hence, reduced viability of the cells. The measured luminescence of *B. subtilis* and *E. coli* after addition of ranging concentrations of either **1** or CHX can be seen in Figure 4. At concentrations above the MIC (6.25 μM), **1** affected the viability of *B. subtilis* within the 3 minutes assay time (Figure 4(A)). Indeed, **1** elevated light emission by the strain at a similar level to CHX at 3.1 μM , resulting in a decrease of around 40% of relative luminescence units after 3 minutes. The decrease in light emission within 3 minutes at concentrations above the MIC confirmed that cell viability was affected relatively fast. However, even at concentrations above the MIC, viability does not drop below 50%, which was the case for CHX. In addition, the ATP dependent membrane assay showed elevated light emission at these concentrations indicating that ATP levels are not the limiting factor. No effect was observed toward *E. coli* (Figure 4(B)).

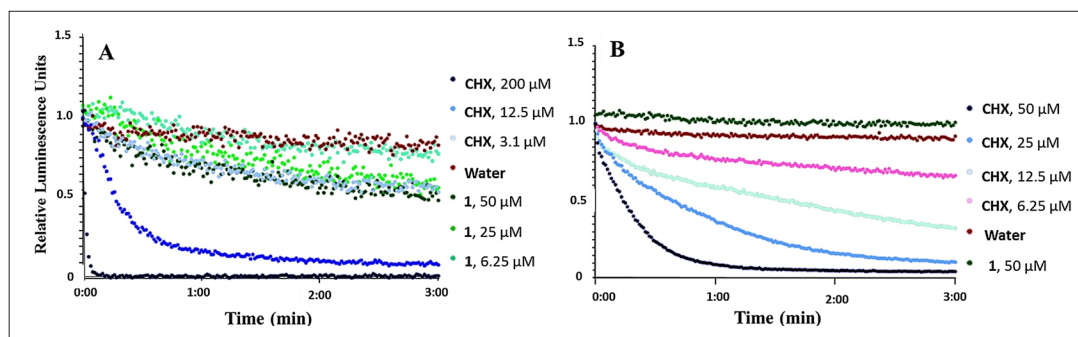


Figure 4. Kinetics of the relative luminescence emission by **A**) *B. subtilis* (pCGLS-11) and **B**) *E. coli* (pCGLS-11) treated with ranging concentrations of either securamine H (**1**) or chlorhexidine (CHX).

Table 2. List of Sensor Strains With the Promoter Region Fused to the *luxABCDE* Operon Located in the *sacA* Region of the *B. subtilis* 168 Chromosome. Respective Positive Control Antibiotics Used Are Shown in the Last Column.

Strain number	Target	Promoter	Control antibiotic
EM10	DNA replication	<i>yorB</i>	Ciprofloxacin
EM11	Transcription	<i>belD</i>	Rifampicin
EM12	Translation	<i>ybeI</i>	Erythromycin
HMB67	Wall and membrane	<i>liaI</i>	Vancomycin/Bacitracin
HMB69	Fatty acid synthesis	<i>fabH</i>	Triclosan/Irgasan
HMB70	Folic acid synthesis	<i>panB</i>	Trimethoprim
HMB62	Viability control	<i>laiG</i>	all

In summary, the results from the membrane integrity and metabolic activity assays show an influx of D-luciferin at concentrations higher than the MIC, no effect on membrane potential, and reduction of metabolic activity in *B. subtilis* exposed to **1**. The effect of **1** on *B. subtilis* viability is thus most likely not caused by direct effects on the cell membrane, but rather by interference with one or more metabolic processes in *B. subtilis*.

Investigation of Possible Intracellular Targets of **1**

In an attempt to gather information regarding the mode of action of **1**, the compound was tested against a panel of six biosensors responding to interference with some major metabolic pathways in *B. subtilis*. Compound **1** was tested for interference with DNA replication, transcription, translation and interference with fatty acid, cell wall and folic acid synthesis. Antibiotics of the respective modes of action, as shown in Table 2, served as positive controls. None of the strains reacted to co-incubation with **1** at the assayed concentrations during the 8 hours the assays were run (twofold dilution series between 50 and 0.39 μ M). The purpose of the sensors is to detect similar activity, but negative results do not exclude a given mode of action. While, for example, erythromycin efficiently induces the sensor for translation interference, kanamycin does not.²⁷ Similarly, the cell envelope stress sensor, which is based on the *liaI* promoter and the *liaRS* two-component system, is most sensitive when challenged with antibiotics affecting the lipid II cycle, as is the case for bacitracin and vancomycin, while they remain uninduced by penicillin.²⁸ This hampers the interpretation of the results since all the assays for the activity of **1** were negative. However, **1** seems not to belong to the subgroups of antibiotic mode of actions that the sensors recognize. Interestingly, the *liaI* based cell envelope stress sensor is known to respond to membrane active compounds such as nisin.²⁸ Therefore, the negative response to **1** was in accordance with earlier results indicating a different mode of action than interference with membrane integrity.

Conclusions

Securamine H (**1**) was found to inhibit the viability of G+ bacteria and to reduce metabolic activity in *B. subtilis*. The effect was shown not to be caused by interference with DNA replication, transcription, or translation, nor by interference with fatty acid, cell wall and folic acid synthesis, and could not be explained by disruption of the cell membrane. The mode of action of **1** thus remains to be deconvoluted. However, as the result indicates that **1** has an intracellular target, the compound serves as an interesting starting point for further investigations. The herein presented results demonstrate that marine bryozoans can be used as a source of compounds with antibacterial activity.

Experimental

Animal Material, Extraction, Fractionation, Compound Isolation, and Structure Elucidation

Specimens of *S. securifrons* were collected off the coast of Hjelmsøya, Norway in 2014 using an Agassi's dredge trawl at 72 m depth. The specimens were prepared as an organic extract, which was further fractionated into eight fractions using RP-flash chromatography and tested for bioactivity. The compounds were isolated using mass-guided semi-preparative HPLC and their structure elucidated using spectroscopic methods (HRMS, 1D- and 2D-NMR), all as previously described in detail.¹⁴

Microorganism Strains, Growth Media, and Assay Temperature

Enterococcus faecalis (ATCC: 29212) and *Streptococcus agalactiae* (Gr. B) (ATCC: 12386) were grown and assayed in brain-heart infusion broth (BHI; Oxoid, Hampshire, England). *Staphylococcus aureus* (ATCC: 25923), *Escherichia coli* (ATCC: 25922), *Pseudomonas aeruginosa* (ATCC: 27853), and *Bacillus subtilis* (ATCC: 23857) and its derivatives were grown and assayed in Mueller Hinton Broth (MH; Merck, Darmstadt, Germany). *Staphylococcus epidermidis* (ATCC: 35984) was grown and assayed in tryptic soy broth (TS; Merck, Darmstadt, Germany). All bacteria were grown and assayed at 37 °C. The yeast strains *Candida albicans* (ATCC: 10231) and *Rhodotorula* sp. and the *Aureobasidium pollulans* mold (*Rhodotorula* sp and *A. pollulans*) were obtained from Professor Arne Tronsmo, the Norwegian College of Life Sciences, Ås, Norway, were cultivated and assayed on potato dextrose agar (PD, Difco, Detroit, MI, USA) with 2% D(+)-glucose (Merck, Darmstadt, Germany) at room temperature.

Antimicrobial and Anti Biofilm Formation Assays

Antibacterial assay. MIC values of **1-5** were determined using the broth microdilution method, as previously described.¹⁵ Briefly, suspended bacteria in log phase were added to 96-well

microtiter plates at a concentration of 1,500-15,000 colony forming units/mL. Serial dilutions of **1-5** (assay cons: 50-0.78 μM) were subsequently added and left to inoculate for 24 hours before growth inhibition was measured using a Victor multi-label counter (Perkin Elmer, Singapore) at 600 nm. Growth medium diluted with water (1:1) was used as negative control and bacteria suspension diluted with water (1:1) as positive control. For *B. subtilis*, oxytetracycline was used as the positive assay control, and for the remaining strains, gentamycin was used. The assays were repeated three times.

Inhibition of biofilm formation. *S. epidermidis* was used to assess the effect of **1-5** on biofilm formation. An overnight culture of *S. epidermidis* was diluted with fresh TS broth with 1% glucose (1:100), transferred to the wells of 96-well microtiter plates, and ranging concentrations (assay cons: 50-0.39 μM) of **1-5** were added. After overnight incubation, the bacterial suspension was carefully discarded, the biofilm fixed by incubation at 55 °C for 1 hour and stained with 0.1% crystal violet for 5 minutes before being washed away with water. The plates were once more left to dry at 55 °C for 1 hour before 70 μL 70% ethanol was added to each well and the plates left to incubate for 10 minutes before biofilm formation was observed by visual inspection of the plates. The MIC was defined as the lowest concentration where no biofilm formation was visible. *S. epidermidis* suspension, diluted with 50 μL of water, was used as a positive control, and 50 μL *Staphylococcus haemolyticus* suspension with 50 μL of water as negative control. A mixture of 50 μL water and 50 μL TS broth was used as assay control. The assay was repeated three times.

Antifungal assay. Fungal spores of yeast strains *Candida albicans* and *Rhodotorula* sp. and the *A. pollulans* mold were added to PD broth and the cell concentration determined and adjusted after counting in a Bürker chamber. A final fungal spore concentration of 2×10^5 spores/mL was inoculated in 96-well Nunc microtiter plates (100 μL total well volume) along with ranging concentrations of **1-5** (assay cons: 50-0.78 μM). The assay plates were incubated at room temperature for either 24 hours (*C. albicans*) or 48 hours (*A. pollulans* and *Rhodotorula* sp.). Ranging concentrations of amphotericin-B was used as positive control (32-0.25 $\mu\text{g}/\text{mL}$), and water as a negative (growth) control. After incubation, the OD value (600 nm) was measured in a Synergy H1 Hybrid Reader (BioTek, Winooski, VT, USA). MIC values of **1-5** were defined as the lowest concentration of the compounds that showed >90% inhibition compared to the negative growth control (as measured by OD). The assays were repeated three times.

Mode of Action Studies

Real-time membrane integrity assay measuring immediate membrane disruption. The real-time membrane integrity assay was performed using *B. subtilis* 168 and *E. coli* K12 (MC1061), both carrying the plasmid pCSS962 with the eukaryotic luciferase

gene *lucGR*. Luciferase is dependent on D-luciferin as substrate to emit light, a substrate that does not penetrate intact cell membranes. The assay is a modification of a previously described protocol.¹⁹ *B. subtilis* and *E. coli* were cultured overnight in MH broth with 5 $\mu\text{g}/\text{mL}$ chloramphenicol (Merck KGaA, Darmstadt, Germany) and a mixture of 20 $\mu\text{g}/\text{mL}$ chloramphenicol/100 $\mu\text{g}/\text{mL}$ ampicillin, respectively, before being centrifuged at 4500 rpm for 10 minutes. The supernatant was removed and the pellet resuspended in MH broth to give an OD_{600} of 0.1. D-luciferin potassium salt (assay concentration: 1 mM) was added and background luminescence measured. Ranging concentrations of **1** (assay conc.: 50-0.78 μM) dissolved in water were added to black round-bottom 96-well microtiter plates (Nunc, Roskilde, Denmark), as well as a ranging concentrations of the control, CHX acetate (assay conc.: 50 μM -1.6 μM). The plates were placed in a Synergy H1 Hybrid Reader (BioTek, Winooski, VT, USA). Aliquots (90 μL , to give a total assay volume of 100 μL) of the prepared bacterial suspension were added to the test wells by an automatic injector with tracking of the luminescence emission every second for 180 s. The assays were repeated 3 times.

Membrane potential assay. To analyze the effects of **1** on the membrane potential of *Bacillus subtilis* 168, the BacLight bacterial membrane potential kit (Invitrogen, Carlsbad, CA, USA) was used. The assays were performed in 96 well 1.8 ml deepwell-plates (Corning, Corning, NY, USA) and analyzed by a Cube8 flow cytometer with an auto sampler (Sysmex, Kobe, Japan). The assay is based on the dye DiOC₂(3), which causes green fluorescence in all bacterial cells. The fluorescence shifts to red when the dye molecules self-associate due to their accumulation in the cytoplasm of viable bacteria with intact membrane potential.²¹ Differences in fluorescence emission were detected by flow cytometry. The ratiometric values of red/green fluorescence were used to analyze if the proton gradient of the tested cells was affected or not. The experiment was performed according to the manufacturer's suggestions, but adapted to the 96 well format and therefore conducted with reduced volumes. Briefly, 5 μL 3 mM DiOC₂(3) solution was added to 500 μL cell suspension, which contained approximately 10^6 bacteria and had been pretreated for 3 minutes with different concentrations of the respective analytes. Before starting the measurement, the samples were incubated in the dark for 30 minutes at room temperature. The samples were then measured in the Cube8 and analyzed with excitation by the blue laser (488 nm) and forwards scatter (FSC), side scatter (SSC), FL1 (emission 536/40 nm) and FL3 (emission 675/20 nm). Data analysis was performed by the freely available flowing software using the first 2000 events of the bacterial population in each measurement for ratiometric analysis (flowingsoftware.btk.fi).

Real-time cell viability assay. The real-time cell viability assay was performed using *B. subtilis* 168 (ATCC: 23857) and *E. coli* K12 (ATCC: MC1061) carrying either a chromosomal integration of

the *lux*ABCDE operon or the plasmid pCGLS-11 with the *lux* operon *lux*CDABE, respectively. The assay is a modification of a previously described protocol.²⁹ *B. subtilis* and *E. coli* were cultured overnight in MH broth with 5 µg/mL chloramphenicol and 100 µg/mL ampicillin (Merck KGaA, Darmstadt, Germany), respectively, before being centrifuged at 4500 rpm for 10 minutes. The supernatant was removed and the pellet resuspended in MH broth to give an OD₆₀₀ of 0.1. Ranging concentrations of **1** (assay conc.: 50–0.78 µM) dissolved in water were added to black round-bottom 96-well microtiter plates (Nunc, Roskilde, Denmark), as well as ranging concentrations of the control, CHX acetate (assay conc.: 50 µM – 1.6 µM). The plates were placed in a Synergy H1 Hybrid Reader (BioTek, Winooski, VT, USA). Aliquots (90 µL, to give a total assay volume of 100 µL) of the prepared bacterial suspension were added to the test wells by an automatic injector with tracking of the luminescence emission every second for 180 s. The assays were repeated three times.

Promotor activity-based whole-cell biosensor assay. Whole cell mode of action, specific biosensors were used to determine if the activity of **1** correlates with some previously known modes of actions. The biosensors were generated by cloning promoter fusions to *lux*ABCDE in the plasmid pBS3*lux*C and subsequent recombination into the *sacA* site on the *B. subtilis* chromosome, as described.²³ Interference with DNA replication, transcription, translation and fatty acid synthesis was tested by *B. subtilis* strains containing *lux*ABCDE fusions to the promoters of the genes *yorB*, *helD*, *ybeI* and *fabHB*, respectively, as described for firefly luciferase.²⁷ Inhibition of cell wall synthesis was tested by a bacitracin inducible promoter construct described²³ based on the promoter of *liaI* fused to *lux*ABCDE. The *veg* promoter fusion described in the same paper was used as a luminescence control. In addition, a *panB-lux*ABCDE promoter fusion described as a *lacZ*-fusion in patent US20020164602A1³⁰ was used to test for inhibition of folic acid synthesis (details in Table 2). Compound **1** was tested in a two-fold dilution series starting with two × *B. subtilis* MIC (MIC = 6.25 µM). The respective control antibiotics were set up similar to the tested compound. The experiments were run at room temperature. Otherwise, the identical setup to the antimicrobial assay protocol was used with additional measurement of luminescence every 15 minutes for 8 hours. Peak luminescence of the controls was compared to luminescence of cells treated with **1**. The assays were repeated three times.

Acknowledgments

The authors are grateful for the help received by Dr. Hans-Matti Blencke in the mode of action studies and the preparation of this manuscript. We are grateful to Marbank for collecting the specimens of *S. securifrons* and to R. Johansen for taxonomic identification of the bryozoan.

Declaration of Conflicting Interests

The author(s) declared no potential conflicts of interest with respect to the research, authorship, and/or publication of this article.

Funding

The author(s) disclosed receipt of the following financial support for the research, authorship, and/or publication of this article: The publication fee was covered by the open access publishing fund, UiT.

ORCID IDs

Kine Ø. Hansen  <https://orcid.org/0000-0002-9023-1958>

Céline S. Richard  <https://orcid.org/0000-0001-5061-1676>

Espen H. Hansen  <https://orcid.org/0000-0003-0354-986X>

Supplemental Material

Supplemental material for this article is available online.

References

1. Medernach RL, Logan LK. The growing threat of antibiotic resistance in children. *Infect Dis Clin North Am.* 2018;32(1):1-17. doi:10.1016/j.idc.2017.11.001
2. Newman DJ, Cragg GM. Natural products as sources of new drugs from 1981 to 2014. *J Nat Prod.* 2016;79(3):629-661. doi:10.1021/acs.jnatprod.5b01055
3. Genilloud O. The re-emerging role of microbial natural products in antibiotic discovery. *Antonie Van Leeuwenboek.* 2014;106(1):173-188. doi:10.1007/s10482-014-0204-6
4. Newman DJ, Cragg GM, Snader KM. Natural products as sources of new drugs over the period 1981-2002. *J Nat Prod.* 2003;66(7):1022-1037. doi:10.1021/np030096l
5. McKinney FK, Jackson JBC. Bryozoan evolution. *University of Chicago Press.* 1991;1(1):1-252.
6. Simpson C, Jackson JBC, Herrera-Cubilla A. Evolutionary determinants of morphological polymorphism in colonial animals. *Am Nat.* 2017;190(1):17-28. doi:10.1086/691789
7. Kutuyumov VA, Maltseva AL, Kotenko N, Ostrovsky AN. Functional differentiation in bryozoan colony: a proteomic analysis. *Tsitologiya.* 2016;58(1):152-159. doi:10.1134/S1990519X16020073
8. Figuerola B, Angulo-Preckler C, Núñez-Pons L, et al. Experimental evidence of chemical defence mechanisms in Antarctic bryozoans. *Mar Environ Res.* 2017;129:68-75. doi:10.1016/j.marenvres.2017.04.014
9. Gray CA, McQuaid CD, Davies-Coleman MT. A symbiotic shell-encrusting bryozoan provides subtidal whelks with chemical defence against rock lobsters. *Afr J Mar Sci.* 2005;27(3):549-556. doi:10.2989/18142320509504115
10. Newman DJ, Cragg GM. Marine natural products and related compounds in clinical and advanced preclinical trials. *J Nat Prod.* 2004;67(8):1216-1238. doi:10.1021/np040031y
11. Kornberg MD, Smith MD, Shirazi HA, Calabresi PA, Snyder SH, Kim PM. Bryostatin-1 alleviates experimental multiple sclerosis. *Proc Natl Acad Sci USA.* 2018;115(9):2186-2191. doi:10.1073/pnas.1719902115
12. Nelson TJ, Sun M-K, Lim C, et al. Bryostatin effects on cognitive function and PKCε in Alzheimer's disease phase IIA and expanded access trials. *J Alzheimers Dis.* 2017;58(2):521-535. doi:10.3233/JAD-170161

13. Kollár P, Rajchard J, Balounová Z, Pazourek J. Marine natural products: bryostatins in preclinical and clinical studies. *Pharm Biol.* 2014;52(2):237-242. doi:10.3109/13880209.2013.804100
14. Hansen Kine Ø, Isaksson J, Bayer A, Johansen JA, Andersen JH, Hansen E. Securamine derivatives from the Arctic bryozoan *Securiflustra securifrons*. *J Nat Prod.* 2017;80(12):3276-3283. doi:10.1021/acs.jnatprod.7b00703
15. Michael P, Hansen Kine Ø, Isaksson J, Andersen JH, Hansen E. A novel brominated alkaloid securidine A, isolated from the marine bryozoan *Securiflustra securifrons*. *Molecules.* 2017;22(7):1236. doi:10.3390/molecules22071236
16. Clardy J, Fischbach MA, Currie CR. The natural history of antibiotics. *Curr Biol.* 2009;19(11):437-441. doi:10.1016/j.cub.2009.04.001
17. Fair RJ, Tor Y. Antibiotics and bacterial resistance in the 21st century. *Perspect Medicin Chem.* 2014;6(6):25-64. doi:10.4137/PMC.S14459
18. Wencewicz TA. New antibiotics from Nature's chemical inventory. *Bioorg Med Chem.* 2016;24(24):6227-6252. doi:10.1016/j.bmc.2016.09.014
19. Virta M, Akerman KE, Saviranta P, Oker-Blom C, Karp MT. Real-time measurement of cell permeabilization with low-molecular-weight membranolytic agents. *J Antimicrob Chemother.* 1995;36(2):303-315. doi:10.1093/jac/36.2.303
20. Kuyyakanond T, Quesnel LB. The mechanism of action of chlorhexidine. *FEMS Microbiol Lett.* 1992;100(1-3):211-215. doi:10.1111/j.1574-6968.1992.tb05705.x
21. Novo D, Perlmutter NG, Hunt RH, Shapiro HM. Accurate flow cytometric membrane potential measurement in bacteria using diethyloxycarbocyanine and a ratiometric technique. *Cytometry.* 1999;35(1):55-63. doi:10.1002/(SICI)1097-0320(19990101)35:1<55::AID-CYTO8>3.0.CO;2-2
22. Kasianowicz J, Benz R, McLaughlin S. The kinetic mechanism by which CCCP (carbonyl cyanide m-chlorophenylhydrazone) transports protons across membranes. *J Membr Biol.* 1984;82(2):179-190. doi:10.1007/BF01868942
23. Radeck J, Kraft K, Bartels J, et al. The Bacillus BioBrick Box: generation and evaluation of essential genetic building blocks for standardized work with *Bacillus subtilis*. *J Biol Eng.* 2013;7(1):29. doi:10.1186/1754-1611-7-29
24. Frackman S, Anhalt M, Neelson KH. Cloning, organization, and expression of the bioluminescence genes of *Xenorhabdus luminescens*. *J Bacteriol.* 1990;172(10):5767-5773. doi:10.1128/JB.172.10.5767-5773.1990
25. Galluzzi L, Karp M. Whole cell strategies based on lux genes for high throughput applications toward new antimicrobials. *Comb Chem High Throughput Screen.* 2006;9(7):501-514. doi:10.2174/138620706777935351
26. Galluzzi L, Karp M. Intracellular redox equilibrium and growth phase affect the performance of luciferase-based biosensors. *J Biotechnol.* 2007;127(2):188-198. doi:10.1016/j.jbiotec.2006.06.019
27. Urban A, Eckermann S, Fast B, et al. Novel whole-cell antibiotic biosensors for compound discovery. *Appl Environ Microbiol.* 2007;73(20):6436-6443. doi:10.1128/AEM.00586-07
28. Mascher T, Zimmer SL, Smith T-A, Helmann JD. Antibiotic-inducible promoter regulated by the cell envelope stress-sensing two-component system LiaRS of *Bacillus subtilis*. *Antimicrob Agents Chemother.* 2004;48(8):2888-2896. doi:10.1128/AAC.48.8.2888-2896.2004
29. Vesterlund S, Palta J, Lauková A, Karp M, Ouwehand AC. Rapid screening method for the detection of antimicrobial substances. *J Microbiol Methods.* 2004;57(1):23-31. doi:10.1016/j.mimet.2003.11.014
30. Murphy CK, inventor; High throughput screen for inhibitors of the folate biosynthetic pathway in bacteria patent application US20020164602A1. 2002.

Paper II

Article

Outer Membrane Integrity-Dependent Fluorescence of the Japanese Eel UnaG Protein in Live *Escherichia coli* Cells

Céline S. M. Richard , Hymonti Dey , Frode Øyen , Munazza Maqsood and Hans-Matti Blencke * 

The Norwegian College of Fishery Science, Faculty of Biosciences, Fisheries and Economics, UiT The Arctic University of Norway, N-9037 Tromsø, Norway

* Correspondence: hans-matti.blencke@uit.no

Abstract: Reporter genes are important tools in many biological disciplines. The discovery of novel reporter genes is relatively rare. However, known reporter genes are constantly applied to novel applications. This study reports the performance of the bilirubin-dependent fluorescent protein UnaG from the Japanese eel *Anguilla japonicas* in live *Escherichia coli* cells in response to the disruption of outer membrane (OM) integrity at low bilirubin (BR) concentrations. Using the *E. coli* wild-type strain MC4100, its isogenic OM-deficient mutant strain NR698, and different OM-active compounds, we show that BR uptake and UnaG fluorescence depend on a leaky OM at concentrations of 10 μ M BR and below, while fluorescence is mostly OM integrity-independent at concentrations above 50 μ M BR. We suggest that these properties of the UnaG–BR couple might be applied as a biosensor as an alternative to the OM integrity assays currently in use.

Keywords: reporter gene; synthetic biology; UnaG; outer membrane; bilirubin; biosensor



Citation: Richard, C.S.M.; Dey, H.; Øyen, F.; Maqsood, M.; Blencke, H.-M. Outer Membrane Integrity-Dependent Fluorescence of the Japanese Eel UnaG Protein in Live *Escherichia coli* Cells. *Biosensors* **2023**, *13*, 232. <https://doi.org/10.3390/bios13020232>

Received: 9 December 2022

Revised: 28 January 2023

Accepted: 3 February 2023

Published: 7 February 2023



Copyright: © 2023 by the authors. Licensee MDPI, Basel, Switzerland. This article is an open access article distributed under the terms and conditions of the Creative Commons Attribution (CC BY) license (<https://creativecommons.org/licenses/by/4.0/>).

1. Introduction

Reporter genes are important tools and are widely used in synthetic biology and cellular biosensors. Due to the ease of use and signal detection, fluorescent and bioluminescent reporter genes are utilized in different types of applications. They are usually fused to either a promoter–operator regulatory sequence or genes of interest and convert biological events into optically detectable signals, which can easily be read by appropriate instrumentation. The most common reporter genes currently in use are the green fluorescent protein *gfp* from the cnidarian *Aequorea victoria* [1–3] and the red fluorescent protein *rfp* from *Discosoma coral* [4–6], as well as different luciferases [7–9]. During the last decade, several alternatives to the traditional fluorescent proteins have emerged, most notably fluorescent proteins belonging to the fatty-acid-binding protein family, such as UnaG and SmurfP [10], as well as RNA-based light-up aptamers [11–13] such as spinach, broccoli, and pepper. They all have in common that they require a fluorogenic ligand for fluorescence, which often must be provided externally.

In this work, we tried to apply the fluorescent protein from a Japanese eel (*Anguilla japonica*), UnaG, for the ligand-dependent labeling of *Escherichia coli* cells [14]. This protein belongs to the fatty-acid-binding protein (FABP) family and produces fluorescence by binding to its ligand bilirubin (BR) (C₃₃H₃₆N₄O₆), a yellow–orange pigment. This molecule is an antioxidant tetrapyrrole, formed by the breakdown of heme—for example, from hemoglobin from dead red blood cells in the mammalian body. UnaG and the unconjugated BR bind noncovalently, but with high specificity and affinity. This protein has been successfully used as an imaging tool for live-cell fluorescence microscopy in mammalian cells [15–17], in yeast [18], as well as in bacteria for anaerobic imaging [19,20], or as a dark-to-green photoswitchable fluorescent protein for super-resolution imaging [17].

The necessity of ligands is not problematic if the host readily provides the molecules in sufficient quantities through its inherent metabolism. Therefore, the use of UnaG does not

require the addition of BR in vertebrate systems. However, when UnaG is used as a reporter in bacteria, BR must be added externally, and, in the case of cytoplasmic expression of the protein, BR must pass the cell envelope and plasma membrane. As BR is a hydrophobic molecule with a size (584.7 Dalton) close to the exclusion threshold of outer membrane (OM) porins (ca. 600 Daltons) [21], sufficient access to BR inside the cell might be a limiting factor when expressed in Gram-negative bacteria. On the other hand, ligands, fluorophores, and enzyme substrate exclusion by cellular barriers such as the OM or plasma membrane can be used in assays or cellular biosensors to evaluate barrier integrity. This principle is used, for instance, in live–dead assays based on the fluorophores [22,23], where plasma membrane disruption is probed by propidium iodide access to the nucleic acids in the cytoplasm. Similarly, the exclusion of D-luciferin of intact plasma membranes is used in assays for plasma membrane integrity [24].

Several methods that are used to study the permeabilization of the OM of Gram-negative bacteria are based on similar principles—for instance, the use of the fluorescent probes 1-*N*-phenyl-naphthylamine (NPN) [25–29] or 8-anilino-1-naphthylsulfonic acid (ANS) [27,30], and ethidium bromide (EtBr) in a different assay [31], and spectrophotometric assays based on periplasmic β -lactamase activity and cytoplasmic β -galactosidase and the activation of respective enzyme-activated dyes [32]. In addition, GFP exported to the periplasm of Gram-negative bacteria has been used to assess damage to the OM in microscopy-based assays [33]. The latter principle has been further applied to multi-color fluorescent flowcytometry assays with GFP localized in the cytoplasm and mCherry in the periplasm [34,35]. The currently most widely applied approach seems to be the use of the fluorescent probe NPN.

The toxicity of ligand, substrate, or probe to the cells of interest might negatively affect experiments or limit the usability for end point measurements rather than real-time assays. For example, a common assay for the evaluation of membrane potential in bacteria is based on the fluorescent dye DiOC2 [36]. The dye itself is cytotoxic and is therefore only used in end point assays. It has been found that also BR affects bacterial viability in the gut. A study by Nobles et al. [37] showed that BR can have a positive effect on the Gram-negative bacteria by protecting them from reactive oxygen species (ROS) but also a negative effect on Gram-positive bacteria by disrupting the plasma membrane at concentrations of at least 100 μ M.

In this study, we show that UnaG-dependent fluorescence in living *E. coli* cells depends on OM disruption under the in vitro conditions that we tested when BR is added externally at relatively low concentrations.

2. Materials and Methods

2.1. Media and Growth Conditions

For cloning, *E. coli* strains were routinely grown in Luria–Bertani (LB) broth at 37 °C with aeration. For fluorescence measurements, the bacteria were grown in Mueller–Hinton (MH; Merck, Darmstadt, Germany) broth medium at room temperature (RT) overnight, which was then diluted 1:100 in MH broth medium and grown to an OD₆₀₀ of approximately 0.5 at RT. To avoid a fluorescence background, after centrifugation at 3000 \times *g* for 5 min, the bacteria pellet was washed by careful pipetting in 0.9% NaCl solution, 0.9% NaCl solution with 20 mM Tris HCl pH 7.5, phosphate-buffered saline (PBS), or 5 mM HEPES buffer (Sigma-Aldrich, St Louis, MO, USA), free of bilirubin (BR), before measuring fluorescence. Then, 1 mM BR (Sigma-Aldrich, St Louis, MO, USA) stocks were created in dimethyl sulfoxide (DMSO; Sigma-Aldrich, St Louis, MO, USA). Different concentrations of ampicillin (Merck KGaA, Darmstadt, Germany), 100 μ g/mL and 5 μ g/mL, were used for the plasmid selection in *E. coli* MC4100 and NR698, respectively.

2.2. Bacterial Strains and Plasmids

In this study, we used the isogenic *E. coli* K-12 strains MC4100 and NR698. To express UnaG constitutively in the cytoplasm, the plasmid pMM001 (Figure S11 and Sequence S1)

was designed and then synthesized through Invitrogen GeneArt Gene Synthesis (ThermoFisher, Waltham, MA, USA) with codon optimization for *E. coli*. In this plasmid, the synthetic construct UnaG [14] is expressed from the constitutive OBX15 promoter [38]. The strain NR698 was constructed by Ruiz et al. [39], where the permeability of the OM increases by introducing the *imp4213* allele of *E. coli* BE100 [40] into the *E. coli* MC4100. This in-frame deletion of the *imp* gene, which encodes an essential protein of the OM assembly, results in a loss of OM integrity. For the membrane integrity assay, the strains were transformed with plasmid pCSS962 containing a constitutively expressed gene, *LucGR* [24].

2.3. Transformation

Competent *E. coli* MC4100 and NR698 were prepared by the transformation and storage solution (TSS) method [41]. Here, 100 μ L of the competent strain was transformed with 100–500 ng plasmid. Cells were incubated at 37 °C, with agitation for 1 h, before being spread on LB agar plates with the appropriate antibiotics and incubated at 37 °C overnight.

2.4. Fluorescence Detection

A Synergy H1 Hybrid Reader (BioTek, Winooski, VT, USA) was used to measure the UnaG fluorescence of bacterial populations. To avoid excessive background fluorescence, the monochromator was set to an excitation wavelength of 508/8 nm and an emission wavelength of 538/8 nm, and fluorescence was measured in 30 s intervals at RT (the temperature inside the device was at 25.5 °C, slightly above ambient, throughout the measurements). The gain was kept at 100 in all experiments. Then, 90 μ L of the bacterial suspension was added to a black round-bottom 96-well microtiter plate (Nunc, Roskilde, Denmark). BR and outer- and plasma-membrane-active compounds were added to the indicated concentrations. The following compounds were used: polymyxin B sulfate (PMB; Sigma-Aldrich, St Louis, MO, USA), polymyxin B nonapeptide (PMBN; GLPBIO, Montclair, CA, USA), chlorhexidine acetate (CHX; Fresenius Kabi, Halden, Norway). BR-free bacterial suspension served as the background, with water instead of PMB as a negative control. Data were processed with GraphPad Prism 9 software version 9.5.0 (GraphPad Software; Boston, MA, USA).

2.5. NPN Assays for Outer Membrane Integrity

The increased permeability of the OM was analyzed by measuring increased fluorescence as kinetics of 1-N-phenylnaphthylamine (NPN) uptake following the protocol described by Helander and Mattila-Sandholm [42]. Briefly, *E. coli* MC4100 and NR698 were grown overnight in MH broth medium. The cultures were further diluted and grown to OD₆₀₀ 0.5, rinsed once using centrifugation at 3000 \times *g* for 5 min, and suspended in 5 mM HEPES buffer supplanted with 5 mM glucose (pH 7.2) and diluted to OD₆₀₀ 0.5. NPN was added to a concentration of 20 μ M containing 1 mL of cell suspension in HEPES buffer immediately prior to fluorescence monitoring using 96-well black-bottom microtiter plates. After 10 μ L of the permeating agent was added to 90 μ L of the cell suspension with NPN, fluorescence was measured using a microplate reader with excitation and emission wavelengths set to 350 and 420 nm, respectively. For the NPN OM assay with BR, *E. coli* cells were grown, harvested, and suspended as described above, before they were preincubated with different concentrations of BR for 10 min. BR-treated cells were washed once and resuspended in HEPES buffer, followed by the addition of NPN to obtain a final concentration of 20 μ M for the measurement of fluorescence for 15 min.

2.6. Luminescence Assays for Plasma Membrane Integrity

The *E. coli* strains MC4100 and NR698 constitutively expressing the luciferase LucGR from the pCSS692 plasmid were cultured overnight in MH broth medium supplemented with 5 μ g/mL chloramphenicol (Merck KGaA, Darmstadt, Germany) for *E. coli* NR698 and 20 μ g/mL for MC4100. New day cultures were made by 1% inoculation in MH broth medium and incubated at RT with aeration until the OD₆₀₀ reached 0.5. The final

concentration of D-luciferin potassium salt (Synchem Inc., Elk Grove Village, IL, USA) in the medium was 2 mM.

The real-time membrane integrity assay was modified from a previously described protocol for the membrane integrity assay [24]. This assay was performed on different strains of *E. coli*, including the wild-type (WT) MC4100 and the OM-deficient NR698 strains. The LucGR protein is dependent on its substrate D-luciferin to emit luminescence. PMB at a final concentration of 10 µg/mL was used as a positive control. Milli-H₂O was used as a negative control.

All values were normalized to the water control for the normalization of the luminescence. Data were processed with GraphPad Prism 9 software.

2.7. Microscopy

Suspensions of UnaG-expressing *E. coli* strains MC4100 and NR698 in PBS buffer were prepared as described earlier. Sample preparation was identical as for the assays in the plate reader in PBS. First, 5 µL of bacterial suspension was transferred onto a microscopic slide and covered with a cover slip for immediate microscopic analysis. Fluorescence was analyzed at several time points after the addition of BR to 5 µM and PMB 10 µg/mL with a Leica DM6000B fluorescence microscope and an excitation light source, a Leica CTR6000, with the filter system Cube I3 DM 513828. Fluorescence was documented with a camera, a Leica DFC7000T, attached to the microscope. Identical camera settings were applied for all images taken. The imaging software used for image analysis was the Leica application suite LAS X, where identical settings for contrast enhancement were applied to the original micrographs. In addition, the brightness of the fluorescent images as a whole was increased to 150% in Photoshop CS6 version 13.0 (Adobe; San Jose, CA, USA) for better on-screen visibility. The original figure without enhanced brightness is supplied as Figure S12.

3. Results and Discussion

3.1. UnaG Fluorescence in Complex Growth Media

To evaluate the fluorescence of UnaG expressed from a plasmid-based, constitutive promoter construct (pMM001) in the wild-type (WT) strain *E. coli* MC4100, the bacteria were grown in either MH or LB broth medium, two different complex media typically in use for different purposes and assays in our laboratory. Green fluorescence was analyzed after incubation in the presence of 5 µM BR. However, within the 15 min measurement window, no UnaG/BR-dependent increase in fluorescence was observed (Figure 1a). In addition, the background fluorescence of complex media is very high. It has been speculated that BR is excluded from entering bacterial cells by the wall of Gram-negative bacteria [43]. Therefore, we tried to compromise the OM with PMB, which is known to affect OM integrity [44]. Again, the addition of PMB did not result in an increase in UnaG-dependent fluorescence.

3.2. The Effect of Different Buffers and Solutions on UnaG Fluorescence Signal-to-Noise Ratio after Membrane Disruption

To investigate whether the background fluorescence of complex media might camouflage any UnaG-dependent changes in fluorescence, we measured the fluorescence of the bacteria suspended in different buffers and solutions, which are often used with viable cells. Again, the WT strain *E. coli* MC4100 carrying the plasmid pMM001 was tested for UnaG-specific fluorescence. In addition, the influence of bacterial concentrations on signal-to-noise ratios was evaluated by testing the fluorescence of the bacterial suspension in HEPES buffer and in 0.9% NaCl solution at an OD₆₀₀ of 0.1, 0.3, 0.5, 0.7, and 1.0. The signal-to-noise ratio seemed to increase with increasing cell concentrations until an OD₆₀₀ of 0.5. Above this concentration, the fluorescence ratio of PMB+BR-treated cells to BR-treated cells stabilized (Figure S13). Hence, an OD₆₀₀ of 0.5 was chosen for further experiments.

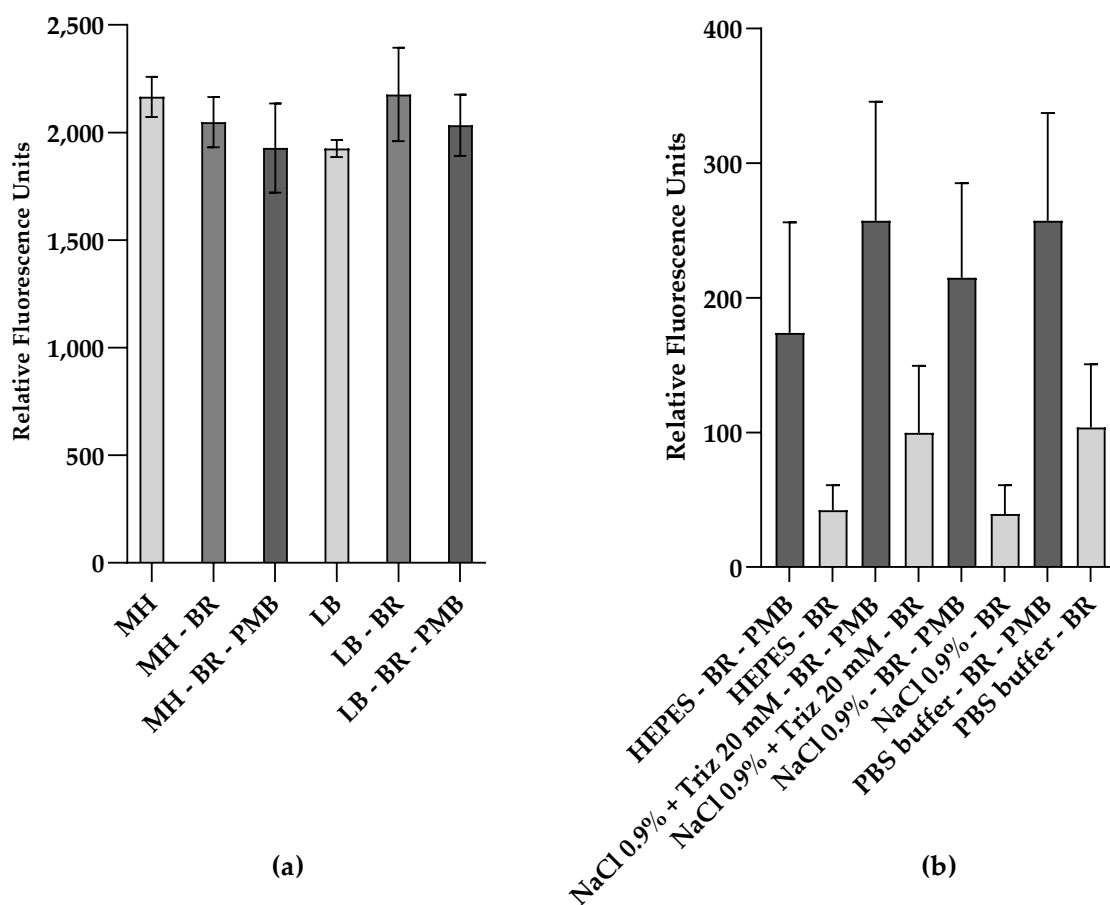


Figure 1. Relative fluorescence of UnaG in live *E. coli* cells is affected by the fluorescent background and the cell envelope active peptide polymyxin B (PMB). Relative fluorescence of *E. coli* MC4100 constitutively expressing UnaG from pMM001 after 15 min exposure to 5 μ M bilirubin (BR) and 10 μ g/mL of PMB in (a) MH medium or LB medium; (b) buffers and solutions, at an OD_{600} of 0.5. Relative fluorescence values are blanked to the respective control without BR. Each data point is the mean of three independent measurements.

Figure 1b shows the comparison of the relative fluorescence emission of UnaG in the different buffer conditions at an OD_{600} of 0.5, after 15 min in the presence and absence of PMB at a final concentration of 10 μ g/mL. The relative fluorescence was blanked to the background fluorescence in the absence of BR in each buffer/solution. Overall, the relative fluorescence of UnaG is strongest in cells treated with PMB when the cells are resuspended in PBS and HEPES, while the fluorescence increase in response to PMB treatment is most pronounced in 0.9% NaCl solution. In all tested conditions, the fluorescence increased at least two-fold after the addition of PMB, while the increase in 0.9% NaCl solution was approximately five-fold. The individual differences in UnaG fluorescence between the independent replicates resulted in a relatively high standard deviation. At the same time, the fold changes in all individual measurements were always largest when conducted in 0.9% NaCl solution. Comparing the effect of PMB on fluorescence in complex media with corresponding data in buffers and solutions clearly indicated that the complex media affected the PMB-induced UnaG fluorescence (Figure 1a,b). Therefore, 0.9% NaCl solution was chosen for further experiments. This difference in fluorescence in response to PMB might be explained by the OM being impermeable to BR at these low concentrations. However, PMB also affects the membrane permeability of the plasma membrane, and, in our construct, UnaG was expressed and localized in the cytoplasm.

3.3. Outer-Membrane-Dependent Uptake of Bilirubin

To determine whether the fluorescence increase after the addition of PMB was caused by OM damage, the OM-deficient *E. coli* strain NR698 was transformed with pMM001. To study the effect of this OM deficiency on BR uptake, we compared the fluorescence kinetics of this mutant and its isogenic WT strain *E. coli* MC4100, both carrying the pMM001 plasmid. Figure 2a illustrates that the addition of BR alone immediately increases the fluorescence only in NR698, while the fluorescence of MC4100 remains at a constant low level. Within the 15 min measuring window used in this experiment, the fluorescence in the OM-deficient strain increases to four-fold compared to the WT strain. The addition of PMB, on the other hand, increases the relative fluorescence in the WT two-fold. Interestingly, the fluorescence of the OM-deficient strain also increases and stabilizes at approximately five-fold after the addition of PMB. This might be caused by the effect of PMB on the plasma membrane or additional damage to the OM. Moreover, when extending the measurement window to 3 h, the fluorescence of MC4100 stays at a low level, while the fluorescence of NR698 is constantly rising (Figure 2b).

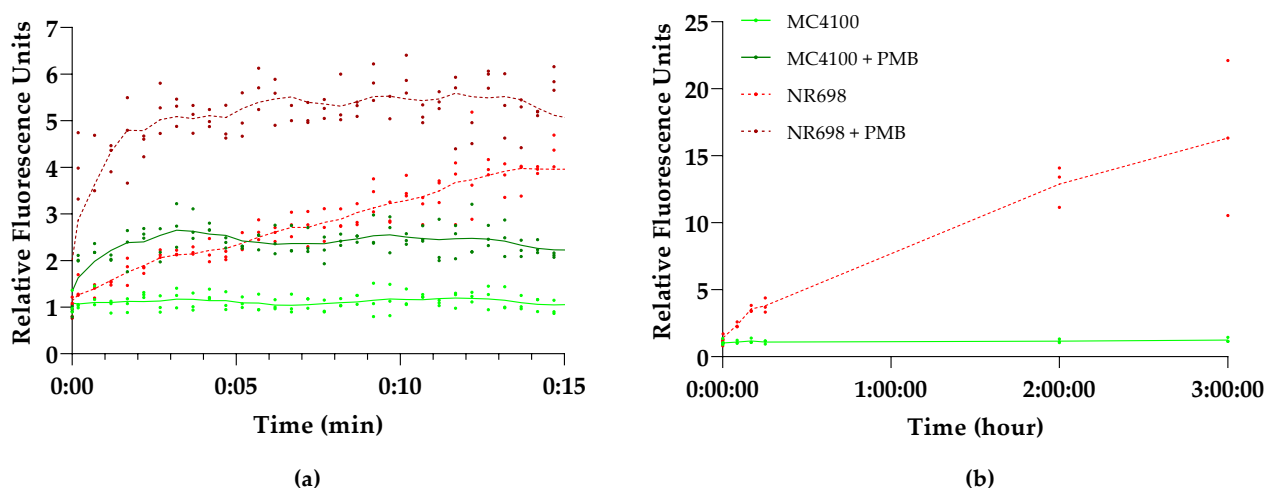


Figure 2. *E. coli* outer membrane (OM) integrity affects UnaG fluorescence. Kinetics of UnaG fluorescence in *E. coli* wild-type (WT) strain MC4100 (solid shades of green) and the isogenic *E. coli* OM-defective mutant NR698 (dashed shades of red) after (a) 15 min exposure of 10 µg/mL PMB and subsequent addition of 5 µM BR (dark shades) or 5 µM BR only (light shades); (b) 3 h exposure of 5 µM BR only. The data points represent three independent measurements normalized to the negative control of MC4100 in the presence of BR only. The mean is represented by the line of the same color.

The results indicate that the OM indeed excludes BR from entering the cells as only the OM-compromised cells allow for the emission of fluorescence, either by mutation (NR698) or a permeabilizing agent (PMB). This seems to confirm the prediction by Chia et al. that the impermeability of bacterial cell walls to BR limits the use of UnaG to outer cell wall targets [43]. This might be caused by the size of BR as the exclusion threshold of OM porins is around 600 Daltons [21] and the molecular weight of BR is 584.7 Daltons. Possibly, BR is also actively removed from the cells with the help of efflux pumps. However, these experiments were conducted at relatively low concentrations of BR. At higher concentrations of BR, a rapid and concentration-dependent increase of fluorescence could be observed in the absence of compounds affecting OM integrity (see Figure S3 in Supplementary Materials), which coincides with the results from the original study in *E. coli* [14] and studies conducted in anaerobic conditions with different *Bacteroidetes* species [43] at 200 µM and 25 µM, respectively. We were not able to rule out or confirm that BR itself has an OM-permeabilizing effect at higher concentrations, as its absorbance spectrum interferes with the NPN-based fluorescence. To exclude any major damage to the OM by BR, we also conducted synergy studies incubating both strains in

Minimum Inhibitory Concentration (MIC) assays with different combinations of BR and erythromycin or vancomycin. These antibiotics are efficiently excluded by the OM and therefore render Gram-negative bacteria relatively insensitive, compared to Gram-positive bacteria [45–48]. While the NR698 was sensitive to all antibiotic concentrations tested, MC4100 did not become more sensitive in the presence of BR. On the contrary, the highest BR concentrations seemed to reduce sensitivity at the MIC (see Table S1 in Supplementary Materials). This observation seems to be in accordance with BR protecting *E. coli* against oxidative stress, as shown in earlier studies [37].

3.4. Confirming Outer Membrane Integrity by NPN Assays

To confirm the hypothesis that the OM is responsible for BR exclusion at low concentrations, we wanted to test the differences in OM integrity in both strains with the fluorescent probe 1-N-phenyl-naphthylamine (NPN), which is often used in OM integrity assays [25–29]. In addition, we confirmed the effects of PMB and EDTA on the OM of these *E. coli* strains. As mentioned above, PMB is known to disrupt the LPS layer of Gram-negative bacteria. NPN is a small hydrophobic molecule (219 Da) that cannot effectively cross the OM and fluoresces only weakly in aqueous solution but strongly when it is in close contact with phospholipid (PL) moieties, which become exposed in response to OM damage. When we compared the background fluorescence taking the same number of cells, the WT strain with intact OM (MC4100) produced weaker fluorescence than the strain with deficient OM (NR698). This difference in fluorescence decreases over time, since the fluorescence intensity of the OM-compromised strain decreases over time, as shown in Figure 3. It seems that NPN can easily access the periplasmic space and bind to the PL of the OM and outer leaflet of the inner membrane when the OM is compromised.

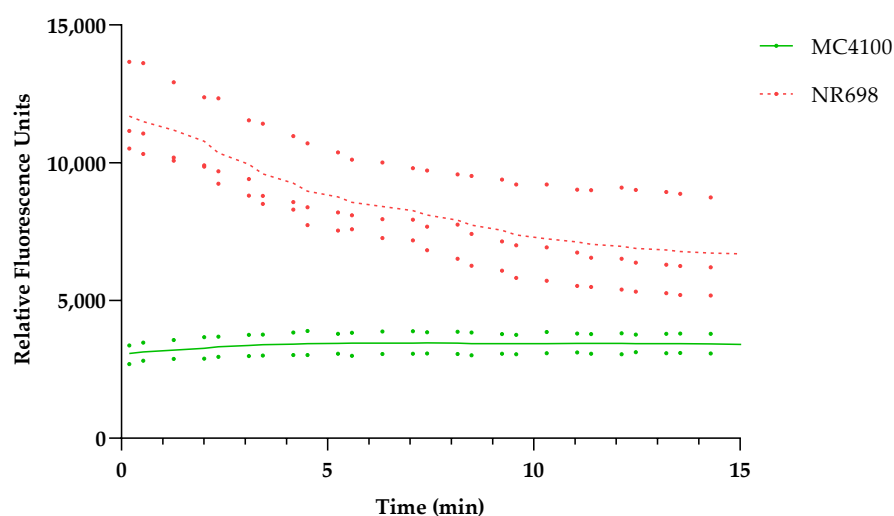


Figure 3. *E. coli* MC4100 and NR698 cells were used to detect fluorescence resulting from OM permeability to the small hydrophobic molecule 1-N-phenyl-naphthylamine (NPN). The data points represent two (MC4100, solid shade of green) or three (NR698, dashed shade of red) independent measurements normalized to the water-treated control (bacteria in 5 mM HEPES buffer). The mean is represented by the line of the same color.

We then compared the effect of different OM-active compounds on the NPN fluorescence of both strains (Figure 4). MC4100 treated with 10 $\mu\text{g}/\text{mL}$ PMB fluoresced almost six-fold more compared to the non-treated control, whereas CHX and EDTA showed a four-fold increase in fluorescence at the 2 min point, which is usually used for OM effects in the NPN assay [25,26]. It is worth noting that MC4100 became slightly more fluorescent in the presence of 10 $\mu\text{g}/\text{mL}$ PMB and 5 mM EDTA than NR698 alone, even though a 1.5–2-fold increase in fluorescence was observed when NR698 cells were treated with 10 $\mu\text{g}/\text{mL}$ PMB. However, MC4100 cells were less permeable when treated with 100 $\mu\text{g}/\text{mL}$ CHX, which

is known to be a strong membranolytic agent with an immediate effect on the viability of bacterial cells, although its OM activity at a sub-MIC level has not been established yet. In our assay, the higher fluorescence values in the NR698 strain with porous OM indicated that NR698 was already more permeable to NPN and reached its higher saturation level in the absence of membrane permeabilizers.

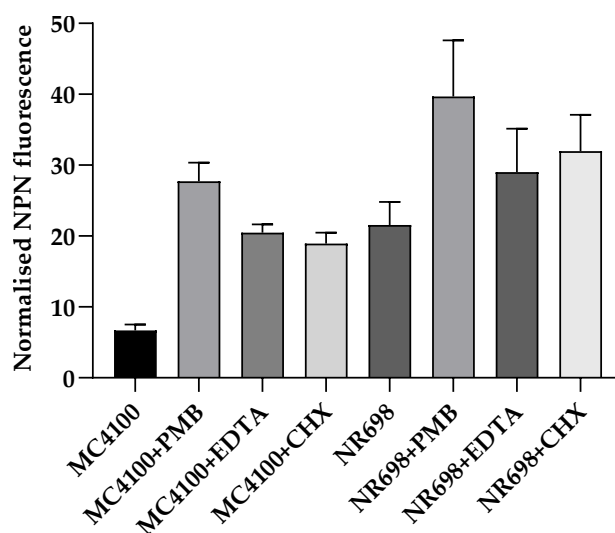


Figure 4. Relative NPN fluorescence in response to different membrane- and OM-active compounds. The permeability of the OM was assessed by measuring the fluorescence of NPN in both *E. coli* strains (MC4100 and NR698) after 2 min in the presence of 10 $\mu\text{g}/\text{mL}$ PMB, 5 mM EDTA, or 100 $\mu\text{g}/\text{mL}$ chlorhexidine (CHX). The fluorescence emission was plotted after normalizing all the samples to the bacteria in 5 mM HEPES buffer.

3.5. Bilirubin Uptake Is Mostly Independent of Plasma Membrane Integrity

To evaluate the plasma membrane integrity of the mutant strain NR698 and the isogenic WT MC4100, we transformed both strains with plasmid pCSS962 coding for a constitutively expressed eukaryotic luciferase LucGR. This construct was used to evaluate the integrity of the plasma membrane [24]. In addition, we wanted to confirm that a derivative of PMB, the PMB nonapeptide (PMBN), did not affect the plasma membrane of either strain at 10 $\mu\text{g}/\text{mL}$, as we planned to use it as an example for a substance specifically damaging the OM. This peptide is described to be highly specific for the efficient perturbation of the OM and affects the plasma membrane only at high concentrations [49]. The integrity of the plasma membrane of *E. coli* MC4100 and NR698 (Figure 5) was tested in response to PMB and PMBN at a concentration of 12.5 $\mu\text{g}/\text{mL}$, and the kinetics of the bioluminescence of the protein LucGR was measured for 10 min after the addition of each compound. The luminescence increased directly after the addition of PMB in both strains. This indicates that the plasma membrane is compromised, allowing D-luciferin to diffuse into the cells and the enzyme to emit luminescence. PMBN, on the other hand, did affect luminescence to a lower extent in either strain at the tested concentration. Furthermore, the luminescence stabilized to a level similar to the non-treated control, confirming that plasma membrane integrity is not severely perturbed by PMBN in either *E. coli* strain and that the plasma membrane of the mutant NR698 in the absence of antimicrobial compounds is still excluding D-luciferin. As BR itself has earlier been described to affect membrane stability [37,50–52], we also analyzed how different concentrations of BR affect plasma membrane integrity. Although the highest concentration of BR resulted in a two-fold increase in luminescence in MC4100, the luminescence levels did not reflect the same pattern as known for membrane-active compounds (see Figures S4 and S5). We also tested different concentrations of BR against an *E. coli* viability sensor based on the *lux* operon, without observing a concentration-dependent specific effect apart from partial light

absorption by bilirubin (see Figures S7 and S8). This is also in agreement with MIC studies conducted earlier, where BR, even at the highest concentrations tested, did not inhibit growth [53], and which we have confirmed in our lab for both strains used in this study.

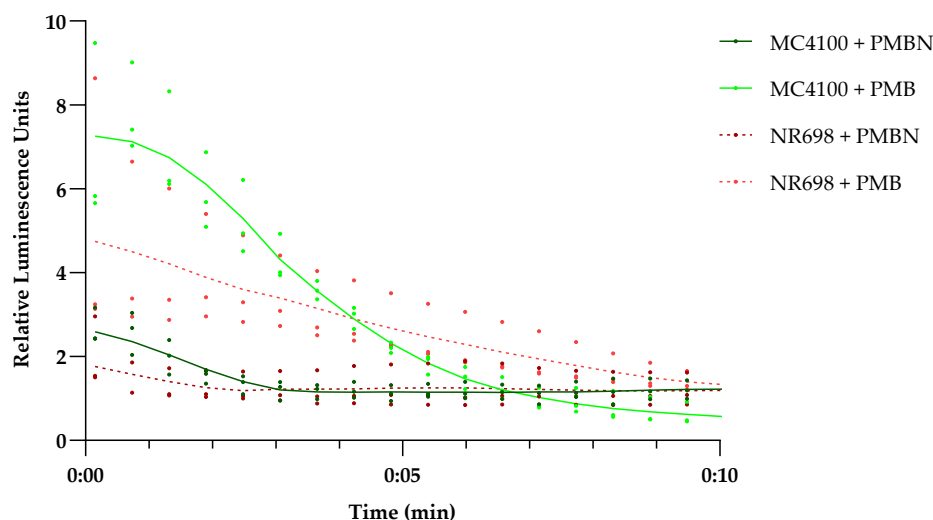


Figure 5. Effect of PMB and PMBN on plasma membrane integrity of *E. coli* MC4100 and NR698. Luminescence kinetics of LucGR in *E. coli* MC4100 (solid shades of green) and *E. coli* NR698 (dashed shades of red) in response to the presence of 12.5 $\mu\text{g}/\text{mL}$ PMB (light color) or polymyxin B nonapeptide (PMBN) (dark color) and due to D-luciferin influx caused by plasma membrane permeabilization. The data points represent three independent measurements normalized to the negative control in the presence of D-luciferin only. The mean is represented by the solid line of the same color. An initial luminescence increase represents membrane permeabilization, the subsequent luminescence decrease represents ATP depletion due to bacterial cell death because of lost membrane integrity, while luminescence stabilization on the level of the control indicates survival of the main population with limited or no plasma membrane damage.

3.6. Is UnaG a Suitable Sensor for Outer Membrane Damage?

To evaluate whether UnaG-expressing *E. coli* strains could be used as indicators of OM damage, the effect of PMBN on UnaG fluorescence, and therefore BR diffusion through the OM, was tested. *E. coli* MC4100 was subjected to PMB and PMBN carrying the plasmid pMM001 with the constitutively expressed UnaG gene. Figure 6 shows the kinetics of the fluorescence increase after the addition of 10 $\mu\text{g}/\text{mL}$ of either peptide. It is evident that both peptides substantially increase the fluorescence. As we showed earlier that the PMBN does not seem to have a major effect on plasma membrane integrity at the tested concentration, this effect is specific for OM damage. However, as studies with *Bacteroidetes* [19] grown anaerobically have shown that BR is taken up by the cells when provided with the growth medium over time, use of the UnaG–BR combination might require strict control of the assay conditions. Although there are already several different assays to test OM damage, in some cases, there might be advantages of using UnaG in combination with BR. Interestingly, the long-term stability of the system over several hours (Figure 2b) suggests a possible application of the system in assays with living bacterial biosensors for the longer-term monitoring of OM integrity in real time.

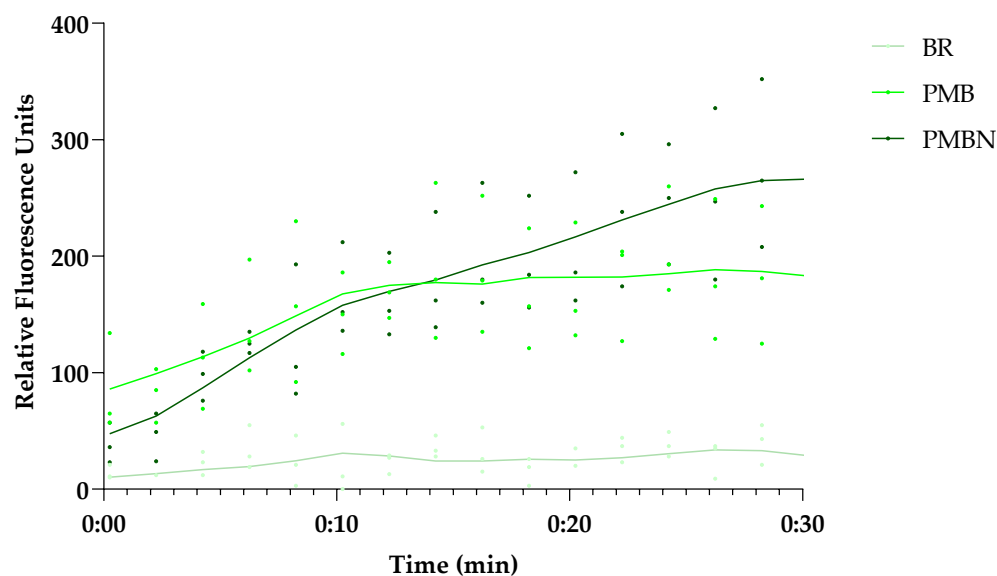


Figure 6. Both the OM-active PMBN and PMB induce UnaG fluorescence in the presence of BR, but show differences in the kinetics over time. The 30 min fluorescence kinetics of UnaG in *E. coli* MC4100 after exposure to 10 $\mu\text{g}/\text{mL}$ PMB and 5 μM BR (medium green), 10 $\mu\text{g}/\text{mL}$ PMBN and 5 μM BR (dark green), or 5 μM BR only (light green). The data points represent three independent measurements normalized to the negative control in the presence of bacteria only. The mean is represented by the solid line of the same color.

To test this hypothesis, the fluorescence of *E. coli* MC4100 carrying the plasmid pMM001 was measured for 10 h in the presence of different concentrations of compounds that are known or suspected to show OM-disrupting activity, plasma-membrane-disruptive activity, or both. PMB has been described to affect the integrity of Gram-negative membranes [44,54], while its derivative PMBN seems to permeabilize the OM down to concentrations around 1 $\mu\text{g}/\text{mL}$ [55] and it does not seem to affect plasma membrane activity at 12.5 $\mu\text{g}/\text{mL}$ (compare Figure 5); hence, its permeabilizing activity is likely exclusively affecting the OM at concentrations between 1 and 10 μM . Here, we show that PMB induces UnaG fluorescence only at the lowest concentration tested (2.5 $\mu\text{g}/\text{mL}$), while PMBN-induced fluorescence is up to three-fold higher at all concentrations tested, including 10 μM . The fluorescence intensities of bacteria treated with PMBN resemble the fluorescence intensity of the OM mutant NR698. The concentration-dependent fluorescence of PMB might be explained by its bacteriostatic effect at low concentrations and its bactericidal effect at high concentrations [54]. Chlorhexidine (CHX), on the other hand, only slightly induces fluorescence at the tested concentrations, while both PMB and CHX permeabilize the plasma membrane at the higher concentrations. This possibly indicates that CHX attacks the OM to a lesser extent, with the plasma membrane being the main target. In addition, we tested two recently described cyclic antimicrobial peptide (Turgencins) derivatives, the peptide analogue cTurg-2 as well as the lipopeptide analogue C₁₂-cTurg-1 [56], against the prospective UnaG-based biosensor. Again, the fluorescence levels in response to the analytes varied. C₁₂-cTurg-1, which was previously described to disrupt both the plasma membrane and OM, causes an increase in UnaG fluorescence at both concentrations tested, while the observed fluorescence is more than two-fold stronger at the lower concentration. cTurg-2, on the other hand, was described as mostly OM-active and, in its presence, UnaG fluorescence rose to above the level of the lower concentration of C₁₂-cTurg-1 at both concentrations tested (Figure 7). This might indicate that cTurg-2 is indeed mostly active against the OM. NPN assays conducted for chlorhexidine published previously [56], and related unpublished data on PMB and the Turgencin derivatives summarized in Figure 7b, all show increasing fluorescence with increasing concentrations of active analytes. The NPN assay seems to quantify the combined membrane damage of both the OM and the

plasma membrane. Therefore, the fluorescence intensity tends to increase with increasing analyte concentrations as opposed to the UnaG-based fluorescence, which decreases with increasing analyte concentrations. It is tempting to speculate that plasma-membrane-active compounds kill the bacterial cells due to plasma membrane permeabilization at and above the MIC. Loss of viability shuts down all cellular metabolism, including protein/UnaG synthesis. On the other hand, OM-active compounds such as PMBN will not damage the plasma membrane and cells stay alive, constantly expressing UnaG, with BR diffusing through the compromised OM as it is bound to the protein in the cytoplasm. The steady fluorescence increases over 10 h is represented in the kinetic fluorescence curves shown in Figures S9 and S10 for all the compounds tested. Therefore, we propose that this sensor construct could be used in assays to identify outer membrane active compounds as illustrated in Figure 8.

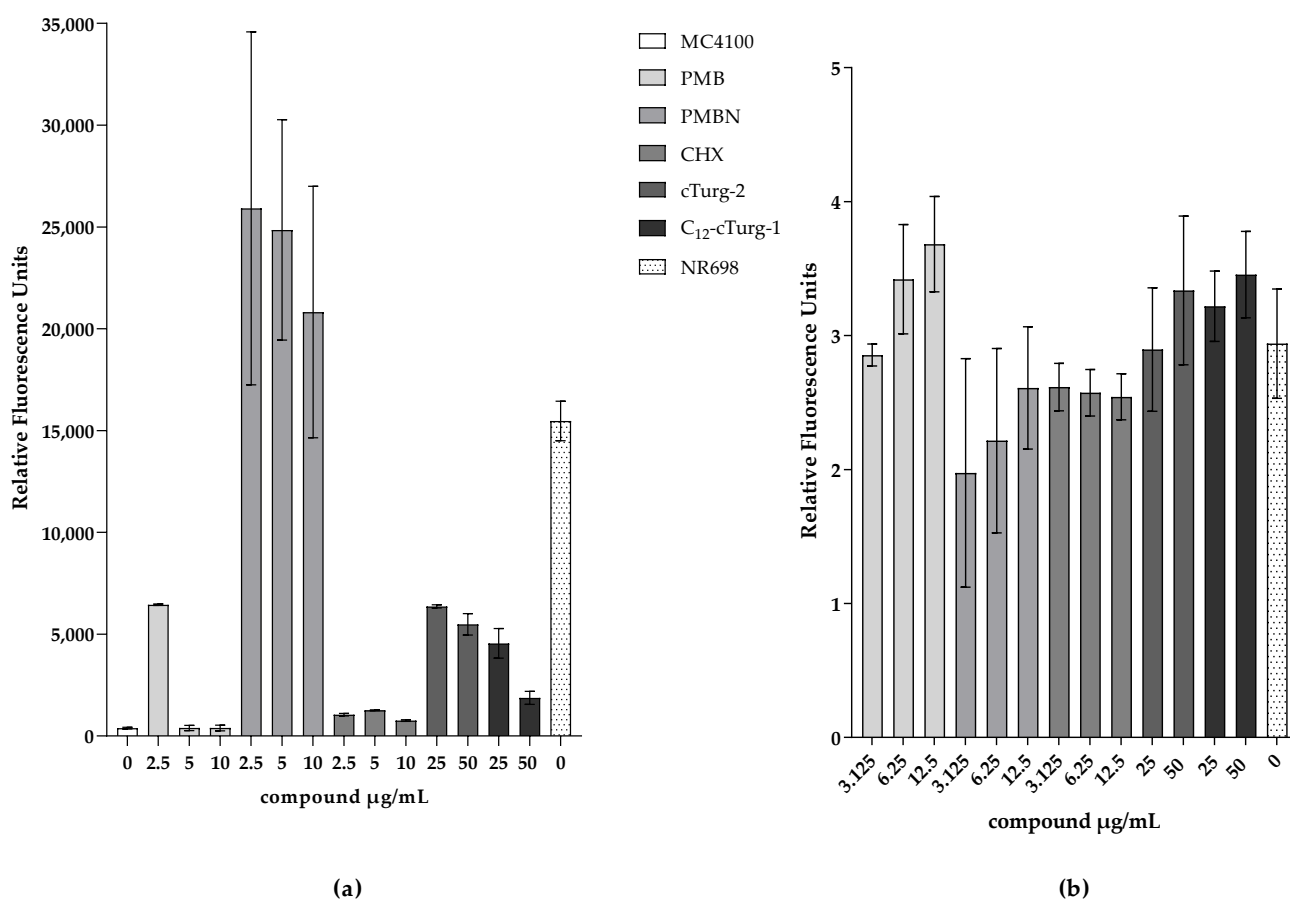


Figure 7. Comparison of relative fluorescence readouts of the proposed UnaG-based OM integrity biosensor and the traditional NPN assay in response to membrane damage. Representative fluorescence values from three independent measurements are shown. (a) Fluorescence of MC4100 constitutively expressing UnaG from pMM001 in 0.9% NaCl 10 h after addition of 5 µM BR and indicated concentrations of OM- or plasma-membrane-active compounds. The measurements were blanked to the respective control without BR. (b) Normalized fluorescence in presence of NPN and different concentrations of OM- or plasma-membrane-active compounds in 5 mM HEPES after 3 min to the MC4100 control with NPN and only water.

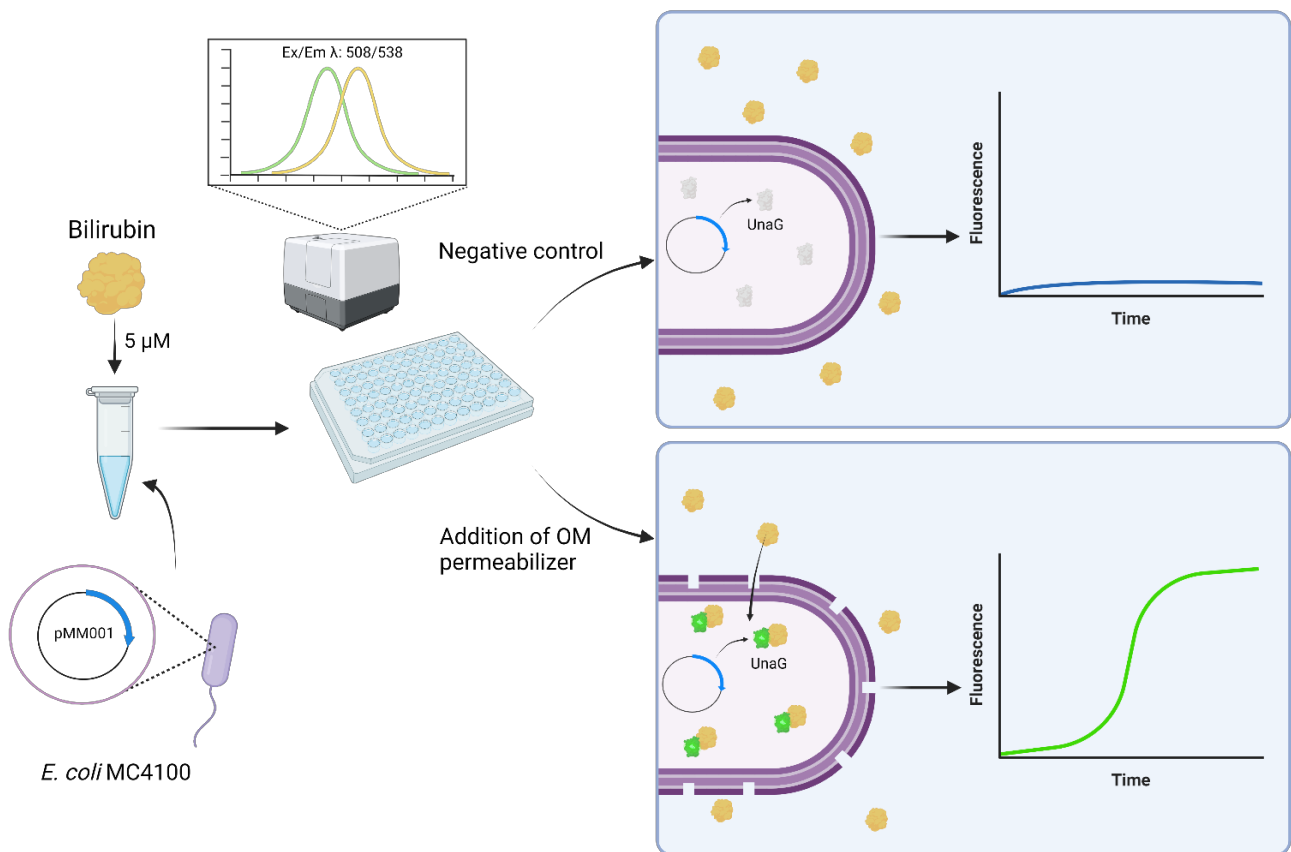


Figure 8. Schematic of the use of the reporter protein UnaG as an OM permeabilization whole-cell biosensor. Created with BioRender.com (accessed on 6 December 2022).

3.7. Is There a Variation in the OM Effect within the Population?

To rule out the possibility that a minor subpopulation is responsible for the increase in fluorescence in response to treatment with OM-disrupting agents observed by the experiments in the plate reader, samples treated in a similar fashion with PMB were analyzed under a fluorescence microscope. Several fluorescent microscope images of the different suspensions of UnaG-expressing *E. coli* strains MC4100 and NR698 in PBS were taken at two different time points after exposure to PMB at 10 μg/mL and BR at 5 μM or BR only (Figure 9). The bacteria were planktonic, viable, and freely moving in the buffer. Therefore, the exposure time could not be increased to achieve brighter images as the moving bacteria resulted in blurry images; this is also visible as a slight positional change between phase contrast and fluorescent images. The fluorescence of the WT MC4100 after exposure to BR was significantly lower compared to the fluorescence after exposure to BR and PMB. Moreover, fluorescence seemed to be mostly constant throughout the population in the focal plane. The effect of PMB was detectable 5 min after its addition. As expected, the fluorescence was significantly lower in the WT compared to the OM-deficient strain when exposed to BR only. This confirms the results observed with PMB performed in the plate reader and indicates that the observed fluorescence is due to the relatively equal fluorescence of the whole population, rather than strongly fluorescent subpopulations. However, an earlier study used the protein UnaG for the imaging of anaerobic bacteria without any OM-disrupting agent [19]. In their study, the concentration of BR in the medium was 25 μM—a concentration only five-times higher than used in this study. Therefore, higher concentrations of BR might increase the diffusion rate to an extent, where sufficient BR molecules accumulate inside the cytoplasm to induce fluorescence also in the absence of OM permeabilizers. It is important to note that this microscopic study was conducted before deciding on the use of 0.9 % NaCl solution as

the medium of choice for conducting experiments, and it was conducted in PBS. More importantly, in the microscopic study, PMB was used as the OM-permeabilizing agent at 10 $\mu\text{g}/\text{mL}$. We later showed, in microtiter plate assays, that the addition of PMBN or PMB at 2.5 $\mu\text{g}/\text{mL}$ resulted in substantially higher fluorescence emission than PMB at 10 $\mu\text{g}/\text{mL}$, indicating a more OM-specific effect (Figures 7 and S9). However, in the presence of BR, the untreated OM-compromised NR698 strain emitted strong fluorescence, which was independent of any compromising agents used, and it can therefore serve as a benchmark to compare fluorescence between the assays conducted in the plate reader and the microscopic observations. In conclusion, the microscopic images show that the fluorescence throughout the treated and untreated populations seems to be mostly homogenous and confirms that a breach in OM integrity is necessary for strong fluorescence.

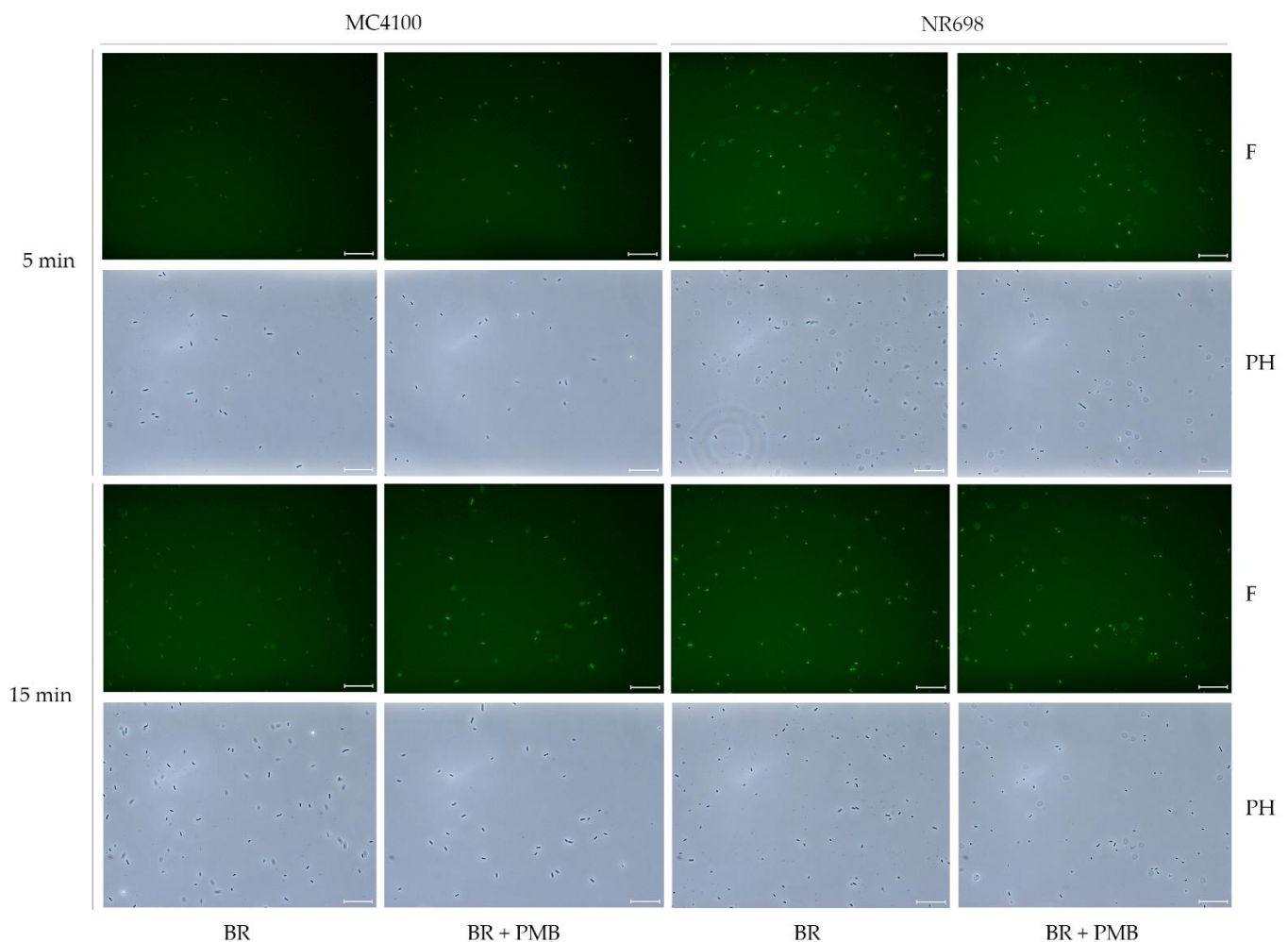


Figure 9. PMB induces population-wide fluorescence of UnaG-expressing *E. coli* cells. Fluorescence images of *E. coli* MC4100 and NR698 at time points of 5 min and 15 min after exposure to BR (5 μM) (BR) or BR and PMB (10 $\mu\text{g}/\text{mL}$) (BR + PMB) at $\times 400$ magnification. The images were taken with the phase contrast (PH) and with fluorescence (F) through the software LAS X. The scale bars represent 25 μm . For better visibility on all monitors, the brightness of the fluorescent pictures (F) was equivalently increased to 150 with Adobe Photoshop CS6 version 13.0.

4. Conclusions

UnaG fluorescence in *E. coli* is completely dependent on the external addition of its ligand BR. At concentrations of 50 $\mu\text{g}/\text{mL}$ and above, the presence of BR alone ensures the sufficient diffusion of BR through the cell envelope for maximal fluorescence in live cells. At low concentrations of BR (5 $\mu\text{g}/\text{mL}$), diffusion and subsequent fluorescence is

dependent on OM disruption. Furthermore, BR does not seem to affect plasma membrane integrity or the survival of *E. coli* cells negatively. Therefore, the UnaG–BR couple might be used as a real-time reporter system in OM integrity biosensors, especially in cases where non-immediate activity and/or OM-specific activity needs to be detected over an extended period, beyond the 2 min mostly used for NPN-based assays. Due to the relatively simple setup, the system might be used as a biosensor that can distinguish OM from OM- and plasma-membrane-active compounds in high-throughput screening applications.

Supplementary Materials: The following supporting information can be downloaded at: <https://www.mdpi.com/article/10.3390/bios13020232/s1>, Figure S1: NPN kinetics in response to different permeabilizing analytes; Figure S2: The dose-dependent short-term effect of PMB and PMBN on UnaG fluorescence kinetics; Figure S3: Fluorescence kinetics of UnaG of *E. coli* MC4100 after exposure of different concentrations of BR; Figure S4: Luminescence kinetics of LucGR in *E. coli* NR698 after exposure of different concentrations of BR; Figure S5: Luminescence kinetics of LucGR in *E. coli* MC4100 after exposure of different concentrations of BR; Figure S6: Plasma membrane remains intact after exposure to PMBN; Figure S7: No effect of BR concentrations on short-term viability of *E. coli* MC4100; Figure S8: *E. coli* NR698 stays alive after exposure to different BR concentrations; Figure S9: Long-term fluorescence kinetics of the proposed OM biosensor to well-known model peptides; Figure S10: Long-term fluorescence kinetics of the proposed OM biosensor to novel cyclic peptide derivatives; Figure S11: Map of the plasmid pMM001 (Benchling.com; accessed on 2 December 2022); Figure S12: PMB induces population-wide fluorescence of UnaG-expressing *E. coli* cells; Figure S13: The influence of bacterial density on UnaG fluorescence; Table S1: Antimicrobial activity (MIC in µg/mL); Sequence S1: DNA sequence of the plasmid pMM001.

Author Contributions: Conceptualization, C.S.M.R., M.M. and H.-M.B.; methodology, C.S.M.R., H.D. and H.-M.B.; software and validation, C.S.M.R., H.D. and H.-M.B.; formal analysis, C.S.M.R.; investigation, C.S.M.R., H.D., M.M. and F.Ø.; resources, H.-M.B.; data curation and writing—original draft preparation, C.S.M.R. and H.-M.B.; writing—review and editing, C.S.M.R., H.D., F.Ø., M.M. and H.-M.B.; visualization, C.S.M.R.; supervision, H.-M.B.; project administration, H.-M.B.; funding acquisition, H.-M.B. All authors have read and agreed to the published version of the manuscript.

Funding: This work was supported by a grant (no. 217/6770) from UiT, the Arctic University of Norway, and a PhD fellowship also granted through the UiT. The publication charges for this article have been covered by the publication fund of UiT, the Arctic University of Norway.

Institutional Review Board Statement: Not applicable.

Informed Consent Statement: Not applicable.

Data Availability Statement: Not applicable.

Acknowledgments: We thank Chun Li for the fruitful discussions, valuable advice, and review of the manuscript. We acknowledge Danijela Simonovic and Ingrid Norberg-Schulz Hagen for synthesizing the marine antimicrobial peptide Turgencin A analogues cTurg-2 and C₁₂-cTurg-1 used in this paper.

Conflicts of Interest: The authors declare no conflict of interest.

References

1. Soboleski, M.R.; Oaks, J.; Halford, W.P. Green fluorescent protein is a quantitative reporter of gene expression in individual eukaryotic cells. *FASEB J.* **2004**, *19*, 440–442. [[CrossRef](#)]
2. Prasher, D.C. Using GFP to see the light. *Trends Genet.* **1995**, *11*, 320–323. [[CrossRef](#)]
3. Martin Chalfie. Green Fluorescent Protein. *Photochem. Photobiol.* **1995**, *62*, 651–656. [[CrossRef](#)]
4. Matz, M.; Fradkov, A.F.; Labas, Y.A.; Savitsky, A.; Zaraisky, A.G.; Markelov, M.L.; Lukyanov, S.A. Fluorescent proteins from nonbioluminescent Anthozoa species. *Nat. Biotechnol.* **1999**, *17*, 969–973. [[CrossRef](#)]
5. Schalén, M.; Anyaogu, D.C.; Hoof, J.B.; Workman, M. Effect of secretory pathway gene overexpression on secretion of a fluorescent reporter protein in *Aspergillus nidulans*. *Fungal Biol. Biotechnol.* **2016**, *3*, 3. [[CrossRef](#)]
6. Fradkov, A.F.; Chen, Y.; Ding, L.; Barsova, E.V.; Matz, M.V.; Lukyanov, S.A. Novel fluorescent protein from *Discosoma* coral and its mutants possesses a unique far-red fluorescence. *FEBS Lett.* **2000**, *479*, 127–130. [[CrossRef](#)]
7. Olsson, O.; Koncz, C.; Szalay, A.A. The use of the luxA gene of the bacterial luciferase operon as a reporter gene. *Mol. Genet. Genom.* **1988**, *215*, 1–9. [[CrossRef](#)]

8. Stewart, G.S.A.B.; Williams, P. lux genes and the applications of bacterial bioluminescence. *J. Gen. Microbiol.* **1992**, *138*, 1289–1300. [[CrossRef](#)]
9. Williams, T.M.; Burlein, J.E.; Ogden, S.; Kricka, L.J.; Kant, J.A. Advantages of firefly luciferase as a reporter gene: Application to the interleukin-2 gene promoter. *Anal. Biochem.* **1989**, *176*, 28–32. [[CrossRef](#)]
10. Rodriguez, E.A.; Tran, G.N.; Gross, L.A.; Crisp, J.L.; Shu, X.; Lin, J.Y.; Tsien, R.Y. A far-red fluorescent protein evolved from a cyanobacterial phycobiliprotein. *Nat. Methods* **2016**, *13*, 763–769. [[CrossRef](#)]
11. Paige, J.S.; Nguyen-Duc, T.; Song, W.; Jaffrey, S.R. Fluorescence Imaging of Cellular Metabolites with RNA. *Science* **2012**, *335*, 1194. [[CrossRef](#)]
12. Ouellet, J. RNA Fluorescence with Light-Up Aptamers. *Front. Chem.* **2016**, *4*, 29. [[CrossRef](#)]
13. Swetha, P.; Fan, Z.; Wang, F.; Jiang, J.-H. Genetically encoded light-up RNA aptamers and their applications for imaging and biosensing. *J. Mater. Chem. B* **2020**, *8*, 3382–3392. [[CrossRef](#)]
14. Kumagai, A.; Ando, R.; Miyatake, H.; Greimel, P.; Kobayashi, T.; Hirabayashi, Y.; Shimogori, T.; Miyawaki, A. A Bilirubin-Inducible Fluorescent Protein from Eel Muscle. *Cell* **2013**, *153*, 1602–1611. [[CrossRef](#)]
15. Shitashima, Y.; Shimozawa, T.; Asahi, T.; Miyawaki, A. A dual-ligand-modulable fluorescent protein based on UnaG and calmodulin. *Biochem. Biophys. Res. Commun.* **2018**, *496*, 872–879. [[CrossRef](#)]
16. To, T.-L.; Zhang, Q.; Shu, X. Structure-guided design of a reversible fluorogenic reporter of protein-protein interactions. *Protein Sci.* **2015**, *25*, 748–753. [[CrossRef](#)]
17. Kwon, J.; Park, J.S.; Kang, M.; Choi, S.; Park, J.; Kim, G.T.; Lee, C.; Cha, S.; Rhee, H.W.; Shim, S.H. Bright ligand-activable fluorescent protein for high-quality multicolor live-cell super-resolution microscopy. *Nat. Commun.* **2020**, *11*, 273.
18. Zahradník, J.; Dey, D.; Marciano, S.; Kolářová, L.; Charendoff, C.I.; Subtil, A.; Schreiber, G. A Protein-Engineered, Enhanced Yeast Display Platform for Rapid Evolution of Challenging Targets. *ACS Synth. Biol.* **2021**, *10*, 3445–3460. [[CrossRef](#)]
19. Chia, H.E.; Zuo, T.; Koropatkin, N.M.; Marsh, E.N.G.; Biteen, J.S. Imaging living obligate anaerobic bacteria with bilin-binding fluorescent proteins. *Curr. Res. Microb. Sci.* **2020**, *1*, 1–6. [[CrossRef](#)]
20. Chia, H.E.; Koebke, K.J.; Rangarajan, A.A.; Koropatkin, N.M.; Marsh, E.N.G.; Biteen, J.S. New Orange Ligand-Dependent Fluorescent Reporter for Anaerobic Imaging. *ACS Chem. Biol.* **2021**, *16*, 2109–2115. [[CrossRef](#)]
21. Decad, G.M.; Nikaiko, H. Outer Membrane of Gram-Negative Bacteria XII. Molecular-Sieving Function of Cell Wall. *J. Bacteriol.* **1976**, *128*, 325–336. [[CrossRef](#)]
22. Boulous, L.; Prévost, M.; Barbeau, B.; Coallier, J.; Desjardins, R. LIVE/DEAD BacLight: Application of a new rapid staining method for direct enumeration of viable and total bacteria in drinking water. *J. Microbiol. Methods* **1999**, *37*, 77–86. [[CrossRef](#)]
23. *LIVE/DEAD BacLight Bacterial Viability Kits Technical Sheet*; Molecular Probes: Eugene, OR, USA, 2004.
24. Virta, M.; Åkerman, K.E.O.; Saviranta, P.; Oker-Blom, C.; Karp, M. Real-time measurement of cell permeabilization with low-molecular-weight membranolytic agents. *J. Antimicrob. Chemother.* **1995**, *36*, 303–315. [[CrossRef](#)]
25. Loh, B.; Grant, C.; Hancock, R.E. Use of the fluorescent probe 1-N-phenyl-naphthylamine to study the interactions of aminoglycoside antibiotics with the outer membrane of *Pseudomonas aeruginosa*. *Antimicrob. Agents Chemother.* **1984**, *26*, 546–551. [[CrossRef](#)]
26. Hancock, R.E.; Farmer, S.W.; Li, Z.S.; Poole, K. Interaction of aminoglycosides with the outer membranes and purified lipopolysaccharide and OmpF porin of *Escherichia coli*. *Antimicrob. Agents Chemother.* **1991**, *35*, 1309–1314. [[CrossRef](#)]
27. Domadia, P.N.; Bhunia, A.; Ramamoorthy, A.; Bhattacharjya, S. Structure, Interactions, and Antibacterial Activities of MSI-594 Derived Mutant Peptide MSI-594F5A in Lipopolysaccharide Micelles: Role of the Helical Hairpin Conformation in Outer-Membrane Permeabilization. *J. Am. Chem. Soc.* **2010**, *132*, 18417–18428. [[CrossRef](#)]
28. Briers, Y.; Walmagh, M.; Lavigne, R. Use of bacteriophage endolysin EL188 and outer membrane permeabilizers against *Pseudomonas aeruginosa*. *J. Appl. Microbiol.* **2011**, *110*, 778–785. [[CrossRef](#)]
29. Saravanan, R.; Mohanram, H.; Joshi, M.; Domadia, P.N.; Torres, J.; Ruedl, C.; Bhattacharjya, S. Structure, activity and interactions of the cysteine deleted analog of tachyplesin-1 with lipopolysaccharide micelle: Mechanistic insights into outer-membrane permeabilization and endotoxin neutralization. *Biochim. Biophys. Acta (BBA)-Biomembr.* **2012**, *1818*, 1613–1624. [[CrossRef](#)]
30. Lamers, R.P.; Cavallari, J.F.; Burrows, L.L. The Efflux Inhibitor Phenylalanine-Arginine Beta-Naphthylamide (PABN) Permeabilizes the Outer Membrane of Gram-Negative Bacteria. *PLoS ONE* **2013**, *8*, e60666. [[CrossRef](#)]
31. Miki, T.; Hardt, W.-D. Outer Membrane Permeabilization Is an Essential Step in the Killing of Gram-Negative Bacteria by the Lectin RegIII_B. *PLoS ONE* **2013**, *8*, e69901. [[CrossRef](#)]
32. Lehrer, R.I.; Barton, A.; Ganz, T. Concurrent assessment of inner and outer membrane permeabilization and bacteriolysis in *E. coli* by multiple-wavelength spectrophotometry. *J. Immunol. Methods* **1988**, *108*, 153–158. [[CrossRef](#)] [[PubMed](#)]
33. Rangarajan, N.; Bakshi, S.; Weisshaar, J.C. Localized Permeabilization of *E. coli* Membranes by Antimicrobial Peptide Cecropin A. *Biochemistry* **2013**, *52*, 6584–6594. [[CrossRef](#)] [[PubMed](#)]
34. Heesterbeek, D.A.C.; Martin, N.I.; Velthuisen, A.; Duijst, M.; Ruyken, M.; Wubbolts, R.; Rooijackers, S.H.M.; Bardoel, B.W. Complement-dependent outer membrane perturbation sensitizes Gram-negative bacteria to Gram-positive specific antibiotics. *Sci. Rep.* **2019**, *9*, 3074. [[CrossRef](#)] [[PubMed](#)]
35. Heesterbeek, D.A.C.; Muts, R.M.; van Hensbergen, V.P.; Aulaire, P.D.S.; Wennekes, T.; Bardoel, B.W.; van Sorge, N.M.; Rooijackers, S.H.M. Outer membrane permeabilization by the membrane attack complex sensitizes Gram-negative bacteria to antimicrobial proteins in serum and phagocytes. *PLOS Pathog.* **2021**, *17*, e1009227. [[CrossRef](#)]

36. Novo, D.; Perlmutter, N.G.; Hunt, R.H.; Shapiro, H.M. Accurate flow cytometric membrane potential measurement in bacteria using diethyloxycarbocyanine and a ratiometric technique. *Cytometry* **1999**, *35*, 55–63. [[CrossRef](#)]
37. Nobles, C.L.; Green, S.I.; Maresso, A.W. A Product of Heme Catabolism Modulates Bacterial Function and Survival. *PLOS Pathog.* **2013**, *9*, e1003507. [[CrossRef](#)]
38. Oxford Genetics. pSF-OXB15 (OG558) Strong Promoter *E. coli*. Available online: <https://connex.oxgene.com/Products/Details?code=OG558> (accessed on 25 January 2016).
39. Ruiz, N.; Falcone, B.; Kahne, D.; Silhavy, T.J. Chemical Conditionality: A Genetic Strategy to Probe Organelle Assembly. *Cell* **2005**, *121*, 307–317. [[CrossRef](#)]
40. Eggert, U.S.; Ruiz, N.; Falcone, B.V.; Branstrom, A.A.; Goldman, R.C.; Silhavy, T.J.; Kahne, D. Genetic Basis for Activity Differences Between Vancomycin and Glycolipid Derivatives of Vancomycin. *Science* **2001**, *294*, 361–364. [[CrossRef](#)]
41. Chung, C.T.; Niemela, S.L.; Miller, R.H. One-step preparation of competent *Escherichia coli*: Transformation and storage of bacterial cells in the same solution. *Proc. Natl. Acad. Sci. USA* **1989**, *86*, 2172–2175. [[CrossRef](#)]
42. Helander, I.M.; Mattila-Sandholm, T. Fluorometric assessment of Gram-negative bacterial permeabilization. *J. Appl. Microbiol.* **2000**, *88*, 213–219. [[CrossRef](#)]
43. Chia, H.E.; Marsh, E.N.G.; Biteen, J.S. Extending fluorescence microscopy into anaerobic environments. *Curr. Opin. Chem. Biol.* **2019**, *51*, 98–104. [[CrossRef](#)] [[PubMed](#)]
44. Evans, M.E.; Feola, D.J.; Rapp, R.P. Polymyxin B Sulfate and Colistin: Old Antibiotics for Emerging Multiresistant Gram-Negative Bacteria. *Ann. Pharmacother.* **1999**, *33*, 960–967. [[CrossRef](#)] [[PubMed](#)]
45. Watanakunakorn, C. Mode of action and in-vitro activity of vancomycin. *J. Antimicrob. Chemother.* **1984**, *14*, 7–18. [[CrossRef](#)]
46. Dhanda, G.; Sarkar, P.; Samaddar, S.; Haldar, J. Battle against Vancomycin-Resistant Bacteria: Recent Developments in Chemical Strategies. *J. Med. Chem.* **2019**, *62*, 3184–3205. [[CrossRef](#)]
47. Delcour, A.H. Outer membrane permeability and antibiotic resistance. *Biochim. Et Biophys. Acta (BBA)-Proteins Proteom.* **2009**, *1794*, 808–816. [[CrossRef](#)] [[PubMed](#)]
48. Chollet, R.; Chevalier, J.; Bryskier, A.; Pagès, J.-M. The AcrAB-TolC Pump Is Involved in Macrolide Resistance but Not in Telithromycin Efflux in *Enterobacter aerogenes* and *Escherichia coli*. *Antimicrob. Agents Chemother.* **2004**, *48*, 3621–3624. [[CrossRef](#)]
49. Tsubery, H.; Ofek, I.; Cohen, S.; Fridkin, M. Structure–Function Studies of Polymyxin B Nonapeptide: Implications to Sensitization of Gram-Negative Bacteria. *J. Med. Chem.* **2000**, *43*, 3085–3092. [[CrossRef](#)] [[PubMed](#)]
50. Vázquez, J.; García-Calvo, M.; Valdivieso, F.; Mayor, F. Interaction of bilirubin with the synaptosomal plasma membrane. *J. Biol. Chem.* **1988**, *263*, 1255–1265. [[CrossRef](#)]
51. Cowger, M.L.; Mustafa, M.G. Some membrane effects of bilirubin. *Pediatr. Res.* **1971**, *5*, 419–420. [[CrossRef](#)]
52. Rodrigues, C.M.; Solá, S.; Brito, M.A.; Brites, D.; Moura, J.J. Bilirubin directly disrupts membrane lipid polarity and fluidity, protein order, and redox status in rat mitochondria. *J. Hepatol.* **2002**, *36*, 335–341. [[CrossRef](#)]
53. Terzi, H.A.; Kardes, H.; Atasoy, A.R.; Aykan, S.B.; Karakece, E.; Ustundag, G.H.; Ermis, B.; Ciftci, I.H. The antibacterial effects of bilirubin on gram-negative bacterial agents of sepsis. *Biomed. Res.* **2016**, *27*, 207–209.
54. Storm, D.R.; Rosenthal, K.S.; Swanson, P. Polymyxin and Related Peptide Antibiotics. *Annu. Rev. Biochem.* **1977**, *46*, 723–763. [[CrossRef](#)]
55. Vaara, M. The outer membrane permeability-increasing action of linear analogues of polymyxin B nonapeptide. *Drugs Under Exp. Clin. Res.* **1991**, *17*.
56. Dey, H.; Simonovic, D.; Hagen, I.N.-S.; Vasskog, T.; Fredheim, E.G.A.; Blencke, H.-M.; Anderssen, T.; Strøm, M.B.; Haug, T. Synthesis and Antimicrobial Activity of Short Analogues of the Marine Antimicrobial Peptide Turgencin A: Effects of SAR Optimizations, Cys-Cys Cyclization and Lipopeptide Modifications. *Int. J. Mol. Sci.* **2022**, *23*, 13844. [[CrossRef](#)] [[PubMed](#)]

Disclaimer/Publisher’s Note: The statements, opinions and data contained in all publications are solely those of the individual author(s) and contributor(s) and not of MDPI and/or the editor(s). MDPI and/or the editor(s) disclaim responsibility for any injury to people or property resulting from any ideas, methods, instructions or products referred to in the content.

Supporting Information

Outer Membrane Integrity-Dependent Fluorescence of the Japanese Eel UnaG Protein in Live *Escherichia coli* Cells

Céline S. M. Richard, Hymonti Dey, Frode Øyen, Munazza Maqsood and Hans-Matti Blencke

Methods

Minimum inhibitory concentration (MIC) assay

Stock solutions of Bilirubin and further dilutions were prepared by dissolving them in 100% DMSO. The final DMSO concentration remained 2% in all the concentration of each antibiotic, Bilirubin or DMSO alone. A modified broth microdilution susceptibility assay, based on the CLSI M07-A9 protocol, was used to determine minimal inhibitory concentrations (MIC) [1]. Briefly, overnight bacterial cultures were grown in Mueller-Hinton (MH) medium (Difco Laboratories, USA) for 2 hours at room temperature. The bacterial inoculum was diluted to 5×10^5 cells/mL in MH medium and added in 96-well plates (Nunc, Roskilde, Denmark) preloaded with two-fold dilution series of Bilirubin (200 to 1.6 μ M) and antibiotic solutions (64 to 0.5 μ g/mL) in a ratio of 1:10 giving a final well volume of 100 μ L with bacterial inoculum. The microplates were incubated in an EnVision 2103 microplate reader (PerkinElmer, Llantrisant, UK) at 35 °C, with OD₅₉₅ recorded every hour for 24 h. The minimal inhibitory concentration (MIC) value was defined the lowest concentration of antibiotics either in presence or absence of Bilirubin showing an optical density less than 10% of the negative (growth) control, consisting of bacteria and MQ- water.

Bacterial viability assay (luminescence based)

The *E. coli* strains MC4100 and NR698 were transformed with plasmid pCGLS-11 [2] expressing a *luxCDABE* operon from a constitutive promoter. Both strains were cultured overnight in MH broth medium supplemented with 100 and 5 μ g/mL Ampicillin (Merck KGaA, Darmstadt, Germany), respectively. New day cultures were made by 1% inoculation in MH broth medium and incubated at RT with aeration until the OD₆₀₀ reached 0.5. This was changed from earlier use of the viability assay to adjust the cell density to the UnaG assays. To evaluate the effect of Bilirubin on bacterial viability the luminescence values were normalized to the DMSO control to account for DMSO related increase of luminescence. Data were processed with GraphPad Prism 9 software.

Figures and tables

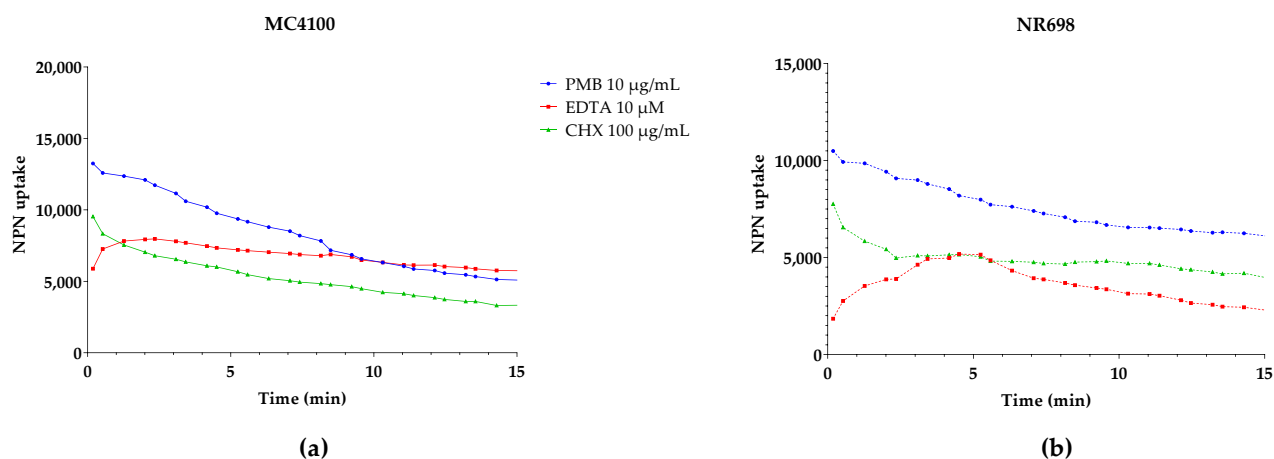


Figure S1. NPN kinetics in response to different permeabilizing analytes. *E. coli* MC4100 (a) and NR698 (b) cells were used to detect fluorescence as a result of outer membrane (OM) permeabilization to the small hydrophobic molecule 1-N-phenyl-naphthylamine (NPN). Fluorescence emission normalized to the water treated control (bacteria in HEPES buffer) is plotted as NPN uptake over time (min).

Table S1. Antimicrobial activity (MIC in $\mu\text{g/mL}$)

Antibiotic	MIC ($\mu\text{g/mL}$)	
	MC4100	NR698
Vancomycin in 2% DMSO	64	0.25 – 0.4
Vancomycin + BR (2% DMSO)	>64	>0.4
Erythromycin 2% DMSO	16	0.25 – 0.4
Erythromycin + BR (2% DMSO)	32	>0.8

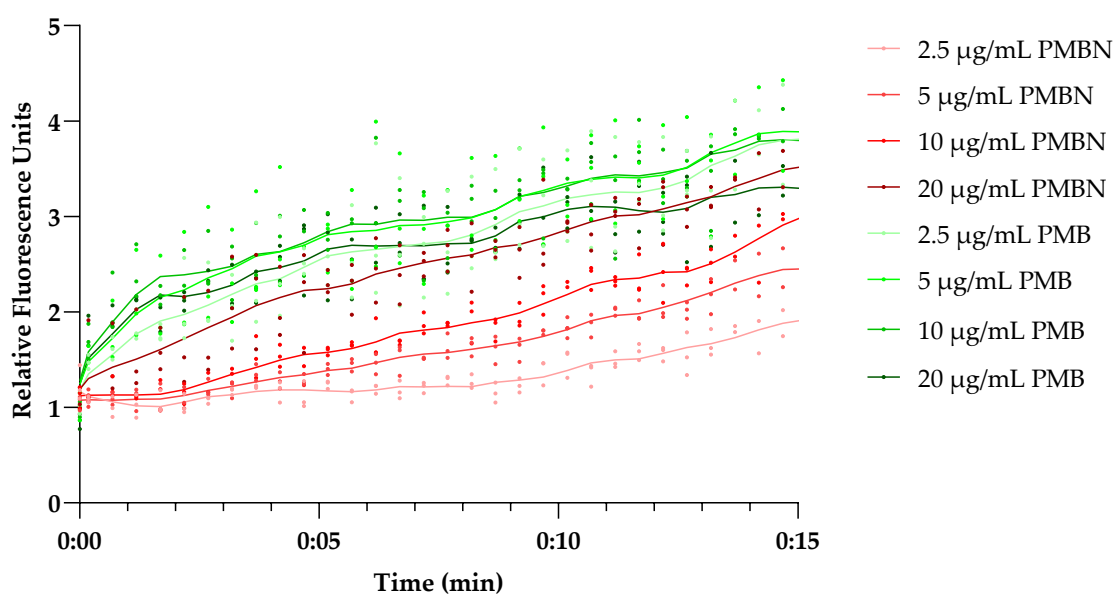


Figure S2. The dose dependent short-term effect of PMB and PMBN on UnaG fluorescence kinetics. Fluorescence kinetic of UnaG of *E. coli* MC4100 after exposure of different concentrations of polymyxin B (PMB; solid shades of green) or polymyxin B nonapeptide (PMBN; solid shades of red).

The data points represent three independent measurements normalized to the negative control in presence of BR only. The mean is represented by the solid line of the same color.

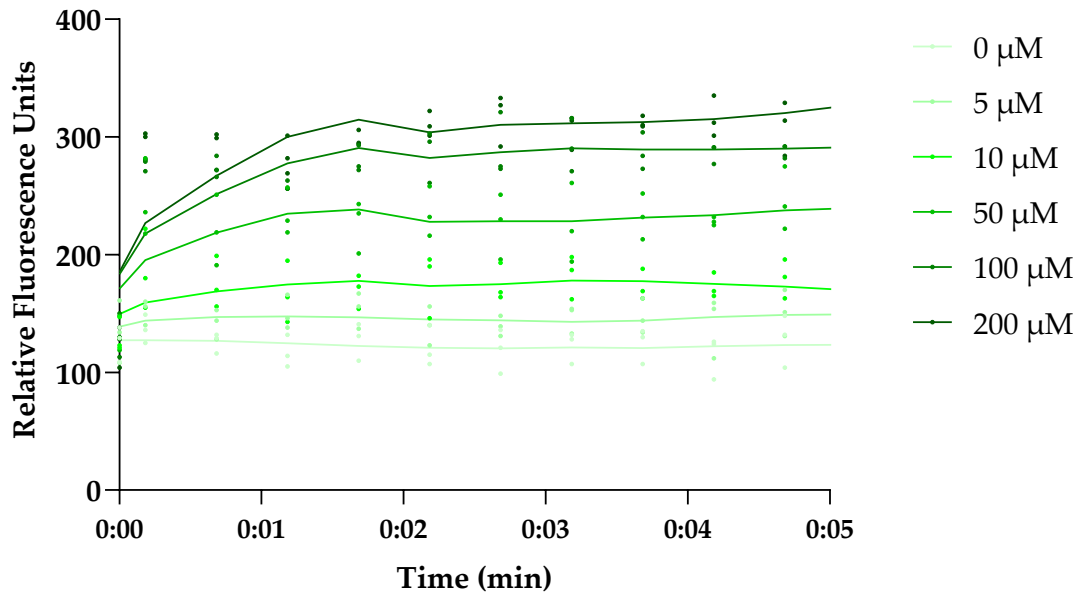


Figure S3. Fluorescence kinetic of UnaG of *E. coli* MC4100 after exposure of different concentration of BR. The data points represent three independent measurements normalized to the negative control in presence of bacteria only. The mean is represented by the solid line of the same color.

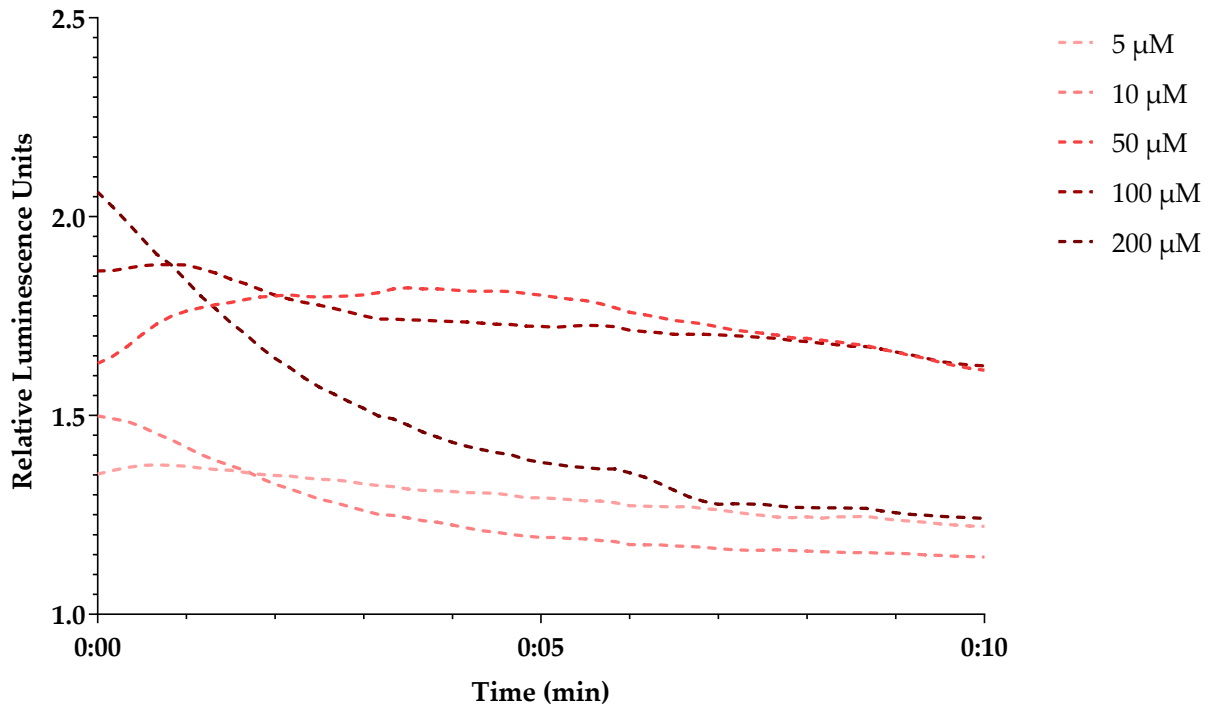


Figure S4. Luminescence kinetic of LucGR in *E. coli* NR698 after exposure of different concentration of BR. The mean of three independent measurements normalized to the negative control in presence of D-luciferin only is represented by the dashed line of the same color.

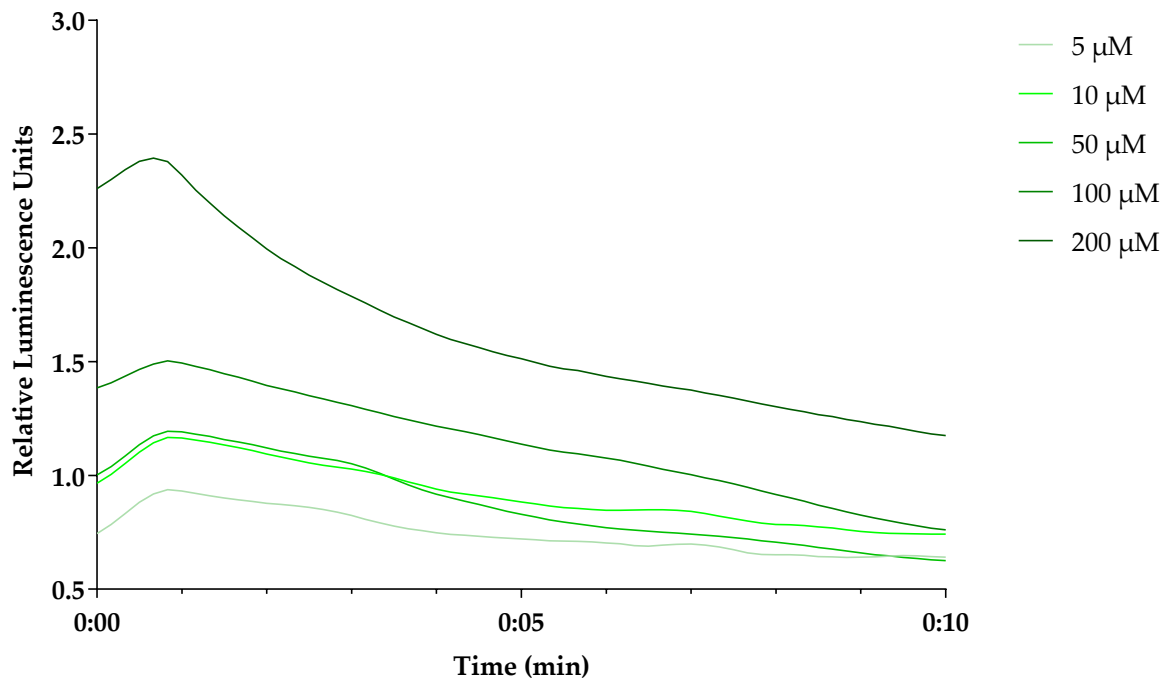


Figure S5. Luminescence kinetic of LucGR in *E. coli* MC4100 after exposure of different concentration of BR. The mean of three independent measurements normalized to the negative control in presence of D-luciferin only is represented by the solid line of the same color.

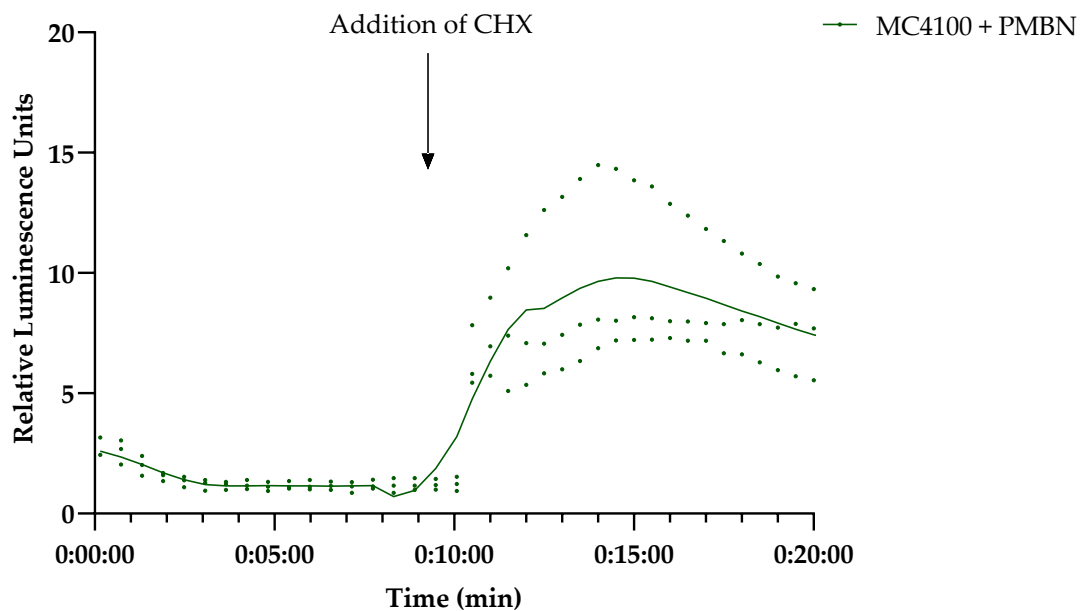


Figure S6. Plasma membrane remains intact after exposure to PMBN. Luminescence kinetic of LucGR in *E. coli* MC4100 after initial exposure to 12,5 μg/mL PMBN and 5 μM of BR and subsequent addition of 5 μg/mL chlorhexidine (CHX) at the 10 minutes mark. The data points represent three independent measurements normalized to the negative control in presence of D-luciferin only. The mean is represented by the solid line of the same color.

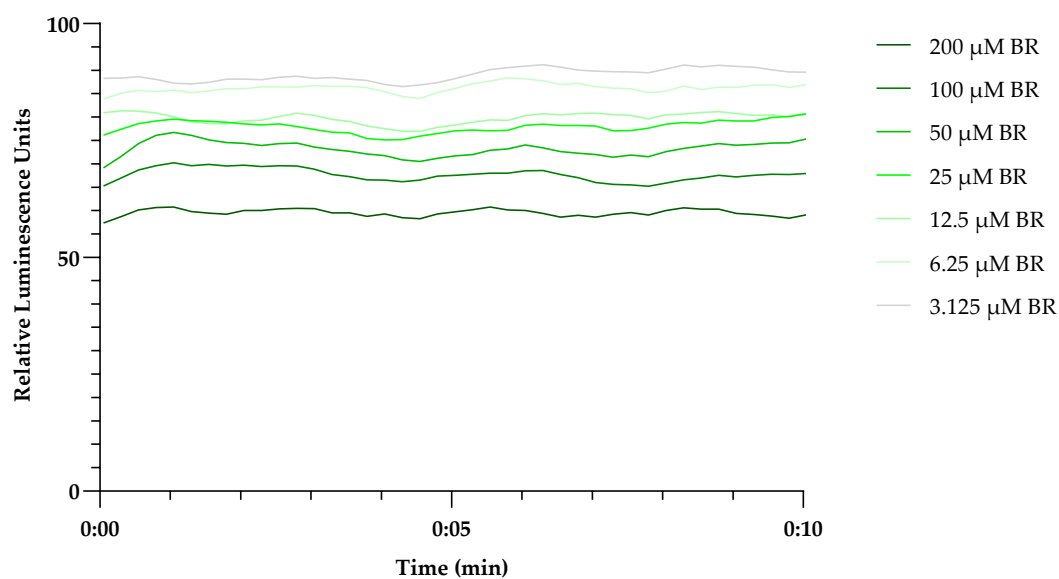


Figure S7. No effect of BR concentrations on short-term viability of *E. coli* MC4100. Luminescence kinetic of lux operon in *E. coli* MC4100 after exposure to different concentrations of BR. The mean of three independent measurements normalized to the negative control in presence of DMSO only is represented by the solid lines. Concentration dependent reduction of luminescence is likely caused by the absorbance spectrum of BR overlapping with the emission spectrum of the luciferase. A decrease in luminescence over time would indicate reduced viability.

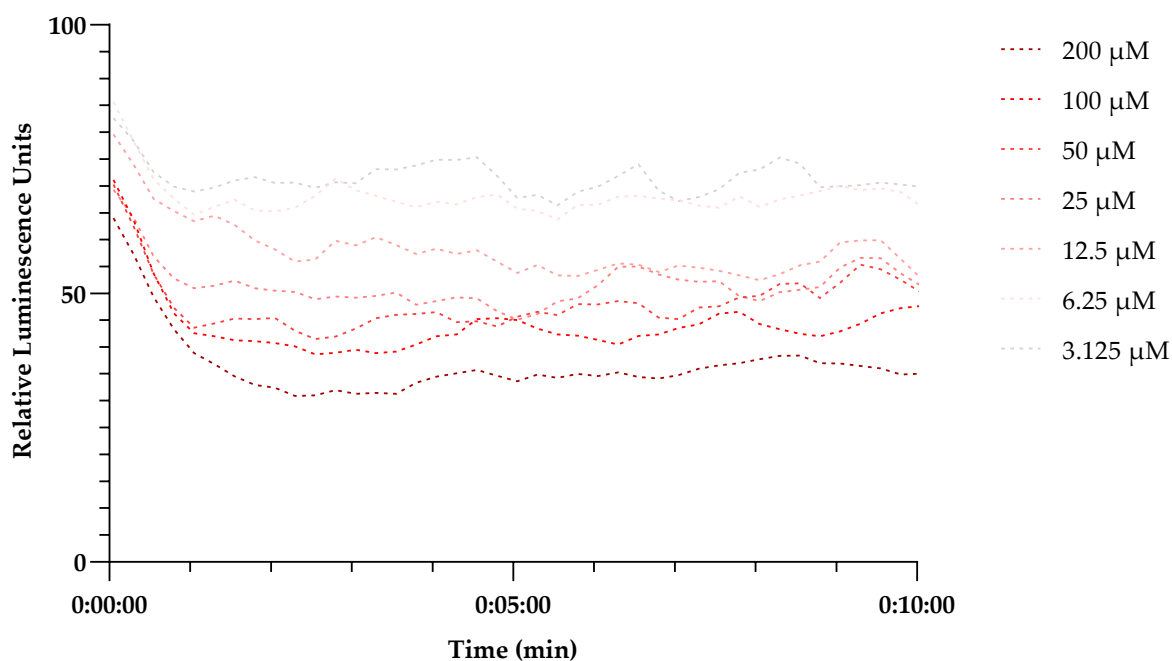


Figure S8. *E. coli* NR698 stays alive after exposure to different BR concentrations. Luminescence kinetic of the lux operon in *E. coli* NR698 after exposure of different concentration of BR. The mean of three independent measurements normalized to the negative control in presence of DMSO only is represented by the dashed line of the same color. Concentration dependent reduction of luminescence is likely caused by the absorbance spectrum of BR overlapping with the emission spectrum of the luciferase.

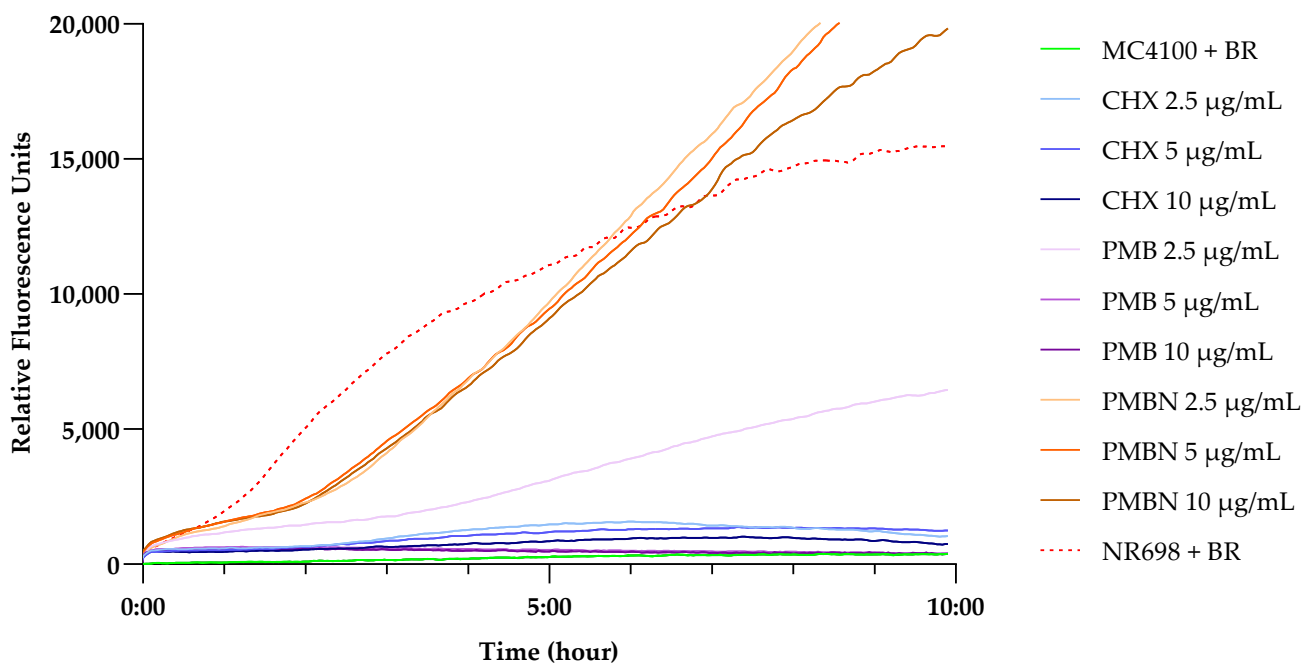


Figure S9. Long-term fluorescence kinetic of the proposed OM biosensor to well-known model peptides. Fluorescence kinetic of UnaG of *E. coli* MC4100 after exposure to different concentrations of PMB (solid shades of purple), PMBN (solid shades of orange), and CHX (solid shades of blue) for 10 hours. The *E. coli* MC4100 negative control with bilirubin only is represented by a solid green line and *E. coli* NR698 with bilirubin only by a dashed red line. All the data are normalized to bacteria with no addition of bilirubin. The mean of three independent measurements is represented by the solid line of the same color.

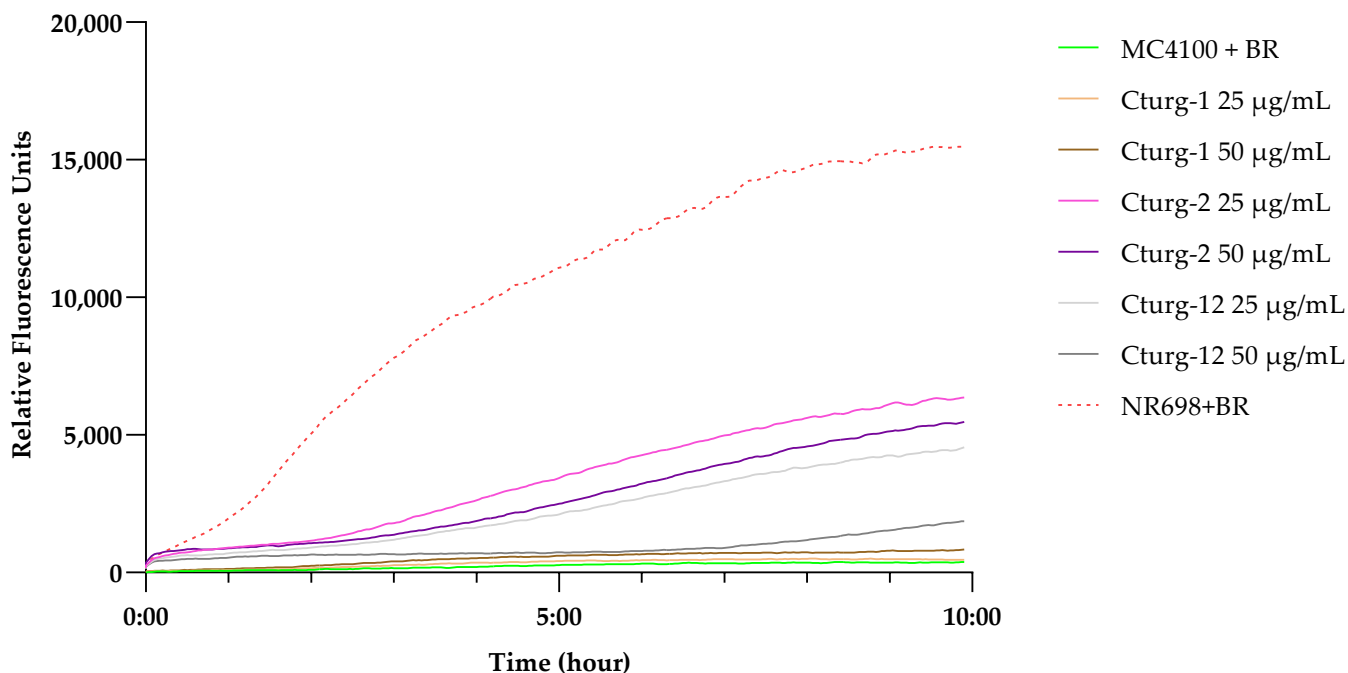


Figure S10. Long term fluorescence kinetic of the proposed OM biosensor to novel cyclic peptide derivatives. Fluorescence kinetic of UnaG in *E. coli* MC4100 after exposure to different concentrations of cyclic marine antimicrobial peptide derivatives cTurg-1 (solid shades of brown), cTurg-2

(solid shades of pink), and derivative C₁₂-Turg-1 (solid shades of blue) for 10 hours. The control of *E. coli* MC4100 with bilirubin only is represented by a solid green line and *E. coli* NR698 with bilirubin only by a dashed red line. All the data are normalized to bacteria with no addition of bilirubin. The mean of three independent measurements is represented by the solid line of the same color.

TGCGTATTGGGCGCTCTCCGCTTCCTCGCTCACTGACTCGCTGCGCTCGGTTCGTT
GGTAAAGCCTGGGGTGCCTAATGAGCAAAAGGCCAGCAAAAGGCCAGGAAC
CGTAAAAAGGCCGCGTTGCTGGCGTTTTTCCATAGGCTCCGCCCCCTGACGAGC
ATCACAAAATCGACGCTCAAGTCAGAGGTGGCGAAACCCGACAGGACTATAA
AGATACCAGGCGTTTTCCCCTGGAAGCTCCCTCGTGCGCTCTCTGTTCCGACCC
TGCCGTTACCGGATACCTGTCCGCTTTCTCCCTTCGGGAAGCGTGGCGCTTTCT
CATAGCTCACGCTGTAGGTATCTCAGTTCGGTGTAGGTTCGTTTCGCTCCAAGCTGG
GCTGTGTGCACGAACCCCCGTTTCAGCCCCGACCGCTGCGCCTTATCCGGTAACTA
TCGTCTTGAGTCCAACCCGGTAAGACACGACTTATCGCCACTGGCAGCAGCCAC
TGGTAACAGGATTAGCAGAGCGAGGTATGTAGGCGGTGCTACAGAGTCTTGAA
GTGGTGGCCTAACTACGGCTACACTAGAAGAACAGTATTTGGTATCTGCGCTCTG
CTGAAGCCAGTTACCTTCGGAAAAAGAGTTGGTAGCTCTTGATCCGGCAAACAA
ACCACCGCTGGTAGCGGTGGTTTTTTTGTTCGCAAGCAGCAGATTACGCGCAGAA
AAAAAGGATCTCAAGAAGATCCTTTGATCTTTTCTACGGGGTCTGACGCTCAGTG
GAACGAAAACCTCACGTTAAGGGATTTTGGTCATGAGATTATCAAAAAGGATCTT
CACCTAGATCCTTTTAAATTAATAAATGAAGTTTTAAATCAATCTAAAGTATATAT
GAGTAAACTTGGTCTGACAGTTACCAATGCTTAATCAGTGAGGCACCTATCTCA
GCGATCTGTCTATTTTCGTTTCATCCATAGTTGCCTGACTCCCCGTCGTGTAGATAAC
TACGATACGGGAGGGCTTACCATCTGGCCCCAGTGCTGCAATGATACCGCGAGA
ACCACGCTCACCGGCTCCAGATTTATCAGCAATAAACAGCCAGCCGGAAGGG
CCGAGCGCAGAAGTGGTCTGCAACTTTATCCGCCTCCATCCAGTCTATTAATTG
TTGCCGGGAAGCTAGAGTAAGTAGTTTCGCCAGTTAATAGTTTTCGCAACGTTGTT
GCCATTGCTACAGGCATCGTGGTGTACGCTCGTCGTTTTGGTATGGCTTCATTCA
GCTCCGGTTCCCAACGATCAAGGCGAGTTACATGATCCCCCATGTTGTGCAAAA
AAGCGGTTAGCTCCTTCGGTCCCTCCGATCGTTGTCAGAAGTAAGTTGGCCGCAGT
GTTATCACTCATGGTTATGGCAGCACTGCATAATTCTTACTGTTCATGCCATCCG
TAAGATGCTTTTCTGTGACTGGTGTGACTCAACCAAGTCATTCTGAGAATAGTG
TATGCGGCGACCGAGTTGCTCTTGCCCGGCGTCAATACGGGATAATACCGCGCC
ACATAGCAGAACTTTAAAAGTGCTCATCATTGGAACCGTTCTTCGGGGCGAAA
ACTCTCAAGGATCTTACCGCTGTTGAGATCCAGTTCGATGTAACCCACTCGTGCA
CCCAACTGATCTTCAGCATCTTTTACTTTTACCAGCGTTTCTGGGTGAGCAAAAA
CAGGAAGGCAAAATGCCGCAAAAAAGGGAATAAGGGCGACACGGAAATGTTG
AATACTCATACTCTTCCTTTTTCAATATTATTGAAGCATTATCAGGGTTATTGTCT
CATGAGCGGATACATATTTGAATGTATTTAGAAAAATAAACAAATAGGGGTTCC
GCGCACATTTCCCGAAAAGTGCCAC

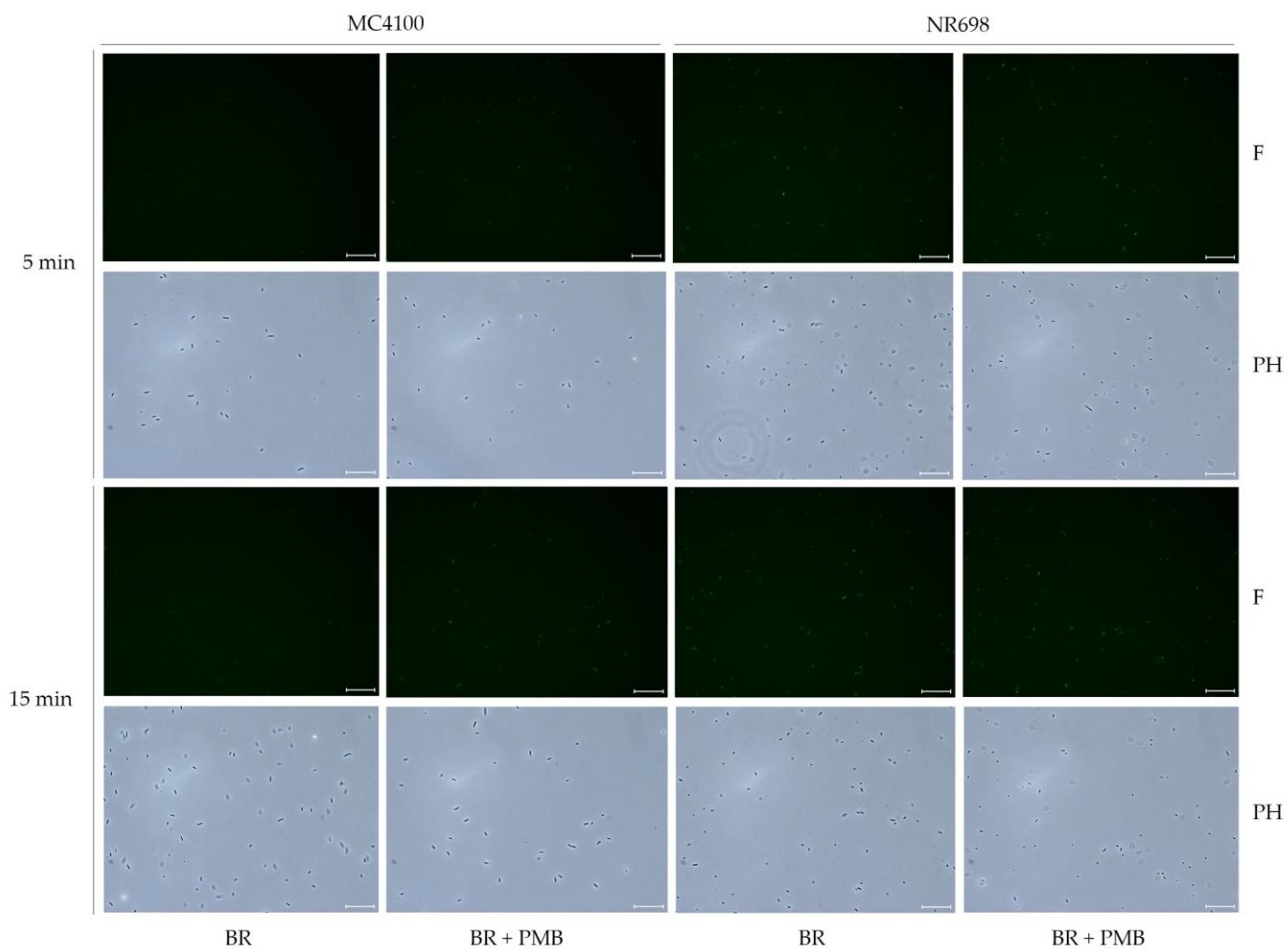


Figure S12. PMB induces population wide fluorescence of UnaG expressing *E. coli* cells. Fluorescence images of *E. coli* MC4100 and NR698 at time points of 5 minutes and 15 minutes after exposure to BR (5 μ M) (BR) or BR and PMB (10 μ g/mL) (BR + PMB) at x400 magnification. The images were taken with the phase contrast (PH) and with fluorescence (F) through the software LAS X. The scale bars represent 25 μ m. Version without the increase of the brightness through Adobe Photoshop CS6 version 13.0.

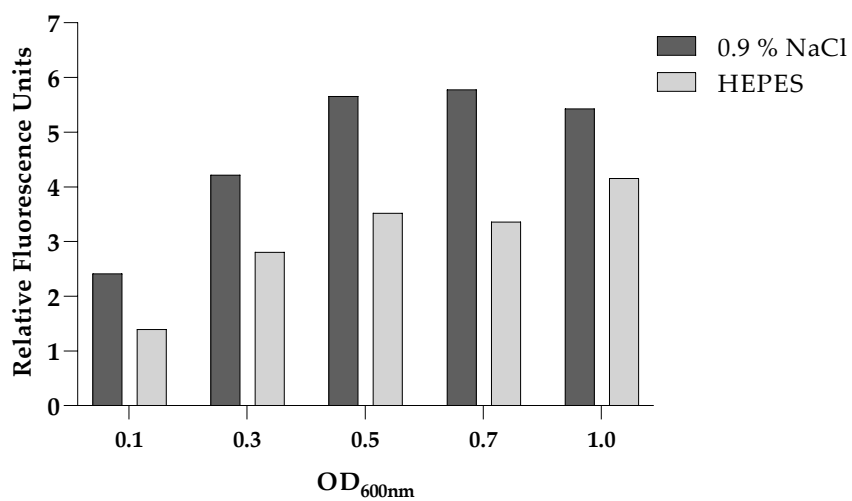


Figure S13. The influence of bacterial density on UnaG fluorescence. Relative fluorescence of UnaG in *E. coli* MC4100 after 15 min exposure to 10 µg/mL PMB normalised to the control in absence of PMB at different ODs in 0.9% NaCl and HEPES buffer

Paper III

Manuscript

Cloning of a dual biosensor relying on UnaG and luciferase for detection of outer and plasma membrane disruption and its application to characterizing the membranolytic effects of green sea urchin *Strongylocentrotus droebachiensis* Centrocin-1-based antimicrobial peptides

Céline S. M. Richard ¹, Hymonti Dey ¹, Emma Murvold ¹, Frode Øyen ¹, Chun Li ¹ and Hans-Matti Blencke ^{1,*}

¹ Norwegian College of Fishery Science, Faculty of Biosciences, Fisheries and Economics, UiT The Arctic University of Norway, Breivika, N-9037 Tromsø, Norway; celine.s.richard@uit.no (C.S.M.R.); hymonti.dey@uit.no (H.D.); emu023@post.uit.no (E.M.); frode.oyen@uit.no (F.Ø.); chun.li@uit.no (C.L.); hans-matti.blencke@uit.no (H.-M.B.)

* hans-matti.blencke@uit.no (H.-M.B.)

Abstract: Antimicrobial peptides (AMPs) are mostly known for their ability to compromise bacterial membranes, thus rapidly killing the cells. Less emphasis has been on differentiating their effect on the plasma membrane (PM) and the outer membrane (OM) in Gram-negatives as separate events. The OM barrier excludes antibiotics (ABs) from Gram-negative bacteria. Hence, peptides specifically disrupting the OM might work in synergy with traditional antibiotics, expanding the use of ABs currently restricted to Gram-positives to treatment of Gram-negative infections. However, discovering novel OM active natural products requires robust OM specific biosensors. In a previous study we established that the Bilirubin (BR) dependent fluorescent protein UnaG can serve as a sensor to detect OM compromising compounds in *Escherichia coli*. In this study we combined UnaG with luciferases in artificial operons to simultaneously but separately evaluate OM and PM disruption or viability. During characterization of these double sensors, we observed that UnaG fluorescence in *E. coli* seems to depend on freshly translated UnaG. We used equally timed expression of apo- and holoUnaG and subsequent fluorescence measurements to evaluate protein stability. We deduced that apoUnaG is less stable than holoUnaG when remaining in the *E. coli* cytoplasm. Finally, we used this novel biosensor as a tool to characterize PM and OM disruption by the green sea urchin *Strongylocentrotus droebachiensis* Centrocin-1 and its derivatives and confirmed that the OM disruption by Centrocin (1-20) works synergistically with Vancomycin and Erythromycin against *E. coli*.

Citation: To be added by editorial staff during production.

Academic Editor: Firstname Last-name

Received: date

Revised: date

Accepted: date

Published: date



Copyright: © 2023 by the authors. Submitted for possible open access publication under the terms and conditions of the Creative Commons Attribution (CC BY) license (<https://creativecommons.org/licenses/by/4.0/>).

Keywords: biosensor; reporter gene; synthetic biology; outer membrane; plasma membrane; synergy

1. Introduction

Natural product discovery represents a fascinating and essential field of scientific exploration characterized by the systematic investigation and elucidation of chemical compounds produced by living organisms, encompassing plants, microbes and marine organisms [1–5]. This field has played a significant role in shaping the world of medicine, agriculture, and biotechnology [6–8]. One well-known class of those naturally occurring molecules are antimicrobial peptides (AMPs). Those crucial components of innate immune defenses [9,10] are characterized by a relatively small size (mostly 3–50 amino acids) and their broad-spectrum antimicrobial activity against bacteria, viruses and fungi [11].

Many of the known AMPs can interact with and destabilize bacterial membranes due to their usually amphipathic nature and net cationic charge. Some AMPs with intracellular targets progress to the cytoplasm and can interfere with synthesis of essential macromolecules [12,13], thereby either killing the cells or arresting their growth. Their notable amino acid sequence and structural diversity contributes to their versatility in targeting a diverse range of microorganisms, rendering AMPs a compelling candidate for the development of innovative antimicrobial therapies.

The marine environment represents more than 70% of the Earth's habitats encompassing between 50% and 80% of all lifeforms and is yet insufficiently explored for potential bioactive molecules in natural product discovery [14]. Aqueous by nature, sea water is an ideal medium for spreading pathogenic bacteria between the immersed hosts. On average sea water contains around 10^6 bacteria/mL. Nonetheless, invertebrates rely solely on innate immunity, including AMPs, to combat infectious agents. Thus, the marine environment selects for the evolution of a large number of AMPs. Marine AMPs differ from their terrestrial counterparts by the prevalence of the amino acids arginine and leucine, as an adaptation to the composition of bacterial membranes in the cold marine environment with an increased prevalence of polyunsaturated fatty acids [13,15–20] as well as brominated amino acids like strongylocins and centrocins [21]. This also makes them interesting for drug discovery. The first marine AMP was discovered by Nakamura *et al.* [22], named tachyplesin, from the hemocytes of horseshoe crab *Tachypleus tridentatus*. Since then, the discovery of AMPs from marine environment continued to intrigue. In 2010, Chun Li *et al.* [21] isolated the AMPs named Centrocin 1 and Centrocin 2 from the green sea urchin *Strongylocentrotus droebachiensis*. These peptides are composed of a light chain (12 amino acids) and a heavy chain (30 amino acids) linked by a cysteine disulfide bond and were active against Gram-positive and Gram-negative bacteria. Moreover, the heavy chain of the Centrocin 1 alone showed pronounced effect against pathogens like methicillin-resistant *Staphylococcus aureus* (MRSA), *Escherichia coli*, *Pseudomonas aeruginosa* or *Klebsiella pneumoniae* and the bacterial cultures failed to develop significant resistance toward this peptide [23], making it very appealing for clinical settings.

Several Gram-negative antibiotic resistant pathogens are strongly impacting the healthcare systems. Among them pathogenic *E. coli* strains such as carbapenem-resistant *Enterobacteriaceae* (CRE) [24–26], extended-spectrum β -lactamase (ESBLs) [27–29] and more recently Colistin-resistant *E. coli* [30–32]. One distinctive feature of Gram-negative bacteria is the outer membrane (OM), which functions as an effective permeability barrier and thus, contributes to their resistance against a large number of antimicrobial compounds [33,34]. This asymmetric bilayer of lipids contains glycolipids, mostly lipopolysaccharides (LPS), exclusively on the outer leaflet, and phospholipids with a composition about 80% phosphatidylethanolamine, 15% phosphatidylglycerol and 5% cardiolipin on the inner leaflet [35]. Furthermore, modifications in the lipid or protein composition of the OM are often found in drug-resistance bacterial species [36]. Consequently, the OM is an interesting target for the new drug discovery [37–39].

In light of the well-established knowledge that for example, the plasma membrane (PM) serves as a universal target for AMPs [9,40], it becomes pertinent to investigate the potential synergistic interactions involving the OM activity. It is noteworthy that a molecule, which may otherwise be hindered from accessing intracellular targets by the OM, could potentially regain its bioactivity in the presence of compounds exhibiting OM activity, like the Polymyxin B nonapeptide [41] or AMPs like thanatin [42,43].

Thus, *E. coli*-based discovery platforms to identify molecules with the potential to permeabilize the OM of Gram-negative bacteria and increasing susceptibility to compounds excluded by the OM might contribute to the identification of novel OM permeabilizers, which could be used synergistically with antibiotics (ABs) already on the market.

The original study showed that the fluorescence of the UnaG protein from the Japanese eel *Anguilla japonica* is dependent on the presence of its ligand bilirubin (BR) [44]. We recently showed that at low BR concentrations the diffusion of BR into *E. coli* cells is

dependent on OM disruption. Moreover we suggested that *E. coli* cells expressing UnaG could serve as real-time biosensors for OM integrity [45].

In this study, we show that the combination of UnaG with different luciferase-based reporter systems could be used as a biosensor that can distinguish OM from OM and PM active compounds in real time. Moreover, we coupled the ability of sensing OM disruption to cell viability measurements into one biosensor strain allowing for one step evaluation of OM and viability in microtiter plate formats.

2. Results and Discussion

2.1. Combining the UnaG outer membrane sensor with luciferase-based reporter systems

To determine if it is possible to measure outer membrane (OM) and plasma membrane (PM) disrupting activities simultaneously, we constructed sensor strains carrying two sensor plasmids. The *E. coli* strains MC4100 and NR698 carrying the plasmid pMM001 and therefore constitutively expressing *unaG*, were transformed with the plasmid pCSS962 for constitutive expression of *lucGR* from Virta *et al.* [46]. The protein LucGR, which is localized in the cytoplasm of the bacterium needs D-luciferin as substrate to emit bioluminescence. At neutral pH, the bacterial PM acts as a barrier for D-luciferin and substantially slows down its diffusion into the cytoplasm, resulting in low luminescence levels in absence of PM disrupting agents. In contrast, the protein UnaG, which is also expressed in the cytoplasm, will only emit fluorescence in presence of BR. In this case the OM seems to constitute an efficient barrier against diffusion of BR, while an intact PM doesn't seem to inhibit its further diffusion into the cytoplasm.

To account for the requirements of both sensor systems, near neutral pH for the plasma membrane sensor and 0,9% NaCl for the OM assay, we tried to find optimal conditions in terms of signal to noise (background of fluorescence and luminescence) ratio in the simultaneous assays by varying the concentration of Tris pH 7.5 in 0,9 % NaCl solution (figure S1a). The highest signal to noise ratio for UnaG fluorescence after exposure to low concentrations of PMB were achieved between 20 mM and 40 mM Tris, with a value of approximately 1.6 to 2.0 relative fluorescence units. The background luminescence after exposure to the ligand D-luciferin in 0,9 % NaCl was high in absence of Tris buffer even without addition of a membrane active compound and dropped to approximately 15% when the buffer contained 5 mM Tris. Background luminescence stabilized to around 5-10% between 20 to 40 mM Tris (figure S1b). Thus, the conditions used for the simultaneous assay were repeated in 0,9 % NaCl, 20 mM Tris HCl and at a pH of pH 7.5.

To investigate if we could follow both, the luminescence and the fluorescence signals from the strains carrying both plasmids simultaneously, the wild type *E. coli* strain MC4100 was used to check the effect of chlorhexidine (CHX) on plasma membrane integrity and Polymyxin on OM integrity (figure 1). The fluorescence emitted by UnaG increases after addition of PMB by 50% while it stays constant in its absence. Addition of chlorhexidine strongly increased luminescence within seconds and then dropped close to the level of the background within only 2 min. These results confirmed that both sensor systems function independently in presence of the other reporter system.

To confirm that expression of *unaG* in the artificial operon with *lucGR* is not affecting UnaG expression, we compared fluorescence levels of the single sensor [45] with the double sensor in similar conditions. To compare general expression levels, we first analyzed expression in the OM deficient strain NR698 carrying either pMM001 or pCSMR01. We observed similar fluorescence levels for both plasmids (figure S2). Then we compared the sensitivity of MC4100 carrying the two plasmids to PMBN. Here the co-expression of *lucGR* did not substantially reduce the fluorescence response to OM perturbation.

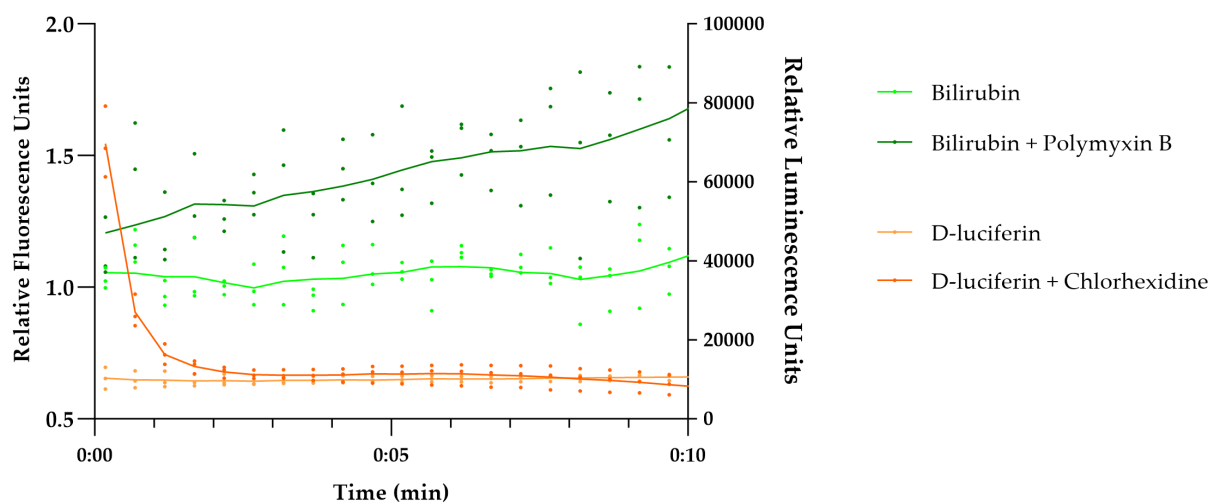


Figure 1. Fluorescence kinetic of UnaG (shades of green) and luminescence kinetic of LucGR (shades of orange) of *E. coli* MC4100 carrying pMM001 and pCSS962 after exposure of Polymyxin B or bilirubin only for UnaG and Chlorhexidine or D-luciferin only for LucGR. Each data point is the mean of three independent measurements. Water was used as negative control.

2.2. Does export of UnaG to the periplasm improve assay sensitivity?

To evaluate the behavior of OM integrity dependent fluorescence when UnaG is localized in the periplasm instead of the cytoplasm, different localization-tags responsible for protein export in *E. coli* cells were fused to *unaG*. In the original pMM001 UnaG is constitutively expressed in the cytoplasm without a transport-tag; pCSMR03 represents the Sec pathway with constitutively expressed *unaG* fused to the signal sequence of *dsbA* and pCSMR04 the TAT pathway with constitutively expressed *unaG* fused to the signal sequence of *torA*. However, fluorescence assays with the constructs supposedly expressing and exporting UnaG to the periplasm were inconclusive sometimes lacking all fluorescence completely, other times returning fluorescence also in absence of OM disrupting agents. Microscopic analysis revealed that fluorescent *E. coli* cells with plasmids for export of UnaG to the periplasm were fluorescent, though abnormally long (figure S3). Transporting strongly and constitutively expressed UnaG to the periplasm seemed to negatively affect cell growth and division. It is not clear if the effect is the mere result of too high expression of UnaG or a protein specific interaction with cell division. However, Stanley *et al.* [47] reported that blocking the *tat*-pathway by deleting genes essential for protein transport, resulted in a prolonged phenotype likely due to incomplete septation. This phenotype resembles *lpxC* mutants, resulting in a defect in biosynthesis of the OM. Thus, the export of UnaG might merely outcompete export of components necessary for cell septation and thereby induce long cell phenotypes. To alleviate this effect, the constitutive promoter was replaced by the inducible arabinose P_{BAD} promoter. The new plasmids were named pMM001B, pCSMR03B, and pCSMR04B. Fluorescence microscopic images revealed that conditional UnaG expression by addition of 1 μ M L-arabinose in advance of microscopy retained normal cell shape and BR-dependent fluorescence (figure 2). Moreover, the fluorescent images confirmed UnaG export to the periplasm in case of Sec pathway dependent use of the *dsbA* signal sequence, indicated by more intense fluorescence in the periphery of the cells in figure 2b. In contrast, when UnaG is tagged with the *torA* signal sequence for export through the TAT pathway (figure 2c), the fluorescence pattern mostly resembles the pattern seen in the cytoplasm control (figure 2a) with

fluorescence throughout the cell and only some cells with stronger fluorescence intensities in the periphery. That can be explained by the fact that Tat secretion pathway transports folded proteins, thus proteins gain their active, and in case of UnaG fluorescent, structure before being exported to the periplasm.

180
181
182
183
184

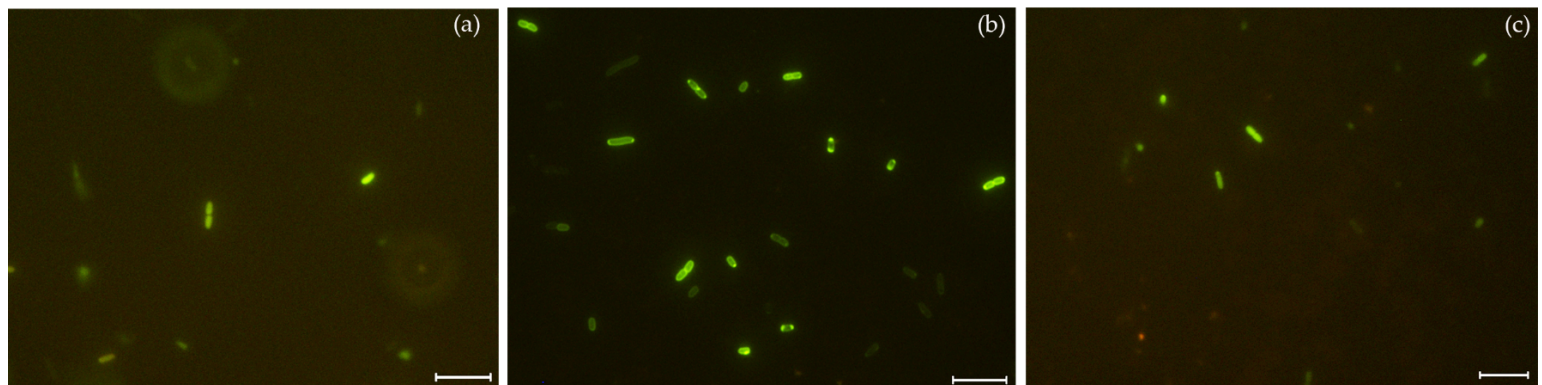


Figure 2: Effect of different export tags on UnaG fluorescence localization. Fluorescence images of *E. coli* MC4100 carrying the plasmid (a) pMm001B, (b) pCSMR03B, (c) pCSMR04B, 45 min after exposure to 5 μ M BR, 1 μ M L-arabinose and 10 μ g/mL PMBN at \times 1000 magnification. The images were taken with fluorescence through the software LAS X. The scale bars represent 7.5 μ m. For better visibility on all electronic devices, the brightness of the images was equivalently increased to 150 with Adobe Photoshop CS6 version 13.0.

185
186
187
188
189
190
191

In order to determine if the periplasmic localization of UnaG affects the response of the outer-membrane assay suggested in our previous study [45] population based fluorescence assays in microtiter plates were conducted. The *E. coli* strain MC4100 and its isogenic OM impaired mutant NR698 carrying the plasmids pMm001B, pCSMR03B and pCSMR04B were grown in presence or absence of 1 μ M L-arabinose, 5 μ M BR and 10 μ g/mL PMBN. Figure 3 illustrates the UnaG fluorescence kinetic of MC4100 and NR698 over a period of 10 hours. In the WT (figure 3a), the fluorescence kinetics are almost identical for plasmids pMm001B and pCSMR04B, where UnaG is folded in the cytoplasm. Fluorescence intensity rises more slowly and to a lower final intensity in the strain carrying the plasmid pCSMR03B, where the protein is folded in the periplasm. In all cases fluorescence is still dependent on the presence of the OM disruptive PMBN. When analyzing fluorescence development in the OM impaired mutant (figure 3b), fluorescence emission is strongest in the strain carrying the plasmid pCSMR04B, where UnaG is folded in the cytoplasm and translocated by the tat-pathway to the periplasm. Fluorescence is weakest, in the strain containing the plasmid pCSMR03B. Interestingly, addition of PMBN further increases fluorescence levels despite the already impaired OM. In both strains MC4100 (figure 3a) and NR698 (figure 3b), there is no signal of fluorescence in presence of 10 μ g/mL PMBN alone but there is an increase of fluorescence in presence of 10 μ g/mL PMBN and 1 μ M L-arabinose (PMBNa) indicating that expression of UnaG is strictly arabinose dependent. Thus, no increase in sensitivity or specificity was observed when UnaG was localized in the periplasm, on the contrary, Sec-dependent transport seems to reduce the sensitivity of the assay.

192
193
194
195
196
197
198
199
200
201
202
203
204
205
206
207
208
209
210
211
212
213
214

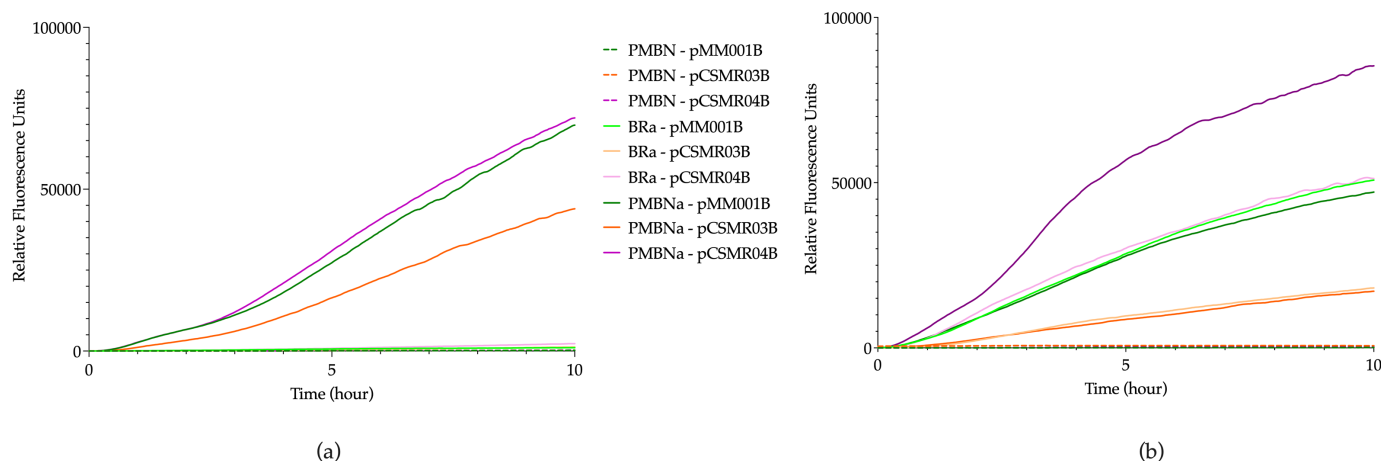


Figure 3: Comparison of the fluorescence kinetic of UnaG of the wild-type MC4100 (a) and the mutant NR698 (b) carrying either the plasmid pMM001B, pCSMR03B, and pCSMR04B in presence of 5 μ M BR and 10 μ g/mL PMBN (PMBN); 1 μ M L-arabinose and 5 μ M BR (Bra); or 1 μ M L-arabinose, 5 μ M BR and 10 μ g/mL PMBN (PMBNa).

2.3. UnaG fluorescence is strongest in metabolically active cells

In our previous study we observed that although *unaG* is expressed from a strong constitutive promoter in the single OM biosensor, its initial fluorescence is relatively weak but increases slowly over time after an OM active compound is added [45]. We also observed that PM active compounds did not invoke UnaG fluorescence, and we speculated that this is caused by the complete metabolic breakdown caused by PM disruption, which stops the translation machinery. The above-mentioned observations indicate that availability of apoUnaG to bind BR is limited and is only increasing while the cells are metabolically active. There are at least three possible explanations for these observations: 1. Only freshly translated apoUnaG can efficiently bind BR to form holoUnaG; 2. apoUnaG expressed from the strong OXB15-promoter is aggregating and therefore not accessible for BR-binding to form holoUnaG; 3. UnaG localized in the cytoplasm of *E. coli* is unstable and possibly proteolytically degraded. We excluded the first explanation as apoUnaG expressed in *E. coli* and purified by affinity chromatography is readily binding BR to form holoUnaG *in vitro* [44]. We also confirmed that the BR concentration used in the experiments is not negatively affecting fluorescence kinetics of UnaG by inducing UnaG expression in the presence of different BR concentrations. We tested how the BR concentrations affected fluorescence when present from the start and added 1 hour after induction. In both cases 5 μ M, which was used for all our studies seemed to achieve the fastest possible fluorescence kinetics.

To study holoUnaG formation unimpeded by the OM acting as a barrier and excluding BR, we conducted the following experiments in the OM impaired NR698 background. First, we compared the fluorescence and luminescence emissions from the dual biosensors immediately after addition of ligand, and in case of lucGR substrate. To compare the measurements in one figure, the highest fluorescence value of each reporter gene was normalized to 100%. Luminescence is strong from the start for both luciferase constructs, but decreases steadily over time, most likely due to metabolic constraints related to nutrient limitation in the buffer solution (*lucGR* figure 4b; control and *luxABCDE* figure S4b). An inverse kinetic was observed for UnaG fluorescence. UnaG fluorescence intensity starts low and increases slowly over time likely related to fresh UnaG synthesis. To be able to compare UnaG fluorescence kinetics to another fluorescent reporter where the signal is independent of the current metabolic status of the cell, we expressed GFP and mCherry

in a similar setting, i.e. from an identical plasmid backbone and promoter (as a single gene, not in an artificial operon with luciferases). mCherry-specific fluorescence starts at around 15% and increases to 100% in the end of the measurement, indicating that there is active mCherry from the start (mCherry figure 4a; control and GFP figure S4a).

To confirm that the increase of UnaG fluorescence correlates with active translation and is not a result of slowed BR diffusion or binding to previously formed apoUnaG, we added Erythromycin to slow down translation at different timepoints in advance of and after BR addition. We also recorded the effect on concomitant luminescence from the synthetic operon and compared the effect of translation inhibition to fluorescence of mCherry and GFP expressing cells treated in the same way (figure 4a UnaG and mCherry; figure 4b LucGR; figure S4a UnaG and GFP; figure S4b LuxABCDE). Addition of Erythromycin slowed down UnaG-dependent fluorescence almost immediately, however, the fluorescence kept increasing at a reduced rate most likely due to incomplete translation inhibition by Erythromycin. Luminescence was affected to a lesser extent and more slowly, indicating that previously translated luciferase was stable and remained active as the cells remained viable. The effect of Erythromycin on mCherry fluorescence could be detected after 3 hours while the effect on UnaG fluorescence development was almost immediate when BR was present in the cultures. Interestingly, the different timepoints of Erythromycin addition spaced 15 minutes apart over one hour, did not result in detectable differences in mCherry fluorescence signal throughout the experiment. UnaG fluorescence on the other hand was directly related to the timepoints of Erythromycin addition. In addition, the fluorescence increase between timepoints of Erythromycin addition was more pronounced when the antibiotic was added after BR addition. We thus hypothesized that apoUnaG might be less stable in *E. coli*. To confirm this, we expressed UnaG from the arabinose inducible promoter P_{BAD} again in the NR698 background to avoid interference of the OM. We induced expression of UnaG by addition of arabinose and stopped it 15 minutes later by the addition of either glucose (figure 6) and therefore catabolite repression, or a combination of erythromycin and tetracycline (figure 5) for general translation inhibition. We repeated this cycle in 15 minutes intervals for 60 minutes in consecutive wells of microtiter plates. To compare the stability of apoUnaG to the stability of holoUnaG the experiment was conducted in presence and absence of BR. In the latter case, BR was added after the last cycle was complete, i.e. 60 minutes after finishing the first cycle. The resulting fluorescence patterns indicate that UnaG fluorescence after a 15-minute induction remains rather stable when BR is provided from the start (figure 5a and figure 6a). When BR is added to the cultures after all the induction cycles are finished, fluorescence seems to depend on the age of the induction. The younger the cycle at the time of BR addition, the more fluorescence is emitted. We therefore conclude that apoUnaG either is less stable than holoUnaG when remaining in the cytoplasm or that it forms aggregates/inclusion bodies. Presence of inclusion bodies could explain the rather slow fluorescence increase in the UnaG based bacterial biosensors especially when expressing UnaG from the strong constitutive promoter of pCSMR01. We therefore analyzed phase contrast and fluorescence microscopic images of MC4100 cells expressing UnaG from pCSMR01 in presence of BR and Centrocins to permeabilize the outer membrane and allow for fluorescence (figure 10). Phase contrast images show that the cytoplasm looks homogenous with no indications of areas with differences in refractive index. Fluorescence micrographs show homogenous green fluorescence throughout the cells without areas with lower or increased fluorescence as shown in other studies [48,49], which could indicate inclusion bodies of non-fluorescent apoUnaG or fluorescent holoUnaG, respectively. We therefore suggest that apoUnaG is less stable than holoUnaG when in the *E. coli* cytoplasm. A similar observation was made for UnaG expressed in mouse fibroblast cell lines. In a study to make UnaG mutants with reduced stability in its apo-form, it was shown that also the WT apoUnaG expressed in the absence of BR rendered fusion protein constructs with mCherry less fluorescent and less stable than BR treated holoUnaG [50]. Another recombinantly expressed and purified fatty-acid binding protein from the

tapeworm *Spirometra* has been shown to withstand clostriparin proteolysis when bound to palmitin, indicating that the holo-form of this protein is more stable [51]. The increased stability of holo-proteins might be due to conformational changes in protein side chains as observed in a study comparing crystal structures of 305 proteins in their apo- and holo-forms [52], thus possibly protecting potential proteolytic recognition sites.

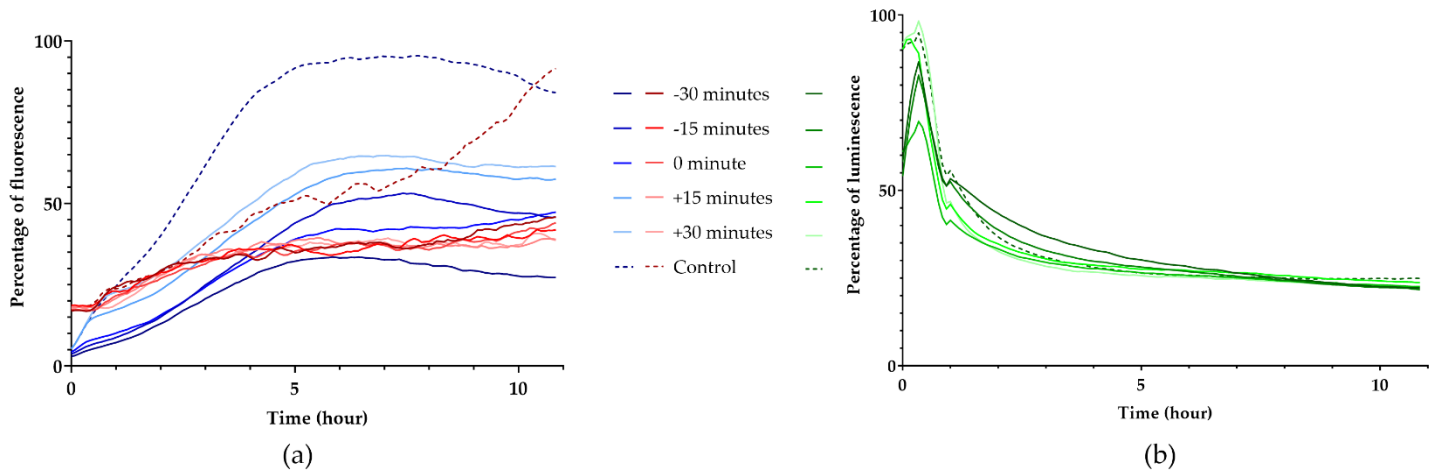


Figure 4: Kinetic of the relative (a) fluorescence of UnaG (shades of blue) and mCherry (shades of red); and (b) luminescence of LucGR for 10 hours after addition 5 μ M BR of *E. coli* NR698 at the 0 min time point and 50 μ g/mL Erythromycin at different time points.

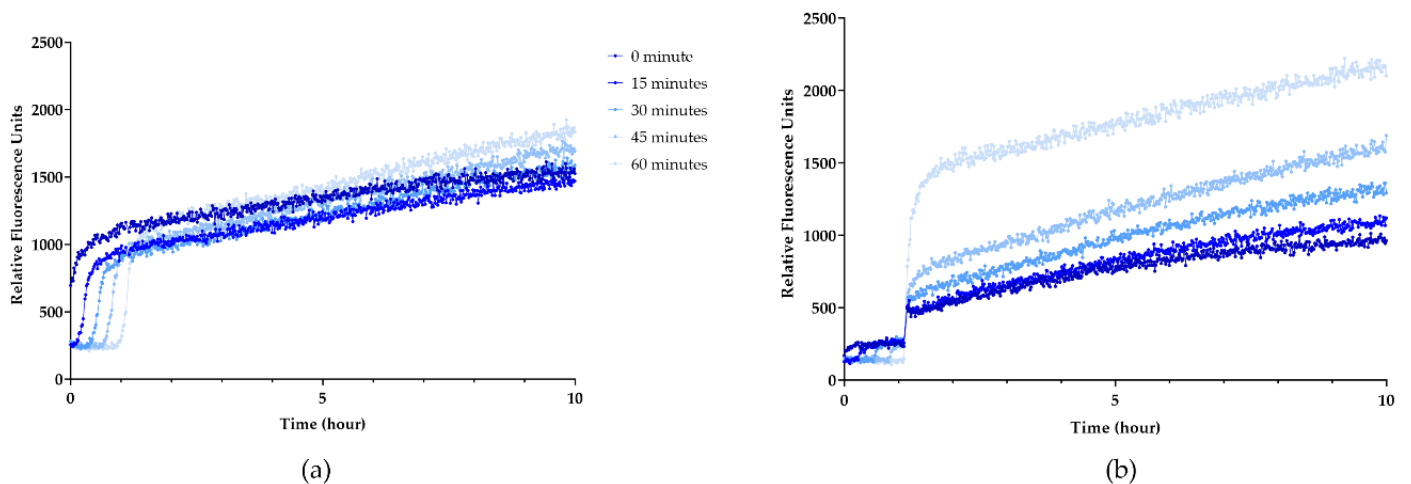


Figure 5: Kinetic of the relative fluorescence of *E. coli* NR698 carrying pCSMR03 with addition of 0.2% L-arabinose at the start and a mix with 25 μ g/mL of erythromycin and 5 μ g/mL of tetracycline every 15 minutes the first hours and of 5 μ M BR at (a) 0 minute and (b) 60 minutes.

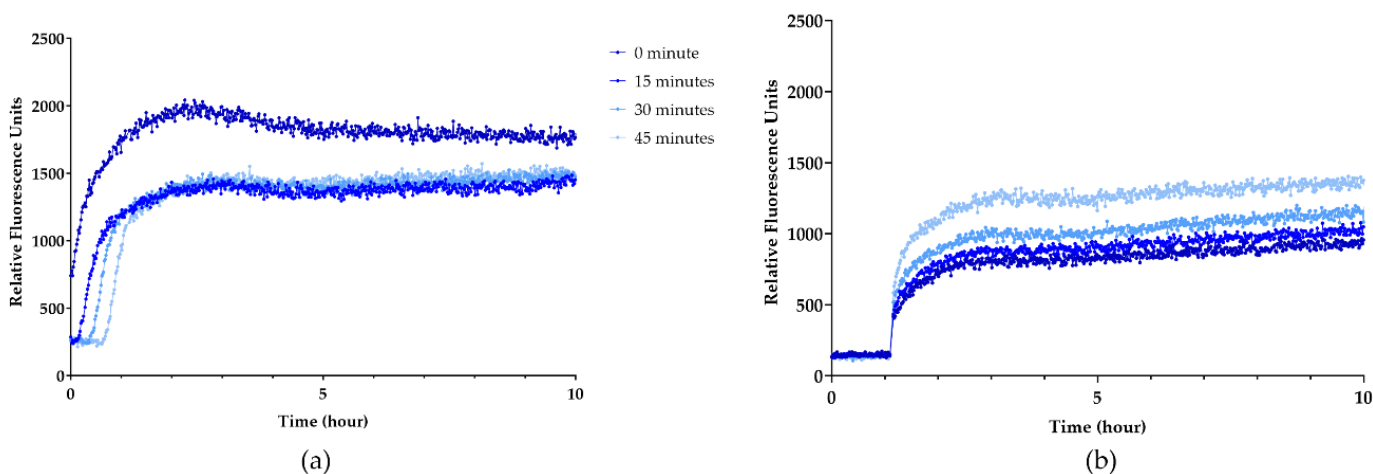


Figure 6: Kinetic of the relative fluorescence of *E. coli* NR698 carrying pCSMR03 with addition of 0.2% L-arabinose at the start and a mix with 0.5% of glucose every 15 minutes the first hours and of 5 μ M BR at (a) 0 minute and (b) 60 minutes

2.4. Investigation of different peptide activities by the *E. coli* double-biosensors

We used the *E. coli* MC4100 with pCSMR01 to characterize the PM and OM permeabilizing activities of three antimicrobial peptides from marine invertebrates (table 3), which were originally isolated from the spider crab *Hyas araneus* [53] and the green sea urchin *Strongylocentrotus droebachiensis* [21]. In addition, we tested two antimicrobial peptides that in earlier studies [54] had served as controls for PM activity (Cecropin P1) and intracellular activity (PR39(1-26)), respectively. Neither spider crab peptide affected luminescence or fluorescence emissions, indicating that neither PM nor OM integrity was affected at the tested concentrations. The original Centrocin consists of a heavy chain (HC) and light (LC) linked by a disulfide bond [21,23]. We only tested each peptide chain separately. Centrocin HC showed strong and rather fast PM activity at 3.1 μ g/mL and above, while we observed UnaG based fluorescence at concentrations between 1.6 and 6.3 μ g/mL. The light chain on the other hand did not affect luminescence or fluorescence output at all. The results from Centrocin HC resembled the results obtained from Cecropin P1, which served as the PM active control peptide. Interestingly, both peptides showed UnaG fluorescence at and below the lowest concentrations not resulting in complete loss of luminescence. This indicates that both PM active peptides also permeabilize the OM, but that this activity is limited to the OM only at concentrations below a certain threshold which was 6.3 μ g/mL for Centrocin HC. PR39 (1-26) did not show a pronounced effect on PM related luminescence and no effect on UnaG fluorescence, indicating no direct effect on either of the membranes at the tested concentrations. From earlier studies [23] we had different peptide fragments of Centrocin HC available (see table 3). We decided to test if any of these shortened fragments of Centrocin HC would show a variation in membrane specificity. Interestingly, only Centrocin HC (1-20) affected fluorescence and luminescence responses of the biosensor. While the effect of the PM was substantially reduced, when compared to the full-length peptide, fluorescence emissions increased and were detectable at a wider range of concentrations 100-3,1 μ g/mL. This indicates that the Centrocin HC (1-20) is mostly effective against the OM. The remaining Centrocin fragments lacked activity both against the PM and the OM, indicating that at least part of the (1-20) amino acid sequence is essential for OM activity and possibly the loss of the positively charged arginine from the full-length peptide for efficient PM activity (figure 7 and figure S5).

322

323

324

325

326

327

328

329

330

331

332

333

334

335

336

337

338

339

340

341

342

343

344

345

346

347

348

349

350

351

352

353

354

355

356

To confirm our hypothesis that Centrocin HC (1-20) specifically damages the OM we decided to microscopically observe the fluorescence pattern of *E. coli* MC4100 expressing arabinose inducible UnaG from plasmids pMM001B and pCSMR03B in response to Centrocin HC and Centrocin HC (1-20). For this purpose, bacteria were treated as described above and incubated in presence of different concentrations of Centrocin HC and Centrocin HC (1-20) for at least 1 h, respectively. Fig. 8 shows the effect of full length Centrocin and Centrocin (1-20) at concentrations between 100 and 12.5 $\mu\text{g}/\text{mL}$. Interestingly the fluorescence intensity of the cells seems to be stronger for the highest concentrations tested of both peptides. However, the conditions are not identical as L-Arabinose had to be added to the medium to induce *unaG* expression. Nonetheless the micrographs correlate with the observations from double sensor in the plate reader. The original Centrocin peptide results in very little fluorescence for both cytoplasmic and periplasmic expression of UnaG. Interestingly, for the highest concentration of Centrocin HC the fluorescence seems to be intracellular also for periplasmic expression, possibly indicating the diffusion of UnaG through the perforated PM to the interior of the cell after treatment with the peptide. Centrocin (1-20) on the other hand leads to a fluorescent halo at all tested concentrations when *unaG* is expressed in the periplasm. However, at the highest concentrations not all cells exhibit strong fluorescence. Possibly due to leakage of UnaG to the exterior of the cell because of excessive OM damage or uneven expression of UnaG within the population due to arabinose-depletion. The intracellularly expressed UnaG fluoresces also at all concentrations but is most prominent at 100 $\mu\text{g}/\text{mL}$.

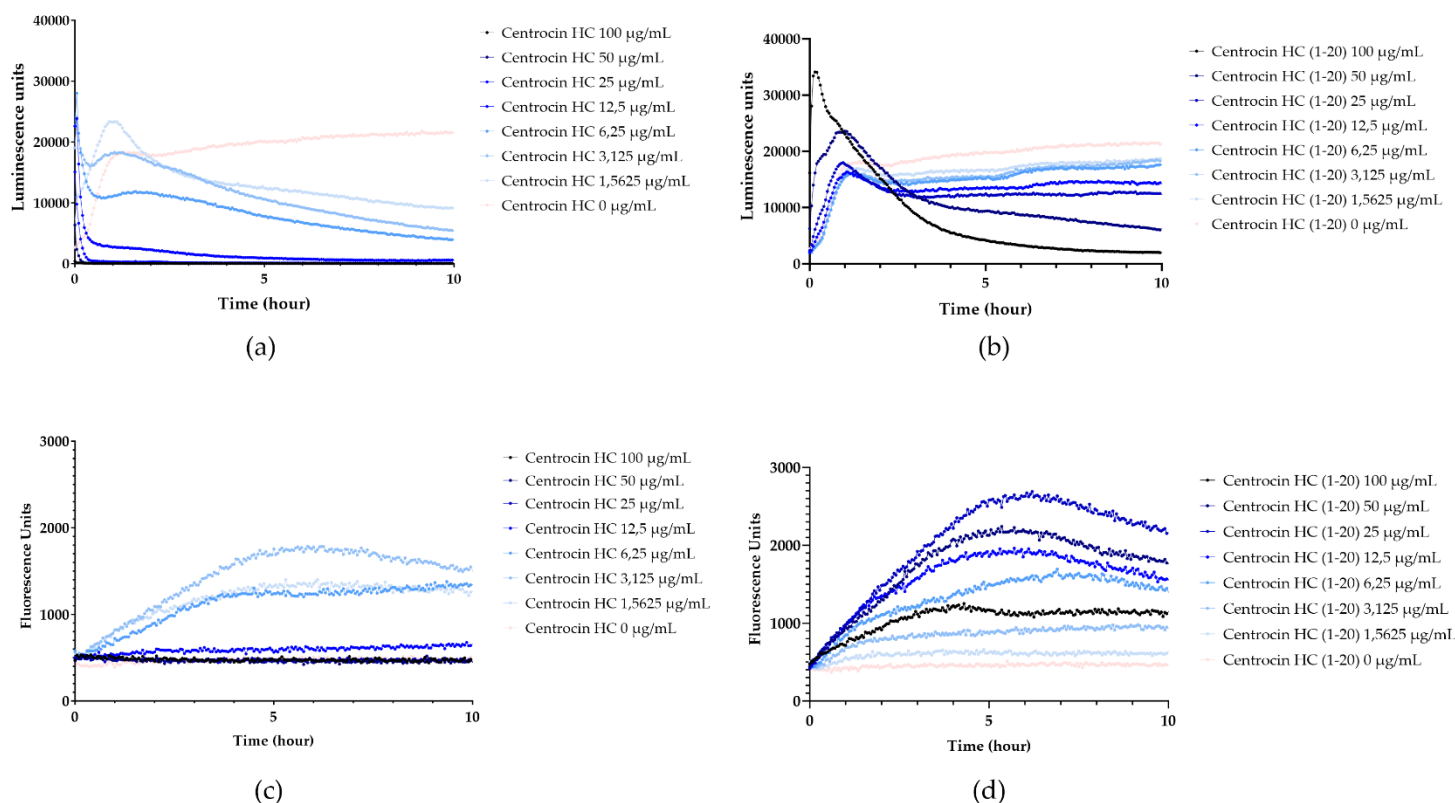


Figure 7: Representative luminescence kinetic of LucGR (a and b) and the fluorescence kinetic of UnaG (c and d) of the wild-type MC4100 in presence of different concentrations of (a and c) centrocin HC; (b and d) centrocin HC (1-20); with 5 μM BR and 1 μM D-luciferin for 10 hours

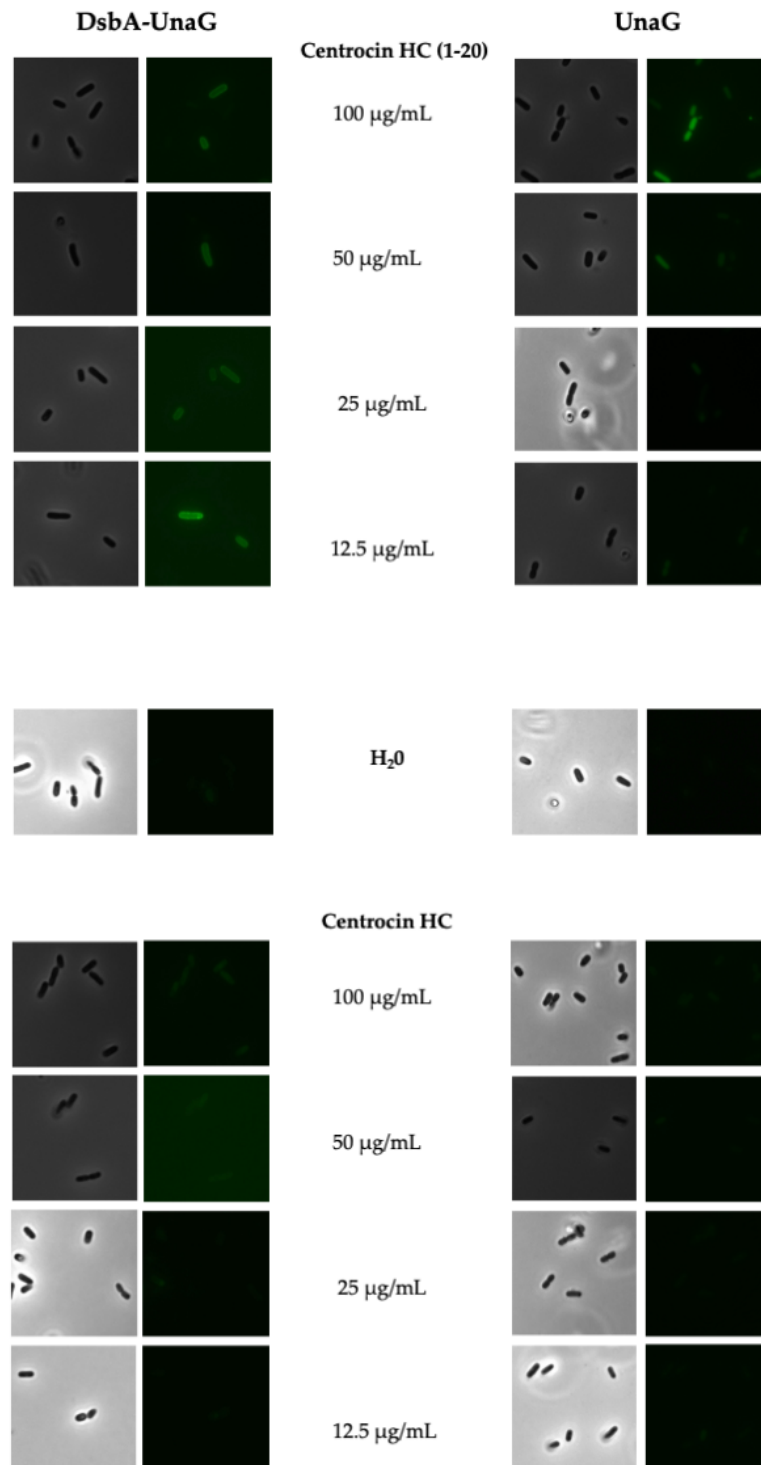


Figure 8: Comparison of the effect of centrocin HC and centrocin HC (1-20) on cytoplasmic and periplasmic UnaG fluorescence in *E. coli* MC4100. Fluorescence and phase contrast images of *E. coli* MC4100 carrying either pMM01 or pCSMR03B (DsbA-UnaG) 60 min after exposure to 5 µM BR, 1 µM L-arabinose and 25 µg/mL of centrocin HC (1-20) at ×1000 magnification. The images were taken with fluorescence through the software LAS X. The sides of each square represent a length of 20 µm.

383

384

385

386

387

388

389

2.5. Does OM activity detected by the double sensor indicate synergistic activity with ABs excluded by the outer membrane?

To evaluate if results from the OM/PM doubles sensor could be used to predict synergism with ABs known to be excluded by the OM, we conducted a checkerboard synergy assay with two ABs with different modes of action, Erythromycin and Vancomycin, respectively. We tested these ABs in combination with the original Centrocin HC and the Centrocin HC (1-20) fragment. We could not discern strong synergy for the full-length peptide as Centrocin HC alone already kills *E. coli* MC4100 cells very effectively. Addition of Vancomycin or Erythromycin did not substantially increase activity. Thus, the fractional inhibitory concentration index (FICI) was above 0.5. Interestingly, the OM active effect observed for Centrocin HC at low concentrations did not seem to increase the availability of either antibiotic to an extent beyond additive activity resulting in a FICI of 0.525 in combination with Centrocin HC and 0.625 in combination with Vancomycin. Centrocin HC (1-20) on the other hand clearly increased AB activity. The high synergy was mostly achieved due to its poor antimicrobial activity on its own. To save peptide the synergy assays were only run with a maximal concentration of 50 µg/ml peptide for both Centrocins. The MIC for Centrocin (1-20) was assayed separately and after 24h incubations *E. coli* K12 was still able to grow at 200 µg/mL. Due to no detected antimicrobial activity of Centrocin (1-20) alone, the MIC was set to 200 µg/ml and used to calculate the FICI. In combination with Erythromycin the calculated FICI value was 0.14 or better, in combination with Vancomycin 0.375. The results indicate that Centrocin HC (1-20) indeed acts synergistically with both Vancomycin and Erythromycin, while the synergism with the latter is substantially more pronounced. Table 1 summarizes the results from 2 independent synergy tests. It has been shown that OM active peptides act synergistically especially with ABs of high molecular weight such as Erythromycin and Vancomycin. This has been shown for PMBN [41,55,56] and for example the AMP Novicidin [57], lactoferricin [58] or tridecaptin M [59].

Table 1. Synergetic and additive effects of Centrocins with Erythromycin and Vancomycin

	Antibiotic	Combined xMIC AB	Combined xMIC Peptide	FICI
Centrocin HC (1-20)	Erythromycin	0.016	0.125	0.14
Centrocin HC (1-20)	Vancomycin	0.125	0.125	0.375
Centrocin HC	Erythromycin	0.125	0.5	0.525
Centrocin HC	Vancomycin	0.0625	0.5	0.625

2.6. Effects of the peptides Centrocin HC and Centrocin HC (1-20) on Gram-positive bacteria

To investigate if the reduced PM activity of the 1-20 Centrocin fragment in *E. coli* might result from the presence of an OM, we tested both peptides against a plasma membrane sensor in the Gram-positive bacterium *Bacillus subtilis* (figure 9). While the full length Centrocin caused plasma membrane disruption at 12.5 µg/mL and above, the Centrocin 1-20 fragment did not cause membrane damage at concentrations up to 100 µg/mL, indicating that the peptide lacks amino acids, which are essential for rapid PM disruption.

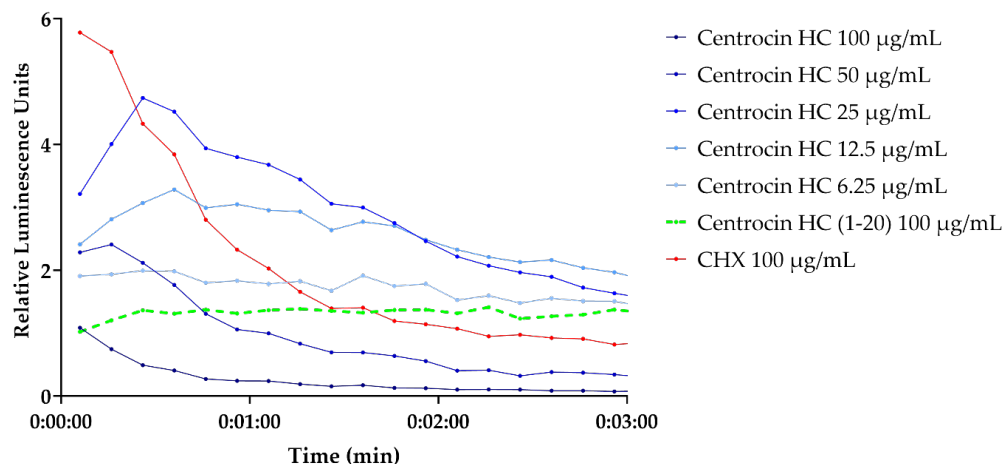


Figure 9: Representative luminescence kinetic of LucGR in *Bacillus subtilis* in presence of 1 μM D-luciferin and different concentrations of centrocin HC, 100 $\mu\text{g}/\text{mL}$ centrocin HC (1-20), or 100 $\mu\text{g}/\text{mL}$ CHX for 3 minutes.

In addition, all peptides were tested against a panel of mode of action specific *B. subtilis* biosensors, based on specific stress-responsive promoter-*luxABCDE* fusions. The sensors respond to inhibitors of DNA replication, transcription, translation, cell envelope synthesis and fatty acid synthesis. None of the peptides with marine origin induced expression of the promoter fusions. However, PR39 (1-26) strongly induced the sensor for translation inhibition from the *yhel*-promoter fusion, indicating that this peptide interferes with translation (figure 10). This is in agreement with earlier studies, which described PR39 to inhibit translation in *E. coli* [60]. Interfering with translation inhibition would lead to false negative results in the OM assay as the reporter genes expression is inhibited. To test if translation in *E. coli* was indeed inhibited by the used concentrations of PR-39(1-26), the assay was repeated in the OM compromised *E. coli* NR698 strain carrying the plasmid pCSMR01 for constitutive expression of *unaG* and *luxABCDE* in an artificial operon. In this strain BR uptake is not restricted by the OM, therefore UnaG fluorescence is directly dependent on UnaG expression. The results of the assay are presented in figure 11. In the wildtype background PR-39 (1-26) does not affect luminescence at the tested concentrations, while fluorescence levels remain low. In the OM compromised background of the NR698 strain on the other hand, strong UnaG fluorescence is only detected in the untreated control, while luminescence is affected in a concentration dependent manner. This indicates that PR-39(1-26) strongly inhibits translation, at least in absence of the OM as a barrier. The effect on luminescence emission, however, is slow and concentration dependent. This indicates that cell viability is not immediately affected, which is in agreement with translation inhibition being the mode of action for reduced cell viability over time. Thus, PR39 (1-26) inactivity against the OM might be a false negative result, camouflaged by the strong activity as a translation inhibitor. However, as no luminescence reduction compared to the untreated control is observed in the WT background, translation inhibition must be substantially lower than in the OM compromised background. To avoid possible false negatives outcomes in screening assays, controls should be run on OM deficient strain NR698 containing pCSMR02 or pCSMR01 possibly allowing to screen for translation inhibitors at the same time.

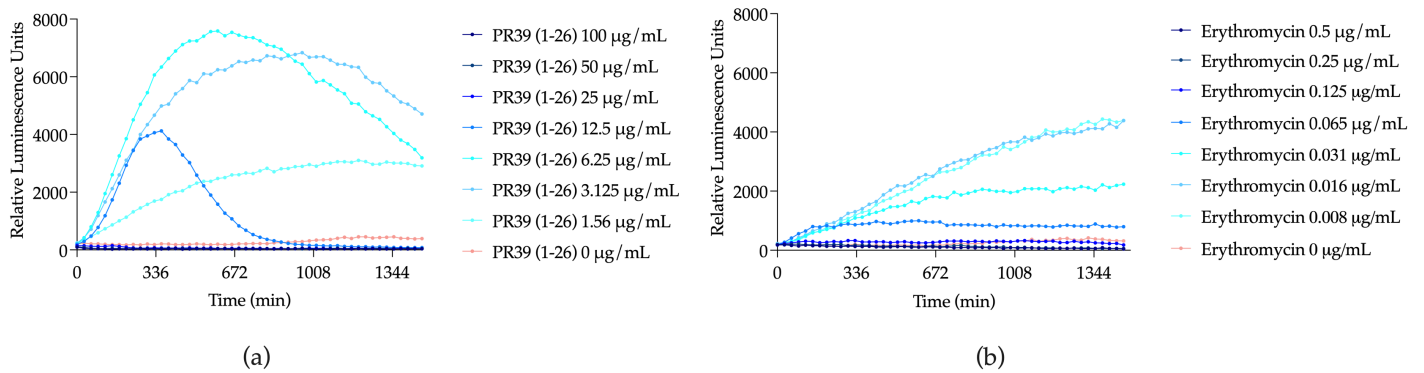


Figure 10: Representative luminescence kinetic of *lux* operon under the control of *yheI*-promoter in *Bacillus subtilis* in response to different concentrations of (a) PR39 (1-26) or (b) Erythromycin (control) for 24 h in 30 minutes time intervals.

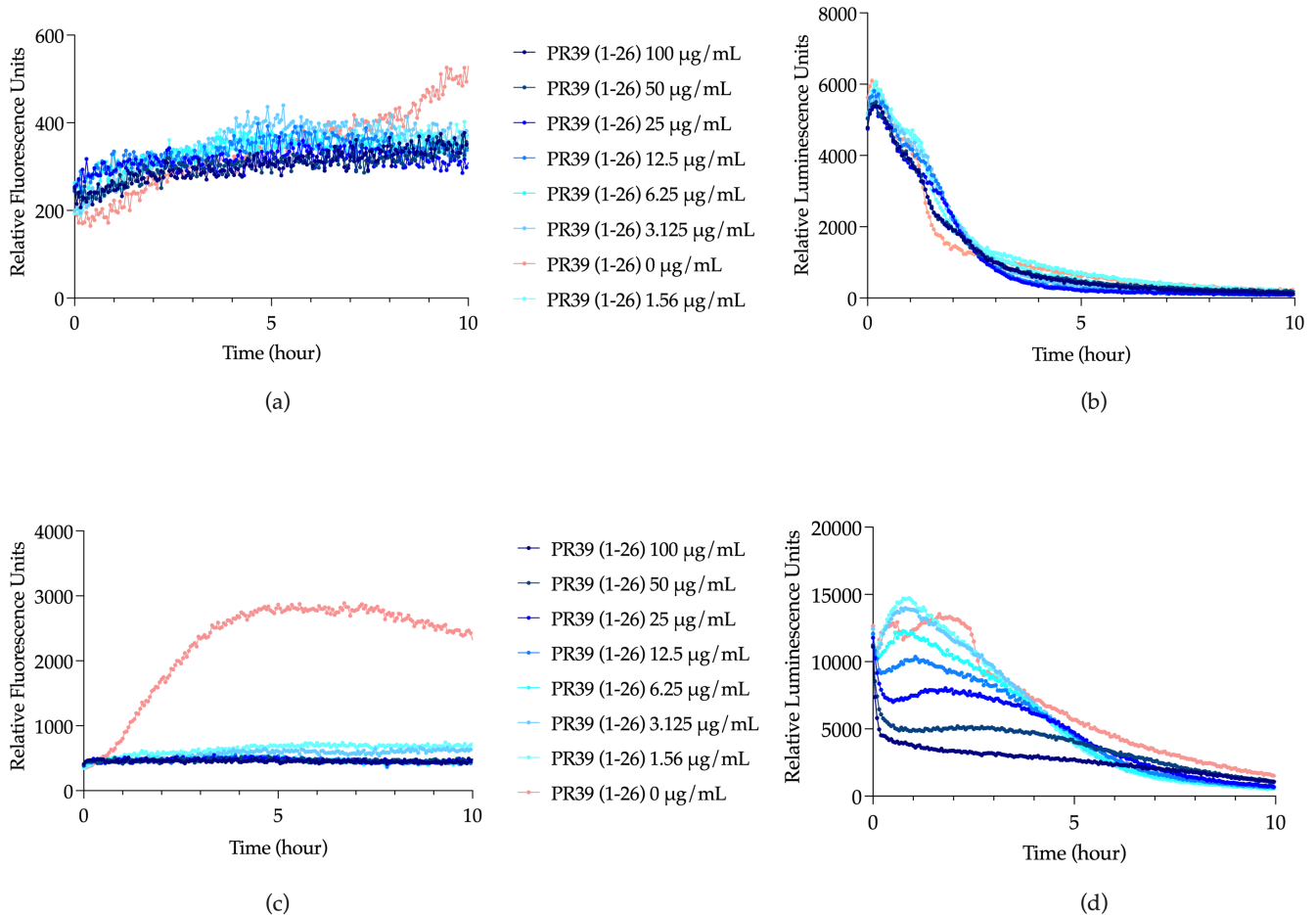


Figure 11: Representative (a and b) fluorescence kinetic of *unaG* and (b and d) luminescence kinetic of *lux* operon of *E. coli* (a and b) MC4100 and (c and d) NR698 in response to different concentration of PR39 (1-26) for 10 hours.

3. Materials and Methods

3.1. Media and Growth Conditions

To perform the cloning, the different *Escherichia coli* and *Bacillus subtilis* strains were routinely grown in Luria-Bertani (LB) broth at 37 °C with aeration. For fluorescence and luminescence measurements, the bacterial cultures were grown in Mueller-Hinton (MH; Merck, Darmstadt, Germany) broth medium at room temperature (RT) overnight. New MH cultures were inoculated to 1% (v/v) of overnight pre-culture and incubated at RT with aeration until the OD₆₀₀ reached 0.5. UnaG fluorescence assays were conducted in presence of 5 mM bilirubin (BR; Sigma-Aldrich, St Louis, MO, USA) stocks were prepared in dimethyl sulfoxide (DMSO; Sigma-Aldrich, St Louis, MO, USA). For the luminescence assays, 20 mM D-luciferin potassium salt (Synchem Inc., Elk Grove Village, IL, USA) stocks were prepared in sterile water.

3.2. Bacterial Strains and Plasmids

In this study we used the *Escherichia coli* K-12 strain MC4100 as a wild-type (WT) and its isogenic OM deficient mutant NR698, both carrying different plasmids with reporter constructs, as well as *Bacillus subtilis* 168 with either plasmid based or chromosomally integrated reporter fusions. The strain NR698 was constructed by Ruiz et al. [61]. *Escherichia coli* DH5 α was used for cloning purposes. A summary of plasmids and oligonucleotides used in this study is listed in table 2 below. Maps of the plasmids assembled for this study are shown in figure S10. To express UnaG under the control of an arabinose inducible promoter for cytoplasmic or periplasmic localization, the pMM001B, pCSMR03B and pCSMR04B were made by integrating the promoter pBad and the gene *araC* from the plasmid pTwist_pBad_RiboJ to the plasmids pMM001, pCSMR03 and pCSMR04 that we designed and synthesized through Invitrogen GeneArt Gene Synthesis (ThermoFisher, Waltham, MA, USA) with codon optimization for *E. coli*.

Table 2. Plasmids and primers used in the study

Plasmid	Characteristic or description	Reference or source
Plasmids		
pCSS962	Plasmid containing lucGR	[46]
pBS3Clux	Plasmid containing lux operon	[62]
pMM001	Plasmid containing unaG	[45]
pCSMR03	Plasmid containing unaG and dsbA	This study
pCSMR04	Plasmid containing unaG and torA	This study
pTwist_pBad_RiboJ	Plasmid containing the promoter pBad with RiboJ	This study
pMM001B	Plasmid containing LucGR and unaG	This study
pCSMR01	Plasmid containing lux operon and unaG	This study
pCSMR02	Plasmid containing unaG under the pBad promoter with RiboJ	This study
pCSMR03B	Plasmid containing unaG with the transporter dsbA under the pBad promoter with RiboJ	This study
pCSMR04B	Plasmid containing unaG with the transporter torA under the pBad promoter with RiboJ	This study
Oligonucleotides		
UnaG-XbaI-XhoI_F	CAATCTAGAATTCTCGAGAGAGGAAGGCCGTCAGGCC	
UnaG-XhoI-SalI_R	CCACTCGAGACAGTCGACACCATTTCGGTTGCACGACGA	
lucGR_NheI_NotI_F	ATCGTCGTGCAACCGAATAAACTAGCTAGCGGCCGCTAAA- GAGGAGAAATTAAGTATG	
lucGR_NheI_HindIII_R	GAAGGCCCATGAGGCCAGACTAGTTAGCTAGCTAAGCTT- GGC	

^a annealing sequences are bold

479

480

481

482

483

484

485

486

487

488

489

490

491

492

493

494

495

496

497

498

499

500

501

502

503

504

3.3. Peptides

Table 3: Peptides used in the study.

Name	Sequence	Origin
Cecropin P1	SWLSKTAKKLENSAKKRISEGIAIAI-QGGPR	<i>Ascaris suum</i> , Parasitic nematode
PR39 (1-26)	RRRPRPPYLPRPRPPFFPPRLPPRI	<i>Sus scrofa</i> , Pig leukocytes
Hyasin unmodified	WQRPLTRPRPFSRPRPYRPNYG	<i>Hyas araneus</i> , Spider Crab
Arasin (1-23)	SRWPSGRPRPFPGRPKPIFRPR	<i>Hyas araneus</i> , Spider Crab
Centrocin HC	GWFKKTFHKVSHAV-KSGIHAGQRGCSALGF	<i>Strongylocentrotus droebachiensis</i> , Green Sea Urchin
Centrocin HC (1-20)	GWFKKTFHKVSHAVKSGIHA	<i>Strongylocentrotus droebachiensis</i> , Green Sea Urchin
Centrocin HC (1-10)	GWFKKTFHKV	<i>Strongylocentrotus droebachiensis</i> , Green Sea Urchin
Centrocin HC (1-5)	GWFKK	<i>Strongylocentrotus droebachiensis</i> , Green Sea Urchin
Centrocin HC (11-20)	SHAVKSGIHA	<i>Strongylocentrotus droebachiensis</i> , Green Sea Urchin
Centrocin HC (21-30)	GQRGCSALGF	<i>Strongylocentrotus droebachiensis</i> , Green Sea Urchin
Centrocin LC	DLRGACAAHAL	<i>Strongylocentrotus droebachiensis</i> , Green Sea Urchin

3.4. Cloning and Transformation

To express UnaG in the cytoplasm or in the periplasm under the inducible arabinose promoter, the promoter OXB15 was cut out by enzymatic digestion from the plasmids pMM001 [45], pCSMR03 and pCSMR04. The same restriction enzymes were used to cut out the genetic insulator RiboJ [63], as well as the pBad promoter with araC gene from the new plasmid pTwist_pBad_RiboJ, before being ligated in the three plasmids, instead of pOXB15. The transformations were performed in competent *Escherichia coli* DH5 α with the Inoue method [64] and the new plasmids were then extracted with the BOMB methods [65] before the TSS transformation [66] in the two isogenic strains *E. coli* MC4100 and NR698. The transformants carrying the new plasmids were selected on LB agar plates with 100 μ g/mL ampicillin or 5 μ g/ml in case of the more sensitive NR698 strain.

To express UnaG in artificial operons with luc and lux luciferases two different strategies were employed. To co-express *unaG* with the *lux* operon, *unaG* together with the strong constitutive promoter OXB15 was amplified from pMM001 by PCR to add restriction enzyme sites necessary for classical cloning (table 2). The BS3Clux backbone containing the *lux*-operon under the control of the was then ligated with the *unaG* insert resulting in a synthetic operon under the control of the OXB15 promoter, resulting in plasmid pCSMR02.

To express *unaG* together with *lucGR* in an artificial operon, *lucGR* was amplified from pCSS962 adding 20 bp overhangs homologous to the flanking regions of the SpeI restriction site downstream of *unaG*. This amplicon was combined with pMM001 linearized by SpeI using Gibson assembly [67] resulting in plasmid pCSMR01.

The PCR products were purified by the NucleoSpin® Gel and PCR Clean-up kit (Macherey-Nagel, Dueren, Germany). Plasmid isolation was done by the open protocol ([65] Bomb.bio.)

Transformants were selected on LB agar plates with 20 µg/mL chloramphenicol for pCSMR01 and 100 µg/mL ampicillin for pCSMR02 (table 1).

3.5. Reporter gene detection and biosensor analysis

To measure UnaG and GFP fluorescence of the biosensor constructs, a Synergy H1 Hybrid Reader (BioTek, Winooski, VT, USA) was used. Depending on the assay, fluorescence was measured regular time intervals for up to 10 hours at 25.5 °C with an excitation wavelength of 508 / 8 nm and an emission wavelength of 538 / 8 nm. mCherry controls were measured at 580 / 8 nm excitation and 610 / 8 nm emission wavelength. The gain was kept at 100 in all experiments. The experiments were conducted in black round-bottom 96-well microtiter plate (Nunc, Roskilde, Denmark) at a final volume of 100 µL, and a bacterial concentration adjusted to OD₆₀₀=0,3 in 0,9 % NaCl 20mM TrisHCl pH7.5. For induction of the P_{BAD} promoter-based constructs 0,2 % L-arabinose was added at the specified timepoints. When necessary, translation of reporter genes was arrested by the addition of translation inhibiting antibiotics or 0,5% Glucose. Where not otherwise specified, BR was added to a final concentration of 5 µM, D-luciferin to a final concentration of 1 mM and peptide compounds to the specified concentrations (PMNM; GLPBIO, Montclair, CA, USA). Addition of water instead of PMBN was used as negative control and BR-free bacteria as background. All the data were processed with GraphPad Prism 9 software version 9.5.0 (GraphPad Software; Boston, USA).

The *E. coli* strains MC4100 and NR968 carrying the double reporter gene plasmids, the eukaryotic luciferase LucGR (pCSMR01) or the lux operon (pCSMR02) coupled with UnaG, were cultured overnight in MH broth medium supplemented with 5 µg/mL or 20 µg/mL of chloramphenicol for pCSMR01, or 5 µg/mL or 100 µg/mL of ampicillin for pCSMR02, for MC4100 and NR968 respectively. Day cultures were then prepared by inoculating at 1% new MH broth medium, until the OD₆₀₀ reached 0.5.

3.6 Mode of action specific biosensor assay in *B. subtilis*

A mode of action specific biosensor assay was used to analyze the activity of the peptides against previously known modes of action. The assays tested specific stress responses related to interference with DNA replication, transcription, translation as well as cell envelope- and fatty acid synthesis using *B. subtilis* 168 derivatives containing the *luxA-BCDE* operon fused to the promoter regions of *yorB*, *belD*, *yheI*, *yupA*, *liaI* or *fabHB*. Fresh colonies of each sensor strain were transferred from agar plates to 5 mL MH medium containing 5 µg/mL chloramphenicol and incubated at 37 °C overnight. Overnight cultures were diluted to an OD₆₀₀ = 0.05 and grown to an OD₆₀₀ = 0.2 before addition to the assay plates already containing the analytes. The analytes and control antibiotics were diluted in two-fold dilution series in water. Then, 5 µL of each dilution was combined with 45 µL bacterial suspension in each well of the 386-well white plates with transparent bottom (6007490, PerkinElmer, Waltham, MA, USA). The wells were covered by an oxygen permeable breatheasy sealing membrane (Z380059, Sigma-Aldrich, Darmstadt, Germany) to reduce evaporation. The assay was run in a plate reader (EnVision(R), PerkinElmer, Waltham, MA, USA) placed in an incubator at 35 °C. Luminescence and growth kinetics were recorded every 30 min for 24 hours. The strains used in this study have been described previously [68].

3.7. Checkerboard synergy assay

The synergistic interaction of the synthetic peptides in combination with either erythromycin or vancomycin were investigated following the established checkerboard method [69]. Briefly, working concentration of both peptides and antibiotics were prepared by two-fold serial dilutions starting at the four-fold of desired concentrations. Next, 25 µL of peptide and antibiotic dilutions with different concentrations were added to the

96-well plates. Then, 50 μ L of diluted bacterial suspension (5×10^5 CFU/mL) was added to each well containing dilution of peptide and antibiotic combinations to give the final desired concentrations. The plates were subsequently incubated for 24 h at 35°C. The FICI values were calculated using the FICI formula with the highest combination effects: $FICI = MIC \text{ of drug A in combination} / MIC \text{ of drug A alone} + MIC \text{ of drug B in combination} / MIC \text{ of drug B alone}$. The antimicrobial combination was defined as synergy when the FICI was ≤ 0.5 , no interaction when $0.5 < FICI < 4$, and antagonism when the FICI was ≥ 4 .

3.8. Microscopy

Bacterial suspensions of *E. coli* strains MC4100 and NR698 expressing UnaG under inducible pBad promoter were prepared in 0.9% NaCl solution. Each isogenic strain contains either the plasmid pMM001B (UnaG cytoplasmic expression), pCSMR03B (UnaG tagged with the *dsbA* export sequence, exported and folded in the periplasm) or pCSMR04B (UnaG tagged with the TorA export sequence, folded in the cytoplasm and exported to the periplasm) were investigated with a Leica DM6000B fluorescence microscope and an excitation light source, a Leica CTR6000 with a filter system Cube I3 DM 513828. The fluorescence of the different strains was measured with a camera Leica DFC7000T 1 hour after addition of 0,2% L-arabinose, 5 μ M BR and 10 μ g/mL PMBN. Identical camera settings were used for all images. When necessary, the brightness of the images was increased by 150% for better on-screen visibility in Photoshop CS6 version 13.

4. Conclusions

Two novel biosensors were established combining the gene for the ligand dependent fluorescent protein UnaG and the eukaryotic luciferase *lucGR* and *unaG* and the bacterial *luxABCDE* in artificial operons. The biosensors can detect OM disruption in addition to either disturbance of plasma membrane integrity or general cell viability, simultaneously. UnaG fluorescence kinetics are tightly coupled to freshly translated UnaG as apoUnaG is less stable than holoUnaG when present in the *E. coli* cytoplasm. Application of the double membrane sensor showed that Centrocin HC disrupts both PM and OM while the Centrocin HC (1-20) fragment mostly interferes with OM integrity. This observation is supported by the synergistic activity of Centrocin HC (1-20) and both Vancomycin and Erythromycin.

Supplementary Materials: The following supporting information can be downloaded at: www.mdpi.com/xxx/s1, Figure S1: Optimization of the medium for better signal to noise ratio for simultaneous fluorescence and luminescence emissions; Figure S2: Comparison of UnaG expression levels in the single and the double sensors; Figure S3: Microscopy of abnormally long cells with periplasm transporters; Figure S4: Effect of translation inhibitor at different time points on GFP fluorescence and lux luminescence; Figure S5: Effect of Centrocin HC and Centrocin HC (1-20) on the plasma membrane of *E. coli*; Figure S6: Effect of Cecropin P1 on the plasma- and the outer-membrane of *E. coli*; Figure S7: Effect of PR39 (1-26) on the plasma- and the outer-membrane of *E. coli*; Figure S8: Effect of Centrocin LC on the plasma- and the outer-membrane of *E. coli*; Figure S9: Comparison of the effect of PR39 (1-26) and Erythromycin on the growth of *Bacillus subtilis*; Figure S10: Maps of the plasmids used in this study; Sequence S1: DNA sequence of pCSMR01; Sequence S2: DNA sequence of pCSMR02; Sequence S3: DNA sequence of pTwist-Pbad-riboJ-0015T; Sequence S4: DNA sequence of pMM001B; Sequence S5: DNA sequence of pCSMR03B; Sequence S6: DNA sequence of pCSMR04B.

Author Contributions: Conceptualization, C.S.M.R., and H.-M.B.; methodology, C.S.M.R., H.D. and H.-M.B.; software and validation, C.S.M.R., H.D. and H.-M.B.; formal analysis, C.S.M.R.; investigation, C.S.M.R., H.D., E.M., and F.Ø.; resources, H.-M.B.; data curation and writing—original draft

preparation, C.S.M.R. and H.-M.B.; writing—review and editing, C.S.M.R., H.D., F.Ø., C.L., and H.-M.B.; visualization, C.S.M.R.; supervision, H.-M.B.; project administration, H.-M.B.; funding acquisition, H.-M.B. All authors have read and agreed to the published version of the manuscript

Funding: This work was supported by a grant (no. 217/6770) from UiT, the Arctic University of Norway, and a PhD fellowship also granted through the UiT. The publication charges for this article have been covered by the publication fund of UiT, the Arctic University of Norway.

Institutional Review Board Statement: Not applicable.

Data Availability Statement: Not applicable.

Acknowledgments:

Conflicts of Interest: The authors declare no conflict of interest.

References

1. Arnold L. Demain From Natural Products Discovery to Commercialization: A Success Story. *J. Ind. Microbiol. Biotechnol.* **2006**, *33*, 486–495, doi:https://doi.org/10.1007/s10295-005-0076-x.
2. Arnold L. Demain Importance of Microbial Natural Products and the Need to Revitalize Their Discovery. *J. Ind. Microbiol. Biotechnol.* **2014**, *41*, 185–201, doi:https://doi.org/10.1007/s10295-013-1325-z.
3. Tobias AM Gulder; Bradley S. Moore Chasing the Treasure of the Sea - Bacterial Marine Natural Products. *Curr. Opin. Microbiol.* **2009**, *12*, 252–260, doi:https://doi.org/10.1016/j.mib.2009.05.002.
4. M. D. Ivorra; M. Payá; A. Villar A Review of Natural Products and Plants as Potential Antidiabetic Drugs. *J. Ethnopharmacol.* **1989**, *27*, 243–275.
5. Adam M. Burja; Bernard Banaigs; Eliane Abou-Mansour; J. Grant Burgess; Phillip C. Wright Marine Cyanobacteria - a Prolific Source of Natural Products. *Tetrahedron* **2001**, *57*, 9347–9377.
6. Martin J. Rice; Mike Legg; Keith A. Powell Natural Products in Agriculture - A View from the Industry. *Pestic. Sci.* **1998**, *52*, 184–188, doi:Pestic.Sci. 0031-613X/98/\$17.5.
7. A. Bhanot; R. Sharma; Malleshappa N. Noolvi Natural Sources as Potential Anti-Cancer Agents: A Review. *Int. J. Phytomedicine* **2011**, *3*, 09–26.
8. Franck E. Dayan; Charles L. Cantrell; Stephen O. Duke Natural Products in Crop Protection. *Bioorg. Med. Chem.* **2009**, *17*, 4022–4034, doi:doi:10.1016/j.bmc.2009.01.046.
9. Michael Zasloff Antimicrobial Peptides of Multicellular Organisms. *Nature* **2002**, *415*, 389–395, doi:https://doi.org/10.1038/415389a.
10. Håvard Jenssen; Pamela Hamill; Robert E. W. Hancock Peptide Antimicrobial Agents. *Clin. Microbiol. Rev.* **2006**, *19*, 491–511, doi:10.1128/CMR.00056-05.
11. Ankit Javia; Jitendra Amrutiya; Rohan Lalani; Vivek Patel; Priyanka Bhatt; Ambikanandan Misra Antimicrobial Peptide Delivery: An Emerging Therapeutic for the Treatment of Burn and Wounds. *Ther. Deliv.* **2018**, *9*, doi:https://doi.org/10.4155/tde-2017-0061.
12. Kim A. Brogden Antimicrobial Peptides: Pore Formers or Metabolic Inhibitors in Bacteria? *Nat. Rev. Microbiol.* **2005**, *3*, 238–250.
13. Annarita Falanga; Lucia Lombardi; Gianluigi Franci; Mariateresa Vitiello; Maria Rosaria Iovene; Giancarlo Morelli; Massimiliano Galdiero; Stefania Galdiero Marine Antimicrobial Peptides: Nature Provides Templates for the Design of Novel Compounds against Pathogenic Bacteria. *Int. J. Mol. Sci.* **2016**, *17*, doi:10.3390/ijms17050785.
14. Laila Ziko; Omnia AbdelRaheem; Marina Nabil; Ramy K. Aziz; Rania Siam Bioprospecting the Microbiome of Red Sea Atlantis II Brine Pool for Peptidases and Biosynthetic Genes with Promising Antibacterial Activity. *Microb. Cell Factories* **2022**, *21*.

15. Raymond C. Valentine; David L. Valentine Omega-3 Fatty Acids in Cellular Membranes: A Unified Concept. *Prog. Lipid Res.* **2004**, *42*, 383–402. 679
680
16. Nicholas J. Russel; David S. Nichols Polyunsaturated Fatty Acids in Marine Bacteria - a Dogma Rewritten. *Microbiology* **145**, 767–681
779. 682
17. Randy Chi Fai Cheung; Tzi Bun Ng; Jack Ho Wong Marine Peptides: Bioactivities and Applications. *Mar. Drugs* **2015**, *13*, 4006–683
4043, doi:doi: 10.3390/md13074006. 684
18. Sigmund V. Sperstad; Tor Haug; Hans-Matti Blencke; Olaf B. Styrvold; Chun Li; Klara Stensvåg Antimicrobial Peptides from 685
Marine Invertebrates: Challenges and Perspectives in Marine Antimicrobial Peptide Discovery. *Biotechnol. Adv.* **2011**, *29*, 519–686
530, doi:10.1016/j.biotechadv.2011.05.021. 687
19. Mohammad H. Semreen; Mohammed I. El-Gamal; Shifaa Abdin; Hajar Alkhazraji; Leena Kamal; Saba Hammad; Faten El-688
Awady; Dima Waleed; Layal Kourbaj Recent Updates of Marine Antimicrobial Peptides. *Saudi Pharm. J.* **2018**, *26*, 396–409. 689
20. Shuocun Wang; Liming Fan; Hanyu Pan; Yingying Li; Yan Qiu; Yiming Lu Antimicrobial Peptides from Marine Animals: 690
Sources, Structures, Mechanisms and the Potential for Drug Development. *Front. Mar. Sci.* **2023**, 691
doi:10.3389/fmars.2022.1112595. 692
21. Chun Li; Tor Haug; Morten K. Moe; Olaf B. Styrvold; Klara Stensvåg Centrocins: Isolation and Characterization of Novel Di-693
meric Antimicrobial Peptides from the Green Sea Urchin, *Strongylocentrotus Droebachiensis*. *Dev. Comp. Immunol.* **2010**, *34*, 959–694
568, doi:doi:10.1016/j.dci.2010.04.004. 695
22. Takanori Nakamura; Hiromi Furunaka; Toshiyuki Miyata; Fuminori Tokunaga; Tatsushi Muta; Sadaaki Iwanaga Tachyplesin, 696
a Class of Antimicrobial Peptide from the Hemocytes of the Horseshoe Crab (*Tachyplesus Tridentatus*). Isolation and Chemical 697
Structure. *J. Biol. Chem.* **1988**, *263*, 16709–16713. 698
23. Camilla Björn; Joakim Håkansson; Emma Myhrman; Veronika Sjöstrand; Tor Haug; Kerstin Lindgren; Hans-Matti Blencke; 699
Klara Stensvåg; Margit Mahlapuu Anti-Infectious and Anti-Inflammatory Effects of Peptide Fragments Sequentially Derived 700
from the Antimicrobial Peptide Centrocin 1 Isolated from the Green Sea Urchin, *Strongylocentrotus Droebachiensis*. *AMB Express* 701
2. 702
24. P. L. Ho; Y. Y. Cheung; Y. Wang; W. U. Lo; E. L. Y. Lai; K. H. Chow; V. C. C. Cheng Characterization of Carbapenem-Resistant 703
Escherichia Coli and *Klebsiella Pneumoniae* from a Healthcare Region in Hong Kong. *Eur. J. Clin. Microbiol. Infect. Dis.* **2016**, *35*, 704
379–385. 705
25. Rabab R. Makharita; Iman El-kholy; Helal F. Hetta; Moahmed H. Abdelaziz; Fatma I. Hagagy; Amara A. Ahmed; Abdelazeem 706
M. Algammal Antibiogram and Genetic Characterization of Carbapenem-Resistant Gram-Negative Pathogens Incriminated 707
in Healthcare-Associated Infections. *Infect. Drug Resist.* **2020**, *13*, 3991–4002. 708
26. A. Balkhair; K. Al. Saadi; B. Al Adawi Epidemiology and Mortality Outcome of Carbapenem- and Colistin-Resistant *Klebsiella* 709
Pneumoniae, *Escherichia Coli*, *Acinetobacter Baumannii*, and *Pseudomonas Aeruginosa* Bloodstream Infections. *IJID Reg.* **2023**, *7*, 1–710
5, doi:https://doi.org/10.1016/j.ijregi.2023.01.002. 711
27. Sarah S. Tang; Anucha Apisarnthanarak; Li Yang Hsu Mechanisms of β -Lactam Antimicrobial Resistance and Epidemiology of 712
Major Community- and Healthcare-Associated Multidrug-Resistant Bacteria. *Adv. Drug Deliv. Rev.* **2014**, *78*, 3–13. 713
28. Borna Mehrdad; Nina M. Clark; George G. Zhanell; Lynch Joseph Antimicrobial Resistance in Hospital-Acquired Gram-Negative 714
Bacterial Infections. *Contemp. Rev. Crit. Care Med.* **2015**, *147*, 1413–1421, doi:https://doi.org/10.1378/chest.14-2171. 715
29. Yihienew M. Bezabih; Alemayehu Bezabih; Michel Dion; Eric Batard; Samson Teka; Abiy Obole; Noah Dessalegn; Alelegn 716
Enyew; Anna Roujeinikova; Endalkachew Alamneh; et al. Comparison of the Global Prevalence and Trend of Human Intesti- 717
nal Carriage of ESBL-Producing *Escherichia Coli* between Healthcare and Community Settings: A Systematic Review and Meta- 718
Analysis. *JAC-Antimicrob. Resist.* **2022**, *4*, doi:https://doi.org/10.1093/jacamr/dlac048. 719

30. Hadir A. El-Mahallawy; Marwa El Swify; Asmaa Abdul Hak; Mai M. Zafer Increasing Trends of Colistin Resistance in Patients at High-Risk of Carbapenem-Resistant *Enterobacteriaceae*. *Ann. Med.* **2022**, *54*, 2748–2756, doi:https://doi.org/10.1080/07853890.2022.2129775.
31. Yasuhide Kawamoto; Norihito Kaku; Norihiko Akamatsu; Kei Sakamoto; Kosuke Kosai; Yoshitomo Morinaga; Norio Ohmagari; Koichi Izumikawa; Yoshihiro Yamamoto; Hiroshige Mikamo; et al. The Surveillance of Colistin Resistance and Mobilized Colistin Resistance Genes in Multidrug-Resistant *Enterobacteriaceae* Isolated in Japan. *Int. J. Antimicrob. Agents* **2022**, *59*, doi:https://doi.org/10.1016/j.ijantimicag.2021.106480.
32. Masoud Dadashi; Fatemeh Sameni; Nazila Bostanshirin; Somayeh Yaslianifard; Nafiseh Khosravi-Dehaghi; Mohammad Javad Nasiri; Mehdi Goudarzi; Ali Hashemi; Bahareh Hajikhani Global Prevalence and Molecular Epidemiology of Mcr-Mediated Colistin Resistance in *Escherichia Coli* Clinical Isolates: A Systematic Review. *J. Glob. Antimicrob. Resist.* **2022**, *29*, 444–461, doi:https://doi.org/10.1016/j.jgar.2021.10.022.
33. Umji Choi; Chang-Ro Lee Distinct Roles of Outer Membrane Porins in Antibiotic Resistance and Membrane Integrity in *Escherichia Coli*. *Front. Microbiol.* **2019**, *10*, doi:https://doi.org/10.3389/fmicb.2019.00953.
34. Hiroshi Nikaiko Outer Membrane Barrier as a Mechanism of Antimicrobial Resistance. *Antimicrob. Agents Chemother.* **1989**, *33*, 1831–1836.
35. *Escherichia Coli and Salmonella, Cellular and Molecular Biology*; Frederick C. Neidhardt, Ed.; ASM Press, 1996;
36. Anne H. Delcour Outer Membrane Permeability and Antibiotic Resistance. *Biochim. Biophys. Acta* **2009**, *1794*, 808–816.
37. Kristina Klobucar; Eric D. Brown New Potentiators of Ineffective Antibiotics: Targeting the Gram-Negative Outer Membrane to Overcome Intrinsic Resistance. *Curr. Opin. Chem. Biol.* *66*, doi:https://doi.org/10.1016/j.cbpa.2021.102099.
38. Scott S. Walker; Todd A. Black Are Outer-Membrane Targets the Solution for MDR Gram-Negative Bacteria? *Drug Discov. Today* **2021**, *26*, 2152–2158, doi:10.1016/j.drudis.2021.03.027.
39. Craig R. MacNair; Caressa N. Tsai; Eric D. Brown Creative Targeting of the Gram-Negative Outer Membrane in Antibiotic Discovery. *Ann. N. Y. Acad. Sci.* **2020**, *1459*, 69–85, doi:10.1111/nyas.14280.
40. Yechiel Shai Mode of Action of Membrane Active Antimicrobial Peptides. *Pept. Sci.* **2002**, *66*, 217–284, doi:https://doi.org/10.1002/bip.10260.
41. Haim Tsubery; Itzhak Ofek; Sofia Cohen; Mati Fridkin Structure-Function Studies of Polymyxin B Nonapeptide: Implications to Sensitization of Gram-Negative Bacteria. *J. Med. Chem.* **2000**, *43*, 3085–3092, doi:10.1021/jm0000057.
42. Bo Ma; Chao Fang; Linshan Lu; Mingzhi Wang; Xiaoyan Xue; Ying Zhou; Mingkai Li; Yue Hu; Xiaoxing Luo; Zheng Hou The Antimicrobial Peptide Thanatin Disrupts the Bacterial Outer Membrane and Inactivates the NDM-1 Metallo- β -Lactamase. *Nat. Commun.* **2019**, *10*, 3517, doi:https://doi.org/10.1038/s41467-019-11503-3.
43. Swaleeha Jaan Abdullah; Bernice Tan Siu Yan; Nithya Palanivelu; Vidhya Bharathi Dhanabal; Juan Pablo Bifani; Surajit Bhattachariya Outer-Membrane Permeabilization, LPS Transport Inhibition: Activity, Interactions, and Structures of Thanatin Derived Antimicrobial Peptides. *Int. J. Mol. Sci.* **2024**, *25*, 2122, doi:https://doi.org/10.3390/ijms25042122.
44. Akiko Kumagai; Ryoko Ando; Hideyuki Miyatake; Peter Greimel; Toshihide Kobayashi; Yoshio Hirabayashi; Tomomi Shimogori; Atsushi Miyawaki A Bilirubin-Inducible Fluorescent Protein from Eel Muscle. *Cell* **2013**, *153*, 1602–1611.
45. Céline S. M. Richard; Hymonti Dey; Frode Øyen; Munazza Maqsood; Hans-Matti Blencke Outer Membrane Integrity-Dependent Fluorescence of the Japanese Eel UnaG Protein in Live *Escherichia Coli* Cells. *Biosensors* **2023**, *13*, doi:https://doi.org/10.3390/bios13020232.
46. Marko Virta; Karl E. O. Åkerman; Petri Saviranta; Christian Oker-Blom; Matti T. Karp Real-Time Measurement of Cell Permeabilization with Low-Molecular-Weight Membranolytic Agents. *J. Antimicrob. Chemother.* **1995**, *36*, 303–315.
47. Nicola R. Stanley; Kim Findlay; Ben C. Berks; Tracy Palmer *Escherichia Coli* Strains Blocked in Tat-Dependent Protein Export Exhibit Pleiotropic Defects in the Cell Envelope. *J. Bacteriol.* **2001**, *183*, 139–144, doi:10.1128/JB.183.1.139–144.2001.

48. Kwang Kook Lee; Cheol Seong Jang; Ju Yeon Yoon; Se Yoon Kim; Tae Ho Kim; Ki Hyun Ryu; Wook Kim Abnormal Cell Division Caused by Inclusion Bodies in *E. Coli*; Increased Resistance against External Stress. *Microbiol. Res.* **2008**, *163*, 394–402, doi:https://doi.org/10.1016/j.micres.2008.03.004. 762
763
764
49. Bihong Zhou; Lei Xing; Wei Wu; Xian-En Zhang; Zhanglin Lin Small Surfactant-like Peptides Can Drive Soluble Proteins into Active Aggregates. *Microb. Cell Factories* **2012**, *11*, doi:http://dx.doi.org/10.1186/1475-2859-11-10. 765
766
50. Raul Navarro; Ling-chun Chen; Rishi Rakhit; Thomas J. Wandless A Novel Destabilizing Domain Based on a Small-Molecule Dependent Fluorophore. *ACS Chem. Biol.* **2016**, *11*, 2101–2104. 767
768
51. Shinan Liu; Fei Gao; Ruijie Wang; Wen Li; Siyao Wang; Xi Zhang Molecular Characteristics of the Fatty-Acid-Binding Protein (FABP) Family in *Spirometra Mansoni* - A Neglected Medical Tapeworm. *Animals* **2023**, *13*, doi:https://doi.org/10.3390/ani13182855. 769
770
771
52. Jordan J. Clark; Mark L. Benson; Richard D. Smith; Heather A. Carlson Inherent versus Induced Protein Flexibility: Comparisons within and between Apo and Holo Structures. *PLOS Comput. Biol.* **2019**, *15*, doi:https://doi.org/10.1371/journal.pcbi.1006705. 772
773
53. Klara Stensvåg; Tor Haug; Sigmund V. Sperstad; Oystein Rekdal; Bård Indrevoll; Olaf B. Styrvold Arasin 1, a Proline-Arginine-Rich Antimicrobial Peptide Isolated from the Spider Crab, *Hyas Araneus*. *Dev. Comp. Immunol.* **2007**, *32*, 275–285, doi:10.1016/j.dci.2007.06.002. 774
775
776
54. Victoria S. Paulsen; Hans-Matti Blencke; Monica Benincasa; Tor Haug; Jacobus J. Eksteen; Olaf B. Styrvold; Marco Scocchi; Klara Stensvåg Structure-Activity Relationships of the Antimicrobial Peptide Arasin 1 - And Mode of Action Studies of the N-Terminal, Proline-Rich Region. *PLOS ONE* **2013**, *8*. 777
778
779
55. Itzhak Ofek; Sofie Cohen; Rita Rahmani; Kisra Kabha; Dove Tamarkin; Yaacov Herzig; Ethan Rubinstein Antibacterial Synergism of Polymyxin B Nonapeptide and Hydrophobic Antibiotics in Experimental Gram-Negative Infections in Mice. *Antimicrob. Agents Chemother.* **1994**, *38*, 374–377, doi:https://doi.org/10.1128/aac.38.2.374. 780
781
782
56. M. Vaara The Outer Membrane Permeability-Increasing Action of Linear Analogues of Polymyxin B Nonapeptide. *Drugs Exp. Clin. Res.* **1991**, *17*, 437–443. 783
784
57. Odel Soren; Karoline Sidelmann Brinch; Dipesh Patel; Yingjun Liu; Alexander Liu; Anthony Coates; Yanmin Hu Antimicrobial Peptide Novicidin Synergizes with Rifampin, Ceftriaxone, and Ceftazidime against Antibiotic-Resistant *Enterobacteriaceae* In Vitro. *Antimicrob. Agents Chemother.* **2015**, *59*, doi:https://doi.org/10.1128/aac.01245-15. 785
786
787
58. Thein Zaw Oo; Nerida Cole; Linda Garthwaite; Mark D. P. Willcox; Hua Zhu Evaluation of Synergistic Activity of Bovine Lactoferricin with Antibiotics in Corneal Infection. *J. Antimicrob. Chemother.* **2010**, *65*, 1243–1251, doi:https://doi.org/10.1093/jac/dkq106. 788
789
790
59. Manoj Jangra; Vrushali Raka; Hemraj Nandanwar In Vitro Evaluation of Antimicrobial Peptide Tridecaptin M in Combination with Other Antibiotics against Multidrug Resistant *Acinetobacter Baumannii*. *Molecules* **2020**, *25*, 3255, doi:https://doi.org/10.3390/molecules25143255. 791
792
793
60. Hans G. Boman; Birgitta Agerberth; Anita Boman Mechanisms of Action on *Escherichia Coli* of Cecropin P1 and PR-39, Two Antibacterial Peptides from Pig Intestine. *Infect. Immun.* **1993**, *61*, 2978–2984. 794
795
61. Natividad Ruiz; Brian Falcone; Daniel Kahne; Thomas J. Silhavy Chemical Conditionality: A Genetic Strategy to Probe Organelle Assembly. *Cell* **2005**, *121*, 307–317, doi:10.1016/j.cell.2005.02.014. 796
797
62. Jara Radek; Korinna Kraft; Julia Bartels; Tamara Cikovic; Franziska Dürr; Jennifer Emenegger; Simon Kelterborn; Christopher Sauer; Georg Fritz; Susanne Gebhard; et al. The Bacillus BioBrick Box: Generation and Evaluation of Essential Genetic Building Blocks for Standardized Work with *Bacillus Subtilis*. *J. Biol. Eng.* **2013**, *7*:29, doi:10.1186/1754-1611-7-29. 798
799
800
63. Kalen P. Clifton; Ethan M. Jones; Sudip Paudel; John P. Marken; Callan E. Monette; Andrew D. Halleran; Lidia Epp; Margaret S. Saha The Genetic Insulator RiboJ Increases Expression of Insulated Genes. *J. Biol. Eng.* **2018**, *12*, doi:https://doi.org/10.1186/s13036-018-0115-6. 801
802
803

-
64. Hogune Im; Joseph Sambrook; David W. Russell The Inoue Method for Preparation and Transformation of Competent *E.Coli*: “Ultra Competent” Cells. *Bio-Protoc.* **2011**, *1*, doi:https://doi.org/10.21769/BioProtoc.143. 804
805
65. Phil Oberacker; Peter Stepper; Donna M. Bond; Sven Höhn; Jule Focken; Vivien Meyer; Luca Schelle; Victoria J. Sugrue; Gert-Jan Jeunen; Tim Moser; et al. Bio-On-Magnetic-Beads (BOMB): Open Platform for High-Throughput Nucleic Acid Extraction and Manipulation. *PLOS Biol.* **2019**, *17*, doi:https://doi.org/10.1371/journal.pbio.3000107. 806
807
808
66. C. T. Chung; Suzanne L. Niemela; Roger H. Miller One-Step Preparation of Competent *Escherichia Coli*: Transformation and Storage of Bacterial Cells in the Same Solution. *Proc. Natl. Acad. Sci. USA* **1989**, *86*, 2172–2175. 809
810
67. Daniel G. Gibson; Lei Young; Ray-Yuan Chuang; J. Craig Venter; Clyde A. Hutchison III; Hamilton O. Smith Enzymatic Assembly of DNA Molecules up to Several Hundred Kilobases. *Nat. Methods* **2009**, *6 No. 5*, 343–345. 811
812
68. Kine Ø. Hansen; Ida K. Ø. Hansen; Céline S. Richard; Marte Jenssen; Jeanette H. Andersen; Espen H. Hansen Antimicrobial Activity of Securamines From the Bryozoan *Securiflustra Securifrons*. *Nat. Prod. Commun.* **2021**, *16*, 1–8, doi:DOI: 10.1177/1934578X21996180. 813
814
815
69. Youwen Zhang; Xiukun Wang; Xue Li; Limin Dong; Xinxin Hu; Tongying Nie; Yun Lu; Xi Lu; Jing Pang; Guoqing Li; et al. Synergistic Effect of Colistin Combined with PFK-158 against Colistin-Resistant *Enterobacteriaceae*. *Antimicrob. Agents Chemother.* **2019**, *63*, e00271-19, doi:https://doi.org/10.1128/aac.00271-19. 816
817
818
819

Disclaimer/Publisher’s Note: The statements, opinions and data contained in all publications are solely those of the individual author(s) and contributor(s) and not of MDPI and/or the editor(s). MDPI and/or the editor(s) disclaim responsibility for any injury to people or property resulting from any ideas, methods, instructions or products referred to in the content. 820
821
822

Supporting Information

Cloning of a dual biosensor relying on UnaG and luciferase for detection of outer and plasma membrane disruption and its application to characterizing the membranolytic effects of green sea urchin *Strongylocentrotus droebachiensis* Centrocin-1-based antimicrobial peptides

Céline S. M. Richard, Hymonti Dey, Emma Murvold, Frode Øyen, Chun Li and Hans-Matti Blencke

Figures and tables

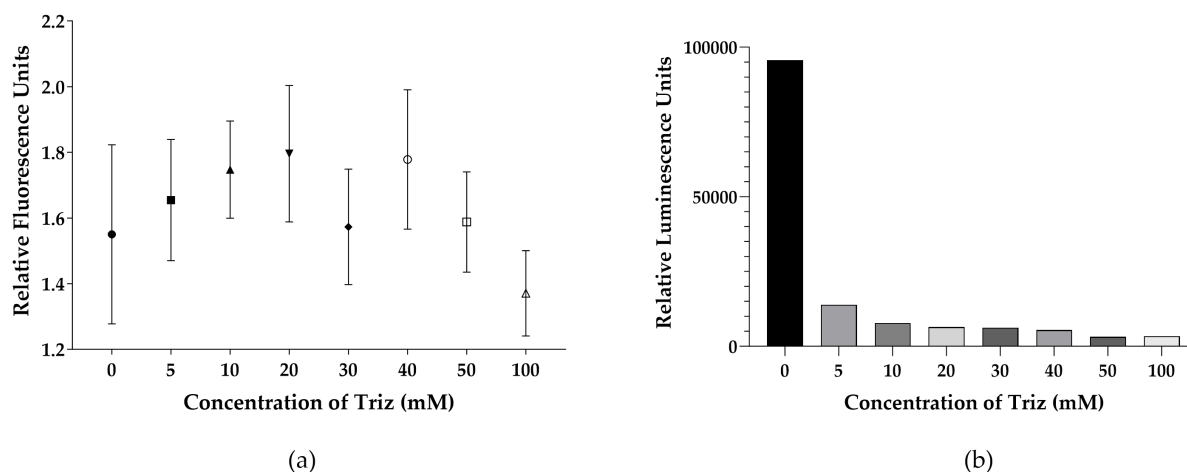


Figure S1. Optimization of medium for better signal to noise ratio for simultaneous fluorescence and luminescence emissions. Relative fluorescence (a) and luminescence (b) of *E. coli* MC4100 in NaCl 0,9 % with different concentrations of Triz pH 7.5 after 10 min exposure of 10 $\mu\text{g}/\text{mL}$ of polymyxin B or without exposure, respectively. The relative fluorescence corresponds to the ratio of the cells after exposure of polymyxin B to the background fluorescence after exposure of 5 μM of BR only. The relative luminescence corresponds to the background of D-luciferin only.

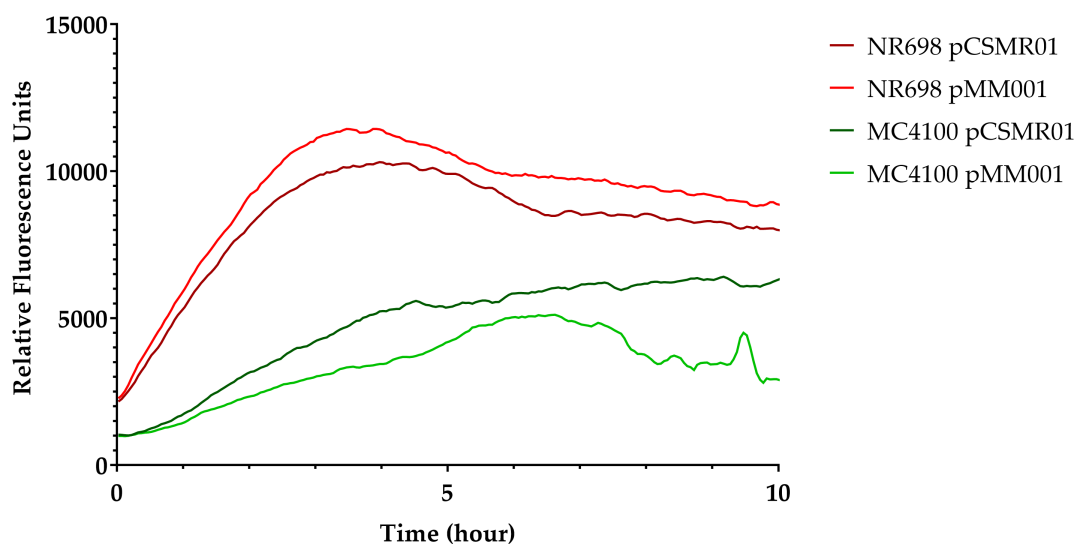


Figure S2: Comparison of UnaG expression levels in the single and the double sensors. Relative fluorescence of both *E. coli* strains carrying the single sensor plasmid (pMM001) or double sensor plasmid (pCSMR01) in presence of 10 $\mu\text{g}/\text{mL}$ Polymyxin B nonapeptide (PMBN) and 5 μM of BR. 25
26
27

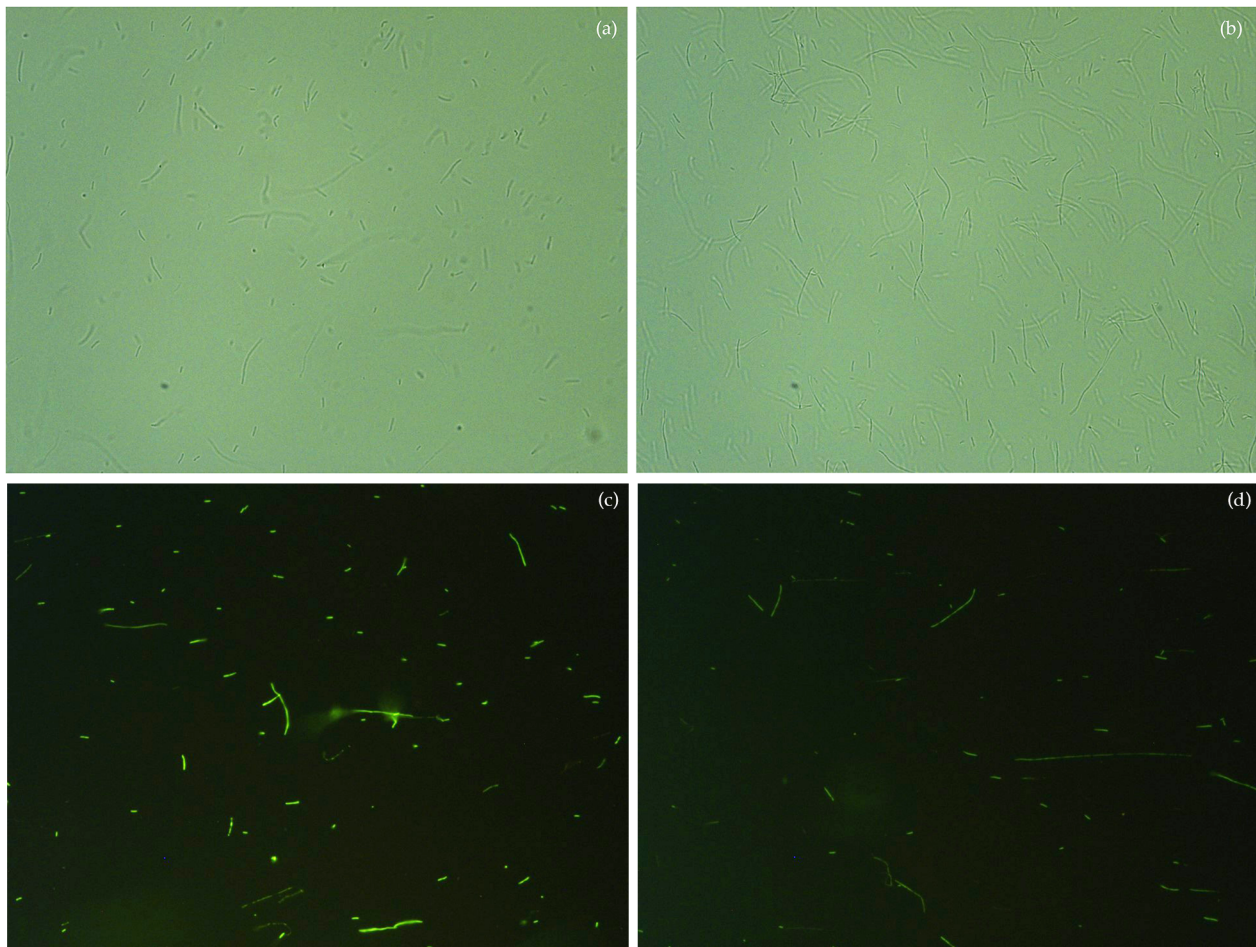


Figure S3: Microscopy of abnormally long cells with periplasm transporters. Images of *E. coli* MC4100 carrying the plasmid **(a and c)** pMM002 (UnaG-dsbA), **(b and d)** pMM003 (UnaG-torA) at x400 magnification. The images were taken with **(a and b)** the phase contrast or **(c and d)** fluorescence through the software Las X. For better visibility, the brightness of the pictures was equivalently increased to 100 with Adobe Photoshop CS6 version 13.0.

31

32
33
34
35
3637
38
39
40
41
42
43
44
45
46

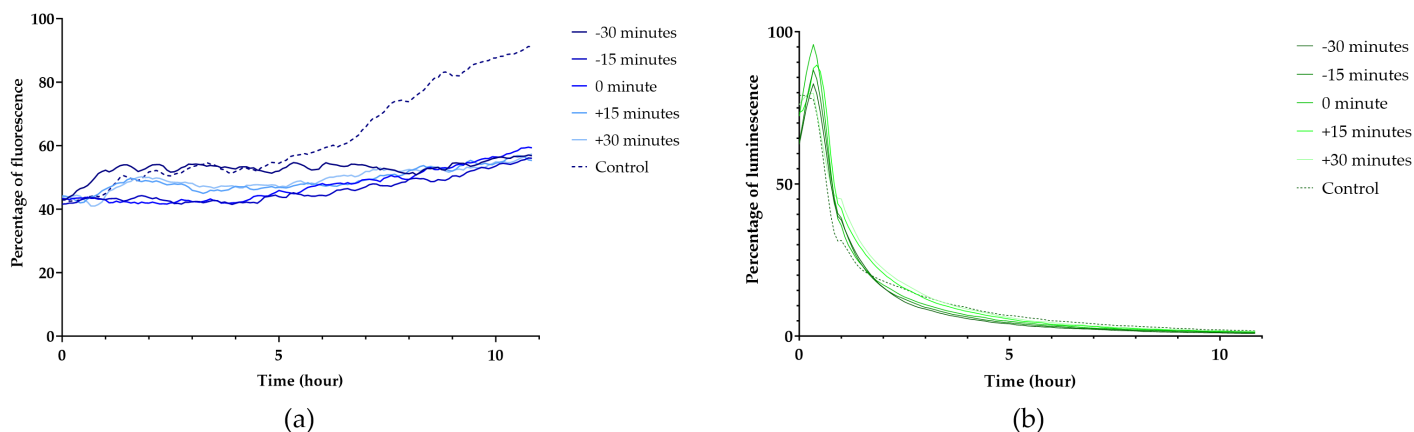


Figure S4: Effect of translation inhibitor at different time points on GFP fluorescence and lux luminescence. Kinetic of the relative (a) fluorescence of GFP; and (b) luminescence of LuxABCDE for 10 hours after addition of 5 μ M BR of *E. coli* NR698 at the 0 min time point and 50 μ g/mL Erythromycin at different time points.

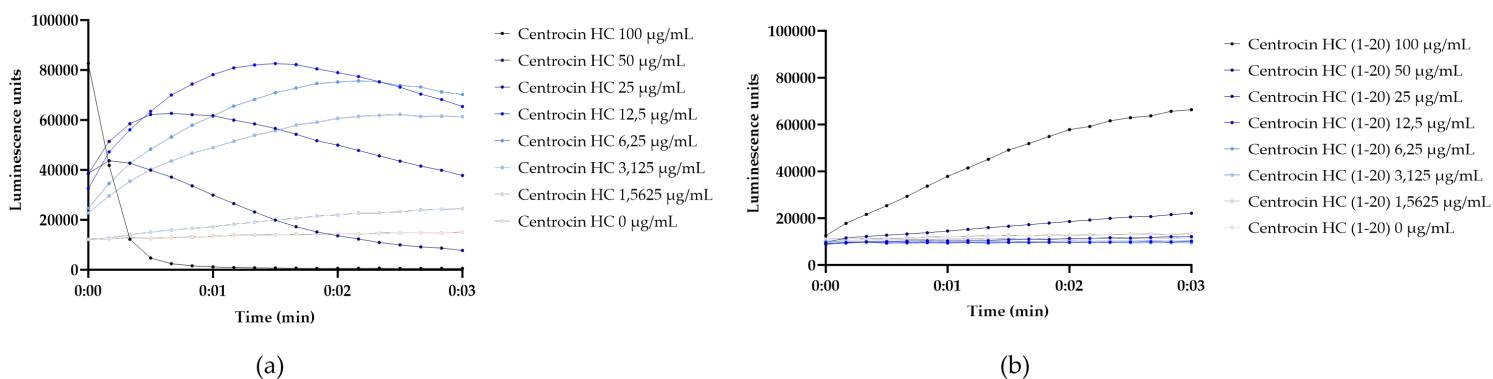


Figure S5: Effect of Centrocin HC and Centrocin HC (1-20) on the plasma membrane of *E. coli*. Representative luminescence kinetic of LucGR of the wild-type MC4100 in presence of different concentrations of (a) centrocin HC; (b) centrocin HC (1-20) with 5 μ M BR and 1 μ M D-luciferin for 10 hours.

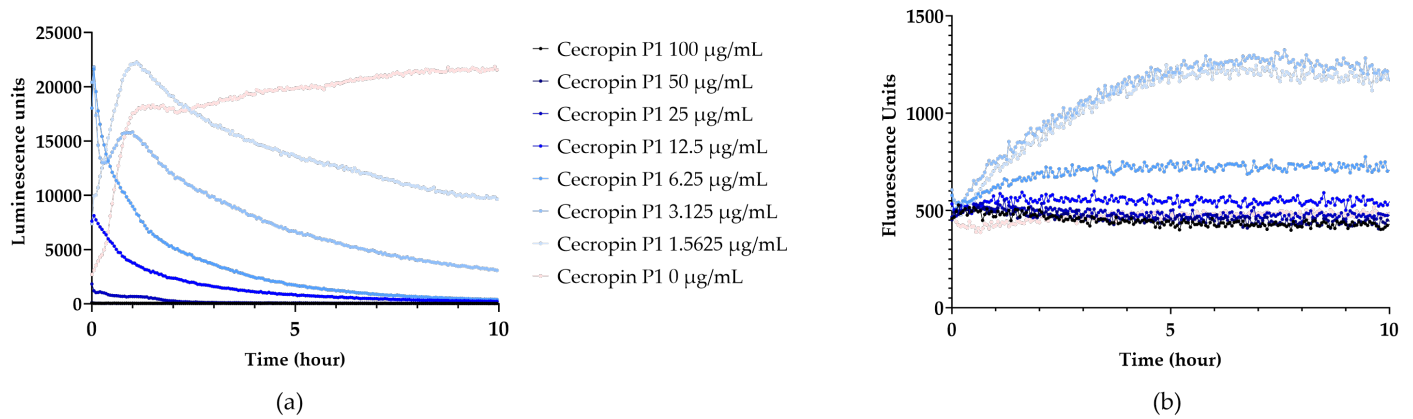


Figure S6: Effect of Cecropin P1 on the plasma- and the outer-membrane of *E. coli*. Representative of (a) the luminescence kinetic of LucGR; (b) the fluorescence kinetic of UnaG of the wild-type MC4100 in presence of different concentrations of cecropin P1 with 5 μM BR and 1 μM D-luciferin for 10 hours.

58

59

60

61

62

63

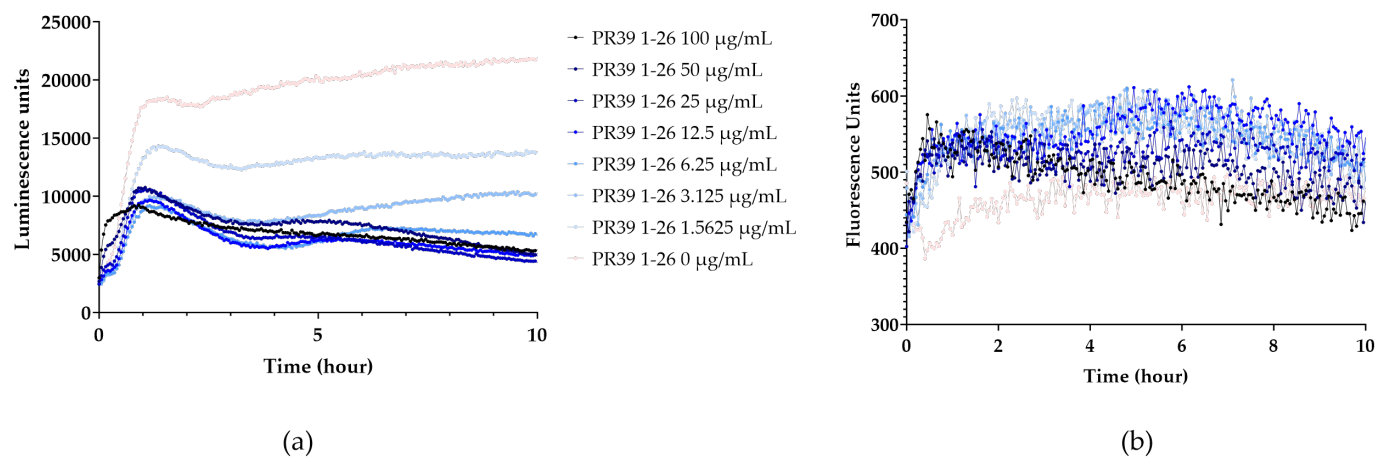


Figure S7: Effect of PR39 (1-26) on the plasma- and the outer-membrane of *E. coli*. Representative (a) luminescence kinetic of LucGR; (b) fluorescence kinetic of UnaG of the wild-type MC4100 in presence of different concentrations of PR39 (1-26) with 5 μM BR and 1 μM D-luciferin for 10 hours.

64

65

66

67

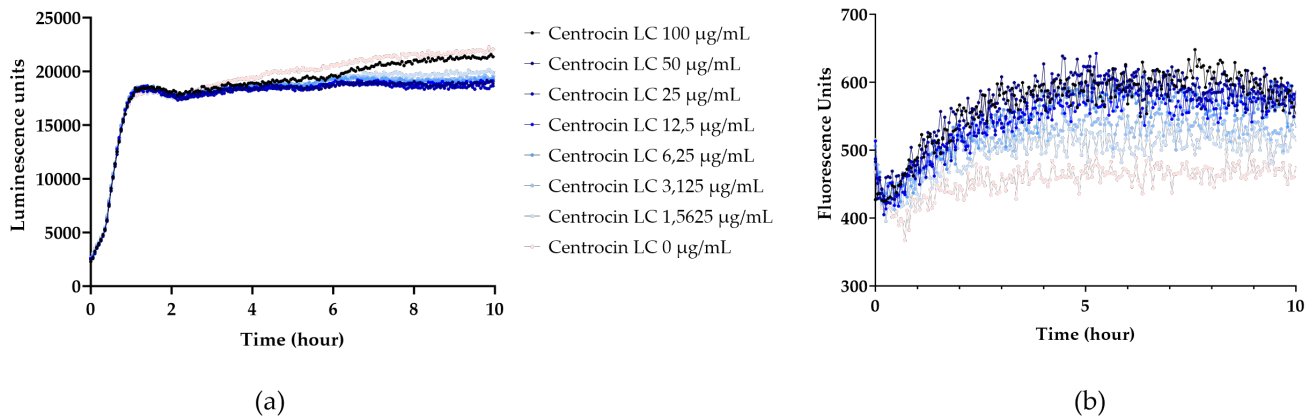


Figure S8: Effect of Centrocin LC on the plasma- and the outer-membrane of *E. coli*. Representative (a) luminescence kinetic of LucGR; (b) fluorescence kinetic of UnaG of the wild-type MC4100 in presence of different concentrations of centrocin LC with 5 μM BR and 1 μM D-luciferin for 10 hours.

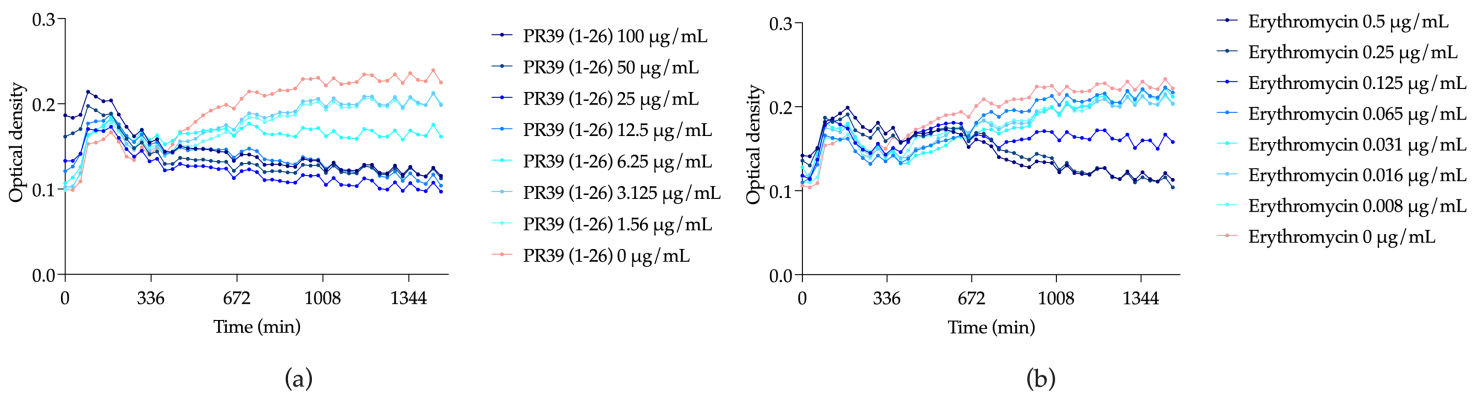


Figure S9: Comparison of the effect of PR39 (1-26) and Erythromycin on the growth of *Bacillus subtilis*. Representative growth of *B. subtilis* in response to different concentrations of (a) PR39 (1-26) or (b) Erythromycin (control) for 24 h in 30 minutes time intervals.

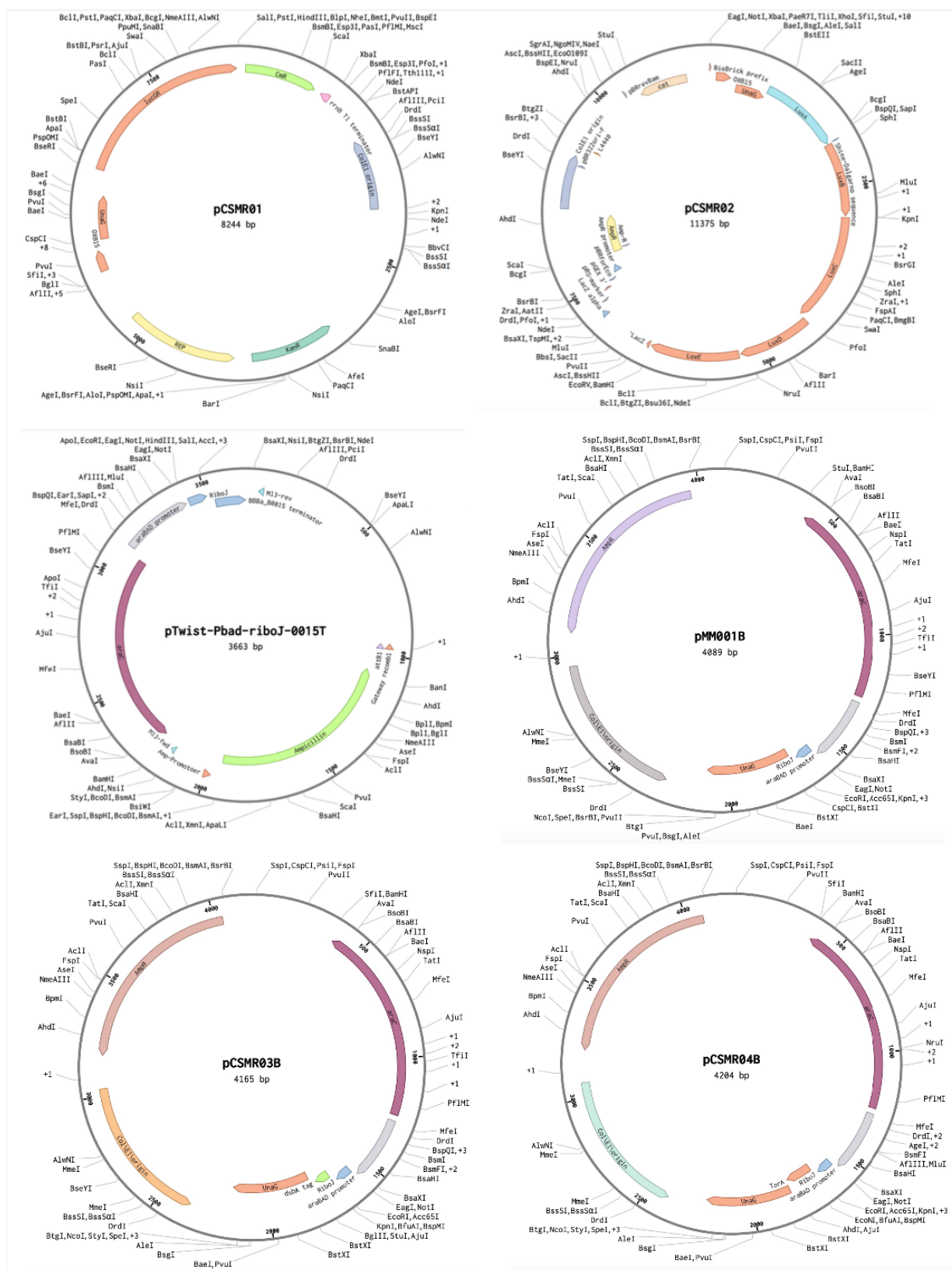


Figure S10: Maps of plasmids used in this study. (Benchling.com; accessed on 29th March 2024).

Sequence S1: DNA sequence of pCSMR01

87

TCGACCTGCAGCCAAGCTTAGCTAGCTAGAGCTTGGCGAGATTTTCAGGAGCTAAGGAAGCTAAAATGGAGAAAAAATCACTGGATATAC 88
CACCGTTGATATATCCCAATGGCATCGTAAAGAACATTTTGAGGCATTTTCAGTCAGTTGCTCAATGTACCTATAACCAGACCGTTTCAGCTGGA 89
TATTACGGCCTTTTAAAGACCGTAAAGAAAAATAAGCACAAGTTTTATCCGGCCTTTATTACATTCTTGCCCGCTGATGAATGCTCATCC 90
GGAATTTTCGTATGGCAATGAAAGACGGTGAGCTGGTGATATGGGATAGTGTTCACCCTTGTACACCGTTTTCCATGAGCAAACCTGAAACGT 91
TTTCATCGCTCTGGAGTGAATACCACGACGATTTCCGGCAGTTTCTACACATATATTTCGCAAGATGTGGCGTGTACGGTGAAAACCTGGCCT 92
ATTTCCCTAAAGGGTTTTATTGAGAATATGTTTTTCGTCTCAGCCAATCCCTGGGTGAGTTTACCAGTTTTGATTTAAACGTGGCCAATATGGA 93
CAACTTCTTCGCCCCGTTTTACCATGGGCAAATATTATACGCAAGGGCACAAGGTGCTGATGCCGCTGGCGATTTCAGGTTTCATCATGCCGT 94
CTGTGATGGCTTCATGTCCGAGAAATGCTTAATGAATTACAACAGTACTGCGATGAGTGGCAGGGCGGGGCGTAATTTTTTAAAGGCAGTT 95
ATTGGTGCCCTTAAACGCCTGGGGTAATGACTCTCTAGCTTGAGGCATCAAATAAAACGAAAGGCTCAGTCGAAAGACTGGGCCTTTCGTTT 96
TATCTGTTGTTTTCGGTGAACGCTCTCCTGAGTAGGACAAATCCGCCGCTCTAGAGCTGCCGCGTTTCGGTGATGACGGTGAAAACC 97
TCTGACACATGCAGTCCCGGAGACGGTCACAGCTTGTCTGTAAGCGGATGCCGGGAGCAGACAAGCCCGTCAGGGCGCGTCAGCGGGTG 98
TTGGCGGTGTCCGGGCGCAGCCATGACCCAGTCACGTAGCGATAGCGGAGTGATACTGGCTTAACTATGCGGCATCAGAGCAGATTGTA 99
CTGAGAGTGCACCATATGCCGTGTGAAATACCGCACAGATGCCGTAAGGAGAAAATACCGCATCAGGCGCTCTCCGCTTCTCCGCTCACTG 100
ACTCGCTGCGCTCGGTGCTTCGGCTGCGGCGAGCGGTATCAGCTCACTCAAAGGCGGTAATACGGTTATCCACAGAATCAGGGGATAACGC 101
AGGAAAGAACATGTGAGCAAAAGGCCAGCAAAAGGCCAGGAACCGTAAAAAGCCGCGTTGCTGGCGTTTTTCCATAGGCTCCGCCCC 102
CTGACGAGCATCACAAAATCGACGCTCAAGTCAGAGGTGGCGAAAACCCGACAGGACTATAAAGATACCAGGCGTTTCCCCCTGGAAGCT 103
CCCTCGTGCCTCTCCTGTTCCGACCCTGCCGCTTACCGGATACTGTCCGCTTTCTCCCTTCGGGAAGCGTGGCGCTTTCTCAATGCTCAC 104
GCTGTAGGTATCTCAGTTCGGTGTAGGTCGTTCCGCTCAAGCTGGGCTGTGTGCACGAACCCCCCGTTACGCCGACCGCTGCGCCTTATCC 105
GGTAACTATCGTCTTGAGTCCAACCCGTAAGACACGACTTATCGCCACTGGCAGCAGCCACTGGTAAACAGGATTAGCAGAGCGAGGTATG 106
TAGGCGGTGCTACAGAGTTCTTGAAGTGGTGGCCTAACTACGGCTACACTAGAAGGACAGTATTTGGTATCTGCGCTCTGCTGAAGCCAGTT 107
ACCTTCGGAAAAAGAGTTGGTAGCTTTGATCCGGCAAACAACCACCGCTGGTAGCGGTGGTTTTTTTTGTTTGAAGCAGCAGATTACGC 108
GCAGAAAAAAGGATCTCAAGAAGATCCTTTGATCTTTTCTACGGGGTCTGACGCTCAGTGAACGAAAACCTCACGTTAAGGGATTTTGGT 109
CATGAGATTATCAAAAAGGATCTTACCTAGATCCTTTTCGGTACCGCTGATTTCACTTTTTGCATTCTACAAACTGCATAACTCATATGTAAA 110
TCGCTCCTTTTTAGGTGGCACAAATGTGAGGCATTTTCGCTCTTTCCGGCAACCACTTCCAAGTAAAGTATAACACACTATACTTTATATTCAT 111
AAAGTGTGTCTCTGCGAGGCGTCCAGTGCCGACCAAAACCATAAAACCTTTAAGACCTTTCTTTTTTTTACGAGAAAAAAGAAACAAAA 112
AACCTGCCCTCTGCCACCTCAGCAAAGGGGGTTTTGCTCTCGTCTGTTTAAAAATCAGCAAGGGACAGGTAGTATTTTTGAGAAGATC 113
ACTCAAAAATCTCCACCTTTAAACCTTGCCAATTTTTATTTGTCCGTTTTGTCTAGCTTACCGAAAGCCAGACTCAGCAAGAATAAAATT 114
TTTATTGTCTTTTCGGTTTTCTAGTGTAACGGACAAAACCACTCAAATAAAAAAGATAACAAGAGAGGTCTCTCGTATCTTTTATTTCAGCAATC 115
GCGCCCCGATTGCTGAACAGATTAATAATAGATTTTAGCTTTTTATTGTTGAAAAAAGCTAATCAAATTGTTGTCCGGATCAATTACTGCAAA 116
GTCTCGTTCATCCCACCACTGATCTTTAATGATGATTGGGGTGCAAAATGCCCAAAGGCTTAATATGTTGATATAATTCATCAATCCCTCTA 117
CTTCAATGCGGCAACTAGCAGTACCAGCAATAAACGACTCCGCACCTGTACAAAACCGGTGAATCATTACTACGAGAGCGCCAGCTTCATCA 118
CTTGCTCCCATAGATGAATCCGAACCTCATTACACATTAGAACTGCGAATCCATCTTCATGGTGAACCAAAGTGAACCTAGTTTATCGCA 119
ATAAAAACCTATACTCTTTTAAATATCCCGACTGGCAATGCCGGGATAGACTGTAACATTCTCACGCATAAAATCCCTTTTCATTTTCTAATG 120
TAAATCTATTACCTTATTATTAATTCAATTCGCTCATAATTAATCCTTTTTCTTATTACGCAAAAATGGCCCCGATTTAAGCACACCCCTTTATCCGT 121
TAATGCGCCATGACAGCCATGATAATTAATACTAGGAGAAGTTAATAAATACGTAACCAACATGATTAACAATTATTAGAGGTATCGTT 122
CAAAATGGTATGCGTTTTGACACATCCACTATATATCCGTGTGCTTCTGTCCACTCCTGAATCCATTCCAGAAATCTCTAGCGATTCCAGAA 123
GTTTCTCAGAGTCGAAAAGTTGACCAGACATTACGAACTGGCACAGATGGTCATAACCTGAAGGAAGATCTGATTGCTTAACTGCTTCAGTT 124
AAGACCGAAGCGCTCGTCTATAACAGATGCGATGATGCAGACCAATCAACATGGCACCTGCCATTGCTACCTGTACAGTCAAGGATGGTA 125
GAAATGTTGTCCGTCCTTGACACGAATATTACGCCATTTGCCTGCATATTCAAACAGCTTCTTACGATAAGGGCACAAATCGCATCGTGA 126
ACGTTTGGGCTTCTACCGATTTAGCAGTTGGATACACTTCTCTAAGTATCCACCTGAATCATAAATCGGCAAAAATAGAGAAAAAATTGACCAT 127

GTGTAAGCGGCCAATCTGATTCCACCTGAGATGCATAATCTAGTAGAATCTCTTCGCTATCAAATTCACCTCCACTCACC GGTTG 128
TCCATTCATGGCTGAACCTCTGCTTCTCTGTTGACATGACACACATCATCTCAATATCCGAATAGGGCCCATCAGTCTGACGACCAAGAGAG 129
CCATAAACACCAATAGCCTTAACATCATCCCCATATTTATCCAATATTCGTTCCCTAATTTTCATGAACAATCTTCATTCTTTCTCTAGTCATT 130
ATTATTGGTCCATTCACTATTCTCATTCCCTTTTCAGATAATTTTAGATTGCTTTTCTAAATAAGAATATTTGGAGAGCACCGTTCTTATTCAGC 131
TATTAATAACTCGTCTTCCTAAGCATCCTTCAATCCTTTTAATAACAATTATAGCATCTAATCTTCAACAAACTGGCCCGTTTGTGAACTACTC 132
TTAATAAAAATAATTTTCCGTTCCCAATTCCACATTGCAATAATAGAAAAATCCATCTTCATCGGCTTTTTCGTCATCATCTGTATGAATCAAAT 133
CGCTTCTTCTGTGTCATCAAGGTTTAAATTTTTATGTATTTCTTTTAAACAAACCACCATAGGAGATTAACCTTTTACGGTGTAACCTTCTCC 134
AAATCAGACAAACGTTTCAAATCTTTTCTTCATCATCGGTATAAAAATCCGTATCCTTTACAGGATATTTTGCAGTTTCGTCAATTGCCGATT 135
GTATATCCGATTTATATTTATTTTTCGGTGAATCATTGAACTTTTACATTGGATCATAGTCTAATTTTATTGCCTTTTCCAAAATTGAATCCA 136
TTGTTTTGATTACAGTAGTTTTCTGTATTCTAAAATAAGTTGGTTCCACACATACCAATACATGCATGTGCTGATTATAAGAATTATCTTTATT 137
ATTTATTGTCACCTCCGTTGCACGCATAAAAACCAACAAGATTTTTATTAATTTTTTATATTGCATCATTCGGCGAAATCCTTGAGCCATATCTG 138
ACAAACTCTTATTTAATTCTTCGCCATCATAAACATTTTTAACTGTTAATGTGAGAAACAACCAACGAACGTTGGCTTTTGTTAATAACTTC 139
AGCAACAACCTTTTGTGACTGAATGCCATGTTTCATTGCTCTCCTCCAGTTGCACATTGGACAAAAGCCTGGATTTACAAAACCACACTCGAT 140
ACAACCTTCTTTCGCCTGTTTCAGGATTTGTTTATACTCTAATATTTTCAGCACAATCTTTTACTCTTTCAGCCTTTTAAATTCAGAATATGCA 141
GAAGTTCAAAGTAATCAACATTAGCGATTTCTTTTCTCTCCATGGTCTCACTTTTCCACTTTTGTCTTGTCCACTAAAACCCTTGATTTTCA 142
TCTGAATAAATGCTACTATTAGGACACATAATATTA AAAAGAAACCCCATCTATTTAGTTATTTGTTTAGTCACTTATAACTTTAACAGATGGG 143
GTTTTTCTGTGCAACCAATTTAAGGGTTTTCAATACTTTAAAACACATACATACCAACACTTCAACGCACCTTTCAGCAACTAAAATAAAAA 144
TGACGTTATTTCTATATGTATCAAGATAAGAAAGAACAAGTTCAAAAACCATCAAAAAAAGACACCTTTTCAGGTGCTTTTTTTATTTTATAAA 145
CTCATTCCCTGATCTCGACTTCGTTCTTTTTTACCTCTCGGTTATGAGTTAGTTCAAATTCGTTCTTTTTAGGTTCTAAATCGTGTTTTTCTTGGA 146
ATTGTGCTGTTTTATCCTTTACCTGTCTACAAACCCCTTAAAAACGTTTTTAAAGGCTTTTAAAGCCGTCTGTACGTTCTTAAAGGAATTAATTC 147
CTCGAGAGAGGAAGGCCGTC AAGGCCTTGGCGGAAGGCCGTC AAGGCCGTCATGGATCCCCAGATCTAAGCTGTTGTGACCGCTTGCTCTA 148
GCCAGCTATCGAGTTGTGAACCGATCCATCTAGCAATTGGTCTCGATCTAGCGATAGGCTTCGATCTAGCTATGTAGAAACGCCGTGTGCTCG 149
ATCGCTTGATAAGGTCCACGTAGCTGCTATAGTTGCTTCAACAGAACATATTGACTATCCGGTATTACCCGGCAGATCTTTGTGATCCTACCA 150
TCCACTCGACACACCCGCCAGCGCCGCTGCCAAGCTTCCGAGCTCTCGAATTCAAAGGAGGTACCCACCATGGTTGAAAAATTTGTTGGC 151
ACCTGGAAAATTGCCGATAGCCATAATTTGGCGAATACCTGAAAGCCATTGGTGCACCGAAAGAACTGAGTGATGGTGGTGATGCAACCA 152
CACCGACACTGTATATTAGCCAGAAAGATGGTGATAAGATGACCGTGAAAATTGAAAATGGTCCGCCTACCTTTCTGGATACCCAGGTTAAA 153
TTCAAACCTGGGCGAAGAATTTGATGAATTTCCGAGCGATCGTCGTAAAGGTGTTAAAAGCGTTGTTAATCTGGTGGGTGAAAAACTGGTTTA 154
TGTGCAGAAATGGGATGGTAAAGAAACCACCTATGTGCGGAAATCAAAGATGGTAAACTGGTTGTTACCCTGACCATGGGTGATGTTGTT 155
GCAGTTCGTAGCTATCGTCGTGCAACCGAATGGTGTGACTGTCTCGAGGCTGGCATCCCTAACATATCCGAATGGTACTTAAACAACGGA 156
GGACTAGCGTATCCCTTCGCATAGGGTTGAGTTAGATAAAGTATATGCTGAACTTCTTCTTTGCTCAAAGAATCATAAAAAATTTATTTGCT 157
TTCAGGAAAATTTTTCTGTATAATAGATTCAAATTTGTGAGCGGATAACAATTTGAATTCATTAAGAGGAGAAATTAACATGAGGGGATCCA 158
TGATGAAGAGAGAGAAAAATGTTGTATATGGACCCGAACCCCTACACCCCTTGGAAAGACTTAACAGCAGGAGAAATGCTCTTCAGGGCCC 159
TTCGAAAACATTTCTATTTACCGCAGGCTTTAGTAGATGTGTATGGTGAAGAATGGATTCATATAAAGAGTTTTTTGAAACTACATGCCTACT 160
AGCACAAAAGTCTTCACAATTGTGGATACAAGATGAGTGATGATGAGTGTGCTGATCTGCGCGGAGAACATAAAAAGATTTTTTGTGCCATTATTG 161
CAGCTTGGTATATTGGTATGATTGTAGCACCTGTTAATGAGGGCTACATCCCAGATGAACTCTGTAAGGTCATGGGTATATCGAGACCACAAC 162
TAGTTTTTTGTACAAAGAATATTCTAAATAAGGTATTGGAGGTACAGAGCAGAACTGATTTCAATAAAAAGGATTATCATACTAGATGCTGTAG 163
AAAACATACACGGTTGTGAAAGTCTTCCCAATTTATTTCTCGTTATTTCGGATGGAAAATATTGCCAACTTCAAACCTTTACATTACGATCCTGT 164
TGAACAAGTGGCAGCTATCTTATGTTTCGTCAGGCACAACCTGGATTACCGAAAGGTGTAATGCAAACTCATAGAAATGTTTGTGTCCGACTTA 165
TACATGCTTTAGACCCAGGGTAGGAACGCAACTTATTCTGGTGTGACAGTCTTAGTATATCTGCCTTTTTTCCATGCTTTTGGGTTCTCTATA 166
AACTTGGGATACTTCATGGTGGTCTTCGTGTTATCATGTTAAGACGATTGATCAAGAAGCATTCTAAAAGCTATTACAGGATTATGAAGTTC 167
GAAGTGTAATTAACGTTCCAGCAATAATATTGTTCTTATCGAAAAGTCTTTGGTTGACAAAATACGATTTATCAAGTTTAAAGGGAATTGTGTTG 168
CGGTGCGGCACCATAGCAAAGGAAGTTGCTGAAATTGCAGTAAAACGATTAACCTTGCCAGGAATTCGCTGTGGATTGGTTTGACAGAA 169

TCTACTTCAGCTAATATACACAGTCTTAGGGATGAATTTAAATCAGGATCACTTGGAAAAGTTACTCCTTTTATGGCAGTTAAAATAGCAGAT 170
AGGGAAACTGGTAAAGCATTGGGACCAAATCAAGTTGGTGAATTATGCGTCAAAGGTCCCATGGTATCGAAAGGTTACGTAAACAATGTAG 171
AAGTACCAAAGAGGCTATTGATGATGATGGTTGGCTTCACTCTGGAGACTTTGGATACTATGATCAGGATGAGCATTCTATGTGGTGGACC 172
GTTACAAGGAATTGATTAATATAAGGGCTCTCAGGTAGCACCTGCAGAACTAGAAGAGATTTTATTGAAAAATCCATGTATCAGAGATGTT 173
GCTGTGGTTGGTATTCTGATCTAGAAGCTGGAGAAGTCCATCTGCGTTTGTGGTTATACAGCCCCGAAAGGAGATTACAGCTAAAGAAGT 174
TTACGATTATCTTGCCGAGAGGGTCTCCCATACAAAGTATTGCGTGGAGGGGTTTCGATTTCGTTGATAGCATACCAAGGAATGTTACAGGTAA 175
AATTACAAGAAAGGAAGTCTGAAGCAGTTGCTGGAGAAGAGTTCTAAACTTTAAAGTCTTCATGGATCCG 176

Sequence S2: DNA sequence of pCSMR02

gaattcgcggccgcttCTAGAATTCTCGAGAGAGGAAGGCCGTCAAGGCCTTGGCGGAAGGCCGTCAAGGCCGATGGATCCCCAGATCTAAGCTG 179
TTGTGACCGCTTGTCTAGCCAGCTATCGAGTTGTGAACCGATCCATCTAGCAATTGGTCTCGATCTAGCGATAGGCTTCGATCTAGCTATGTA 180
GAAACGCCGTGTGCTCGATCGCTTATAAGTCCACGTAGCTGCTATAGTTGCTTCAACAGAACATATTGACTATCCGGTATTACCCGGCAG 181
ATCTTTGTCGATCCTACCATCCACTCGACACACCCGCCAGCGGCCGTCCAAGTTCGAGCTCTCGAATTCAAAGGAGGTACCCACCAT 182
GGTTGAAAAATTGTTGGCACCTGAAAATTGCCGATAGCCATAATTTGGCGAATACCTGAAAGCCATTGGTGCACCGAAAAGAACTGAGT 183
GATGGTGGTATGCAACCACACCGACACTGTATATTAGCCAGAAAAGATGGTGATAAGATGACCGTGAAAATTGAAAATGGTCCGCCTACCT 184
TTCTGGATACCCAGGTTAAATTCAAAGTGGCGAAGAATTGATGAATTCGAGCGATCGTCGTAAAGGTGTTAAAAGCGTTGTTAATCTG 185
GTGGGTGAAAACTGGTTTATGTGCAGAAATGGGATGGTAAAGAAACCACCTATGTGCGCGAAATCAAAGATGGTAAACTGGTTGTTACCC 186
TGACCATGGGTGATGTTGTTGCAGTTCGTAGCTATCGTCGTGCAACCGAATGGTGtcgacaggaggactctctatgaaattggaacttttcttacataccaacctcccaa 187
tttctcaaacagaggaatgaaacgfttggtaaaataggtcgcctctgaggagtggtttgatacctgatggtactgagcatcttccaggagttggttctggttaaccctatgctcgtcgtcatalttactgg 188
cgcgactaaaaatgaaatgtaggaactccgctattgtctccacagccatccagtagccaactgaagatgtaatttattggatcaaatgcaaaaggacgatttcggttgggtatttgcgagggctttacaacaag 189
gactttcgcgtattcgcacagatatgaaatacagtcgacctagcgggaatctggtacgggctgataaagaatggcgtgacagaggatataggaagctgataatgaaatcaatcaaggttaaaagtaaa 190
ccccgcggctatagcagagggtggcaccggtttatggtggctgaaatcagctcgcagactgagtggtgctcaatttggcctaccgatataaagttggattataaactaacgaaagaaagcacaactga 191
gctttataatgaagtggtcaagaatagggcacgataatcataatcagcaactgtatcatatataacatctgtagatcatgactcaattaaagcgaagagatttccggaatttctggggcattggtatgattctatgt 192
gaaatgctacgactattttgatgattcagacaaacaagaggtatgattcaataaaggcgactggcgtgactttgtatataaaggacataaagataactatcgccgtattgattacagttacgaaatcaatcccgtgggaaac 193
gcccaggaatgattgacataatcaaaagacattgatgctacaggaatcaaatatttgggtgattgaaagctaatggaacagtagacgaaatattgcttcatgaagctctccagctgatgcatgcaattctta 194
aagaaaaaacgctgctattatagtaagaggtaaagaatgaaattggattgtcttcaactcatcaattcaacaactgtcaagaacaaagatagttcgcagcaggaataacgggatgattgataagt 195
tgaattttgaacagattttatgtagtaaaatcattttcagataatggtggtgctggcctctctgactgtttctggtttctgctcgggttaacagagaaaataaattggttcattaatcacatcattacaactcatctctgt 196
ccgcatagcggaggaagcttcttattgtagcgttaagtgaggagatttttttagggtttagtgattgcaaaaaaagatgaaatgcaatttttaacgcccgttgaatatacagcaactatttgaagagtgattat 197
gaaatcattaacgatgcttaacaacaggctattgtaatccagataacgattttatagcttccctaaaatactgtaaatccccatgcttacgccagggcgacctcgaaatagtaacagcaaccagtcacatattgtga 198
gtgggcccgaaaaaaggtaactctctatcttaagtgggatgattctaatgatgtagatgaatgctgaaagataaaagccgctcgggataaatagcgttgacctatcagagatagaccatcagttaatgatatt 199
agftaactataacgaagatagtaataaagctaaacaagagacgctgcaattattagtgattgttctgaaatgcacctaatagaaattcgaataaaactgaaataaattgcaaaaactgcaaaaacgctgctggaaattatc 200
ggagtgataactcggcgaatggcaattgaaagtggtgctgaaagtgattgctgctttgaaaccaatgaaatgattgatgaccaaaaaatgtaataatgattgatgataatgaaaggtaccacatga 201
aatatacctaaggtaccaggaggaagcaaatatgactaaaaaattcattcattaaacggccaggtgaaatcttcccgaagtgatgatttagtcaatcattaaatttgggtataatgatttactgcaatatt 202
gaaatgactctcatgtaaaaaacattattgattgaaataacgaattacgggtgcataacattgcaattttctctatcggtagggcaagatggaataatgaaataactcaagacgcaggacatacattcgtgactt 203
aaaaaataatagggatattcagaagaaatggctaaagctagaggcaattgatatctatgattttatggtctaaaggcggcctttatgatgttgagaataatgaaactggtctccatcatgatgaaatggctacctcag 204
gatgaaagttatgctgggctttccgaaaggtaaatctgtacatctggtgaggttaatttccattctgggatcatgctctatattacgcgcaattttaaactaagaatcagtgattataaaaactcgtcaaccgatctttac 205
cgtaatgattagcgttaagtttattgatgtagacctaatcatccgataacgcgctcttctgcttatataatggccccaccaaggtgatacatcactgcaaaagaaatgcaacatcggtgatgtattgtcgttgggg 206
agggccagatgcaatggggcgtgagacatgcaatcttattgctgattgaaatttgggtctaaagagcttctgattatcgaataactctgttattgacgtccgcagcaggtgctgctcatgatgtttgtt 207
ttcagcatcagcagctgttttctgcccataatattacatgggaaatcattatgaggaattaaagttagcgttgatagaaaacttaactatgctgcatatattaccgaatgcaaaaaagattttgatgaaaggcg 208
gcctattcttagtcaaaaagaagctgttctggtgaaatagtagaggtgattcaacgttgatgattatgagcgaatgaggtggaatttaacacttggcagatggtgtgtaccttcatcagctga 209
taattattgagcaaatattgcttattgtaaaaaataagacgcaaacatattcttttctggagctcatcattaaatcagagatgctgtagcattaaagggtgcaagagattgtagaagcaggaatgaaatacata 210

tgatgtcggcgatatagcgcagcaaccgcacctgtggcgcgggatgacccggccagatgcgtccggcgtagaggatctggagctgtaataaaaacctcttcaactaacggggcaggttagtgcattagaaaa 253
 ccgactgtaaaaagtagcagtcgacattatctcattataaaaagccagtcattagccctatctgacaattctgaaatagatctcataaacaatctgcatgataaccatcacaaacagaatgatgactgtataagatagcgg 254
 aaatataatgaattaccttttaataatgaatttctgctgtaataatgggtagaaggtaattactattattgatatttaagtaaacccagtaaatgaagccatggaataatagaagagaaaaagcattttcaggtataggt 255
 gtttgggaaacaatttcccgaaccattatatttctctacatcagaaggataaatcataaaactcttgaagtcattcttacaggagtcctcaataccagagaatgttttagataccatcaaaaattgtataaagtggctca 256
 acttaccataaactaacctctcgtctgattgtaaccagttctaaaagctgtatttgagttatcaccttctcactaagaaaataaatgcagggtaaaatttatcttctgttttagtttcgggtataaacactaatatcaatt 257
 tctgtggtatactaaaagtcgtttgtggfcaataatgafaaataatcttttcttccaattgtctaaatcaatttttaaaagtcatttgatagcctcctaaattttatctaaagtgaatttaggaggcttactgtcttctt 258
 cattaagaatcaatccttttaaaagcaatattactgtaacataaataatataatataaaaataaccactttatccaatttctgtttgtaactaatgggtcttttagtgaagaataaaagaccacattaaaaatgtggtctttgtg 259
 ttttttaaggaattgagcgtagcgaataatccttttcttcttctgataataagggtactattgccgatgataagctgcaaacatga 260

Sequence S3: DNA sequence of pTwist-Pbad-riboJ-0015T

AGGCTAGGTGGAGGCTCAGTGATGATAAGTCTGCGATGGTGGATGCATGTGTCATGGTCATAGCTGTTTCTGTGTGAAATGTTATCCGCTC 263
 AGAGGGCACAATCCTATTCGCGCTATCCGACAATCTCCAAGACATTAGGTGGAGTTCAGTTCGGCGTATGGCATATGTCGCTGGAAAGAAC 264
 ATGTGAGCAAAAGGCCAGCAAAAGGCCAGGAACCGTAAAAAGGCCGCGTGTGGCGTTTTTCCATAGGCTCCGCCCCCTGACGAGCAT 265
 CACAAAAATCGACGCTCAAGTCAGAGGTGGCGAAACCCGACAGGACTATAAAGATAACCAGGCGTTTCCCTGGAAGCTCCCTCGTGCGC 266
 TCTCCTGTTCCGACCCTGCCGCTTACCGGATACCTGTCCGCCTTCTCCCTTCGGGAAGCGTGGCGCTTCTCATAGCTCACGCTGTAGGTATC 267
 TCAGTTCGGTGTAGGTGCTTCCGCTCAAGCTGGGCTGTGTGCACGAACCCCGTTCAGCCCGACCGCTGCGCCTTATCCGGTAACTATCGT 268
 CTTGAGTCCAACCCGGTAAAGACGACTTATCGCCACTGGCAGCAGCCACTGGTAAACAGGATTAGCAGAGCGAGGTATGTAGGCGGTGCTA 269
 CAGAGTTCCTGAAGTGGTGGCCTAACTACGGCTACACTAGAAGAACAGTATTTGGTATCTGCGCTCTGCTGAAGCCAGTTACCTTCGGAAAA 270
 AGAGTTGGTAGCTCTTGATCCGGCAAACAACCACCGCTGGTAGCGGTGGTTTTTTTGTGTTGCAAGCAGCAGATTACGCGCAGAAAAAAG 271
 GATCTCAAGAAGATCCTTTGATCTTTTCTACGGGGTCTGACGCTCTATTCAACAAAGCCCGCTCCCGTCAAGTCAGCGTAAATGGGTAGGG 272
 GGCTTCAAATCGTCTCTGATACCAATTCCGAGCCTGCTTTTTGTACAAACTGTGTTGATAATGGCAATTCAAGGATCTTACCTAGATCCTT 273
 TTAAATTAATAAATGAAGTTTTAAATCAATCTAAAGTATATATGAGTAAACTGGTCTGACAGTTACCAATGCTTAATCAGTGAGGCACCTATC 274
 TCAGCGATCTGTCTATTTCTGTTTATCCATAGTTGCCTGACTCCCGTCTGTGATAGATAACTACGATACGGGAGGGCTTACCATCTGGCCCCAGT 275
 GCTGCAATGATACCGCGAGAGCCACGCTCACCGCTCCAGATTATCAGCAATAAACCAGCCAGCCGGAAGGGCCGAGCGCAGAAGTGGT 276
 CCTGCAACTTTATCCGCCTCCATCCAGTCTAATAATTGTTGCCGGGAAGCTAGAGTAAAGTAGTTCGCCAGTTAATAGTTTGCAGCAACGTTGTT 277
 GCCATTGCTACAGGCATCGTGGTGTACGCTCGTCTGTTGGTATGGCTTCATTCAGCTCCGGTCCCAACGATCAAGGCGAGTTACATGATCC 278
 CCCATGTTGTGCAAAAAAGCGTTAGCTCCTTCGGTCTCCGATCGTTGTCAGAAGTAAGTTGGCCGAGTGTATCACTCATGGTTATGGCA 279
 GCACTGCATAATTCTTACTGTATGCCATCCGTAAGATGCTTTTCTGTGACTGGTGTAGTACTCAACCAAGTCATTCTGAGAATAGTGTATGC 280
 GCGGACCGAGTTGCTCTTGCCCGCGTCAATACGGGATAATACCGGCCACATAGCAGAACTTTAAAAGTGCTCATCATTGGAAAAACGTTCT 281
 TCGGGGCGAAAACCTCTCAAGGATTTACCGCTGTTGAGATCCAGTTCGATGTAACCCACTCGTGCACCCAAGTATCTTACAGCATCTTTACT 282
 TTCACCAGCGTTTCTGGGTGAGCAAAAACAGGAAGGCAAAAATGCCGCAAAAAAGGAATAAGGGCGACACGGAAATGTTGAATACTCAT 283
 ACTCTTCCTTTTTCAATATTATTGAAGCATTATCAGGGTTATTGTCTCATGAGCGGATACATATTTGAATGTATTTAGAAAAATAAACAATAG 284
 GGGTTCGCGCACATTTCCCCGAAAAGTGCCAGATACCTGAAACAAAACCCATCGTACGGCCAAGGAAGTCTCCAATAACTGTGATCCACC 285
 ACAAGCGCCAGGGTTTTCCAGTACGACGTTGTAACGACGCGCCAGTTCATGCATAATCCGCACGCATCTGGAATAAGGAAGTGCCATTC 286
 CGCCTGACCTGGATCctatgacaactgacggctacatcattcatttttctcacaaccggcagcgaactcgtcgggctggccccgggctcatttttaataaccgcgagaaatagagttgatcgtcaaaacc 287
 aacattgacgaccgaggtggcgataggcatcgggtgggtctcaaaaagcagcttgcctggctgatacgttggctcctcgcgacgttaagacgtaaatcctaactgctggcggaagatgtgacagacgcgacggc 288
 gacaagcaaacatgctgtgacgctggctatacaaaattgctgtctgccaggtgatcgtgatgactgacaagcctcgcgtaccgattatccatcgggtgatggagcactgftaatcgttccatgcccgcagtaa 289
 caattgctcaagcagattatcgcaccagctccgaatagcgccttccccctgcccggcgttaatgattgcccacaacaggtcgtgaaatcggtgctgcttaccggcggaagaaaccccgtattggcaagattg 290
 acggccagttagccattatcgcagtaggcgcggcagaaagtaaacactgggtgataaccctgcgagcctccggatgacgaccgtgatgaaatctctctggcggaacagcaaaatataccggctggca 291
 acaaaattctgctcctgattttaccaccccctgaccgcgaatgggtgagattgagaatataaccttcatcccagcgtcggctgataaaaaatcgagataacgttggcctcaatcggcgttaaacccgccaccagtg 292
 ggcaataaacagatgccggcagcagggtcattttgctcctcagcactatcttactcctccgactcagagaagaaccaattgtccatattgcatcagacattgcccgtcactgcttcttactgctctctcctaacc 293

caaaccgtaaccccccttattaaagcattctgtaacaaagcgggaccaaagccatgacaaaaacgtaacaaaagtgtctataatcacggcagaaaagtcacaltgattattgcacggcgtcacacttctctatgcc 294
 atagcattttatccataagattagcggatcttactgacgcttttatcgaactctctactgtttccatGCGGCCGCaattagctgtcaccggatgtgtcttccggtctgatgagtcctgaggacgaacacgctctac 295
 aaataatttggttaaGAATTCGCGGCCGCAAGCTTatatGTCGACccaggcatcaataaaaacgaaaggctcagtcgaaagactgggccttctgtttatctgtgtttgctgggtaacgctctctactag 296
 agtcacactggctcaccttgggtggccttctgctgtata 297
 298

Sequence S4: DNA sequence of pMM001B

CTAAATTGTAAGCGTTAATATTTTTGTTAAATTCGCGTTAAATTTTTGTTAAATCAGCTCATTTTTTAACCAATAGGCCGAAATCGGC AAAATC 300
 CCTTATAATCAAAAAG AATAGACCGAGATAGGGTTGAGTGGCCGCTACAGGGCGCTCCCATTCGCCATT CAGGCTGCGCAACTGTTGGGAA 301
 GGGCGTTTCGGTGC GGGCCTCTTCGCTATTACGCCAGCTGGCGAAAGGGGGATGTGCTGCAAGGCGATTAAGTTGGGTAACGCCAGGGTTT 302
 TCCCAGTCACGACGTTG TAAAACGACGGCCAGTGAGCGCGACGTAATACGACTCACTATAGGGCGAAGGAAGGCCGTCAAGGCCTTGGCG 303
 GAAGGCCGTCAAGGCCG CATGGATCCttatgacaactgacggctacatcattcattttctcacaaccggcaggaactcgtcgggctggccccggcgtcatttttaaataccgcgagaaataga 304
 gttgatcgtcaaaaccaacattgcgaccgacggtggcgatagggatccgggtgggtctcaaaagcagcttcgctggctgatacgttggctctcgcgccagcttaagacgctaalcctaactcgtggcgaaaagatgtg 305
 acagacgcgacggcagacaagcaaacatgctgtgcgacgctggtatatacaaaatgctgtctgcagggatgctgctgactgacaagcctcgtaccgattatccatcggtggatggagcactcgttaactcgttc 306
 catgcgccgagtaacaattgctcaagcagattatccagcagctcgaatagcgccttccccctgccccgcttaatgatttgcacaaacaggtcgtgaaatgcggtgggtgcttcatccggcgaaagaacccc 307
 gtattggcaagattgacggccagttaaagcattcatccagtaggcgcgagcaaaagtaaacccactgggtataccattcgcgaccccggtatgacgacctagtgatgaatctctctggcggaacagcaaaat 308
 atcaccggctggcaaaacaaatctcgtcctgattttaccaccccctgaccgcaatgggtgagattgagaatataacccttccatccagcggctgctgataaaaaaatcgagataaccgttggcctcaatcgcgcttaa 309
 accgccaccagatgggcattaaacagataccggcagcaggggatcattttgctcagccatactttcatactccgcattcagagaagaaccaattgtccatattgcatcagacattgccgtcactgctctttact 310
 ggctctctcgtcaacaaacggtaaccccgtattaaaagcattctgtaacaaagcgggaccaaagccatgacaaaaacggtacaaaaggtgtataatcacggcagaaaagtcacattgattattgcacggcgt 311
 cacacttctctatgcatatgattttatccataagattagcggatcttactgacgcttttatcgaactctctactgttttccatGCGGCCGCaattagctgtcaccggatgtgtcttccggtctgatgagtcctgaggga 312
 cgaaacagcctcacaataatttggttaaGAATTC AAGGAGGTACCCACCATGGTTGAAAAATTTGTTGGCACCTGGAAAATTGCCGATAGCCATAATTTT 313
 GGCGAATACCTGAAAGCCATTGGTGACCCGAAAGAACTGAGTGATGGTGGTGATGCAACCACACCGACACTGTATATTAGCCAGAAAAGAT 314
 GGTGATAAGATGACCGTGAAAATTGAAAATGGTCCGCCTACCTTTCTGGATACCCAGGTTAAATTC AACTGGGCGAAGAATTTGATGAATT 315
 TCCGAGCGATCGTCGTA AAGGTGTTAAAAGCGTTGTTAATCTGGTGGGTGAAAAACTGGTTTATGTGCAGAAATGGGATGGTAAAGAAACC 316
 ACCTATGTGCGCGAAATCAAAGATGGTAAACTGGTTGTTACCCTGACCATGGGTGATGTTGTTGCAGTTCGTAGCTATCGTCGTGCAACCGA 317
 ATAAACTAGTCTGGGCTCATGGCCTTCCGCTCACTGCCCGCTTCCAGTCGGGAAACCTGTCGTGCCAGCTGCATTAACATGGTCATAGC 318
 TGTTTCCTTGCGTATTGGGCGCTCTCCGCTTCTCGCTCACTGACTCGCTGCGCTCGGTCTCGGTAAAGCCTGGGGTGCCTAATGAGCAA 319
 AAGGCCAGCAAAAAGCCAGGAACCGTAAAAAGCCGCGTTGCTGGCGTTTTTTCATAGGCTCCGCCCCCTGACGAGCATC AAAAAATC 320
 GACGCTCAAGTCAGAGGTGGCGAAACCCGACAGGACTATAAAGATAACCAGGCGTTTTCCCCTGGAAGCTCCCTCGTGCCTCTCTGTTCC 321
 GACCCTGCCGCTTACCGGATACCTGTCCGCTTTCTCCCTTCGGGAAGCGTGGCGCTTTCTCATAGCTCACGCTGTAGGTATCTCAGTTCGGT 322
 GTAGGTCGTTGCTCCAAGCTGGGCTGTGTGCACGAACCCCGCTTCCAGCCGACCGCTGCGCTTATCCGGTAACTATCGTCTTGAGTCCA 323
 ACCCGGTAAGACACGACTTATCGCCACTGGCAGCAGCCACTGGTAACAGGATTAGCAGAGCGAGGTATGTAGGCGGTGCTACAGATTCTT 324
 GAAGTGGTGGCCTAACTACGGCTACACTAGAAGAACAGTATTTGGTATCTGCGCTCTGCTGAAGCCAGTTACCTTCGAAAAAAGAGTTGGT 325
 AGCTCTTGATCCGGCAAACAACACCCTGGTAGCGGTGGTTTTTTTTGTTGCAAGCAGCAGATTACGCGCAGAAAAAAGGATCTCAAG 326
 AAGATCCTTTGATCTTTTCTACGGGGTCTGACGCTCAGTGGAACGAAAACCTACGTTAAGGGATTTTGGTCATGAGATTATCAAAAAGGATC 327
 TTCACCTAGATCCTTTAAATTA AAAATGAAGTTTTAAATCAATCTAAAGTATATATGAGTAAACTTGGTCTGACAGTTACCAATGCTTAATCA 328
 GTGAGGCACCTATCTCAGCGATCTGTCTATTTCTGTTATCCATAGTTGCTGACTCCCCGTCGTGATATAACTACGATAACGGAGGGCTTAC 329
 CATCTGCCCCAGTGCTGCAATGATACCGGAGAACACGCTACCCGCTCCAGATTTATCAGCAATAAACCAGCCAGCCGGAAGGGCCG 330
 AGCGCAGAAGTGGTCTGCAACTTATCCGCCTCCATCCAGTCTATTAATTGTTGCCGGGAAGCTAGAGTAAGTAGTTCGCCAGTTAATAGTT 331
 TGGCAACGTTGTTGCCATTGCTACAGGCATCGTGGTGTACGCTCGTCTTGGTATGGCTTCAATCAGTCCGGTTCCCAACGATCAAGGC 332
 GAGTTACATGATCCCCATGTTGTGCAAAAAAGCGGTTAGCTCCTTCGGTCTCCGATCGTTGTCAGAAGTAAGTTGGCCGAGTGTATCA 333
 CTCATGGTTATGGCAGCACTGCATAATTCTTACTGTATGCCATCCGTAAGATGCTTTTCTGTGACTGGTGAAGTACTCAACCAAGTCATTCT 334

GAGAATAGTGTATGCGGCGACCGAGTTGCTCTTGCCCGGCGTCAATACGGGATAATACCGCGCCACATAGCAGAACTTTAAAAGTGCTCATC 335
ATTGAAAACGTTCTTCGGGGCGAAAACCTCTCAAGGATCTTACCGCTGTTGAGATCCAGTTCGATGTAACCCACTCGTGCACCCAACTGATC 336
TTCAGCATCTTTTACTTTACACGCGTTTCTGGGTGAGCAAAAAACAGGAAGGCAAAATGCCGCAAAAAAGGGAATAAGGGCGACACGGAA 337
ATGTTGAATACTCATACTCTTCCTTTTCAATATTATTGAAGCATTATCAGGGTTATTGTCTCATGAGCGGATACATATTTGAATGTATTTAGAA 338
AAATAAACAAATAGGGTTCCGCGCACATTTCCCGAAAAGTGCCAC 339

Sequence S5: DNA sequence of pCSMR03B

CTAAATTGTAAGCGTAAATATTTTGTAAAATTCGCGTAAATTTTGTAAAATCAGCTCATTTTTTAACCAATAGGCCGAAATCGGCAAAATC 342
CCTTATAAATCAAAAAGATAGACCGAGATAGGGTTGAGTGGCCGCTACAGGGCGCTCCCATTCGCCATTCAGGCTGCGCAACTGTTGGGAA 343
GGGCGTTTCGGTGCGGGCCTCTTCGCTATTACGCCAGCTGGCGAAAGGGGGATGTGCTGCAAGGCGATTAAGTTGGGTAACGCCAGGGTTT 344
TCCCAGTCACGACGTTGTA AAAACGACGGCCAGTGAGCGCGACGTAATACGACTCACTATAGGGCGAATTGGCGGAAGGCCGTC AAGGCCG 345
CATGGATC Cttatgacaactgacggctacatcattcacttttctcacaaccggcacggaactcgtcgggctgccccggcgcatttttaataaccgcgagaaatagagttgatcgtcaaaaccaacattgcgac 346
cgacggtggcgatagggatccgggtgggtctcaaaagcagctcgtcggctgatacgttggtcctcgcgaccgctaagacgctaaccctactgctggcgaaagatgtgacagacgcgacggcgacaagcaaa 347
catgctgtgcgacgctggctatacaaaattgctgtctccagggtgatcgtgatgtactgacaagcctcgtaccgattatccatcggtgatggagcactcgttaacgctccatgcgccgagtaacaattgctcaa 348
gcagattatccagcagctccgaatagcgccttccccctggcggcgttaatgattgcccacaaggtcgtgaaatcgggctggtgcgcttcatccggcgaaagaaccccgattggcaagattgacggccagtt 349
aagccattcatccagtaggcgcgagcaaaagtaaacccactggtgatacctcgcgagcctccggatgacgacgctagtgatgaatctcctctggcggaacagcaaaatatacccggtcggcaaaacaattctc 350
gtccctgattttaccaccccctgaccgcaatgggtgagattgagaatataaccttccaccagcggctggtcgataaaaaatcgagataaccgtggcctcaatcgcggttaaacccgccaccagatgggcattaaac 351
gagatccggcagcaggggatcattttgctcctcagcactatcttccatctcccgactcagagaagaaaccaattgctcatattgatcagacattgcgctactgctctttactgctcttctcgtcaaccaaacggta 352
accccgcttataaaagcattctgtaacaaagcgggaccaaaagccatgacaaaaacgctgatacaaaaagtgctataatcacggcagaaaagtcacattgattttgacagcgtcacactttgctatgcatatagcatttta 353
tccataagattagcggatctacctgacgcttttatcgcaactctactgtttctccatGCGGCCGCaattagctgtaccggatgtgctttccggctgatgagtcctgagggagaaacagcctctacaataattttgt 354
ttaaGAATTCAAAGGAGGTACCCACCATGAAAAAATCTGGCTGGCACTGGCAGGTCTGGTTCTGGCATTAGCGCAAGCGCAGCACAGTAT 355
GAAGATCTGGAAGGTCCGGCAGGCCTGATGGTTGAAAAATTTGTTGGCACCTGGAAAATTGCCGATAGCCATAATTTTGGCGAATACCTGA 356
AAGCCATTGGTGACCGAAAGA AACTGAGTGTGGTGGTGTGCAACCACACCGACACTGTATATTAGCCAGAAAGATGGTGATAAGATGA 357
CCGTGAAAATTGAAAATGGTCCGCTACCTTTCTGGATACCCAGGTTAAATTCAAACCTGGGCGAAGAATTTGATGAATTTCCGAGCGATCGT 358
CGTAAAGGTGTTAAAAGCGTTGTTAATCTGGTGGGTGAAAAACTGGTTTATGTGCAGAAATGGGATGGTAAAGAAACCACCTATGTGCGCG 359
AAATCAAAGATGGTAAACTGGTTGTTACCCTGACCATGGGTGATGTTGTTGCAGTTCGTAGCTATCGTCGTGCAACCGAATAAACTAGTCTG 360
GGCCTCATGGCCTTCCGCTCACTGCCCCTTTCCAGTCGGGAAACCTGTCGTGCCAGCTGCATTAACATGGTCATAGCTGTTTCCCTTGGCGTA 361
TTGGGCGCTCTCCGCTTCTCGCTCACTGACTCGCTGCGCTCGGTCTGTTCCGGTAAAGCCTGGGGTGCCTAATGAGCAAAAAGGCCAGCAAAA 362
AGGCCAGGAACCGTAAAAAGGCCGCTTGCTGGCGTTTTTCCATAGGCTCCGCCCCCTGACGAGCATCACAAAAATCGACGCTCAAGTC 363
AGAGGTGGCGAAACCCGACAGGACTATAAAGATACCAGGCGTTTCCCCCTGGAAGTCCCTCGTGCCTCTCTGTTCCGACCCCTGCCGCT 364
TACCGGATACTGTCCGCTTTCTCCCTTCGGGAAGCGTGGCGCTTTCTCATAGCTCACGCTGTAGGTATCTCAGTTCGGTGTAGGTCGTTCCG 365
CTCCAAGCTGGGCTGTGTGCACGAACCCCCGTTACGCCCCACCGCTGCGCCTTATCCGGTAACTATCGTCTTGAGTCCAACCCGGTAAGAC 366
ACGACTTATCGCCACTGGCAGCAGCCACTGGTAACAGGATTAGCAGAGCGAGGTATGTAGGCGGTGCTACAGAGTTCTTGAAGTGGTGGCC 367
TAACTACGGCTACACTAGAAGAACAGTATTTGGTATCTGCGCTCTGCTGAAGCCAGTTACCTTCGAAAAAGAGTTGGTAGCTCTTGATCCG 368
GCAAAACAAACCCGCTGGTAGCGGTGGTTTTTTTGTGTTGCAAGCAGCAGATTACGCGCAGAAAAAAGGATCTCAAGAAGATCCTTTGAT 369
CTTTTCTACGGGTCTGACGCTCAGTGAACGAAAACCTCACGTTAAGGGATTTTGGTTCATGAGATTATCAAAAAGGATCTTACCTAGATCC 370
TTTTAAATTA AAAATGAAGTTTTAAATCAATCTAAAGTATATATGAGTAACTTGGTCTGACAGTTACCAATGCTTAATCAGTGAGGCACCTAT 371
CTCAGCGATCTGTCTATTTTCGTTTATCCATAGTTGCTGACTCCCCGCTGCTGTAGATAACTACGATACGGGAGGGCTTACCATCTGGCCCCAG 372
TGCTGCAATGATACCGCGAGAACCACGCTACCGGCTCCAGATTTATCAGCAATAAACCAGCCAGCCGGAAGGGCCGAGCGCAGAAGTGG 373
TCCTGCAACTTTATCCGCTCCATCCAGTCTATTAATTGTTGCCGGAAGCTAGAGTAAAGTAGTTCGCCAGTTAATAGTTTGCACAACGTTGTT 374
GCCATTGCTACAGGCATCGTGGTGTACGCTCGTCTGTTGGTATGGCTTCATTCAGCTCCGGTCCCAACGATCAAGGCGAGTTACATGATCC 375

CCCATGTTGTGCAAAAAAGCGGTTAGCTCCTTCGGTCTCCGATCGTTGTCAGAAGTAAGTTGGCCGCAGTGTATCACTCATGGTTATGGCA 376
 GCACTGCATAATTCTTACTGTATGCCATCCGTAAGATGCTTTTCTGTGACTGGTGAGTACTCAACCAAGTCATTCTGAGAATAGTGTATGC 377
 GGCGACCGAGTTGCTCTTGCCCGCGTCAATACGGGATAATACCGCGCCACATAGCAGAACCTTAAAAAGTGCTCATCATTGGAAAAAGTTCT 378
 TCGGGGCGAAAACTCTCAAGGATCTTACCGCTGTTGAGATCCAGTTCGATGTAACCCACTCGTGCACCCAACTGATCTTCAGCATCTTTTACT 379
 TTCACCAGCGTTTCTGGGTGAGCAAAAAACAGGAAGGCAAAATGCCGCAAAAAAGGGAATAAGGGCGACACGGAAATGTTGAATACTCAT 380
 ACTCTTCCTTTTCAATATTATGAAGCATTATCAGGGTTATTGTCTCATGAGCGGATACATATTTGAATGTATTTAGAAAAATAAACAAATAG 381
 GGGTTCCGCGCACATTTCCCCGAAAAGTGCCAC 382

Sequence S6: DNA sequence of pCSMR04B

CTAAATTGTAAGCGTTAATATTTTGTAAAATTCGCGTTAAATTTTGTAAAATCAGCTCATTTTTAAACCAATAGGCCGAAATCGGCAAAATC 385
 CCTTATAAATCAAAAAGATAGACCGAGATAGGGTTGAGTGGCCGCTACAGGGCGCTCCCATTCGCCATTGAGGCTGCGCAACTGTTGGGAA 386
 GGGCGTTTCGGTGCGGGCTCTTCGCTATTACGCCAGCTGGCGAAAGGGGGATGTGCTGCAAGGCGATTAAGTTGGGTAACGCCAGGGTTT 387
 TCCCAGTCACGACGTTGTAACGACGCGCCAGTGTAGCGCGACGTAATACGACTCACTATAGGGCGAATTGGCGGAAGGCCGTCAGGCCG 388
 CATGGATCCtatgacaactgacggctacatcattcattttcttcacaaccggcacggaactgcctgggctggccccgggtcatttttaaataccgcgagaaatagagtgatcgtaaaacaacattgacgac 389
 cgacgggtggcgataggcatccgggtggtgctcaaaagcagcttcgctggctgatacgttgctcctgcgcagcctaagacgctaatccctaactgctggcgaaagatgtgacagacgacggcgcaagcaaa 390
 catgctgtgacgctgctgctatacaaaftgctgctcagggatgctgctgactgatacagcctcgcgtaccgattatccatcggtggatggagcactcgtaaatcgctccatgacgcccagtaacaattgctcaa 391
 gcagattatccagcagctccgaatagcgccttccccctgccccggctaatgatttgccaaacaggtcgtgaaatgcccgtgctcctccggcgaaagaaccccgtattggcaagattgacggccagtt 392
 aagccattcatgccagtaggcgacgaaagtaaacccactggataccattcgcgaccccgatgacgacgctagtgatgaatctcctctggcggaacagcaaaataaccggctggcaaaacaattctc 393
 gtccctgattttaccaccccctgaccgcaatggtgagattgagaataataactttcattcccagcggctgataaaaaatcgagataaccgtggcctcaatcgcgcttaaacccgccaccagatgggcattaac 394
 gagtatccggcagcaggggatcattttgcttcagccatactttcactcccgcattcagagaagaaccaattgccaatgcatcagacattgcccactgctctttactgctctctcctaaccacccggta 395
 accccgcttataaaagcatttctaacaagcgggacaaagccatgacaaaaacgctaaacaaagtgtctataatcacggcagaaaaagtcacattgattttgacggcgtcacactttgctatgcatatagcatttta 396
 tccataagattagcagcttacctgacgctttttatgcactctctactgttttccatGCGGCCGCaattagctgtaccggatgctttccggctgatgagtcggaggacgaaacagcctctacaaaataattttgt 397
 ttaaGAATTCAAAGGAGGTACCCACCATGGCAAATAACAATGACCTGTTTCAGGCAAGCCGTCGTCGTTTTCTGGCACAGTTAGGTGGTCTGA 398
 CCGTTGCAGGTATGCTGGGTCCGAGCCTGCTGACACCGCGTCGTGCAACCCGACGACAGGCAGCAATGGTTGAAAAATTGTTGGCACCTG 399
 GAAAAATTGCCGATAGCCATAATTTTGGGAATACCTGAAAGCCATTGGTGCACCGAAAGAAGTACTGAGTATGGTGGTATGCAACCACACCCG 400
 AACTGTATATTAGCCAGAAAGATGGTGATAAGATGACCGTGAAAATTGAAAATGGTCCGCCTACCTTTCTGGATAACCAGGTTAAATTCAA 401
 ACTGGGCGAAGAATTTGATGAATTTCCGAGCGATCGTCGTAAAGGTGTTAAAAGCGTTGTAATCTGGTGGGTGAAAAACTGTTTATGTGC 402
 AGAAATGGGATGGTAAAGAAACCACCTATGTGCGCGAAATCAAAGATGGTAAACTGGTTGTTACCCTGACCATGGGTGATGTTGTTGCAGT 403
 TCGTAGCTATCGTCGTGCCACCGAATAAACTAGTCTGGGCCTCATGGGCCTTCCGCTCACTGCCCGCTTCCAGTCGGGAAACCTGTCTGTC 404
 CAGCTGCATTAACATGGTCATAGCTGTTTCTTGCCTATTGGGCGCTCTCCGCTTCTCTGCTCACTGACTCGCTGCGCTCGGTCGTTCCGGTA 405
 AAGCCTGGGGTGCCTAATGAGCAAAAAGGCCAGCAAAAAGGCCAGGAACCGTAAAAAGGCCGCTTGTGCGGTTTTTCCATAGGCTCCGCC 406
 CCCCTGACGAGCATCACAAAAATCGACGCTCAAGTCAGAGGTGGCGAAAACCCGACAGGACTATAAAGATAACCAGGCGTTTCCCCCTGGAA 407
 GCTCCCTCGTGCCTCTCCTGTTCCGACCCCTGCCGTTACCGGATACCTGTCCGCTTTTCTCCCTTCGGAAAGCGTGGCGCTTTTCTCATAGCTC 408
 ACGCTGTAGGTATCTCAGTTCGGTGTAGGTCGTTTCGCTCCAAGCTGGGCTGTGTGCACGAACCCCCGTTACGCCCCACCGCTGCGCCTTAT 409
 CCGGTAACCTATCGTCTTGTAGTCCAACCCGGTAAGACACGACTTATCGCCACTGGCAGCAGCCACTGGTAACAGGATTAGCAGAGCGAGGTA 410
 TGTAGGCGGTGCTACAGAGTCTTGAAGTGGTGGCCTAACTACGGCTACACTAGAAGAACAGTATTTGGTATCTGCGCTCTGCTGAAGCCAG 411
 TTACCTTCGGAAAAAGAGTTGGTAGCTCTTGATCCGGCAAAACAAACCACCGCTGGTAGCGGTGGTTTTTTTTGTTTGAAGCAGCAGATTACG 412
 CGCAGAAAAAAGGATCTCAAGAAGATCCTTTGATCTTTTCTACGGGTCTGACGCTCAGTGGAAACGAAAACCTCACGTTAAGGGATTTTGG 413
 TCATGAGATTATCAAAAAGGATCTTCACCTAGATCCTTTTAAATTAATAAATGAAGTTTTAAATCAATCTAAAGTATATATGAGTAAACTTGGTC 414
 TGACAGTTACCAATGCTTAATCAGTGAGGCACCTATCTCAGCGATCTGTCTATTTTCGTTTCATCCATAGTTGCCTGACTCCCCGTCGTGTAGATA 415
 ACTACGATACGGGAGGGCTTACCATCTGGCCCCAGTGTGCAATGATACCGCGAGAACCACGCTCACCGGCTCCAGATTTATCAGCAATAA 416

ACCAGCCAGCCGGAAGGGCCGAGCGCAGAAGTGGTCCTGCAACTTTATCCGCCTCCATCCAGTCTATTAATTGTTGCCGGAAGCTAGAGT 417
AAGTAGTTCGCCAGTTAATAGTTTGCACAACGTTGTTGCCATTGCTACAGGCATCGTGGTGTACAGCTCGTCGTTTGGTATGGCTTCATTCAG 418
CTCCGGTCCCAACGATCAAGGCGAGTTACATGATCCCCATGTTGTGCAAAAAAGCGGTTAGCTCCTTCGGTCCTCCGATCGTTGTCAGAA 419
GTAAGTTGGCCGAGTGTATCACTCATGGTTATGGCAGCACTGCATAATTCTTACTGTTCATGCCATCCGTAAGATGCTTTTCTGTGACTGG 420
TGAGTACTCAACCAAGTCATTCTGAGAATAGTGTATGCGGCGACCGAGTTGCTCTTGCCCGGCGTCAATACGGGATAATACCGCGCCACATA 421
GCAGAACTTTAAAAGTGCTCATCATTGGAAAACGTTCTTCGGGGCGAAAACTCTCAAGGATCTTACCGCTGTTGAGATCCAGTTCGATGTAA 422
CCCCTCGTGCACCCAACACTGATCTTCAGCATCTTTTACTTTTACCAGCGTTTCTGGGTGAGCAAAAAACAGGAAGGCAAAATGCCGCAAAAA 423
AGGGAATAAGGGCGACACGAAATGTTGAATACTCATACTCTTCCTTTTCAATATTATTGAAGCATTTATCAGGGTTATTGTCTCATGAGCGG 424
ATACATATTTGAATGTATTTAGAAAAATAAACAATAGGGGTTCCGCGCACATTTCCCGAAAAGTGCCAC 425
426
427
428

